226p

Space Sciences Laboratory
University of California
Berkeley, California

Series No. 4
Issue No. ~~56~~ 55

NASA Research Grant NsG 150-61

Principal Investigator: Charles W. Tobias

Technical Report

DYNAMIC ANALYSIS OF A ONE DIMENSIONAL POROUS ELECTRODE MODEL

by

Edward A. Grens II
(Ph.D. Thesis)

September 1963

Space Sciences Laboratory
University of California
Berkeley 4, California

Series No. 4,
Issue No. 55

NASA Research Grant NsG 150-61

Principal Investigator: Charles W. Tobias

Technical Report

DYNAMIC ANALYSIS OF A ONE DIMENSIONAL POROUS ELECTRODE MODEL

by

Edward A. Grens II

(Ph.D. Thesis)

September 1963

DYNAMIC ANALYSIS OF A ONE DIMENSIONAL POROUS ELECTRODE MODEL

Edward Anthony Grens II

Department of Chemical Engineering
University of California, Berkeley, California

ABSTRACT

A one dimensional model is developed to represent flooded porous electrodes in which there is no bulk flow of electrolyte in the pores. In this representation the pore configuration is ignored and the entire electrode treated as a homogeneous macroscopic region of electrolyte with distributed current and species sources. Mass transport in the electrolyte by diffusion and migration is considered. No assumptions of uniformity of electrolyte conductivity or composition are made. The model is capable of incorporating electrode reaction overpotential expressions of quite arbitrary nature.

Analysis of the model is conducted by numerical techniques to furnish descriptions of electrode behavior for both steady state and transient operation. Performance characterization includes electrode overpotential and current and concentration distributions as functions of current drain and system parameters. The computational procedure is implemented on digital computing machinery.

Examples based on the cadmium anode in 5N KOH and on the ferri-ferrocyanide electrode in 2N NaOH are investigated. In these examples overpotential relationships incorporating both forward and reverse reaction terms are used and the inadequacies of approximations to these relationships are demonstrated.

Author

DYNAMIC ANALYSIS OF A ONE DIMENSIONAL POROUS ELECTRODE MODEL

CONTENTS

1. INTRODUCTION

The operation of electrochemical cells requires that a heterogeneous reaction involving charge transfer occur at the interface between the electrolyte phase and the electrode. Since the rate of such a reaction per unit interfacial area is limited by the kinetics of the reacting system, the total rate of reaction for the electrode, and thus the electrode current, is dependent upon the extent of the interface. Therefore, electrodes with extended active surface, usually in the form of porous solids, find wide application, particularly in electrochemical energy conversion devices. It is important to be able to characterize their behavior.

A porous electrode consists of a connected matrix of an electrically conducting solid material (or mixture of materials) interspersed with connected voids, or pores, the characteristic dimensions of which are small compared with the overall size of the electrode. Such a matrix may be formed by compaction or sintering of granular material, by selective dissolution of a heterogeneous solid, or by mechanical shaping and construction. The voids or pores of the electrode are filled in part or completely with the electrolyte solution, in certain cases a portion of the pore volume being occupied by a more or less connected gas phase. Electrical contact is made by appropriate means to the electrode matrix and the exterior surfaces of the electrode are maintained in contact with the bulk electrolyte (and gas phase if one is involved). This arrangement

is illustrated schematically in Figure 1 where an electrode without gas phase (flooded) is shown in (a), one involving a gas phase in (b).

The electrode reaction takes place almost exclusively in the pores, the external surface area being small with respect to pore wall surface. The primary chemical reactant may be supplied in the solid matrix, in the electrolyte, or in the gas phase, if present. The first-mentioned source of supply is appropriate to batteries (primary or secondary); the second and third to fuel cells. The reaction product may also occur in either the solid, electrolyte, or gas phases. The reaction is distributed over the walls of the pores, the rate at any point being dependent upon the conditions of potential, species concentration, etc., prevailing at that location. In turn, the potential and species concentrations at any point in the electrode are governed by the processes of transport of current and species, respectively, to and from that point. Thus, in principle, the rate of reaction at any position in a porous electrode, conveniently expressed as rate per unit volume or transfer current per unit volume, can be determined from the conditions to which the electrode is subjected. Knowledge of distribution of electrode reaction, at any time, is necessary for complete characterization of electrode behavior.

The prediction of the performance of porous electrodes is of considerable interest, because a knowledge of their behavior under varying conditions of operation is essential

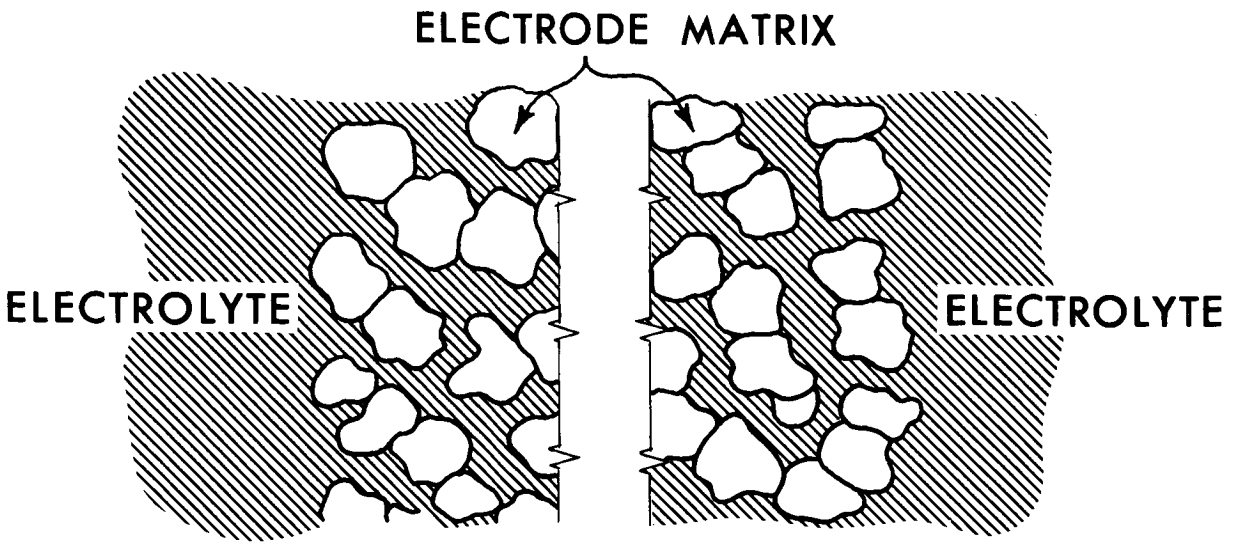

(a) Flooded electrode

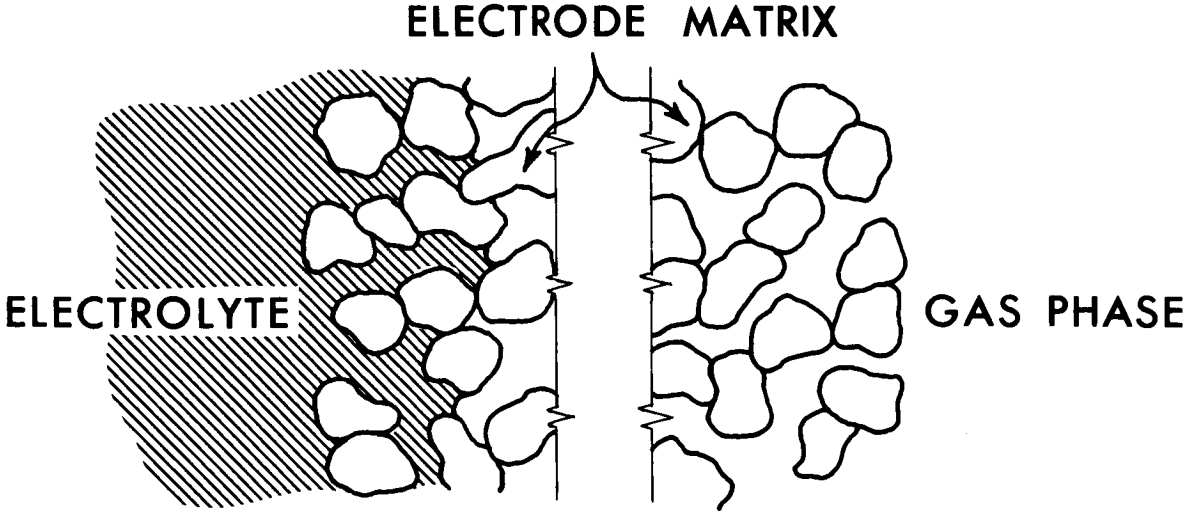

(b) Gas electrode

Figure 1. Representative Porous Electrode Sections. On order of 10^4 actual size.

to rational design and construction of those electrochemical systems which contain such electrodes as elements. Devices making use of these electrodes include all batteries of current commercial importance as well as most other electrochemical energy conversion techniques under investigation or in development. One need only cite such widespread applications as the lead-acid and nickel cadmium storage batteries, the silver-zinc and other primary batteries, and the vast majority of fuel cell types as examples.

With emphasis being placed on high energy density electrochemical devices, as for space vehicle applications, and upon perfecting of practicable fuel cell systems, the need of reliable methods of analyzing porous electrode behavior becomes increasingly important. The wide variety of systems involved and the range of parameters to be considered indicates that something more than a purely empirical approach is desirable. Theoretically based prediction techniques for characterization of the performance of such electrodes are necessary. Such methods of analysis as have been presented in the literature to this time are largely valid only for a very limited set of systems, and then only under steady state conditions. Procedures are required which are applicable to a large variety of electrode systems and which treat dynamic, as well as static, electrode operation.

1.1 Problem Description

It is the purpose of this dissertation to define a model for the flooded porous electrode, and from analysis of this

model to develop a procedure for characterizing the dynamic behavior of the electrode, subject to a set of parameters defining system conditions.

In investigating porous electrodes, the consideration of the actual geometrical configuration of the matrix (or equivalently, of the pores) would lead to overwhelming complexity. Since most such configurations are highly random, the very characterization of the pore geometry is extremely difficult. Extensive simplification would be necessary, turning to consideration of specific, idealized geometrical arrangements (e.g., cylindrical pores). Although models based on such simplified configurations are possible, and in some ways convenient, another approach has been adopted in this study: that is the utilization of the one dimensional porous electrode model. In this model the configuration of the porous body is ignored, and the entire electrode is treated as a homogeneous macroscopic region of electrolyte with a distributed current (and reacting species) source or sink representing the reaction occurring at the electrode-electrolyte interfaces. All gradients perpendicular to the overall direction of current flow (parallel to the face of the electrode) are disregarded. Thus a representation for the porous electrode is derived in which the variables are functions of only one space dimension, that normal to the electrode face. This model is well suited to the investigation of the distribution of current and species concentration in depth in the electrode, and of the gross overpotential of the

electrode. It is a valuable approximation which is amenable to theoretical treatment. It should be noted that the one dimensional model can be applied to situations in which idealized geometry in fact exists, for instance to cylindrical or fissure type pores, so long as the transverse dimensions of electrolyte containing portions of the structure are small.

For the one dimensional model to have validity, it is required that the electrode be macroscopically uniform and that characteristic dimensions of the matrix structure (e.g., grain size) be small compared to distances over which there is significant variation in concentrations or potential. That is to say, an averaging over the local complexities of the system must be permissible. Because of the very small pore dimensions in most electrodes of interest (of micron order), these conditions quite commonly exist. Then the one dimensional approach should be fully as valid as any considering a highly idealized pore geometry in two (or more) dimensions.

This nature of model has been treated quite extensively in the literature[4,7-13,15-19] but always under additional restrictions. These include assumptions of uniformity of species concentrations and electrolyte conductivity, of unrealistically simple local overpotential expressions, and of absence of migration of reacting species. Each such simplification reduces the range of cases covered, sometimes to the extent that no real systems are even approximately described. However, interesting qualitative conclusions

can be, and have been, drawn from such restricted models.

1.2 Previous Work

Previously published work devoted to analysis of behavior of porous electrodes can be divided into treatments applying to flooded systems and treatments of gas electrodes. Only the former will be considered here. These investigations are almost entirely based upon some type of analysis of a one dimensional model, as described above, although in several instances the true nature of the model was apparently not recognized. In a few cases experimental results are cited to confirm certain aspects of the results of the analysis, but no successful empirical characterization of distribution of reaction in a porous electrode has been published.

The principal contributions to the analysis of flooded porous electrodes are reviewed briefly in this section. The basic assumptions involved and type of results obtained are described, although the results themselves are not reproduced. Limitations upon applicability of the treatments are evaluated where results are of such a form that they might be applied to characterization of electrode performance. The papers are mentioned chronologically, except for a few cases where several related articles of a single author are grouped.

Fischbeck and Einecke[1,2,3]: In the consideration of electrochemical reduction of solid materials in the late 1920's, Fischbeck and Einecke were led to the examination of the

porous nature of their electrodes, and the possible effects of such nature, by the unusual behavior of certain chromite electrodes. They discussed the phenomena only briefly and in the context of a solid matrix of sufficiently low conductivity so that its particles acted as intermediate electrodes. No attempt at analysis was made, but they recognized the significance of local conductivity and overpotential and observed and commented on non-uniform distribution of reaction in porous electrodes.

Daniel-Bekh[4]: Daniel-Bekh, in 1948, initiated a series of investigations of porous electrodes in the Soviet Union. He defined a model which embodies most of the features of the one dimensional approach used in this present investigation. Specifically, he represented the electrode by parallel current paths, in the solid and in the electrolyte, each characterized by a constant conductivity. Current transfer between the paths, that is electrode reaction, was governed by an unspecified overpotential relation, with the overpotential assumed a function of transfer current only. Then the transfer current at any point along the path was shown to be proportional to the second derivative of the potential difference between the paths at that point. Daniel-Bekh developed this model for plane and for cylindrical electrode configurations. He realized that species concentration would not be constant in the pores of the electrode but dismissed this effect with a vague reference to accounting for it by use of diffusion potentials.

In order to use this model to characterize current distribution in the electrode, Daniel-Bekh relied on experimentally measured potential distributions for the electrodes, rather than introducing overpotential expressions in his equations and directly calculating distributions. These potentials were measured by use of a Luggin capillary probe inserted in the electrolyte in a 0.3 mm hole drilled into the porous electrode. Although this method eliminates the requirements for known overpotential relationships and for difficult mathematical operations, it is unsatisfactory for several reasons: the accurate measurement of the potentials is very difficult; the presence of the hole and the probe (inserted from the face of the electrode) destroys the electrode structure and creates a false environment at the point of measurement; and the double differentiation of an empirical potential curve introduces additional gross errors. In spite of its shortcomings, this work represents a valuable contribution through establishing the essential features of the one dimensional model.

Coleman[5,6]: In a paper published in 1946, Coleman presented a model for current distribution in the porous cathode of the Leclanché cell. This was essentially one dimensional in nature and was based upon application of Kirchoff's Laws to a current path. The path proceeds from one point in the matrix, through the matrix to another such location, then over into the electrolyte and, in this phase, back to the

starting point (there transferring again to the matrix). Coleman considered his matrix as made up of two kinds of particles, carbon black which carried the current and MnO_2 at which transfer took place, and assigned a constant conductivity to each, as well as to the electrolyte. However, he ignored any consideration of the local overpotential at the point of current transfer and investigated his model only for the unlikely cases of uniform potential and of uniform current distribution in the electrode. In a later paper (1951) Coleman described the results of experiments in which Leclanché type cathodes were divided into three sections (plates 1 cm thick) each provided with a connection for passage of current. Through external resistors various matrix resistances were simulated and current distribution (among the three sections) measured. A modification of the earlier Kirchoff's Law model was applied to this three-section case but experimental and calculated results were not in agreement. These treatments are principally of historical interest and contribute little to the progress of porous electrode analysis.

Ksenzhek and Stender[7,8,9,10]: A series of articles by Ksenzhek and Stender during the years 1956 and 1957 analyzed the behavior of a porous electrode containing electrolyte of a uniform concentration. Initially during the consideration of specific surfaces of porous electrodes and their measurement, these authors developed a one dimensional model with uniform electrolyte conductance (and no matrix resistance), utilizing

an overpotential relationship with transfer current proportional to hyperbolic sine of overpotential.[7] From this model an approximate expression for gross electrode overvoltage as a function of time (for periods short compared to charging times) was derived. Shortly thereafter the analysis was extended to predict current distribution in a porous electrode of infinite thickness at steady state for the same model.[8] Later the model was reinterpreted as applying to the interior surface of a tubular electrode, although in fact it was not modified at all, and solutions for local overpotential for an applied sinusoidal alternating current were derived.[9] This interpretation permitted experimental verification by use of the interior of a nickel plated metal tube as the working electrode, measuring local overpotential with a capillary probe inserted into the tube. Agreement of results with the theory was quite good, but the size of the tube used (about 8 mm) precludes any real comparison with porous electrode behavior. In the final paper in this group, Ksenzhek derived an equivalent activation energy for the overall porous electrode reaction from the steady state results previously obtained.[10]

This work constitutes a considerable advance in the one dimensional treatment of porous electrodes. Here, for the first time an overpotential relationship is used in the equation system. The approach is, however, severely limited by the assumption of uniform species concentrations in the electrode, a condition that is obtained only on initial

completion of a circuit or under AC loading. The transient results are likewise applicable only to sinusoidal or initial transient loadings. These conditions are not compatible with studies of behavior of electrochemical energy conversion devices but may be encountered in certain types of investigations of porous media.

Perskaya and Zaideman[11]: The porous electrode in which reactant is supplied entirely by diffusion in the electrolyte was examined by Perskaya and Zaideman. A redox type overpotential was used and anodic and cathodic diffusion currents assumed equal. The analysis led to a gross overpotential relationship for the porous electrode which was further simplified to an equivalent electrode transfer resistance at vanishing electrode current, given as a function of electrolyte resistance, diffusion limiting current, and overpotential parameters. This transfer resistance was compared with good agreement with experimental results measured for Fe^{2+}, Fe^{3+} system in acid solution.

Euler and Nonnenmacher[12]: The treatment by Euler and Nonnenmacher, published in 1960, employed the same basic one dimensional porous electrode model as the previous authors but, for the first time, indicated the assumptions inherent in its use. The primary concern of these authors was the carbon-MnO_2 porous electrode and this sytem served as a source of parameter values in their development. Constant conductances were assumed for the matrix and for the electrolyte. Effects of species concentration variation in the

electrolyte were disregarded, and the overpotential relationship was represented by an equivalent transfer resistance (linear overpotential). For this model analytic solutions were derived and several examples calculated. Because of the emphasis in application to carbon-MnO_2 electrodes, the effect of low conductivity electrode matrices was stressed.

Euler and Nonnenmacher also described their measurements of gross overpotential of thin carbon-MnO_2 electrode layers and presented results extrapolated to a vanishingly thin electrode. This extrapolated behavior was used to calculate the effective "volume conductivity" for transfer current which served as the basis of their overpotential relationship in the theoretical analysis. No comparison between calculated and measured results was possible because of dependence of calculated overpotential on the polarization parameter (selected from empirical results).

This article, although not basically different from those of Ksenzhek and Stender[7,8,9], presents a clear derivation of the one dimensional model for the case of uniform electrolyte concentration. The resulting expressions for steady state current distribution clearly illustrate the effects of electrolyte and matrix conductivity. The value of these results is, however, somewhat limited, since they are based on the use of a "volume conductivity" which is constant, independent of transfer current density, although the published measurements demonstrate the strong dependence of this

"conductivity" on transfer current. Nevertheless, the authors' insight into the nature of the problem makes a significant contribution to the investigation of porous electrode phenomena.

Buvet, Guillou, and Warszawski[13]: Buvet and his coauthors presented an extensive discussion of porous electrode reactions and a classification of these reactions based on method of reactant supply. They went to considerable effort to justify the existence of a non-uniform transfer current distribution in a porous electrode and then developed a one dimensional electrode ("column electrode") model for the case of constant conductivity of the electrolyte (the matrix is taken as nonresistive) and uniform species concentrations in the electrode. Two types of overpotential relationships were considered, a step function (zero or constant) overpotential and a linear overpotential expression. Both cases were solved for expressions giving gross overpotential for the electrode and potential distribution in the electrolyte.

The essential results of this work are mere restatements of those of Euler and Nonnenmacher[12] for electrode matrices of no resistance.

Euler[14,15]: In a study characterizing the pore dimensions and surface area of MnO_2 electrodes, Euler examined the effective electrical capacitance of the electrodes for various frequencies of applied alternating current.[14] In this application concentrations of species in the electrolyte were

constant since no direct current was passed. The result of primary interest in connection with porous electrode analysis is the value of the time constant for surface capacitance effects, measured at around 10^{-5} sec. Another investigation by Euler, this time into alteration of the potential profile in porous electrodes (again MnO_2) during discharge, was based on a one dimensional model with the assumption of uniform current distribution. It was then assumed that current distribution changed from some initial distribution (as from e.g. Euler and Nonnenmacher[12]) to the final uniform condition with a "buildup" of this profile. The course of this development was not analyzed. An experimental model consisting of a one dimensional network of resistors and Leclanché cells was developed and the alteration of current distribution among the branches of this network used to simulate behavior of porous electrodes during discharge.

Ksenzhek[16,17]: Extending his earlier work with porous electrodes[7,8,9,10], Ksenzhek considered two further special cases of the one dimensional porous electrode model. In considering diffusion controlled electrodes, he assumed reactant supply by diffusion from the surface of the electrode nearer the counterelectrode[16]. He further assumed conditions of operation whereby the potential in the electrolyte within the pore structure was essentially constant. Thus the analysis of the distribution of current in the electrode reduced to that of distribution of a heterogeneous

chemical reaction in a porous material (with potential as a parameter of the rate expression) and results from this field were introduced. Ksenzhek also recognized the concurrent effect on electrode behavior of the transport of reactant from the bulk of the solution through an effective diffusion layer on the surface of the electrode. Results were developed as gross overpotential curves for electrodes of various specific surface areas and as effective depths of penetration of reaction into the electrode. In discussion of the applicability of his steady state solutions, Ksenzhek explored the relation between time constants for electric charging of surface capacitance and for diffusion supply of reactant, showing the time for the former effect to be on the order of 10^{-3} to 10^{-7} times that for the latter.

Investigating polarization of thin porous electrodes Ksenzhek extended his earlier results[8] for the one dimensional electrode with uniform electrolyte concentration to the case where electrode thickness is not large compared to the depth over which significant reaction takes place[17]. He defined a measure of porous electrode efficiency as the ratio of current drawn at a porous electrode to that which would pass at a smooth electrode of same <u>superficial</u> area at the same gross overpotential. The results of this study were given as relations for this efficiency and for electrode current as a function of electrode thickness and overpotential.

Although these investigations are somewhat specialized and restricted in application by the assumptions involved,

Ksenzhek has clarified to a considerable extent the general nature of porous electrode performance at steady state.

Winsel[18]: The electrode model developed by Winsel was the single pore of circular cylindrical configuration in a material of high conductivity. The electrolyte within the pore was assumed to have constant conductivity. The author defined and discussed this model for a general overpotential relationship at the pore wall, deriving a representation as a system of integral equations. In developing solutions to these equations, however, Winsel used variables averaged over the pore cross section, a procedure equivalent to the assumption of a one dimensional model. Cases considered included electrodes with uniform electrolyte concentration and redox type overpotential expressions, as previously treated by Ksenzhek and Stender[7], and electrodes with overpotential relationships which can be represented by an interfacial resistance, as developed by Euler and Nonnenmacher[12]. Winsel also considered the effect of pre and post-transfer reactions, although solutions for these cases were not completed.

The treatments of certain non-steady state phenomena were also presented: namely, the application of alternating current to porous electrodes and the discharge of an electrode with a uniform (and constant) electrolyte composition but a condition of the pore wall which varies with time. These investigations of transient effects can be considered of a preliminary nature only.

In his lengthy paper, Winsel presented several new and interesting approaches to analysis of porous electrode performance. Computational difficulties repeatedly limited the effectiveness of the approach.

Newman and Tobias[19]: The one dimensional pore model with a resistive matrix was analyzed by Newman and Tobias in an extension of the work of Euler and Nonnenmacher[12]. In this steady state treatment a Tafel type overpotential expression was utilized instead of the linear relationship used in the earlier study cited. The model and its inherent assumptions and limitations were fully discussed and solutions derived, both for the case of uniform electrolyte concentration and for the case of binary electrolytes. In addition, approximate solutions were developed for electrodes in which con concentration variations occur but where electrolyte conductivity remains uniform.

This work is the clearest exposition available of the nature of the one dimensional model. The principal limitation of the steady state analysis presented is its restriction to Tafel type overpotential relationships, which lose validity at any point in the electrode where transfer currents become small.

1.3 Scope of Investigation

The development and analysis of a one dimensional porous electrode model which is undertaken herein is intended to unify and extend the results of the previous steady state

treatments and to provide descriptions of transient behavior in porous electrode systems.

The one dimensional model here developed, within the limitations of all one dimensional approximations, is applicable to all flooded porous electrodes in which no forced convection of electrolyte exists and for which the resistivity of the electrode matrix is negligible. The development involves no limitation to electrolytes of uniform, or constant, concentrations or conductivities. The relationships between transfer current, electrode potential, and local species concentrations which are employed in this study are considered realistic and representative of the current knowledge in electrode kinetics; no fundamental restriction is placed upon adoption of any such relationship based upon a rate limiting charge transfer step. However, throughout this work, as in essentially all previous investigations, no account is taken of any variation of the properties of the electrode matrix with extent or rate of electrode reaction.

The consideration of dynamic behavior in porous electrodes is undertaken in the context of phenomena that occur over times significant in a charge or discharge cycle (tenths of a second to many hours) and not in the restrictive (and except for certain measurements, unrealistic) sense of applied alternating currents of the first few milliseconds of discharge. Thus the effects of variations in electrolyte composition with time are explored.

In comparison with the previous work cited in Section 1.2, this study represents an increase in the generality of treatment with respect to the nature of electrolyte systems considered and to the characterization of the electrode reaction rates. It restricts electrode materials to those of low resistivity, a limitation not present in certain other analyses. No previous treatment of the transient phenomena is known.

The present investigation involves no experimental verification of the theoretical results. Moreover, currently no reliable measurements of current distribution in porous electrodes are available. Thus, in a sense equally applicable to previous treatments, this work must be considered the analysis of a <u>model</u> only; an analysis which may, however, approximate the behavior of many real systems to the extent they can be portrayed by the model.

2. FORMULATION OF POROUS ELECTRODE MODEL

2.1 Transport Phenomena in Electrolyte Systems

The characterization of the processes occurring in a flooded porous electrode must be based upon the description of the transport of mass and charge in the electrolyte filling the pores of the electrode, and of the kinetics of the electrode reactions occurring at the pore walls. The latter phenomena is discussed in Section 2.4; it essentially consists in the specification of an overpotential expression relating reaction rate (or transfer current) to the conditions prevailing at the locality in question. Transport effects in electrolyte solutions have been discussed in considerable detail in many books and articles; perhaps the work of Levich[20] presents as clear a development as any. The pertinent transport concepts are presented below in application to the electrolyte in the pores of an electrode.

The electrolyte solution within the pores of the electrode (and that exterior to the electrode) is composed of an undissociated solvent and various dissolved species, which may be either charged (ionic) or uncharged. At any position in this electrolyte the concentrations of the various species, c_j (mols/cm^3), and the potential, ϕ (volts), are necessary to describe the solution at that point. The potential may be specified with respect to any arbitrary reference; here this reference is taken as the constant potential of the electrode matrix. In this electrolyte the

the vector flux, $\underline{N}_j$ (mol/cm^2-sec), of any species, j, is expressed in terms of the gradients of concentration and potential at any point as

$$\underline{N}_j = -D_j \nabla c_j - z_j \epsilon u_j c_j \nabla \phi + \underline{v} c_j \ , \qquad (2.1\text{-}1)$$

where: D_j = diffusion coefficient of species j (cm^2/sec)

z_j = charge number of species j

ϵ = electronic charge (1.60 x 10^{-19} coul)

u_j = mobility of species j (cm/sec-dyne)

$\underline{v}$ = vector hydrodynamic velocity (cm/sec)

The three terms on the right-hand side of this equation represent, respectively, flux components arising in diffusion under a concentration (more correctly chemical potential) gradient, migration under a potential gradient, and convection by bulk fluid movement. The electric current in the electrolyte, $\underline{i}$ (amp/cm^2), is carried by the charged species and may be related to their fluxes.

$$\underline{i} = F \sum_j z_j \underline{N}_j \qquad (2.1\text{-}2)$$

where: F = Faraday's constant (96,500 coul/equiv).

The potential at any point in the solution must be related to the local charge density by Poisson's equation

$$\nabla^2 \phi = - \frac{F}{\epsilon'} \sum_j z_j c_j \qquad (2.1\text{-}3)$$

where: ϵ' = permittivity of the electrolyte solution (coul^2/erg-cm). However, except in the electric double layer at the surface of an electrode, charge separation is

not significant in the solution; that is, the local charge density is never appreciable. Therefore, as is done in almost every study of electrolytic transport phenomena, electroneutrality is assumed. This electroneutrality assumption is expressed as

$$\sum_j z_j c_j = 0 \qquad (2.1\text{-}4)$$

and serves to replace the Poisson equation (2.1-3) in the description of the system. It should be noted that this assumption is <u>not</u> equivalent to replacing the Poisson equation by the Laplace equation, $\nabla^2\phi = 0$, since the constant, F/ϵ', in equation (2.1-3) has a very large value, on the order of 10^{18} volt-cm/coul in units consistent with the expressions given above.

For conservation of species j, the continuity relation can be written

$$\frac{\partial c_j}{\partial t} = -\nabla \cdot \underline{N}_j + S_j \qquad (2.1\text{-}5)$$

where: t = time (sec)

S_j = species j source term (mol/cm^3-sec).

This source term represents a production of the species and, barring homogeneous chemical reactions in the body of the electrolyte, is zero except at the electrolyte-electrode interface where the electrode reaction takes place. Here the source can be related to the reaction rate, or rather to the transfer current density, i^s, for the electrode reaction. In transition to a one dimensional model, this source term represents the pseudo-homogeneous reaction in the one

dimensional space, which accounts for the electrode reaction at the interface.

A general reaction may be expressed as

$$\sum_j \nu_j M_j^{z_j} \longrightarrow - ne^- \qquad (2.1\text{-}6)$$

where: ν_j = stoichiometric coefficient for species j

M_j = chemical symbol for species j

e^- = chemical symbol for 1 mol of electrons.

Here the number of Faradays of charge passed per mol of reaction, n, is given by

$$n = \sum_j z_j \nu_j \ , \qquad (2.1\text{-}7)$$

where the summation is over the N species present in the electrolyte. Then the source for species j is

$$S_j = - \frac{a\nu_j}{nF} i^s \qquad (2.1\text{-}8)$$

where a = surface area per unit volume (cm^2/cm^3). In the absence of significant capacitive effects (see Appendix I) the transfer current, i^s, also represents the <u>sink</u> in a conservation equation for charge

$$0 = - \nabla \cdot \underline{i} + S_i \qquad (2.1\text{-}9)$$

where the current source is then

$$S_i = - ai^s . \qquad (2.1\text{-}10)$$

Thus the source of any species, j, can also be represented in terms of the divergence of current in the electrolyte

$$S_j = \frac{\nu_j}{nF} \nabla \cdot \underline{i} \ . \qquad (2.1\text{-}11)$$

Furthermore, the overpotential expression mentioned earlier as a description of the kinetics of the electrode reaction can, in general, be represented by a relationship of the type

$$i^s = f\ (\phi, c_j, \underline{r})\ . \qquad (2.1\text{-}12)$$

If the expressions for component flux, equation (2.1-1), and those for the source terms, in form (2.1-11), are substituted into the continuity equations (2.1-5) for each species, then a system of conservation equations, one for each species, j, is derived.

$$\frac{\partial c_j}{\partial t} = \nabla\cdot(D_j \nabla c_j) + z_j \epsilon \nabla\cdot(u_j c_j \nabla\phi) + \underline{v}\nabla c_j + \frac{\nu_j}{nF}\nabla\cdot\underline{i} \qquad j=1,\ldots,N \quad (2.1\text{-}13)$$

This system of equations, together with the electroneutrality condition

$$\sum_j z_j c_j = 0, \qquad (2.1\text{-}4)$$

serves to describe the transport phenomena taking place in the electrolyte. With a suitable overpotential expression

$$\nabla \cdot \underline{i} = -\, af(\phi, c_j, \underline{r}) \qquad (2.1\text{-}14)$$

the transport processes occurring in the electrolyte under isothermal and isobaric conditions are completely characterized.

2.2 Basic Assumptions for Porous Electrode Model

The characterization of processes occurring within the electrolyte in the pores of a porous electrode (and at the electrode surface) which has been stated in Section 2.1 is,

in theory at least, sufficient for complete solutions for the dynamic behavior of the system. However, the equations (2.1-13) which describe transport in the electrolyte are of a nature such that no analytic solutions are possible and numerical analysis is impractical for realistic cases. Moreover, as indicated in Section 1.1, the configuration of the regions over which (2.1-13) are to be applied is not subject to any practicable mathematical description for real porous bodies. In addition, other data for application of these equations, notably diffusion coefficients, D_j, and mobilities, u_j, for various species as functions of solution composition and potential gradient are not available. Therefore, certain simplifying assumptions must be made in order to permit analysis of the system and prediction of electrode behavior. These assumptions define the model treated in this dissertation within the already stated general consideration of flooded porous electrodes.

Three basic assumptions, or limitations of considerations, have previously been mentioned. These are:

1. The electrode can be described by a one dimensional approximation. This requires that all gradients perpendicular to the overall direction of current flow (direction of distance into the electrode) be negligible; that the electrode be macroscopically uniform; and that the characteristic dimensions of the pore structure be small compared to distances over which there is significant variation in concentration or potential. By this assumption the pore electrolyte can be treated as a one dimensional

region of electrolyte with a distributed homogeneous reaction representing the actually heterogeneous electrode reaction.

2. There is no hydrodynamic (bulk) flow of electrolyte in the pores. This assumption requires that no flow be impressed by an applied pressure gradient and that, further, any changes in electrolyte volume accompanying the electrode reaction generate no significant fluid velocity. It should be noted that if a significant flow is introduced by exterior means, the transport of reactant (and product) will be largely by forced convection, the convection term in equation (2.1-13) becoming dominant even at extremely low velocities (order 10^{-4} cm/sec).
3. The matrix is isopotential. This condition prevails for porous bodies of high (metallic) conductivity and is approximately satisfied as long as the solid phase conductivity is large compared with that representative of the electrolyte. Many, but certainly not all, porous electrodes satisfy this condition.

Further assumptions of a fundamental nature are introduced at this time. They are:

4. Transport parameters, that is diffusion coefficients and mobilities, are constant, independent of concentration, over the ranges of variables encountered in the electrode. At the high electrolyte concentrations

encountered in most important electrolytic cells, this assumption is certainly not satisfied (nor even approximately satisfied). It is dictated by the lack of adequate knowledge of the behavior of the properties of concentrated electrolytes and further by the difficulty in using any complex expressions for the parameters in equations (2.1-13). All known treatments of porous electrodes, and of other electrolytic transport problems, have been forced to employ the assumptions. It certainly can impose a limit upon the degree to which the model represents an actual electrode.

5. The electric double layer can be considered as part of the electrode matrix and its effects accounted for in whatever overpotential relationship is used. Given an appropriate overpotential expression (see assumption 7) this condition is very well satisfied so long as pore dimensions are large compared to the double layer thickness (order 10^{-7} cm); that is, so long as the double layer occupies only an insignificant portion of the pore cross section.
6. The solid phase of the porous electrode (the matrix) undergoes no significant modification in the course of the process considered; that is, its properties do not change with the amount of current passed nor with the condition of the adjacent electrolyte. Such an assumption is necessary to provide a well defined model of any generality but must be considered a

serious limitation. In most batteries, as opposed to fuel cells, very significant changes in the solid phase do occur during charging or discharging. No means of describing this effect is known and many aspects of this phenomena are little understood.

7. The relationship between local electrode reaction rate (transfer current) and conditions prevailing at that locality can be satisfactorily represented by an overpotential expression of the form (2.1-12). This requires a reaction whose rate depends only upon species concentration in the electrolyte and potential difference between the electrolyte and the matrix. If assumption 6 is met, then this situation will ordinarily follow for flooded systems (no gas present). It is further assumed that such overpotential expression is known.
8. The effect of transport phenomena in the electrolyte exterior to the porous electrode can be accounted for by an equivalent "transfer layer" (diffusion layer) expressed as a thickness of electrode structure within which no electrode reaction can occur. This assumption presupposes known solutions of exterior "convective-diffusion" problems and their translation into the terms specified. It imposes no essential limitation upon the model.
9. The electrolyte is isothermal. This assumption is truly valid only at low current drains. It allows

avoiding the problems of heat transfer, which are usually dependent on factors exterior to the electrode itself.

The assumptions enumerated above define a model for the porous electrode which will be developed in detail in the next section. Further assumptions will be made, from time to time, in the course of the analysis, but they will not be basic to the development of the model. The validity of the fundamental assumptions as applied to any real electrode will determine the applicability of the results of this analysis to that electrode.

2.3 Development of One Dimensional Porous Electrode Model

The assumptions of Section 2.2 define an idealized porous electrode which may be regarded as a one dimensional region of electrolyte throughout which a current and species source is distributed. The strength of this source at any point is given by equation (2.1-8). The region, which represents the electrode, will be described as extending in the single significant direction, y, from y=0 at the face of the electrode to $y=\ell$ cm at the plane of symmetry (or sealed termination of the electrode). The face of the electrode has another one dimensional region of electrolyte, without species or current sources, adjoining to it; this represents the equivalent transfer layer and extends from y=0 to $y=-\delta$ cm. Beyond the transfer layer in the negative y direction is the completely mixed bulk electrolyte and the counterelectrode, both exterior to the consideration of this model. The

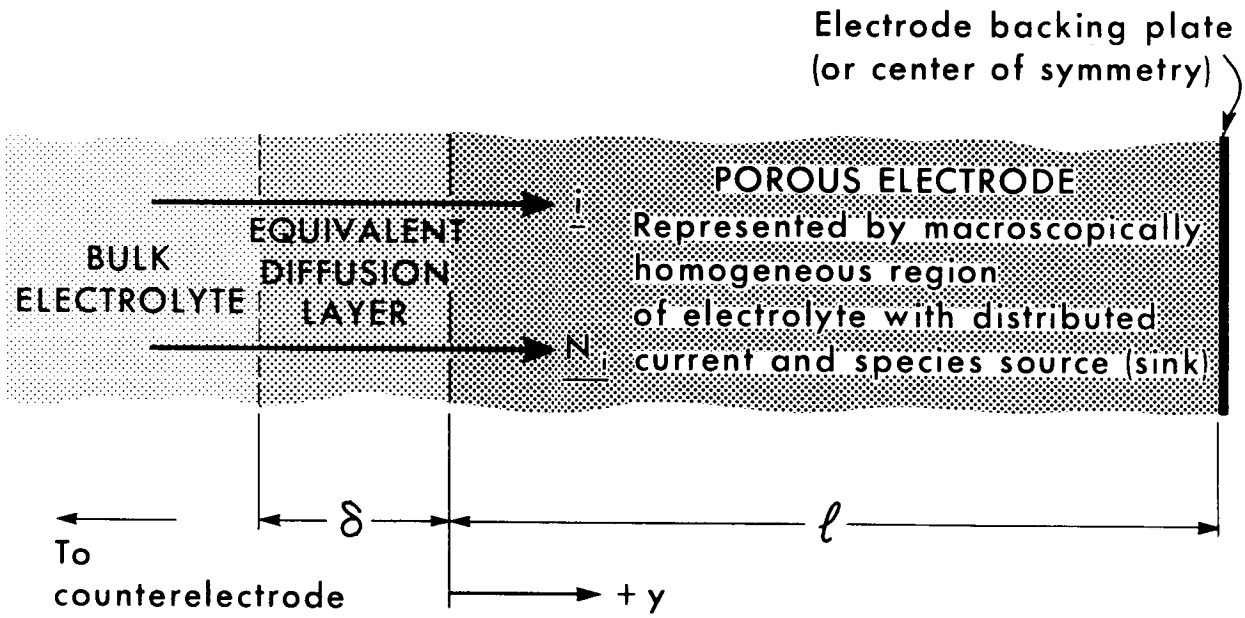

Figure 2. One-dimensional Porous Electrode Model.

arrangement just described is depicted in Figure 2.

For the one dimensional approximation with constant transport parameters and no hydrodynamic flow (assumptions 1, 2 and 4) equations (2.1-13) become

$$\frac{\partial c_j}{\partial t} = D_j \frac{\partial c_j}{\partial y} + z_j \epsilon u_j \frac{\partial}{\partial y}\left(c_j \frac{\partial \phi}{\partial y}\right) + \frac{\nu_j}{nF} \frac{\partial i}{\partial y} \qquad (2.3\text{-}1)$$

where ϕ is the potential in the solution less the assumed constant potential of the matrix, i.e., the electrode potential. Similarly, (2.1-14) becomes

$$\frac{\partial i}{\partial y} = - af(\phi, c_j) \ . \qquad (2.3\text{-}2)$$

From the description of the model in the first paragraph of this section, the side conditions for equation (2.3-1) can be formulated. Initially, before any electrode reaction has taken place, the bulk electrolyte is unaltered in the pores; thus the initial condition is:

$$\text{At} \quad t = 0: \qquad c_j = c_j^o \qquad (2.3\text{-}3)$$

where c_j^o is bulk concentration of species j. In the bulk electrolyte the concentrations remain unaltered. Thus the condition exists:

$$\text{At} \quad y = -\delta: \qquad c_j = c_j^o \qquad (2.3\text{-}4)$$

Also, at the face of the electrode, so at the face of the transfer layer, the current density in the electrolyte must be the total current density applied.

$$\text{At } y = -\delta \text{ and at } y = 0: \quad i = i^* \qquad (2.3\text{-}5)$$

where i^* = applied current density in pore electrolyte (amp/cm^2). At the plane of symmetry (or equivalent

termination) of the electrode the condition of symmetry must be met. This is expressed as:

$$\text{At} \quad y = \ell: \quad \frac{\partial c_j}{\partial y} = \frac{\partial \phi}{\partial y} = 0; \; i = 0 \; . \tag{2.3-6}$$

Within the accuracy of assumed constant transport parameters, the Nernst-Einstein relation can be introduced (for a discussion of the applicability of this expression see Harned[21]),

$$u_j = \frac{D_j}{kT} \; , \tag{2.3-7}$$

where k = Boltzmann constant (1.38×10^{-6} erg/°K)

T = Absolute temperature (°K)

Substituting (2.3-7) in (2.3-1) and noting

$$\frac{\epsilon}{kT} = \frac{F}{RT} \; ,$$

where R is the gas constant,

$$\frac{\partial c_j}{\partial t} = D_j \frac{\partial c_j}{dy} + z_j D_j \frac{F}{RT} \left(\frac{\partial c_j}{\partial y} \frac{\partial \phi}{\partial y} + c_j \frac{\partial^2 \phi}{\partial y^2} \right) + \frac{\nu_j}{nF} \frac{\partial i}{\partial y} \tag{2.3-8}$$

and, applying the same treatment to equation (2.1-2) for the current

$$i = -F \sum_j z_j D_j \left(\frac{\partial c}{\partial y} + z_j c_j \frac{\partial \phi}{\partial y} \right) . \tag{2.3-9}$$

Equations (2.3-2) through (2.3-6) and (2.3-8) now characterize the model. Thus the problem reduces to the analysis of this mathematical system.

The equation system can now be more conveniently treated if put in dimensionless form. Moreover, such a transformation yields groupings of parameters that reduce the number of independent parameters whose influence may be studied.

A suitable transformation for this model is:

$$Y = \frac{y}{\ell}$$

$$\tau = \frac{D_k t}{\ell^2}$$

$$C_j = \frac{c_j}{c_k^o} \qquad (2.3\text{-}10)$$

$$\Phi = \frac{F(\phi-\phi_e)}{RT}$$

where ϕ_e is the equilibrium electrode potential at bulk electrolyte composition and the component designated k is a convenient non-reacting species present in large concentration in the bulk solution. With this transformation the following dimensionless parameters appear:

$$\pi_j = \frac{D_j}{D_k}\ ; \qquad \gamma_j = \frac{c_j^o}{c_k^o}$$

$$\beta = \frac{i^*\ell}{nF\ D_k\ c_k^o}\ ;\ \Delta = \frac{\delta}{\ell}$$

The equation system representing the electrode model then becomes

$$\frac{1}{\pi_j}\frac{\partial C_j}{\partial \tau} = \frac{\partial^2 C_j}{\partial Y^2} + z_j\left(C_j\frac{\partial^2 \Phi}{\partial Y^2} + \frac{\partial C_j}{\partial Y}\frac{\partial \Phi}{\partial Y}\right) + \frac{\nu_j}{\pi_j}\beta\frac{\partial I}{\partial Y}$$

$$j=1,N \qquad (2.3\text{-}11)$$

$$\sum_j z_j C_j = 0 \qquad (2.3\text{-}12)$$

$$\frac{\partial I}{\partial Y} = -\ a\ f(\Phi, C_j) = -p(\Phi, C_j) \qquad (2.3\text{-}13)$$

where the function, p, representing the overpotential expression is also cast in a form which involves the

dimensionless variables. Equation (2.3-9) is easily rearranged, with nondimensionalization, to the form:

$$\frac{\partial \Phi}{\partial Y} = -\frac{1}{\sum_j z_j^2 \pi_j C_j} \left\{ n\beta\, I + \sum z_j \pi_j \frac{\partial C_j}{\partial Y} \right\} \qquad (2.3\text{-}14)$$

These equations have the side conditions, transformed from (2.3-3) through (2.3-6):

$$\text{At } \tau = 0: \quad C_j = \gamma_j \qquad (2.3\text{-}15)$$

$$Y = -\Delta: \quad C_j = \gamma_j$$

$$Y = 0: \quad I = 1 \qquad (2.3\text{-}16)$$

$$Y = 1: \quad \frac{\partial C_j}{\partial Y} = \frac{\partial \Phi}{\partial Y} = 0;\ I = 0. \qquad (2.3\text{-}17)$$

The conditions on current represented by (2.3-16) and the right-hand expression of (2.3-17) can be combined in an alternate form by integrating $\partial I/\partial Y$ over Y = 0 to 1. Then the restriction appears as

$$-\int_0^1 \frac{\partial I}{\partial Y}\, dY = \int_0^1 p\ (\Phi, C_i)\, dY = 1. \qquad (2.3\text{-}18)$$

2.4 Overpotential Expressions

The present analysis strives to maintain considerable generality in the exact nature of the relationship between local reaction rate and the conditions existing at the point in question. This must be accomplished subject to the restrictions imposed by assumption 7, that the rate may be expressed in the form

$$i^s = f\ (\Phi, c_j) \qquad (2.4\text{-}1)$$

where transfer current, i^s, is used as a measure of rate.

Of course, factors other than those considered in (2.4-1) may influence local electrode reaction rates. However, the current state of knowledge of electrode kinetics for most reactions is such that no characterization, even under near ideal conditions, is well established. That is to say, even when conditions are such that the influence of factors such as electrode history, state of aggregation, presence of traces of catalytic or inhibiting compounds, etc., is absent, usually no unequivocal rate relationship is known. The mechanisms of most reactions are poorly understood. Thus the overpotnetial expressions available are, for the most part, empirical results expressed in forms consistent with some assumed mechanism.

It should be noted that even if electrode reactions were satisfactorily desqribed for local plane surfaces with known histories, application of these descriptions to porous electrodes might be tenuous due to inhomogeniety of matrix materal and changes in material properties during the process of the reaction. Really, the overpotential expression used must represent the electrode reaction as it occurs at a matrix-electrolyte interface <u>within the porous electrode</u>. The development of such information is a field of study requiring considerable emphasis. As stated under the basic assumptions of this model, a valid expression of type (2.4-1) will be regarded as known for this investigation.

The analysis that is undertaken in Chapter 3 requires no further supposition concerning the nature of the rate

expression. However, for application to the calculation of behavior of specific electrode systems, the function f must take some definite form. For utilization in example calculations in this work two forms of overpotential expressions, which are in wide usage, have been selected. One of these is the Tafel type expression,

$$i^s = i_o \cdot \frac{c_r}{c_r^o} \exp\left[\frac{\alpha n F}{RT}(\phi-\phi_e)\right], \qquad (2.4\text{-}2a)$$

where i_o = exchange current density (amp/cm^2)

α = transfer coefficient (between 0 and 1, usually about 1/2)

ϕ_e = equilibrium electrode potential at bulk concentration

and where the subscripts r and p refer to reactant and product, respectively, for the reaction considered (2.1-6). The other form is the redox (or Erdey-Gruz or Volmer) type formula,

$$i^s = i_o\left\{\frac{c_r}{c_r^o}\exp\left[\frac{\alpha n F}{RT}(\phi-\phi_e)\right] - \frac{c_p}{c_p^o}\exp\left[\frac{(\alpha-1)nF}{RT}(\phi-\phi_e)\right]\right\} \qquad (2.4\text{-}2b)$$

Both of these expressions apply to reactions first order in reactant. The Tafel form corresponds to an electrode reaction which may proceed in one direction only, or to reactions at transfer current densities high compared with their exchange current density. The redox formulation is applicable to systems considered "reversible". An extensive discussion of the basis of these and other overpotential expressions, as well as of electrode kinetics, in general, is given in Vetter[22]. While these relationships are certainly subject

to the difficulties and limitations mentioned earlier, it is felt that they are realistic considering the current state of knowledge of kinetics for electrode reactions. For most reactions in flooded electrodes the redox form should be preferred. These expressions are much better descriptions of the vast majority of reactions than any linear approximations (equivalent resistance)* and correspond to the forms chosen in the better work previously published (Tafel by Newman and Tobias[19], redox - for the special case of uniform concentration and $\alpha=\frac{1}{2}$ - by Ksenzhek and Stender[7,8] and by Ksenzhek[16,17]). More accurate relationships should, of course, be used if available for any system being investigated.

Application of the transformation of Section 2.3 (2.3-9) to the expressions (2.4-1) and (2.4-2) gives, for the Tafel case

$$i^s = i_o \frac{C_r}{\gamma_r} \exp\ [\alpha n\Phi] \qquad (2.4\text{-}3)$$

and for the redox relationship

$$i^s = i_o \left\{\frac{C_r}{\gamma_r} \exp\ [\alpha n\Phi] - \frac{C_p}{\gamma_p} \exp\ [(\alpha-1)\ n\Phi]\right\} \qquad (2.4\text{-}4)$$

Then converting to the form of equation (2.3-13) and introducing the dimensionless parameters

---

* For comparison purposes only, a linearized form of (2.5-1) for vanishing transfer current density (and in absence of concentration overpotential) is also used in some calculations. This is

$$i^s = \frac{i_o nF}{RT} (\phi-\phi_e)$$

and involves the further assumption of $\alpha=0.5$. It is comparable to expressions used by Euler and Nonnenmacher[12], and by certain other previous investigators.

$$\xi = \frac{a\ell^2 i_o}{nFD_k c_k^o} ; \qquad \chi = \frac{\xi}{\beta} \tag{2.4-5}$$

the expressions for $\frac{\partial I}{\partial Y} = -p(\Phi, C_i)$ become

$$\text{Tafel:} \quad \frac{\partial I}{\partial Y} = -\chi \frac{C_r}{\gamma_r} \exp\,[\alpha n\Phi] \tag{2.4-6}$$

$$\text{Redox:} \quad \frac{\partial I}{\partial Y} = -\chi \left\{ \frac{C_r}{\gamma_r} \exp\,[\alpha n\Phi] - \frac{C_p}{\gamma_p} \exp\,[(\alpha-1)n\Phi] \right\} \tag{2.4-7}$$

Although a general overpotential function will be used in a large part of following developments, the redox type expression will occasionally be utilized to illustrate the adaptation of the treatment to particular rate relationships.

2.5 Significance of Variables and Parameters

Before proceeding with the analysis of the one dimensional porous electrode model, it may be well to examine the relation of variables and parameters used to describe the system to quantities normally measured for electrolytic processes. There are many ways in which the model may be related to the physically measurable system. The choice among these should be on the basis of having exact correspondence between as many variables of the model and their measurable counterparts as is possible.

In order to relate the model to measured physical quantities, certain characteristics of the porous electrode must be defined. For this purpose consider the structure shown in Figure 1 as a series of separate channels or individual pores as illustrated in Figure 3. Then a tortuosity factor, ω, can be defined as the ratio of average path length through

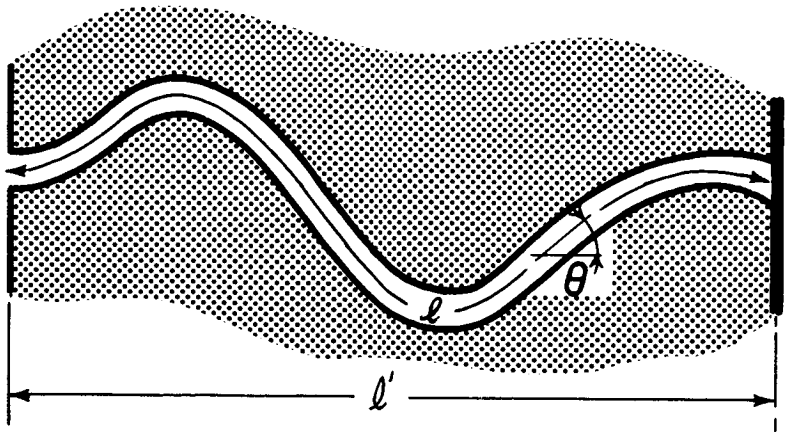

SCHEMATIC ILLUSTRATION OF RELATIONSHIP BETWEEN PORE LENGTH AND ELECTRODE THICKNESS OR HALF-THICKNESS

(Note: Pore diameter greatly exaggerated)

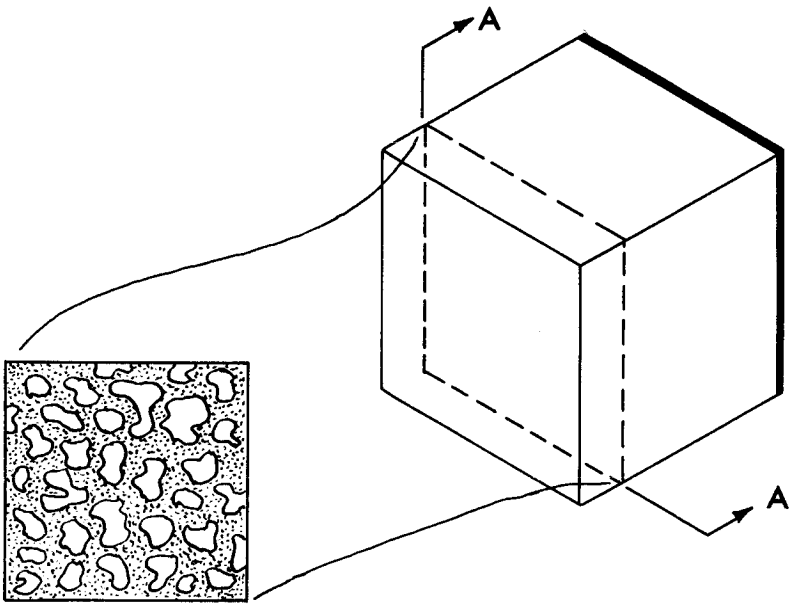

Section A-A

$$\text{POROSITY} = \frac{\text{UNSHADED AREA (VOIDS)}}{\text{TOTAL AREA}}$$

SCHEMATIC ILLUSTRATION OF POROSITY OF ELECTRODE

Figure 3. Characteristic Parameters of Porous Electrode Structure.

a pore, ℓ, to matrix thickness, ℓ', and a divergence angle, θ, as the average angle made by the pore axis with the direction perpendicular to the electrode face. Also the average fraction of a section of the porous solid, taken parallel to its face, that is void (i.e., consists of pores) can be defined as the porosity, P. Then the effective electrolyte area perpendicular to the direction of the pore axes is P cos θ per unit superficial cross sectional area.

To a good approximation, at least within the domain of cases established by the assumptions of the present model, the properties of the electrolyte within the pores are identical to those of bulk electrolyte at similar composition. That is, the presence of the pore walls does not significantly affect the transport parameters of the constituents of the solution as long as the double layer occupies a negligible portion of the pore cross section. Accordingly, the transport of species in the one dimensional model may be compared to that in an average pore along the path of the pore. In any such comparison the concentrations in the model must be referred to electrolyte volume only, in order to correspond to bulk concentrations at the boundary and at initial time. Therefore fluxes must be referred to electrolyte cross section area alone. If primed symbols represent superficial (referred to total frontal area) flows, i.e., those that would be measured,

$$N_j = \frac{N'_j}{P \cos \theta} \qquad (2.5\text{-}1)$$

$$i = \frac{i'}{P \cos \theta} ; \quad i^* = \frac{i^{*\prime}}{P \cos \theta} \qquad (2.5\text{-}2)$$

Moreover, the model boundaries must be expressed, in terms of macroscopic distances δ' and ℓ'

$$\ell = \omega \ell' \quad ; \quad \delta = \omega \delta' \ . \tag{2.5-3}$$

With these adaptations, the bulk transport parameters hold for the model, and the only effect of the pore structure appears in the first two transformations of (2.3-9) where $\omega \ell'$ must replace ℓ, and in the parameter, β, which becomes

$$\beta = \frac{i^{*\prime} \omega \ell'}{nF D_k c_k^o P \cos \theta} \tag{2.5-4}$$

in terms of normally measured values.

If the overpotential relationships of Section 2.4 are to be compared to those measured for elementary plane surfaces, the parameter ξ becomes

$$\xi = \frac{a \omega \ell'^2 i_o P \cos \theta}{nF D_k c_k^o} \tag{2.5-5}$$

where i_o is the exchange current determined for the elementary plane. It must be re-emphasized here, however, that such comparisons are not to be recommended in view of the strong influence of surface conditions (and local configurations) on overpotential properties. Measurements should be made, as mentioned earlier, for the matrix concerned.

In the above comparison the applicability of the assumptions of Section 2.2 are, of course, assumed. Without this condition the model loses significance and no comparisons of its parameters to reality is possible. However, minor deviations from certain of the assumptions may, in some cases, be compensated for by changes in values of certain

quantities entering the model. Thus the effect of a pore structure not homogeneous on a small scale, but rather possessing repeated pore narrowings or restrictions, may be compensated to some extent by variation of the diffusion coefficients used. The influence of certain portions of the pore wall to which transport is unusually difficult may be balanced by reduction of the specific area value, a. Each such situation requires special consideration; in many cases suitable adjustment may be possible but this is not necessarily to be expected. Nor is it a concern of this dissertation to examine at length cases <u>not</u> corresponding to the model developed.

3. ANALYSIS OF POROUS ELECTRODE MODEL

3.1 The Problem of Analysis

The one dimensional model for flooded porous electrodes developed in Chapter 2 is represented by the system of N parabolic partial differential equations (2.3-11), for the N species present in the electrolyte, together with the restrictions imposed by the electroneutrality condition (2.3-12) and the side conditions (2.3-15,17,18). Substituting the given overpotential function, $p(\Phi,C_j)$, into the appropriate equations, the system appears as

$$\frac{1}{\pi_j}\frac{\partial C_j}{\partial \tau} = \frac{\partial^2 C_j}{\partial Y^2} + z_j\left(C_j\frac{\partial^2 \Phi}{\partial Y^2} + \frac{\partial C_j}{\partial Y}\frac{\partial \Phi}{\partial Y}\right) - \frac{\nu_j}{\pi_j}\beta\, p(\Phi,C_i) \qquad (3.1\text{-}1)$$

for $j = 1, \ldots, N$ (note subscript, i, in fuction $p(\Phi,C_i)$ runs from 1 to N) with

$$\sum_j z_j\, C_j = 0 \qquad (3.1\text{-}2)$$

and

$$\begin{aligned} C_j\Big|_{\tau=0} &= C_j\Big|_{Y=-\Delta} = \gamma_j \\ \frac{\partial C_j}{\partial Y}\Big|_{Y=1} &= \frac{\partial \Phi}{\partial Y}\Big|_{Y=1} = 0 \qquad (3.1\text{-}3) \\ \int_0^1 p(\Phi,C_i)\, dY &= 1. \end{aligned}$$

Since the relation (3.1-2) can be used to express any dimensionless concentration, C_k, in terms of the other C_j's, this system appears as N parabolic equations (3.1-1) with appropriate side conditions (3.1-3) involving N-1

concentration variables, C_j, and the potential variable, Φ, as functions of Y and τ. In principle at least, solutions can be derived for this system giving the variation of concentrations and potential, and thus electrode reaction rate, with position and time.

Unfortunately, the partial differential equations (3.1-1) are non-linear, the non-linearities occurring in the second, and in most cases the third, terms on the right-hand side. No analytic solutions are possible. Further, the non-linearities exist in very significant (and frequently dominant) terms. Thus solutions of approximate, linearized equations corresponding to (3.1-1) will not, in most cases, yield results valid for this model. For solutions to this system of equations, recourse must be made to numerical techniques.

The application of numerical analysis to the system of equations of this model encounters several significant difficulties. While the treatment of <u>linear</u> parabolic equations by finite difference methods is a reasonably well developed field, particularaly when coefficients are time independent (see Forsythe and Wasow[23], for example), very little has been established concerning the analysis of non-linear problems (except for a few very special cases). No methods of demonstrated convergence and stability which are applicable to this problem have been described, at least to this investigator's knowledge. In fact, even if consideration is limited to the system of ordinary differential equations representing the model at steady state (equations (3.1-1)

with $\frac{\partial c_j}{\partial \tau}$ set to zero), proven numerical methods are not available.

This situation has led to an "empirical" approach to the numerical analysis problem; that is, methods have been formulated based upon the principles of finite difference analysis and upon expected behavior of the solutions to the equation system; these methods have been repeatedly modified (or completely reformulated) in accordance with the performance of the method applied to the present model. In this manner the numerical procedure described herein has been developed. It is found to yield solutions for the equations of the one dimensional porous electrode model over wide ranges of input parameters. The convergence of this procedure cannot be established, nor can its stability, except for those cases to which it has been applied. The application of this procedure to any other problems (systems of equations) must be undertaken with considerable caution. Nevertheless, it appears to be a powerful tool in predicting the performance of porous electrodes satisfying the assumptions of this work.

3.2 General Numerical Procedure

The general numerical procedure developed in this investigation is outlined here. Details of the method and its implementation are discussed later. Of course, the procedure is actually carried through with high speed digital computing machinery and is designed with this in mind, but the method

is not, in principle, restricted to this form of execution.

The partial differential equations (3.1-1) are first put in finite difference form in terms of increments of the independent variables Y and τ. At each time step (at each value of τ), starting from the initial conduction, the system is then represented by a set of simultaneous, non-linear, algebraic equations involving values of the variables from the preceding time step. This equation set is solved by assuming starting values of all quantities appearing in non-linear terms and finding revised estimates of these quantities by solution of the then linearized equation system, continuing the procedure iteratively until convergence is obtained. The calculation then proceeds to the succeeding time step where the same process is undertaken. Solutions are also obtained (by the same method) for the steady state problem. When the time step calculations yield results satisfactorily close to the steady state condition, the problem is terminated.

In using this method, convergence of the iterative procedure at each time step can only be attained if the overpotential expression, $p(\Phi,C_i)$, is put in a form such that any linear dependence of $p(\Phi,C_i)$ upon the C_j of the equation concerned (3.1-1) is separated. Thus the expression becomes

$$p(\Phi,C_i) = C_j A_j(\Phi,C_i) + B_j(\Phi,C_i) \qquad (3.2\text{-}1)$$

where the terms A_j and B_j will be different in the different equations of (3.1-1). The nature of these terms for the

overpotential types discussed in Section 2.4 is developed in Appendix II. The reason for this procedure lies in the magnitude sometimes assumed by coefficients of any C_j in $p(\Phi,C_i)$ and in the basic requirements of convergent iterations in non-linear systems (see Lapidus[24]). It should be noted that A_j and B_j may include the variable C_j which is then given its value from a preceding iteration in their evaluation.

It is also convenient to replace one of the conservation equations (3.1-1) with the differential expression for potential (2.3-14) in cases where the reactants and products constitute a very small fraction of the current carrying species present in the electrolyte. The conservation equation deleted in this instance is that for the species k. This procedure must be avoided in cases where ionic species participating in the reaction constitute the largest part of current carriers in the electrolyte; under these conditions use of (2.3-14) leads to instability.

Many aspects of the numerical calculations procedure used were dictated by computational requirements (as computer storage limitations) and economics (computer time utilization). Variations of the method are, of course, possible.

3.3 Finite Difference Representation

Transformation to finite difference representation is made by considering the space variable, Y, divided in increments, h, and the time variable, τ, divided in increments, g_i.

The space increments will be constant (h = constant), but the time steps are variable (see Section 3.4). Then if J is designated as the index for Y and K the index for τ, the relations

$$Y(J) = (J - 1)h - \Delta, \tag{3.3-1}$$

$$\tau(K) = \sum_{i=1}^{K} g_i \tag{3.3-2}$$

exist, the second reducing, for constant increments, g, of τ to

$$\tau(K) = Kg \ . \tag{3.3-3}$$

Thus the index J runs from 1 to L, where L is given by

$$L = \frac{1 + \Delta}{h} + 1 \tag{3.3-4}$$

and has a value, LF, corresponding to Y=0 which is

$$LF = \frac{\Delta}{h} + 1 \ . \tag{3.3-5}$$

The index K runs from 0 to some unspecified upper limit.

The values of the dependent variables in finite difference representation are those existing at a point in Y - τ space corresponding to integral values of the indices J and K. Thus these dependent variables become discrete, indexed, sets of values

$$\begin{aligned} &C_j(J,K) \quad \text{for } C_j \text{ at } Y(J),\ \tau(K) \\ &\Phi\ (J,K) \quad \text{for } \Phi \text{ at } Y(J),\ \tau(K) \ . \end{aligned} \tag{3.3-6}$$

In putting the partial differential equations (3.1-1) in finite difference form, representations of space derivatives of error order h^2 have been chosen. These are

$$\left.\frac{\partial^2 U}{\partial Y^2}\right|_{J,K} = \frac{U(J-1,K) - 2U(J,K) + U(J+1,K)}{h^2} + O(h^2) \qquad (3.3\text{-}7)$$

$$\left.\frac{\partial U}{\partial Y}\right|_{J,K} = \frac{U(J+1,K) - U(J-1,K)}{2h} + O(h^2) \; . \qquad (3.3\text{-}8)$$

For representation of the time derivative the form

$$\left.\frac{\partial U}{\partial \tau}\right|_{J,K+\frac{1}{2}} = \frac{U(J,K+1) - U(J,K)}{g} + O(g^2) \qquad (3.3\text{-}9)$$

is used, which, it should be noted, is of order g^2 only for a point midway between index K and index K+1. In the above U represents any dependent variable. Naturally other finite difference forms could have been chosen for the derivatives (perhaps with smaller error terms), but the same order should be maintained for the errors of the $\frac{\partial^2}{\partial Y^2}$ and $\frac{\partial}{\partial Y}$ terms*.

Implicit finite difference representations for the parabolic equations are necessary to maintain the stability of the solution in proceeding from time step to time step. In order to obtain symmetry about the point of evaluation of the time derivative, the Crank-Nicholson symmetric form has been chosen[25]. It must be mentioned, however, that there is some argument over the necessity, or even desirability, of such a choice[26].

The modified form of the overpotential expression (3.2-1) is substituted in equation (3.1-1) giving

---

* That is, the form

$$\left.\frac{\partial U}{\partial Y}\right|_{J,K} = \frac{U(J+1,K) - U(J,K)}{h} + O(h)$$

should not be used with (3.3-7).

$$\frac{1}{\pi_j}\frac{\partial C_j}{\partial \tau} = \frac{\partial^2 C_j}{\partial Y^2} + z_j\left(C_j\frac{\partial^2\Phi}{\partial Y^2} + \frac{\partial C_j}{\partial Y}\frac{\partial \Phi}{\partial Y}\right) - \frac{\nu_j\beta}{\pi_j}\left(C_jA_j(\Phi,C_i) + B_j(\Phi,C_i)\right) . \qquad (3.3\text{-}10)$$

Then such equations for all species save k (recall that k is a nonreacting species present in large concentration) yield finite difference equations in the Crank-Nicholson symmetric form

$$\frac{1}{\pi_j}\left[\frac{C_j(J,K)-C_j(J,K-1)}{g(K)}\right] = \frac{1}{2}\left\{\left[\frac{C_j(J-1,K)-2C_j(J,K)+C_j(J+1,K)}{h^2}\right] + z_j\frac{Q(J,K)}{h^2}C_j(J,K) + z_j\frac{P(J,K)}{2h}\left[\frac{C_j(J+1,K)-C_j(J-1,K)}{2h}\right] - \frac{\nu_j\beta}{\pi_j}\left[A_j(J,K)C_j(J,K)+B_j(J,K)\right]\right\}$$

$$+ \frac{1}{2}\left\{\left[\frac{C_j(J-1,K-1)-2C_j(J,K-1)+C_j(J+1,K-1)}{h^2}\right] + z_j\frac{Q(J,K-1)}{h^2}C_j(J,K-1)+z_j\frac{P(J,K-1)}{2h}\left[\frac{C_j(J+1,K-1)-C_j(J-1,K-1)}{2h}\right] - \frac{\nu\beta}{\pi_j}\left[A_j(J,K-1)C_j(J,K-1)+B_j(J,K-1)\right]\right\} \qquad (3.3\text{-}11)$$

where:
$$P(J,K) = \Phi(J+1,K) - \Phi(J-1,K)$$
$$Q(J,K) = \Phi(J-1,K) - 2\Phi(J,K) + \Phi(J+1,K) . \qquad (3.3\text{-}12)$$

If, for simplicity in representation, the terms are defined

$$T_j = \frac{h^2\nu_j\beta}{\pi_j}$$
$$\lambda_j(K) = \frac{\pi_j g(K)}{h^2} \qquad (3.3\text{-}13)$$

$$F_j(J,K) = -\left\{\left[1-z_j\frac{P(J,K-1)}{4}\right]C_j(J-1,K-1)\right.$$
$$+\left[z_jQ(J,K-1)-T_jA_j(J,K-1)+\frac{2}{\lambda_j(K)}-2\right]C_j(J,K-1)$$
$$\left.+\left[1+z_j\frac{P(J,K-1)}{4}\right]C_j(J+1,K-1)-T_jB_j(J,K-1)\right\}$$

then equations (3.3-11) may be expressed as

$$\left[1-z_j\frac{P(J,K)}{4}\right]C_j(J-1,K)+\left[z_jQ_j(J,K)-T_jA_j(J,K)-\frac{2}{\lambda_j(K)}-2\right]C_j(J,K)$$
$$+\left[1+z_j\frac{P(J,K)}{4}\right]C_j(J+1,K)=F_j(J,K)+T_jB_j(J,K) \qquad (3.3\text{-}14)$$

which have the limit conditions from (3.1-3)

$$C_j(1,K)=C_j(J,0)=\gamma_j$$
$$C_j(L-1,K)=C_j(L+1,K) \qquad (3.3\text{-}15)$$

In the above equations $A_j(J,K)$ and $B_j(J,K)$ are zero for $J < LF$ since this represents the region in the equivalent transfer layer where no reaction can take place. For $J = LF$, the values of $A_j(LF,K)$ and $B_j(LF,K)$ calculated from the overpotential expression must be multiplied by a factor

$$\frac{1}{2}+z_j\frac{P(LF,K)}{8}$$

to account for the absence of species source on one side of the position $J = LF$(see Appendix III). When the expression for $F_j(J,K)$ (3.3-13) is compared to the equation for C_j (3.3-14) for one earlier time step, then a recursion relation for $F_j(J,K)$ becomes apparent,

$$F_j(J,K) = -F_j(J,K-1)-\left(\frac{2}{\lambda_j(K)}+\frac{2}{\lambda_j(K-1)}\right)C_j(J,K-1), \qquad (3.3\text{-}16)$$

which can be used in calculating $F_j(J,K)$ at each time step

except K = 1. The value in the latter case is easily shown to be

$$F_j(J,1) = \left(T_j - z_j \frac{h^2}{\kappa} \gamma_j\right) B_k(J,0) - \frac{2}{\lambda_j(1)} \gamma_j \quad . \qquad (3.3\text{-}17)$$

where κ=constant concentration conductivity= $\sum_j z_j^2 \pi_j \gamma_j / n\beta$.

For the species k, equation (3.3-10) can be put in a form oriented to consideration of Φ as the primary dependent variable, noting species k does not react,

$$C_k \left(\frac{\partial^2 \Phi}{\partial Y^2} + \frac{1}{C_k} \frac{\partial C_k}{\partial Y} \frac{\partial \Phi}{\partial Y} + \frac{1}{C_k} \frac{\partial^2 C_k}{\partial Y^2}\right) = \frac{1}{z_k} \frac{\partial C_k}{\partial \tau} \quad . \qquad (3.3\text{-}18)$$

Then, if a variable

$$\Phi^* = \Phi - \Phi\Big|_{Y=-\Delta} \quad ; \quad \Phi^*(J) = \Phi(J) - \Phi(1) \qquad (3.3\text{-}19)$$

is defined, the finite difference approximation for (3.3-18) can be written in the symmetric form as

$$\begin{aligned}
&\frac{C_k(J,K)}{2}\left\{\left[\frac{\Phi^*(J-1,K)-2\Phi^*(J,K)+\Phi^*(J+1,K)}{h^2}\right]\right. \\
&\quad \left. + \frac{R(J,K)}{2h}\left[\frac{\Phi^*(J+1,K)-\Phi^*(J-1,K)}{2h}\right] + \frac{S(J,K)}{h^2}\right\} \\
&\quad + \frac{C_k(J,K-1)}{2}\left\{\left[\frac{\Phi^*(J-1,K-1)-2\Phi^*(J,K-1)+\Phi^*(J+1,K-1)}{h^2}\right]\right. \\
&\quad \left. + \frac{R(J\ K-1)}{2h}\left[\frac{\Phi^*(J+1,K-1)-\Phi^*(J-1,K-1)}{2h}\right] + \frac{S(J,K-1)}{h^2}\right\} \\
&\quad = \frac{1}{z_k}\left[\frac{C_k(J,K)-C_k(J,K-1)}{g(K)}\right] \qquad (3.3\text{-}20)
\end{aligned}$$

where:

$$R(J,K) = \frac{C_k(J+1,K)-C_k(J-1,K)}{C_k(J,K)} \qquad (3.3\text{-}21)$$

$$S(J,K) = \frac{C_k(J-1,K)-2C_k(J,K)+C_k(J+1,K)}{C_k(J,K)}$$

Rearrangement and definition of the term

$$F_p(J,K) = -\left\{\left[1 - \frac{R(J,K-1)}{4}\right]\Phi^*(J-1,K-1) - 2\Phi^*(J,K-1) + \left[1 + \frac{R(J,K-1)}{4}\right]\Phi^*(J+1,K-1) + \frac{S(J,K-1)}{z_k} + \frac{2}{\lambda_k(K)z_k}\right\} C_k(J,K-1) \qquad (3.3\text{-}22)$$

gives the finite difference expression for $\Phi^*(J,K)$

$$\left[1 - \frac{R(J,K)}{4}\right]\Phi^*(J-1,K) - 2\Phi^*(J,K) + \left[1 + \frac{R(J,K)}{4}\right]\Phi^*(J+1,K) = \frac{F_p(J,K)}{C_k(J,K)} - \frac{S(J,K)}{z_k} + \frac{2}{\lambda_k(K)z_k} \qquad (3.3\text{-}23)$$

which has the limit conditions, from (3.1-3) and from definition of $\Phi^*(J,K)$,

$$\begin{aligned} \Phi^*(1,K) &= 0 \\ \Phi^*(L-1,K) &= \Phi^*(L+1,K). \end{aligned} \qquad (3.3\text{-}24)$$

As with the expressions for $F_j(J,K)$, a recursion relation exists for (3.3-22). This is

$$F_p(J,K) = -F_p(J,K-1) - \frac{2}{z_k}\left(\frac{1}{\lambda_k(K)} + \frac{1}{\lambda_k(K-1)}\right)C_k(J,K-1) \qquad (3.3\text{-}25)$$

and it holds, of course, for time steps excluding K=1. For K=1 the value of $F_p(J,1)$ is

$$F_p(J,1) = -\frac{h^2}{\kappa} B_k(J,0) - \frac{1}{z_k\lambda_k(1)} \qquad (3.3\text{-}26)$$

If equation (2.3-14) is to be used, instead of the conservation relation (3.3-10) for species k, in determining Φ^* values as discussed in Section 3.2, then (2.3-14) is put in the finite difference form*

---

* Since no second derivative terms appear in this equation, the finite difference representation of error order h can be used for $\frac{\partial\Phi^*}{\partial Y}$ in (3.3-27) and has been found a convenient choice in this application.

$$\left[\frac{\Phi^*(J,K)-\Phi^*(J-1,K)}{h}\right] = \frac{-1}{V(J,K)}\left[n\beta I(J,K) + \frac{W(J,K)}{h}\right]$$

$$\Phi^*(J,K) = \Phi^*(J-1,K) - \frac{1}{V(J,K)}\left[n\beta h I(J,K) + W(J,K)\right] \qquad (3.3\text{-}27)$$

where: $V(J,K) = \sum_j z_j^2 \pi_j C_j(J,K)$

$$W(J,K) = \sum_j z_j \pi_j [C_j(J,K) - C_j(J-1,K)] \qquad (3.3\text{-}28)$$

and where $I(J,K)$ is given by numeric integration of $\frac{\partial I}{\partial Y}$ from LF to J. Using the notation Section 2.3 (i.e., (2.3-13))

$$I(J,K) = \underset{(\text{NUMERIC})}{\int_{LF}^{J}} p\left(\Phi(J,K), C_i(J,K)\right) . \qquad (3.3\text{-}29)$$

Equation (3.3-27) has the boundary conditions given by (3.3-24). It can be solved for given values of $C_j(J,K)$ by evaluating $W(J,K)$ and proceeding stepwise from $\Phi^*(1,K) = 0$.

The conversion of the values of $\Phi^*(J,K)$ of the system of (3.3-23) to values of $\Phi(J,K)$ requires a knowledge of $\Phi(1,K)$. This value is determined from the last condition of (3.1-3) by considering the integral as numerically evaluated, thus becoming

$$\underset{(\text{NUMERIC})}{\int_{LF}^{L}} p\left(\Phi^*(J,K), \Phi(1,K), C_i(J,K)\right) - 1 = 0 \qquad (3.3\text{-}30)$$

Although this expression may not be explicit in $\Phi(1,K)$, this quantity can be found by application of a suitable root-seeking procedure such as the Newton-Raphson method (see Lapidus[24]).

The finite difference expressions given in the previous paragraphs of this section are for use at all time steps

except the initial condition, $\tau=0(K=0)$. Here the values of C_j are specified in (3.1-3). Thus solutions are only required for $\Phi(J,0)$. For this purpose equation (2.3 -14) can again be used, becoming under the conditions of $C_j = \gamma_j$ which exist at $\tau=0$

$$I = -\frac{1}{n\beta}\sum_j z_j^2 \pi_j \gamma_j \frac{\partial \Phi}{\partial Y} = -\kappa \frac{\partial \Phi}{\partial Y} \qquad (3.3\text{-}31)$$

where κ is used (as previously defined) to represent $\frac{\sum z_j^2 \pi_j \gamma_j}{n\beta}$. Taking the derivative with respect to Y of (3.3-29)

$$\frac{\partial^2 \Phi}{\partial Y^2} = -\frac{1}{\kappa}\frac{\partial I}{\partial Y} = \frac{1}{\kappa} p(\Phi, C_i) \qquad (3.3\text{-}32)$$

This expression can be put in finite difference form and $B_k(J,0)$ used as equivalent to $p(\Phi(J,0),\gamma_i)$, giving

$$\Phi^*(J-1,0) - 2\Phi^*(J,0) + \Phi^*(J+1,0) = \frac{1}{\kappa} B_k(J,0), \qquad (3.3\text{-}33)$$

which has limit conditions analogous to (3.3-24)

$$\begin{aligned} \Phi^*(1,0) &= 0 \\ \Phi^*(L-1,0) &= \Phi^*(L+1,0) \ . \end{aligned} \qquad (3.3\text{-}34)$$

$\Phi(1,0)$, and thus $\Phi(J,0)$, are then found by a procdure essentially identical with that given for determining $\Phi(1,K)$ in (3.3-30).

The steady state condition of the system is represented by (3.1-1) with the left-hand sides set equal to zero. Finite difference representation for this state can be expressed in the form of equations (3.3-14) and (3.3-23) with their appropriate limit conditions by the simple process of setting the quantities $F_j(J,K)$, $F_p(J,K)$, and $\frac{1}{\lambda_j(K)}$ equal to zero. That is, if K=S signifies the steady state condition,

$$F_j(J,S) = F_p(J,S) = \frac{1}{\lambda_j(S)} = 0. \qquad (3.3\text{-}35)$$

Then a solution of the equation system at steady state is the same as a solution at any time step, but with the special values of the quantities given in (3.3-35) being employed.

These finite difference representations of the porous electrode, equations (3.3-14) and (3.3-23) for a time step, K, (or for K equal zero or S) constitute a large and complex system of simultaneous, non-linear, algebraic equations, the solutions to which will predict the behavior of the porous electrode model.

3.4 Conduct of Calculation Procedures

The finite difference representation of the one dimensional porous electrode model, developed in the previous section, has created in essence a separate problem for each value of τ considered; a problem which is linked, however, to the solutions of the problems for previous time steps. Each of these problems consists of a set of simultaneous algebraic equations (3.3-14) and (3.3-23), which are reproduced again here, in condensed form.

$$\xi_j(J,K)C_j(J-1,K) + \eta_j(J,K)C_j(J,K) + \zeta_j(J,K)C_j(J+1,K) = F_j(J,K) + \Omega_j(J,K) \qquad (3.4\text{-}1)$$

$$\mu(J,K)\Phi^*(J-1,K) - 2\Phi^*(J,K) + \nu(J,K)\Phi^*(J+1,K) = \frac{F_p(J,K)}{C_k(J,K)} + \Lambda(J,K) \qquad (3.4\text{-}2)$$

where:
$$\xi(J,K) = 1 - z_J \frac{P(J,K)}{4}$$
$$\eta(J,K) = z_j Q(J,K) - T_j A_j(J,K) - \frac{2}{\lambda_j(K)} - 2$$
$$\zeta(J,K) = 1 + z_j \frac{P(J,K)}{4}$$
$$\Omega(J,K) = T_j B_j(J,K) \qquad (3.4\text{-}3)$$
$$\mu(J,K) = 1 - \frac{R(J,K)}{4}$$
$$\nu(J,K) = 1 + \frac{R(J,K)}{4}$$
$$\Lambda(J,K) = - \frac{S(J,K)}{z_k} + \frac{2}{\lambda_k(K) z_k}$$

Since $A_j(J,K)$, $B_j(J,K)$, $P(J,K)$, and $Q(J,K)$ are functions of $\Phi(J,K)$, then $\xi_j(J,K)$, $\eta_j(J,K)$, $\zeta_j(J,K)$, and $\Omega_j(J,K)$ are likewise explicitly dependent on $\Phi(J,K)$. Similarly, the dependence of $R(J,K)$ and $S(J,K)$ upon the $C_j(J,K)$ causes $\mu(J,K)$, $\nu(J,K)$, and $\Lambda(J,K)$ to be functions of $C_j(J,K)$. At any time step K, $F_j(J,K)$ and $F_p(J,K)$ are known from preceding time steps, or, in the steady state case, are specified by relation (3.3-33). The above expressions are valid for $J = 2, \ldots, L - 1$, with limit conditions holding for $J = 1$ and $J = L$. Equation (3.4-2) may be replaced by a form of (3.3-27).

Taken with the appropriate side conditions as specified in Section 3.3, there are L of the equations (3.4-1) for each of the N-1 species, $j \neq k$, and L of the equations (3.4-2) for Φ^* (or with condition (3.3-30), for Φ). At any K there are L values of $C_j(J,K)$ $(J=1, \ldots,L)$ for each $j \neq k$ and L values of $\Phi^*(J,K)$ (or $\Phi(J,K)$) to be determined. Thus the system can

be represented by a set of matrix relations: (3.4-4) and (3.4-5) as shown on the following page. The alternate Φ^* equation (3.3-27) does not require matrix calculations. If it were not for the nonlinearities involved, that is if the terms ξ_j, η_j, ζ_j, Ω_j, μ, ν, and Λ were known in (3.4-4) and (3.3-5), these matrix equations could be resolved to give values for all $C_j(J,K)$ and $\Phi^*(J,K)$. However, in the actual case it is necessary to use estimates of $C_j(J,K)$ and $\Phi(J,K)$ to evaluate the matrix coefficients and right-hand vector, and then to develop new values of the variables by solution of the approximated, linearized, system. These new values can then be used to re-evaluate the matrix coefficients in an iterative procedure.

The iteration scheme followed must be quite carefully selected if successive values of $C_j(J,K)$ and $\Phi(J,K)$ determined in the course of iteration are to approach the solution to the non-linear equation system. It has been determined that solution of the entire system (3.4-4)-(3.4-5) for each set of iterates $C_j(J,K)$, $\Phi(J,K)$ does not, except in unusual cases, lead to convergence. Moreover, it is the convergence of this iteration that has dictated the form adopted for the source term in Section 3.2 (3.2-1). Convergence is most easily achieved if starting estimates are close to actual solutions, thus every effort must be made to secure good starting values. A basic iteration procedure, as outlined in the next paragraph, has been developed which converges in most cases to the solutions for the system (3.4-4), (3.4-5)

$$
\begin{bmatrix}
1 & & & & & \\
\xi_j(2,K) & \eta_j(2,K) & \zeta_j(2,K) & & & \\
 & \xi_j(3,K) & \eta_j(3,K) & \zeta_j(3,K) & & \\
 & & \ddots & \ddots & \ddots & \\
 & & & \xi_j(L-1,K) & \eta_j(L-1,K) & \zeta_j(L-1,K) \\
 & & & & 2 & \eta_j(L,K)
\end{bmatrix}
\circ
\begin{bmatrix} C_j(1,K) \\ C_j(2,K) \\ C_j(3,K) \\ \vdots \\ C_j(L-1,K) \\ C_j(L,K) \end{bmatrix}
=
\begin{bmatrix} \gamma_j \\ F_j(2,K) + \Omega_j(2,K) \\ F_j(3,K) + \Omega_j(3,K) \\ \vdots \\ F_j(L-1,K) + \Omega_j(L-1,K) \\ F_j(L,K) + \Omega_j(L,K) \end{bmatrix}
$$

(3.4-4)

$$
\begin{bmatrix}
1 & & & & & \\
\mu(2,K) & -2 & \nu(2,K) & & & \\
 & \mu(3,K) & -2 & \nu(3,K) & & \\
 & & \ddots & \ddots & \ddots & \\
 & & & \mu(L-1,K) & -2 & \nu(L-1,K) \\
 & & & & 2 & -2
\end{bmatrix}
\circ
\begin{bmatrix} \Phi^*(1,K) \\ \Phi^*(2,K) \\ \Phi^*(3,K) \\ \vdots \\ \Phi^*(L-1,K) \\ \Phi^*(L,K) \end{bmatrix}
=
\begin{bmatrix} 0 \\ F_p(2,K) + \Lambda(2,K) \\ F_p(3,K) + \Lambda(3,K) \\ \vdots \\ F_p(L-1,K) + \Lambda(L-1,K) \\ F_p(L,K) + \Lambda(L,K) \end{bmatrix}
$$

(3.4-5)

with reasonable rapidity. Certain computational cases require variations of this procedure, which will be discussed later.

The basic iterative process for the solution of the non-linear finite difference equation system representing the porous electrode at time step K (or at steady state) is as follows:

1. At time step K select initial estimates of $\Phi(J,K)$ for all J. These are based upon the results of the last time step (K-1) or upon solutions of similar problems in the case of steady state.
2. Using estimates of $\Phi(J,K)$ from (1) or values from a previous iteration, evaluate the terms $\xi_j(J,K)$, $\eta_j(J,K)$ and $\zeta_j(J,K)$ for the expression of type (3.4-4) pertaining to the principal <u>reactant</u> and <u>product</u> species for reaction (2.1-6). Then using these values solve the matrix relations for $C_r(J,K)$ and $C_p(J,K)$ (r and p representing reactant and product) simultaneously. Since the matrices concerned are in tridiagonal form, this solution (and other such solutions in this procedure) are conveniently accomplished by a modification of the method attributed to Thomas by Bruce et. al.[27].
3. Repeat step (2) for any other reactants or products not appearing in the overpotential expression.
4. Repeat step (2) for other species $j \neq k$ present.
5. Using the values of $C_j(J,K)$ determined in (2) through (5) above for $j \neq k$, calculate values of $C_k(J,K)$

for J = 2, ..., L by means of the electroneutrality condition, expressed in terms of finite difference variables as

$$C_k(J,K) = \frac{1}{z_k} \sum_{j \neq k} z_j C_j(J,K) \qquad (3.4\text{-}6)$$

6. Evaluate the matrix coefficients and right-hand vector of (3.4-5) in terms of the approximations to $C_k(J,K)$ found in step (5). Then solve the tridiagonal matrix equation for $\Phi^*(J,K)$ for J=2, ..., L. Alternately, for cases previously mentioned, evaluate V(J,K) and W(J,K) and solve (3.3-27) sequentially for $\Phi^*(J,K)$, from J=2 to J=L.

7. Integrate the overpotential relation, $p(\Phi^*(J,K), \Phi(1,K), C_i(J,K))$, numerically over the interval J=LF, ..., L to find $\Phi(1,K)$ as described by (3.3-30). Determine the new approximations (iterates) $\Phi(J,K) = \Phi^*(J,K) + \Phi(1,K)$ for J=1, L.

8. Compare the $\Phi(J,K)$ generated in step (7) with the value from the previous iteration (value used at step (2)). When the values are the same the process has converged. The comparison is most sensitive if, instead of the $\Phi(J,K)$ values themselves, $p(\Phi(J,K), C_i(J,K))$ evaluated with $\Phi(J,K)$ and $C_j(J,K)$ from present iteration is compared with this function evaluated at the end of the previous iteration. The criterion for convergence is that the change in p(J,K) values shall be less than some preset quantity,

epsilon, for all J=LF, ..., L. If this convergence criterion is <u>not</u> satisfied, go to step (2) and commence a new iteration. If it is satisfied, record the values of $C_j(J,K)$, $\Phi(J,K)$ for $\tau=\tau(K)$ and proceed to time step K+1.

The calculational sequence described above yields solutions after a reasonable number of iterations to the "problem" of a single time step, for most values of parameters involved. Excluded, of course, are choices of the parameters which would lead to functions p(J,K) which approach a Dirac delta function at Y=0 (delta functions are not conveniently described or treated numerically). Certain cases (or certain time steps of some cases) do present difficulties which require variations in the basic procedure just described. These difficulties can be attributed either to oscillation from iteration to iteration or to a "creeping" approach to convergence.

The phenomenon of oscillation arises most strongly in cases where the principal current carrying species in the electrolyte (species with large concentration and diffusion coefficients) exhibit large gradients of concentration ($C_j(J,K)$ a strong function of J for j a principal current carrying species). It is accentuated by inaccurate starting estimates. Oscillation manifests itself as a periodic (with the course of the iteration procedure) variation in the approximations to $C_j(J,K)$ and $\Phi(J,K)$, either of relatively constant or increasing amplitude. Oscillations of rapidly decreasing amplitude may

be ignored. The oscillation period is most commonly two iterations but may be more. This behavior precludes convergence of the basic iteration procedure. It is treated by the introduction of iteration to iteration damping on the variable $\Phi(J,K)$ whenever oscillatory behavior appears, and by using two iteration running average values of certain source terms. Damping is imposed by using a weighted average of the values of $\Phi(J,K)$ from the most recent and immediately previous iterations, in place of that from the most recent iteration alone, as the quantity used in evaluating coefficients, etc., in step (2). The weighting factor on the most recent $\Phi(J,K)$ value is started (when damping is introduced) at 0.9 and is decreased each iteration by a factor of 0.9 as long as oscillation persists. When oscillations terminate damping is decreased by multiplying the factor by 1/0.9 each iteration until the factor is unity or oscillations again appear. Any initial degree of damping may be selected. Note that the convergence criterion must be tightened by dividing the quantity epsilon by the weighting factor described above whenever damping is imposed. This simple damping procedure effectively eliminates oscillation difficulties in almost all cases, though sometimes at the expense of large (>50) iteration counts. Improvement of starting estimates of $\Phi(J,K)$ helps alleviate the oscillation phenomenon.

In cases where a redox type overpotential expression (see Section 2.4), or a relationship of similar properties, may exhibit large forward and reverse rate terms and a net reaction

rate very small by comparison, the phenomenon of "creeping" convergence may arise. In this behavior the changes in $\Phi(J,K)$ approximations from iteration to iteration become progressively smaller as convergence is approached, in the end creating a situation where it is impossible to ascertain when convergence has, in fact, occurred. In order to overcome this difficulty, a significant modification of the basic calculational procedure is instituted. In concept, the modification consists in substituting a condition of fixed applied gross overpotential,

$$\Phi(1,K) = E \tag{3.4-7}$$

for that of fixed applied current (3.3-30). Step (6) of the iteration procedure then solves for $\Phi(J,K)$, instead of $\Phi^*(J,K)$, and step (7) is omitted. When convergence for a value of E is obtained the inlet current, $I(1,K)$, is calculated from

$$I(1,K) = \int_{\substack{LF \\ NUMERIC}}^{L} P(\Phi(J,K),\ C_i(J,K)) \tag{3.4-8}$$

and compared with unity. A new value of E is then chosen to reduce the discrepancy between $I(1,K)$ and 1 and the procedure repeated. Successive values of E are used until $I(1,K)$ approaches satisfactorily close to the desired fixed condition, $I(1,K)=1$. While this procedure has been found to effectively improve "creeping" convergence, it must be used judiciously as it imposes a requirement of several convergent iteration processes, and thus many iterations, per time step.

The calculational process described in this section

develops values for $C_j(J,K)$ and $\Phi(J,K)$ for J=2, ..., L from given conditions at K-1. As stated in the first paragraph, this calculation can be considered entirely separate from overall transient problem and will be referenced in further consideration of the transient system analysis.

3.5 Time Step Procedure

The progression from the solutions for $C_j(J,K-1)$, $\Phi(J,K-1)$, determined by the methods of Section 3.4 for any time step, K-1, to the specification of the equation system, (3.4-4)-(3.4-5), for the next succeeding time step, K, constitutes what may be termed the time step procedure. This consists in first establishing the magnitude of the step, g(K), to be used, and then evaluating the terms, $F_j(J,K)$ and $F_p(J,K)$ by the appropriate recursion relations, (3.3-16) and (3.3-25). Once the first of these tasks is accomplished, the second is merely a straightforward substitution using $C_j(J,K-1)$ and $\Phi(J,K-1)$ values.

The choice of a time increment, g(K), for time step K must be based upon the rate of variation of $C_j(J,K)$ and $\Phi(J,K)$ with K <u>at this step</u>. Although the Crank-Nicholson symmetric finite difference form utilized in the calculations is apparently stable, given convergent solutions to iteration procedures at each time step, the cumulative effect of errors made at time steps is of order $h^{-1}g^{-1}$. Thus, choosing g(K) excessively small generates large cumulative deviations in the solution to the finite difference procedure, as well as being prohibitively costly in computation effort. On the

other hand, if an overly large value of g(K) is used, the error in the finite difference representation of the time derivatives may become unacceptable.* Although the value g(K) used should, strictly speaking, be based on the behavior of higher order derivatives of the concentrations, C_j, with respect to τ, such a method is impractical because of lack of knowledge of these derivatives. However, the choice cannot be avoided by selection of a constant value of g which is small enough for the situation at any time step due to the error propagation effect mentioned above. The procedure adopted is based upon the behavior of the terms $F_j(J,K)$ in (3.4-1) or (3.4-4); it generates small values of g(K) under conditions where $C_j(J,K)$ is changing rapidly and its higher derivatives can be expected to be significant. The use of varying time steps should not adversely affect the convergence of the calculations, as shown by Douglas and Gallie for systematically varied time steps[28].

By examination of the system (3.3-11) in its explicit form and the recursion relation (3.3-16), $F_j(J,K)$ can be related to the finite difference approximation for the τ derivative of $C_j(J,K-1)$, evaluated at $\tau=\tau(K-1)$ by the expression

$$F_j(J,K) = -\frac{h^2}{\pi_j}\left[C_j(J,K-1)\right]_\tau - \frac{2}{\lambda_j(K)}\,C_j(J,K-1) \qquad (3.5\text{-}1)$$

---

* For the symmetric form this error can be estimated, for an arbitrary function $U(\tau)$ by considering the realtion

$$\left.\frac{\partial U}{\partial \tau}\right|_{K-\frac{1}{2}} = \frac{U(K) - U(K-1)}{g} - \frac{g^2}{(4)(6!)}\,U'''(\xi)$$

where ξ is some value of τ between those corresponding to the indices K-1 and K. If $U'''(\tau)$ is large in the neighborhood of $\tau=\tau(K)$, the g must be small.

where $[C_j(J,K-1)]_\tau$ signifies the finite difference representation of the τ derivative of C_j at K-1. From (3.3-14) at $\tau=\tau(K)$ the additional expression can be written

$$\frac{h^2}{\pi_j}[C_j(J,K)]_\tau - \frac{2}{\lambda_j(K)} C_j(J,K) = F_j(J,K) \ . \qquad (3.5\text{-}2)$$

Recalling $\lambda_j(K) = \pi_j g(K)/h^2$, (3.5-1) and (3.5-2) become

$$\frac{\pi_j}{h^2} F_j(J,K) = -[C_j(J,K-1)]_\tau - \frac{2}{g(K)} C_j(J,K-1) \qquad (3.5\text{-}3)$$

$$\frac{\pi_j}{h^2} F_j(J,K) = +[C_j(J,K)]_\tau - \frac{2}{g(K)} C_j(J,K) \qquad (3.5\text{-}4)$$

Since $g(K)$ and $C_j(J,K)$ are always >0, if $[C_j(J,K)]_\tau < 0$, then from (3.5-4) $F_j(J,K) < 0$. But then from (3.5-3)

$$\frac{2}{g(K)} C_j(J,K-1) > -[C_j(J,K-1)]_\tau \ . \qquad (3.5\text{-}5)$$

Conversely, if $[C_j(J,K-1)]_\tau > 0$, from (3.5-3) $F_j(J,K) < 0$, and from (3.5-4)

$$\frac{2}{g(K)} C_j(J,K) > [C_j(J,K)]_\tau \qquad (3.5\text{-}6)$$

Thus for either case, the requirement is placed, if $C_j(J,K)$ is to be >0, that

$$g(K) < \frac{2\, C_j(J,K-1)}{|[C_j(J,K-1)]_\tau|} \qquad (3.5\text{-}7)$$

This can be satisfied by the approximation

$$g(K) = \min_{J=LF,L} \left\{ 2 \left(1 + \frac{2}{g(K-1)} \left[\frac{C_j(J,K-1)}{F_j(J,K-1)} \right] \right) \left(\frac{C_j(J,K-1)}{F_j(J,K-1)} \right) \right\} \qquad (3.5\text{-}8)$$

without evaluating $[C_j(J,K-1)]_\tau$. It should be noted that this treatment employs $g(K)$ values which will usually be too large to give a difference equation of the positive type (see

Forsythe and Wasow[29]); this is not a restriction in the usefulness of the computational procedure, nor an adverse influence upon the stability of the process.

If the conservative value of g(K) calculated according to (3.5-8) is used for cases where $C_j(J,K-1)$ get very small for some J, then the time steps may become impossibly small for practical computation. In these cases, that is for situations where some $C_j(J,K-1)$ are less than a set minimum limit, the limitation imposed by (3.5-7) may be avoided by using an extrapolated (toward steady state) value of $F_j(J,K)$. This is accomplished by noting, from (3.3-14) and (3.3-35), that as steady state is approached

$$F_j(J,K) \longrightarrow -\frac{2}{\lambda_j(K)} C_j(J,K) \tag{3.5-9}$$

or in context of the recursion relation (3.3-16)

$$F_j(J,K) = -F_j(J,K-1) - \left(\frac{2}{\lambda_j(K)} + \frac{2}{\lambda_j(K-1)}\right) C_j(J,K-1)$$

$$\longrightarrow -\frac{2}{\lambda_j(K)} C_j(J,K-1) \ . \tag{3.5-10}$$

If it is now assumed that extrapolation can be made in the form

$$C_j(J,K) = C_j(J,K-1) \exp\,[w(J,K)\ g(K)] \tag{3.5-11}$$

where w(J,K) is a coefficient which may be formed from

$$w(J,K) = \frac{[C_j(J,K-1)]_\tau}{C_j(J,K-1)}$$

$$= \frac{\pi_j}{h^2}\left\{\frac{F_j(J,K-1)}{C_j(J,K-1)} + \frac{2}{\lambda_j(K-1)}\right\} , \tag{3.5-12}$$

then the extrapolation of $C_j(J,K)$ is

$$C_j(J,K) = C_j(J,K-1)\ \exp\left[\left(\frac{F_j(J,K-1)}{C_j(J,K-1)} + \frac{2}{\lambda_j(K-1)}\right)\lambda_j(K)\right] \quad (3.5\text{-}13)$$

which leads to the extrapolation for $F_j(J,K)$ of

$$F_j(J,K) = -\frac{2C_j(J,K-1)}{\lambda_j(K)}\ \exp\left[\lambda_j(K)\left(\frac{F_j(J,K-1)}{C_j(J,K-1)} + \frac{2}{\lambda_j(K-1)}\right)\right] \quad (3.5\text{-}14)$$

Although this extrapolation procedure could lead to quite erroneous values for $F_j(J,K)$ if applied too far from steady state, it has no appreciable adverse influence on the course of the calculation because it is only used when $C_j(J,K-1)$, and thus $F_j(J,K)$, are very small. This statement concerning the application of this procedure has been confirmed by comparison of calculations conducted with and without its implementation; in any event, the extrapolation is rarely required.

The time steps determined as outlined above are also subjected to an arbitrary upper bound in magnitude. This is established in order to give a sufficient number of data points in τ for evaluating system performance. Once the time step magnitude, $g(K)$, is determined, the formulation of the equation system as in the previous section is easily accomplished by means of the recursion relations for $F_j(J,K)$ and $F_p(J,K)$ as mentioned at the start of this section. If the alternate calculation of $\Phi^*(J,K)$ is utilized (3.3-27), $F_p(J,K)$ need not be evaluated.

The conduct of the transient solution proceeds as a

series of individual time step solutions, conducted as outlined in Section 3.4, each leading, through the procedures described in this section, to the definition of the "problem" for the next time step. The sequence of operations continues until the values of $C_j(J,K)$ and $\Phi(J,K)$ for some time step approach satisfactorily close to the values of these variables under steady state conditions. These latter values are determined prior to initiation of the transient computations by an iterative procedure on equations (3.4-4) and (3.4-5), exactly as for any time step, with the zero values of $F_j(J,S)$, $F_p(J,S)$, and $\frac{1}{\lambda_s(S)}$ as imposed in (3.3-35). This approach to a previously determined condition also provides a confirmation on the stability of the time step procedure in each case treated.

3.6 Computer Implementation of Calculations

The execution of the calculational procedure presented in the preceding sections of this chapter requires extremely large numbers of arithmetic operations. A single iteration described in Section 3.4 requires on the order of 20,000 manipulations*, and from 10 to 200 iterations may be required at each time step. Thus the technique developed in this investigation is practicable only when implemented by high speed digital computation machinery. This has been carried out with an IBM 7090 Data Processing System**.

---

* Additions and multiplications, not including logical decisions, based on a system with 4 species present in the electrolyte and using a value of h=0.01.

** Computer Center, University of California, Berkeley.

The calculations were adapted for the digital computer through a FORTRAN II* program. This program closely follows the sequence of operations described in Sections 3.4 and 3.5, with necessary formalization of logical decisions; it is described and listed in Appendix IV. The program is applicable to systems of five or fewer species present in the electrolyte. About 5 to 20 minutes are required for calculation of each case treated.

For each case (porous electrode system and operating condition) to be analyzed, the input parameters required for the machine computation are:

N : Number of species present in electrolyte ($N \leq 5$)

z_j : Charge numbers of each species ($j=1,N$)

ν_j : Stoichiometric coefficients of each species for electrode reaction ($j=1,N$)

π_j : Diffusion coefficient ratios ($j=1,N-1$)

α, ξ, η: Overpotential parameters (as required by whatever overpotential expression is being utilized).

γ_j : Bulk concentration ratios ($j=1,N-1$)

β : Dimensionless current drain

Δ : Dimensionless equivalent transfer layer thickness

h : Distance increment

g_o : Initial time increment

ϵ_1, ϵ_2: Convergence criteria for calculations at a time step and for approach to steady state, respectively.**

---

* IBM algorithmic programming language.

** The convergence condition is $p(J,K) - p^*(J,K) \leq \epsilon$ for all J where $p(J,K)$ stands for $A_j(J,K)\, C_j(J,K) + B_j(J,K)$, the transfer current density, and $p^*(J,K)$ is, for ϵ_1, the value of $p(J,K)$ at the last iteration, and for ϵ_2, the value of $p(J,K)$ at steady state.

C_{ins}: Minimum concentration level considered significant (different from zero) for output purposes

In addition, control indicators as explained in Appendix IV are required as input information. These designate program options to be used in regard to auxilliary output material, conditions for terminating unsuccessful calculations, and so forth. All input information for each case is in punched card form. The overpotential expression to be utilized is entered as a subroutine with the parameters α, ξ, η (or any one or two of these).

The program output is in the form of line-printed data sheets, with optional magnetic tape output record for further processing. The primary printed output consist in a listing, at each time step and at steady state, of the values of $\partial I/\partial Y$, Φ, and the C_j for selected values of Y (usually every 0.02 for $-\Delta \leq Y \leq 1$).

The specification of type of overpotential expression by choice of a program subroutine, as mentioned above, lends considerable flexibility to the computation procedure. A subroutine covering Tafel and redox type expressions only is listed in the appendix, but others can be devised, subject to the restrictions of three parameters and adaptability to required form of Section 3.2*.

---

* The form, setting $-\frac{\partial I}{\partial Y} = p(J,K) = A_j(J,K)\, C_j(J,K) + B_j(J,K)$ does not imply linearity as $A_j(J,K)$ and $B_j(J,K)$ may involve $C_j(J,K)$ evaluated at last iteration. Each form poses individual convergence problems.

This mechanized computation procedure provides a quite rapid method of analyzing the behavior, under steady state and transient conditions, of any porous electrode system which can be represented by the one dimensional model of this dissertaion.

4. APPLICATION TO ELECTRODE SYSTEMS

4.1 Characterization of Electrode Systems

The analysis of a particular electrode system requires that the system, and its condition of operation, be described in terms of the input parameters of the computer implemented numerical procedure. These parameters are described in Section 3.6.

The system itself, including the electrode reaction, is characterized by the number of species present in the electrolyte; the charge numbers, stoichiometric coefficients, and diffusion coefficients of each species; and by the overpotential expression for reaction at an element of interface. In terms of the input parameters, this description involves N, z_j, ν_j, π_j, and the overpotential parameters (α, ξ, η as required).

The condition of operation of the system is determined by specification of the concentrations of species in the bulk electrolyte, the equivalent transfer layer thickness, and the superficial current density associated with the electrode current drain. These conditions are represented through values of the parameters γ_j, Δ, and β. The effect of variation of operation on electrode performance is investigated by determining behavior of the model at several values of these operating parameters, distributed over the range of interest.

Application of this model to any real electrode requires,

then, an accurate set of data descriptive of the electrode reaction at an element of interface and of the transport phenomena for the species present in the electrolyte. For most systems of interest such data are not available. In fact, the almost complete lack of data concerning the variation of ionic transport parameters with electrolyte composition leads directly to the necessity of some assumption for this behavior. The simplest assumption, that of constancy, was adopted here (see Section 2.2). The absence of reliable overpotential expressions for most systems has been discussed in Section 2.4, together with the types of expression selected for use in this analysis. These difficulties in finding accurate descriptive parameters for systems to be analyzed have, to a significant extent, dictated the degree of approximation used in this treatment. However, in many cases of porous electrode systems so little is known as to basic behavior of the electrode reactions that no analysis of any type can be undertaken at the present time.

In this investigation two electrode systems have been selected for analysis, both to illustrate the application of the method and to develop description of electrode behavior reasonably typical of many porous electrodes. One of these systems is the metal-insoluble oxide electrode in basic solution, typified by a slightly idealized cadmium anode of a nickel-cadmium cell. The other was the ferricyanide-ferrocyanide redox electrode (cathode) in 2N sodium hydroxide solution. These selections were based upon a desire to

examine systems of quite different natures but of considerable practical interest. The cadmium electrode represents an anodic reaction occurring in a binary electrolyte and yielding an insoluble product; it is of importance due to the wide utilization of nickel-cadmium batteries, and other cells using similar metal-metal oxide couples. The ferri-ferrocyanide system represents, on the other hand, a reaction occurring in the presence of excess inert electrolyte (the NaOH) and having both reactant and product as species present in the electrolyte; it is a system that is well adapted to experimental investigation of transient porous electrode performance. Through these two examples, the salient features of the dynamic behavior of a wide range of porous electrode systems may be demonstrated.

4.2 Analysis of Idealized Cadmium Anode

The cadmium anode in basic solution, treated in slightly idealized form to permit arbitrary choices among conflicting data and characterizations, is representative of a considerable number of metal-metal oxide porous electrodes finding wide commercial application (e.g., Ag-AgO). The electrode is typically composed of a porous metal matrix operating in 20-30% KOH. Here 5N (23%) KOH is used. Temperatures of operation are usually ambient, 25°C being selected for this example. It should be noted that the anodic operation considered corresponds to the discharge of a nickel-cadmium cell.

The discharge reaction for a nickel-cadmium cell in

KOH has been described by Kornfeil as:[30]

$$Cd + \underline{Ox} + 0.84\ H_2O \longrightarrow Cd(OH)_2 + \underline{Red} + 0.067\ KOH \quad (4.2\text{-}1)$$

where Ox and Red represent, respectively, the oxidized and reduced forms of the active species of the nickel oxide plate. There is considerable disagreement about these nickel oxide forms, but this is of no concern in the analysis of the cadmium anode. In any event, reaction (4.2-1) shows that there is not a significant change in the bulk concentration of KOH during discharge. At the cadmium anode, the half cell reaction is

$$Cd + 2OH^- - Cd\ (OH)_2 \longrightarrow 2e^- \ . \quad (4.2\text{-}2)$$

For this system the electrolyte is binary, the significant species present being OH^- and K^+ which are given the indices 1 and 2, respectively. Then, with the 5N bulk KOH concentration:

$$\begin{aligned} z_1 &= -1 \ ; \quad z_2 = +1 \\ \nu_1 &= +2 \ ; \quad \nu_2 = 0 \\ c_1^o &= c_2^o = 5 \times 10^{-3}\ gmol/cm^3 \end{aligned} \quad (4.2\text{-}3)$$

The diffusion coefficients in concentrated KOH are not well known, and of course not independent of concentration. For this analysis, ionic self-diffusion coefficients at 5N concentration were estimated, and these estimates used as the basis for assumed constant values of the model. The estimates were made from limiting equivalent conductance values from Harned and Owen[31], converted to dilute solution diffusion coefficients by the Nernst-Einstein relation (2.3-7).

These values were, in turn, used to derive diffusion coefficients at 5N concentration by means of the expressions developed by Gordon[32] and the procedure outlined by Reid and Sherwood[33]. The activity coefficients required for this estimation were taken from Harned and Owen[34]. The estimates developed in this manner are $D_1 = 4.7 \times 10^{-5}$ cm^2/sec; $D_2 = 1.8 \times 10^{-5}$ cm^2/sec. Due to uncertainty in these values, the diffusion coefficient-Faraday products used for this example were taken as the round number approximations:

$$\begin{aligned} D_1F &= 4 \quad \text{cm}^2 \text{ coul/gmol sec} \\ D_2F &= 2 \quad \text{cm}^2 \text{ coul/gmol sec} \ . \end{aligned} \tag{4.2-4}$$

For the electrode kinetics of this anode, no reliable data are available. Vetter[35] gives a transfer coefficient of 0.55 for Cd oxidation in K_2SO_4, indicating the assumption of $\alpha = \frac{1}{2}$ is not unreasonable. However, exchange current density estimates by battery manufacturers range over several orders of magnitude, even at a fixed KOH concentration. Thus it is desirable to use several values of this parameter and note the effect of its variation on electrode behavior. For the analysis the overpotential is characterized by

$$\begin{aligned} \alpha &= 0.5 \\ i_o &= 10^{-3}, \ 10^{-2}, \text{ and } 10^{-1} \text{ amp/cm}^2 \end{aligned} \tag{4.2-5}$$

The structure of the electrode also enters the calculation, both through the specific surface term in the parameter ξ and in the relation of superficial current densities to those in the pores. Based upon data furnished by U. B. Thomas

of Bell Telephone Laboratories*, this structure may have a porosity of 40 to 80% and a characteristic pore dimension of perhaps 2μ. Plate thicknesses range from 0.06 cm to 0.35 cm, and specific matrix surface area is approximately $\frac{1}{2}$ m^2/cm^3. For the cadmium electrode of this study, the following values are adopted.

$$\ell = 0.1 \text{ cm}$$
$$a = 10^4 \text{ cm}^2/\text{cm}^3 \text{ based on pore volume} \qquad (4.2\text{-}6)$$

A porosity of 50% is assumed.

Equivalent transfer layer thickness is dependent upon conditions exterior to the electrode and may vary widely. For this reason it was decided to study the effect of its variation, using values for the cadmium anode of

$$\delta = 0, \ 0.01 \text{ cm, and } 0.05 \text{ cm} . \qquad (4.2\text{-}7)$$

Since possible operating conditions of a cadmium anode include an extensive range of electrode current drains, operation at superficial current densities from 0.01 to almost** 2 amp/cm^2 was investigated. For the 50% porosity assumed, and using three current density values per decade, values of current density considered were

$$-i^* = 0.02, 0.05, 0.10, 0.20, 0.50, 1.0, 2.0, 3.0, 3.8 \text{ amp/cm}^2 \qquad (4.2\text{-}8)$$

The values of the parameters describing the cadmium electrode, and its operation, given in the preceding paragraphs correspond to the input parameters characteristic of the system

---

* Private communications from U. B. Thomas, Head, Electrochemical Research and Development Department, Bell Telephone Laboratories.

** This is limiting superficial current density for δ=0.01 cm.

$$N = 2$$

$$z_1 = -1 \quad ; \quad z_2 = +1$$

$$\nu_1 = +2 \quad ; \quad \nu_2 = 0$$

$$\pi_1 = 2.00 \qquad (4.2\text{-}9)$$

$$\gamma_1 = 1.00$$

$$\alpha = 0.50$$

$$\xi = 5,\ 50,\ 500.$$

The operating conditions studied are represented by the input parameters

$$\Delta = 0, 0.1, 0.5 \qquad (4.2\text{-}10)$$

$$\beta = 0.10, 0.25, 0.50, 1.00, 2.50, 5.00, 10.0, 15.0, 19.0.$$

To keep the number of cases computed from becoming excessive, the effect of different ξ values was studied only at Δ=0.1, and that of different Δ values only at ξ=50. The cases of operation considered for the cadmium anode were, then, as listed and identified in Table I.

For comparison purposes, certain operational cases were analyzed with a Tafel type overpotential matched to the redox type expression at $i^s \longrightarrow \infty$. These cases are tabulated in Table II.

The calculated operation of the cadmium anode at steady state is presented in Appendix V for each of the cases listed above. The description takes the form of curves of transfer current density (reaction rate) and KOH concentration as functions of position, in depth, in the electrode. In interpreting these curves it must be remembered that they involve non-dimensionalized variables and that for this system the

TABLE I

Cases of Operation Considered for Cadmium Anode in 5N KOH
Redox Overpotential

Case Number	ξ	Δ	β
A1	50.	0.1	0.05
A2(T)	↓	↓	0.10
A3			0.25
A4			0.50
A5(T)			1.0
A6			2.5
A7			5.0
A8(T)			10.
A9			15.
A10	↓		18.
A11	500.		0.10
A12	↓		1.0
A13(T)			10.
A14	↓		15.
A15	5.		0.10
A16	↓		1.0
A17(T)			10.
A18	↓	↓	15.
A19	50.	0.0	0.10
A20	↓	↓	1.0
A21			10.
A22		↓	15.
A23		0.5	0.10
A24		↓	1.0
A25	↓	↓	3.0

TABLE II

Cases of Operation Considered for Cadmium Anode in 5N KOH
Tafel Overpotential

Case Number	ξ	Δ	β
A27	50.	0.1	0.10
A28	↓	↓	1.0
A29(T)			10.
A30	↓	↓	15.

superficial current density is -0.1β (amp/cm^2); the transfer current density is $2\beta \frac{\partial I}{\partial Y}$ (amp/cm^3) or $2 \times 10^{-4} \beta \frac{\partial I}{\partial Y}$ (amp/cm^2 pore wall); distances are 0.1 Y (cm); and overpotentials 0.0256 Φ (volts).

The steady state operation of the system is summarized, and the effect of variations of the parameters β, ξ, and Δ demonstrated, in Figures 4 through 10. These represent predictions of system behavior based upon a redox type overpotential expression. In Figure 4 the distribution of transfer current (in depth) in the electrode is shown for several values of β for ξ=50, Δ=0.1. Similar curves are presented for higher and lower exchange current densities, ξ=500 and 5, respectively, in Figures 5 and 6. It can be seen in Figure 4 that as β is reduced, a distribution is reached (at about β=0.5) which is not affected by further reductions in current drain (β). This same phenomenon occurs for the other values of ξ. Comparison of Figures 4, 5, and 6 reveals the profound effect of exchange current density (ξ) upon current distribution, particularly at lower current drains. This effect is clearly illustrated by the comparison of current distributions at β=1.0, Δ=0.1 for ξ=5, 50, and 500 in Figure 7.

The effect of different transfer layer thicknesses upon current distribution is small at moderate current drains as should be expected for a binary electrolyte. This is shown in Figure 8 for β=1.0, ξ=50. In essence, the presence of a transport layer serves only to decrease the concentration

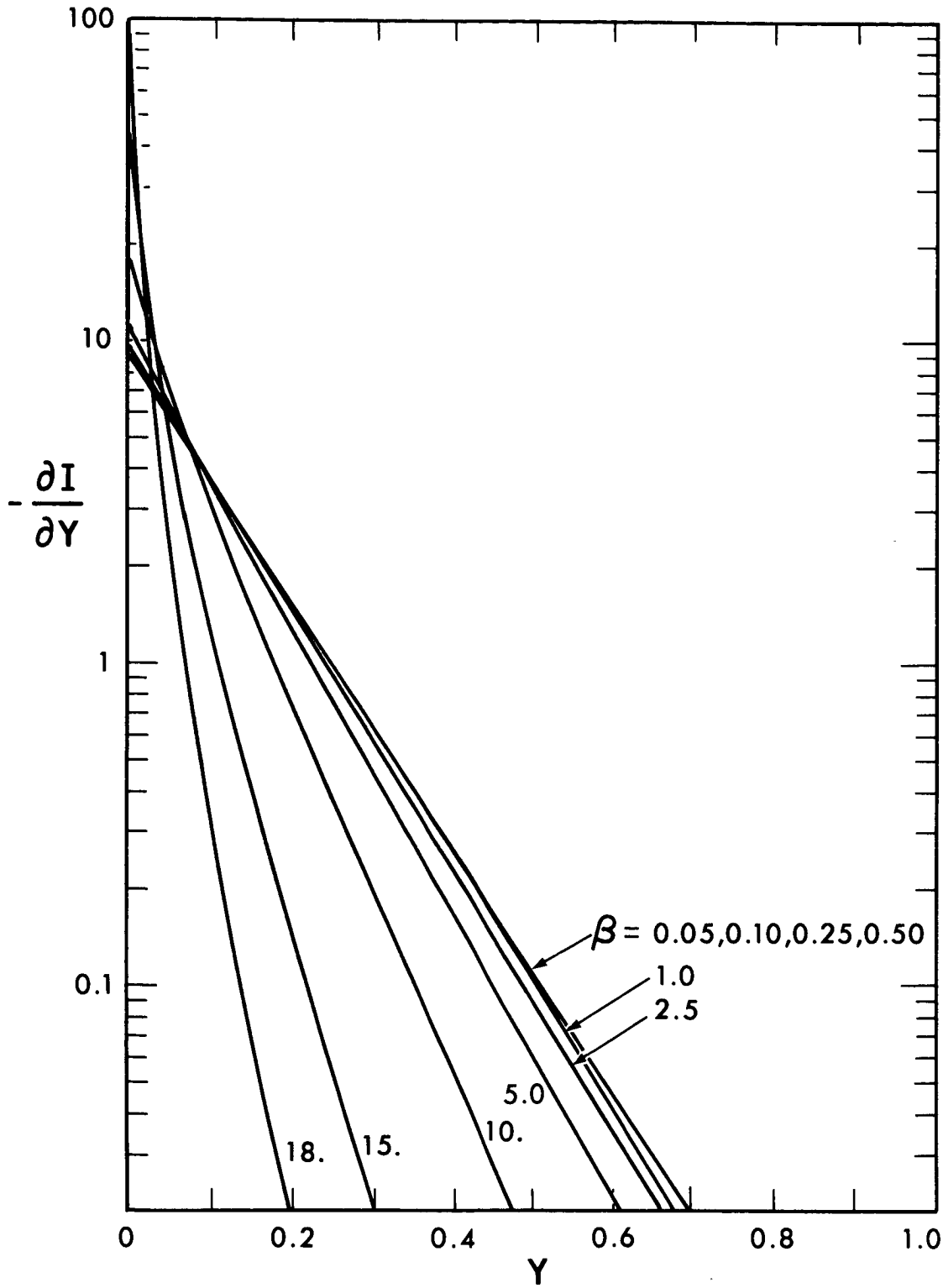

Figure 4. Current Distribution at Steady State for Cadmium Anode (5N KOH). $\xi = 50.$, $\Delta = 0.1$. (Redox Overpotential)

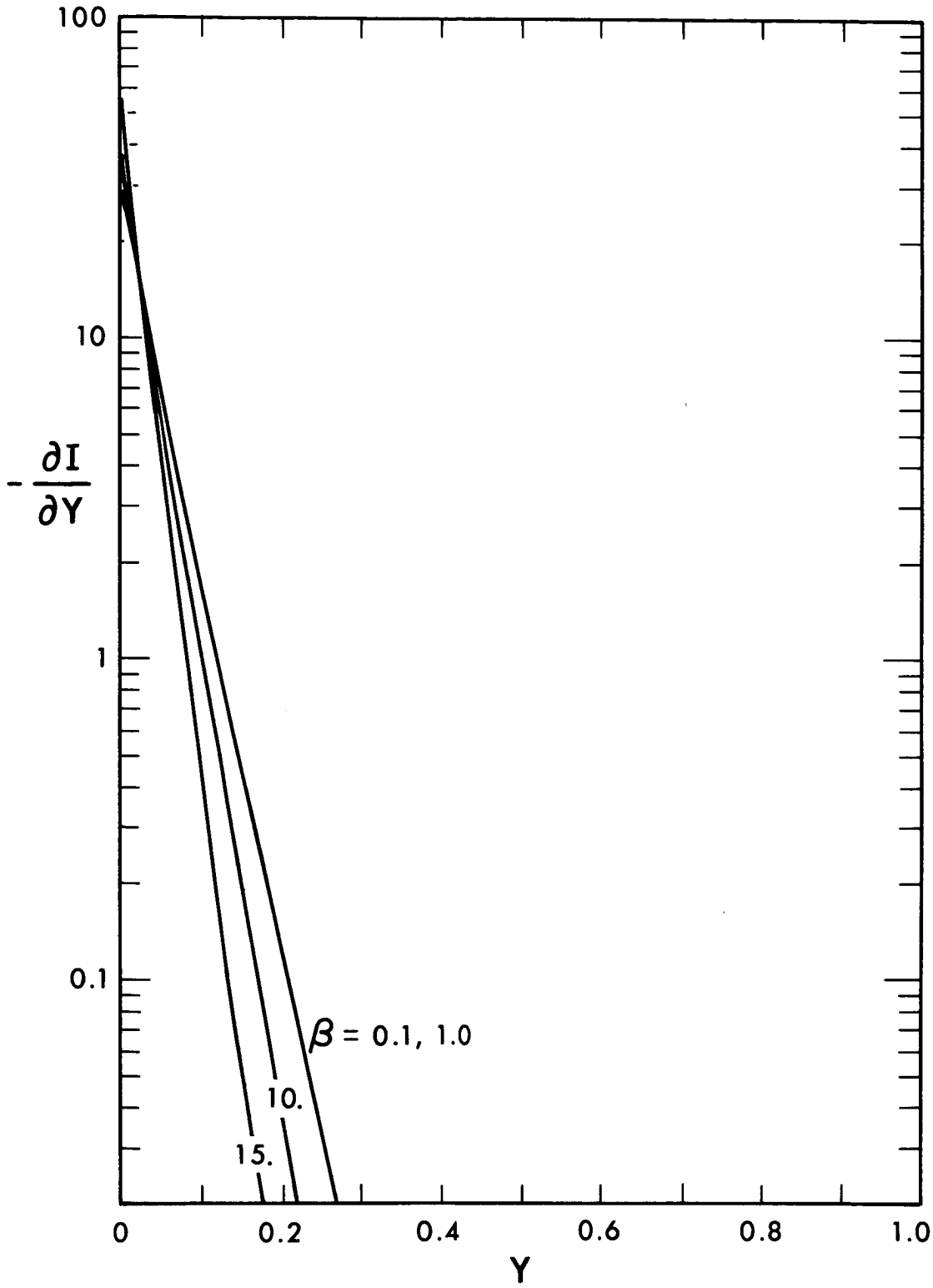

Figure 5. Current Distribution at Steady State for Cadmium Anode (5N KOH). ξ = 500., Δ = 0.1. (Redox Overpotential)

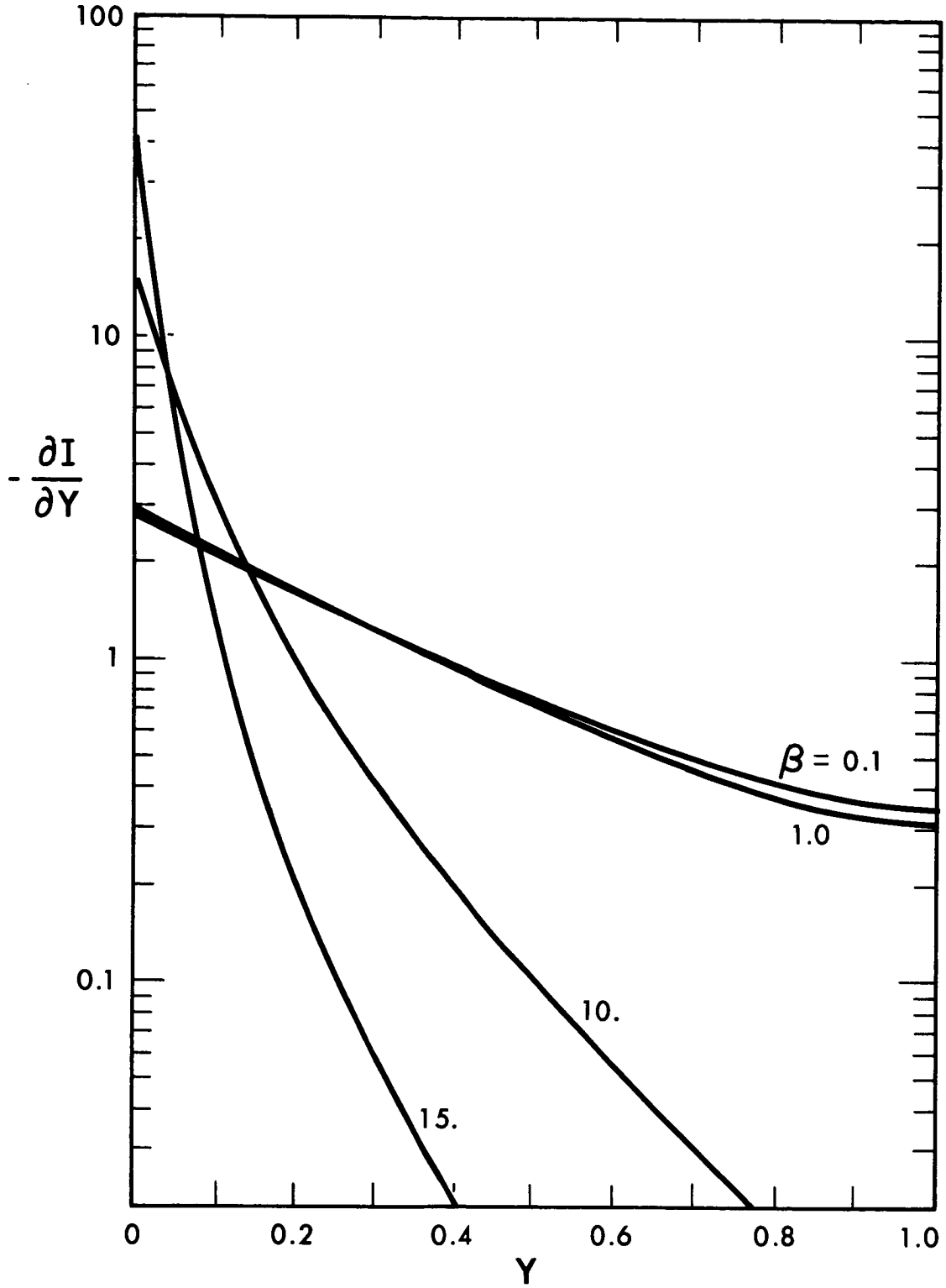

Figure 6. Current Distribution at Steady State for Cadmium Anode (5N KOH). $\xi = 5.$, $\Delta = 0.1$. (Redox Overpotential)

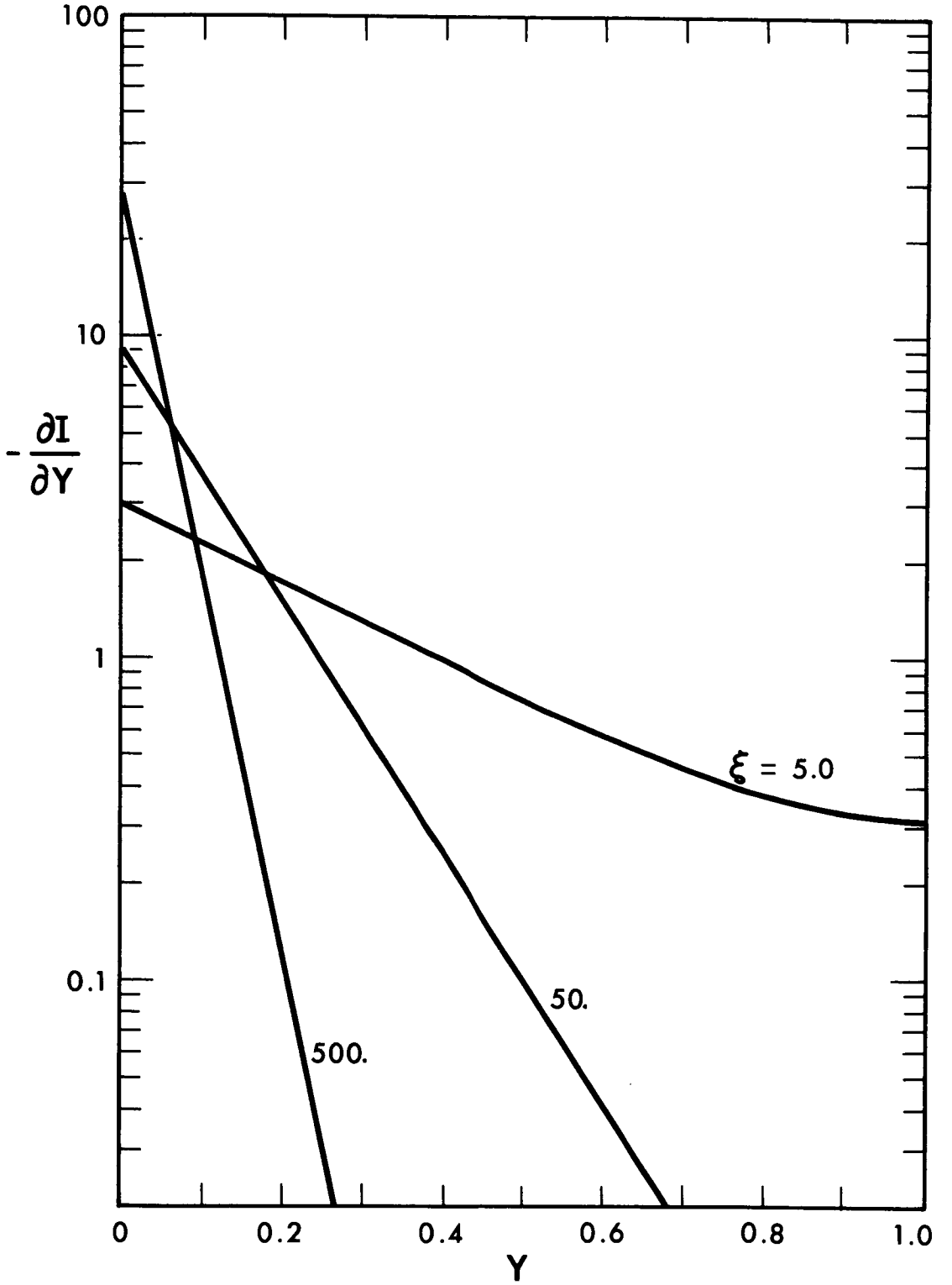

Figure 7. Current Distribution at Steady State for Cadmium Anode (5N KOH). $\Delta = 0.1$, $\beta = 1.0$. (Redox Overpotential)

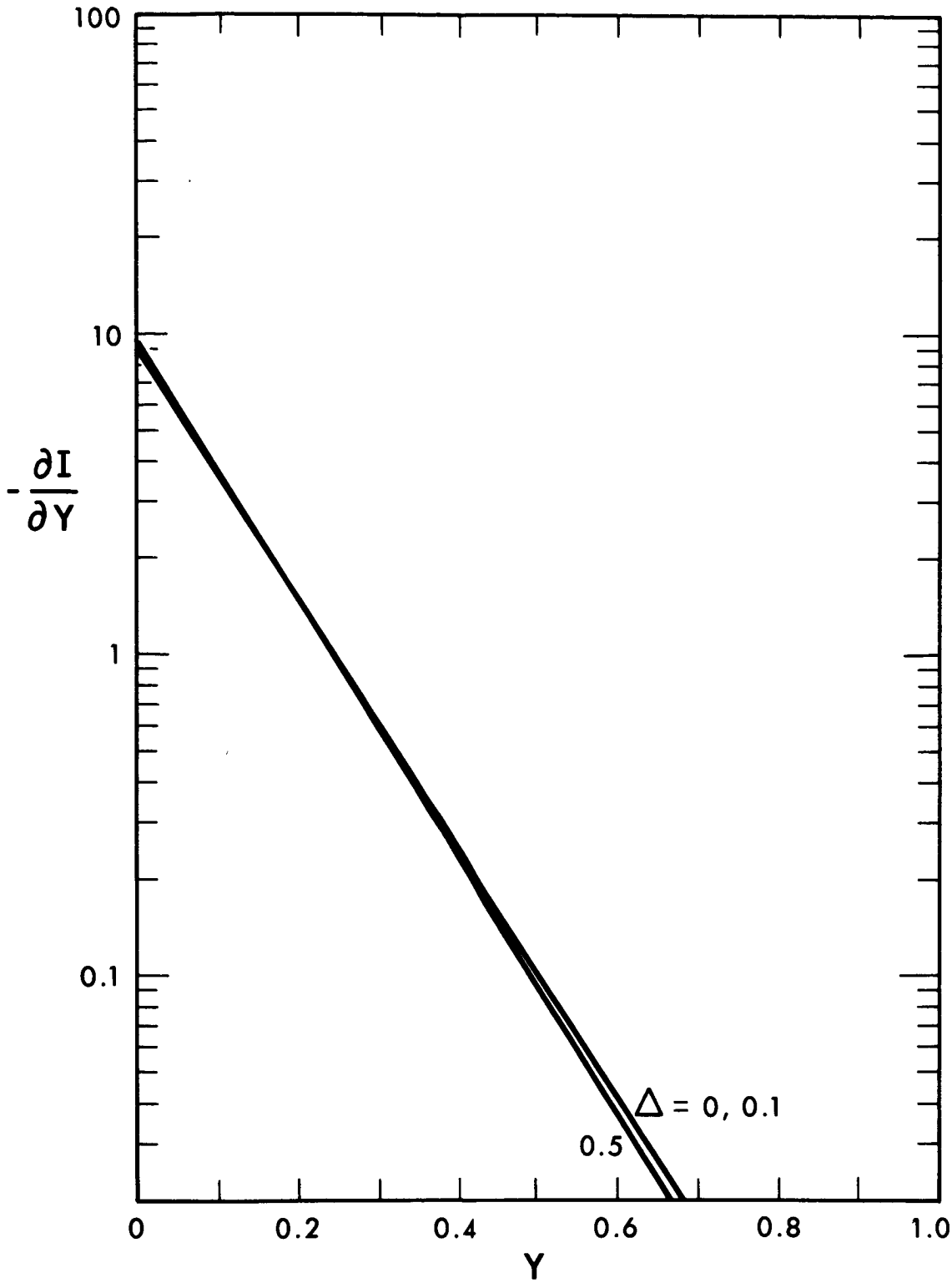

Figure 8. Current Distribution at Steady State for Cadmium Anode (5N KOH). $\xi = 50.$, $\beta = 1.0.$ (Redox Overpotential)

of species at the electrode surface, and, since for a binary electrolyte such as KOH the concentrations of anions and cations are always equal (or in fixed ratio), this effect appears as a change in the "effective" value of β at the electrode surface. Large concentration changes are encountered only as limiting superficial current density is approached. At this juncture, which corresponds here to a value $\beta=2/\Delta$, transfer current becomes concentrated in the very first layer of the electrode and overpotential increases without limit.

The behavior of total electrode overpotential, Φ_o, exclusive of the resistive potential drop across any effective transport layer present, is presented in Figure 9 as a function of current drain. For convenience, a logarithmic representation has been chosen; in this way the behavior over a wide range of conditions may be examined. For all conditions of ξ and Δ, up to quite significant superficial current densities, a linear relationship (unit slope on log plot) exists between Φ_o and β. This linear behavior is characterized by a zero intercept and thus a form

$$\Phi_o = b\ \beta \qquad (4.2\text{-}11)$$

where the slope b is a function of ξ and Δ. Values of these limiting slopes are given in Table III. At higher values of β (say above 1 to 5) this linear relation ceases to hold and the Φ_o vs. β slope increases rapidly. The overpotentials are, at equivalent values of β, higher for low exchange

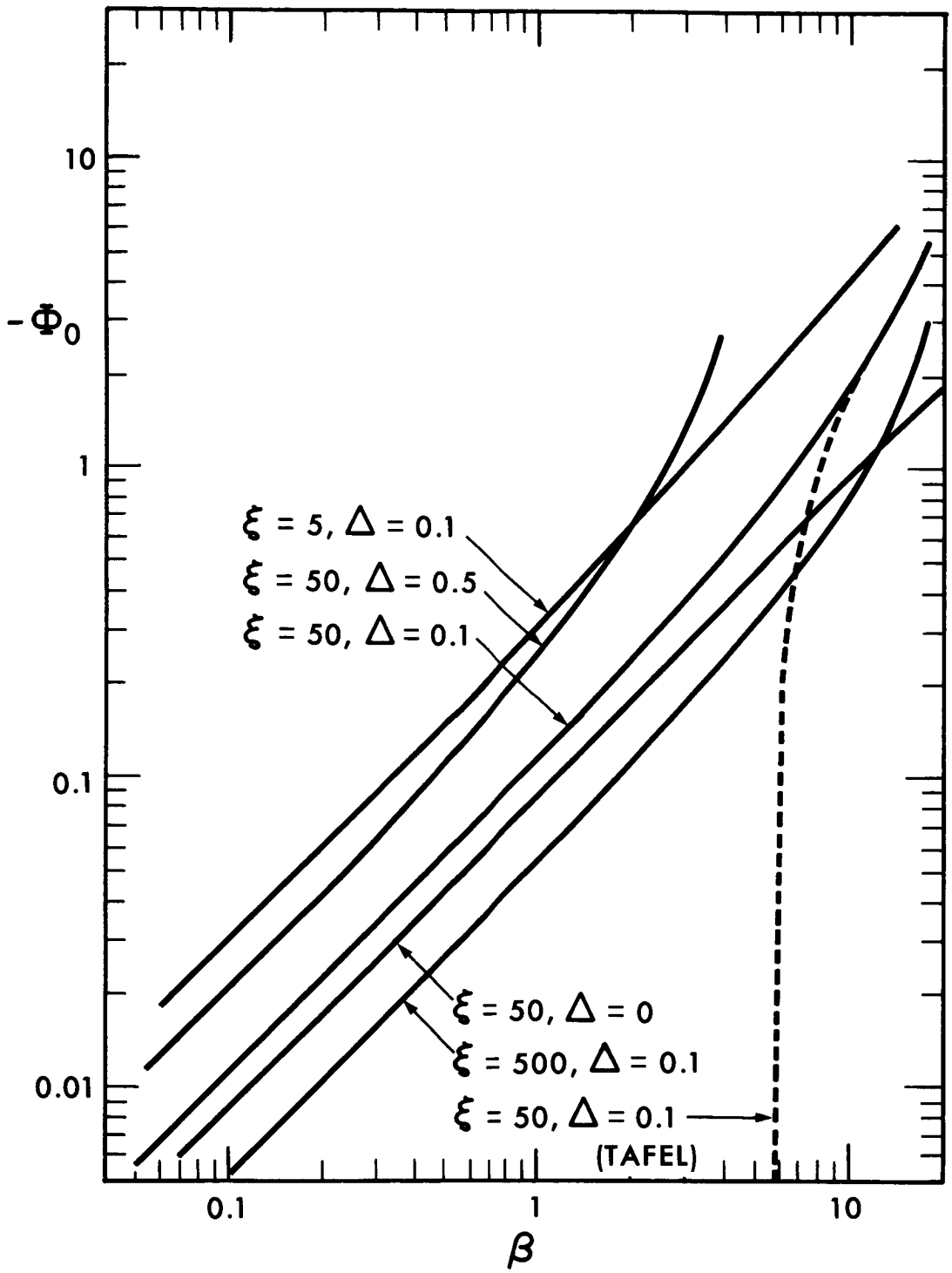

Figure 9. Electrode Overpotential at Steady State for Cadmium Anode (5N KOH).
(Redox Overpotential except for dashed curve)

current densities and high transfer layer thicknesses, as would be expected from elementary considerations. For a vanishing transfer layer thickness, that is in absence of any reduction of electrolyte concentration at the electrode face, the linear behavior persists even under conditions where local transfer current densities in the front section of the electrode (where essentially all reaction occurs) are high compared to the exchange current density.

TABLE III

Limiting Overpotential Slopes
Cadmium Anode in 5N KOH

ξ	Δ	b
5.	0.10	- 0.303
50.	0.00	- 0.087
↓	0.10	- 0.112
↓	0.50	- 0.212
500.	0.10	- 0.053

It is apparent in examining the distribution of transfer current in the one dimensional model of the cadmium anode, in Figures 4, 5, and 6 or in Appendix V, that the portion of the electrode contributing significantly to the current being drawn may be very small indeed. Since this part of the electrode is that closest to the electrode surface (and the counterelectrode), this behavior can be characterized by a "depth of penetration", Y_{90}, of the electrode reaction into the porous matrix, taken as the value of Y at which the current in the electrolyte, I, has fallen to 10% of its value at the electrode face (where I=1.0). This distance,

then, is the depth of the region near the face of the electrode in which 90% of the electrode reaction occurs. Y_{90} is depicted as a function of β in Figure 10. Here curves are given for ξ=5, 50, and 500 at Δ=0.1 and the effect of Δ is illustrated for ξ=50. The depth of penetration has a limiting value at low β which decreases sharply with increasing ξ and is independent of Δ. As β increases the penetration decreases abruptly above β=1, becoming zero at the value of β corresponding to limiting superficial current density for the transfer layer thickness, Δ, under consideration. For high exchange current densities the reaction may be confined to a narrow zone (<0.02 cm) near the face of the electrode for all values of β.

This behavior has been predicted and discussed by many investigators (see Section 1.2) but the influence of the effective transfer layer exterior to the electrode has not been cited. As exchange current densities should be high for favorable overpotential behavior, and in any event are not subject to control, the reduction of transport resistance exterior to the electrode assumes considerable importance in effective utilization of the porous electrode at high current densities. This can also be seen from the overpotential curves of Figure 9.

Transient behavior has been analyzed only for certain cases selected from those examined at steady state and listed in Table I, for reasons of the computational time involved. These are indicated in the aforementioned table by the symbol

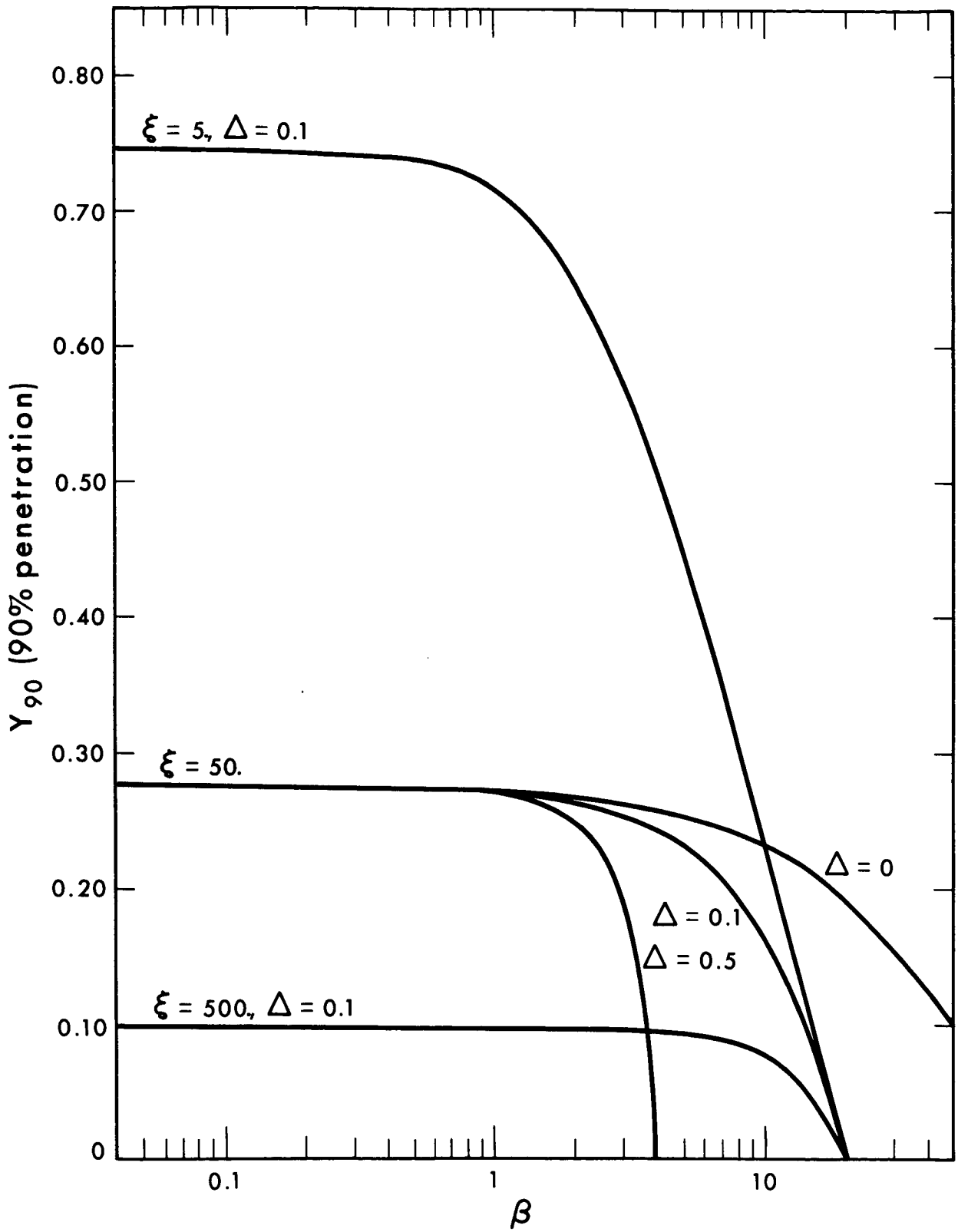

Figure 10. Depth of Penetration of Reaction in Electrode for Cadmium Anode (5N KOH). (Redox Overpotential)

(T) following the case number. Calculated transient operation of the cadmium electrode in each of these instances is presented as plots of transfer current densities, concentration, and electrode overpotential against elapsed time in Appendix VI. The number of transient cases computed is sufficient to illustrate the significant aspects of the non-steady state behavior of the system and the influence of β and ξ upon this behavior.

Representative of the transient operation of this system is the pattern shown in Figure 11 for $\xi=50$, $\Delta=0.1$, and $\beta=10$. In this graph $-\frac{\partial I}{\partial Y}$ and C_1 at Y=0 and 0.1, and Φ_o are given as functions of the dimensionless time, τ, elapsed since completion of the circuit. In its evaluation the conversion of τ to time in seconds according to $t=500\tau$ yields a better insight into the significance of transient effects. In Figure 12 current distribution over the front half of the electrode is shown at several elapsed times, for the same case as in Figure 11. Here the nature of the transient effects can be clearly seen. The initial current densities, except at the very face of the electrode, are depressed in the locations where they are large, due to depletion of reactant. Current densities toward the rear of the electrode, initially small, change little until reactant is consumed at these positions and then decrease. During much of the transient process, the distribution of current is considerably flattened over the rear portion of the electrode.

The transient processes take place over a characteristic

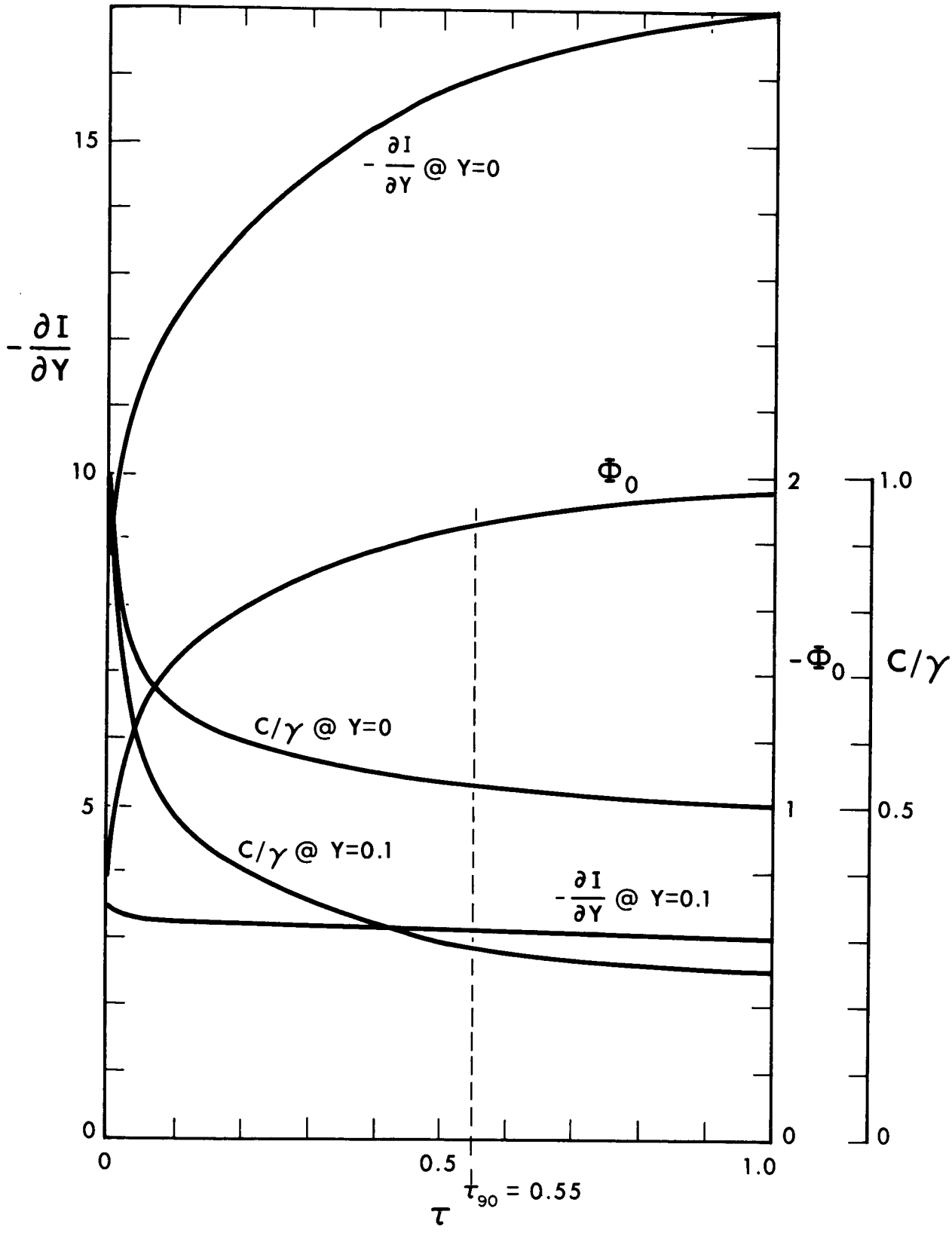

Figure 11. Transient Behavior of Cadmium Anode (5N KOH). $\xi = 50.$, $\Delta = 0.1$, $\beta = 10.$ (Redox Overpotential)

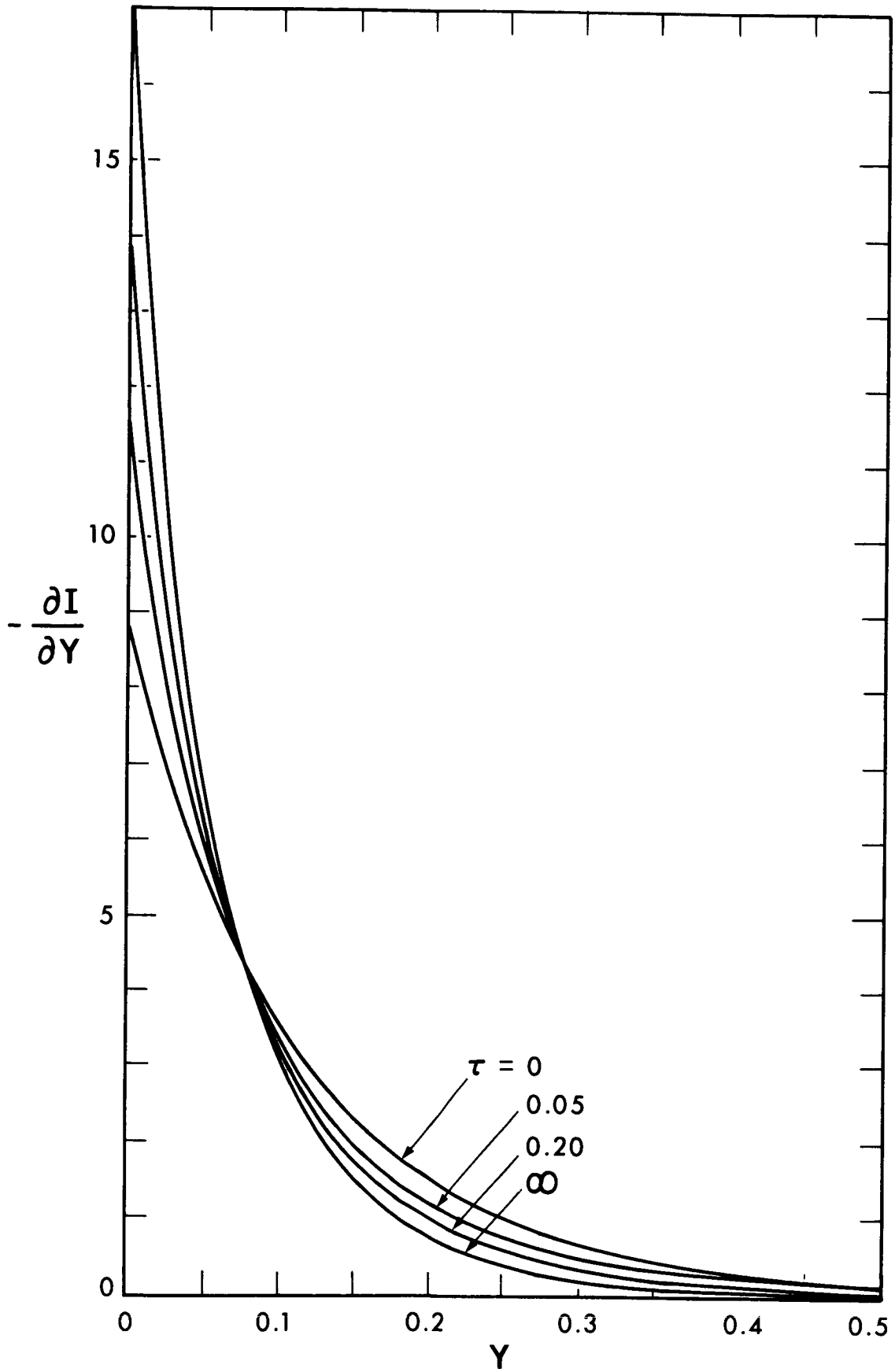

Figure 12. Current Distribution at Several Elapsed Times for Cadmium Anode (5N KOH). ξ = 50., Δ = 0.1, β = 10. (Redox Overpotential)

time, here taken as the time over which the change in overpotential between initial to steady state values is 90% completed, which remains at approximately $\tau_{90}=0.6$ over a wide range of conditions. This corresponds to a transient occurring over a period of 300 seconds.

Use of the Tafel type overpotential expression instead of the redox expression leads to markedly different steady state and transient behavior. Results of calculations of the cases enumerated in Table II are given in Appendix V for steady state and in Appendix VI for transient analyses. Behavior for $\xi=50$, $\Delta=0.1$, is summarized in the steady state in Figure 13 and as a transient time plot for $\beta=10$ in Figure 14. These figures are of the same format as those used for the cases calculated with a redox overpotential expression. The marked influence of the difference in overpotential relationship is apparent in comparing Figures 4 and 13 or 11 and 14. This effect will be discussed in Chapter 5. The electrode overpotential for the Tafel case is depicted by a dashed curve in Figure 9, where it can be seen to approach the behavior of the corresponding redox case at very high current drain.

It is not intended that the results presented in this section should be considered to represent the behavior of any actual cadmium anode. Rather, they represent an illustration of the application of the one dimensional porous electrode model, together with a description of the type of behavior to be expected in such an electrode and the

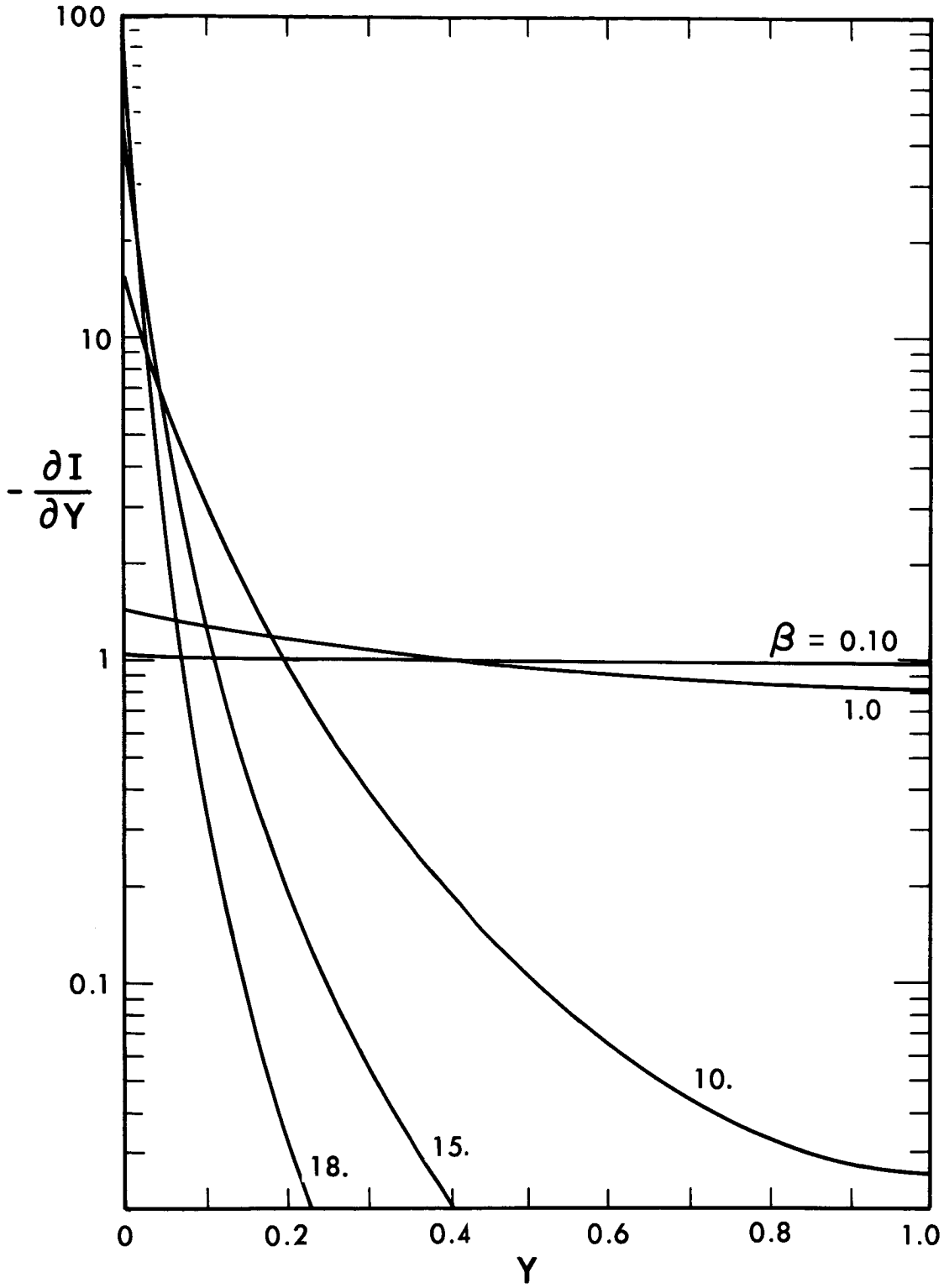

Figure 13. Current Distribution at Steady State for Cadmium Anode (5N KOH). ξ = 50., Δ = 0.1 (Tafel Overpotential)

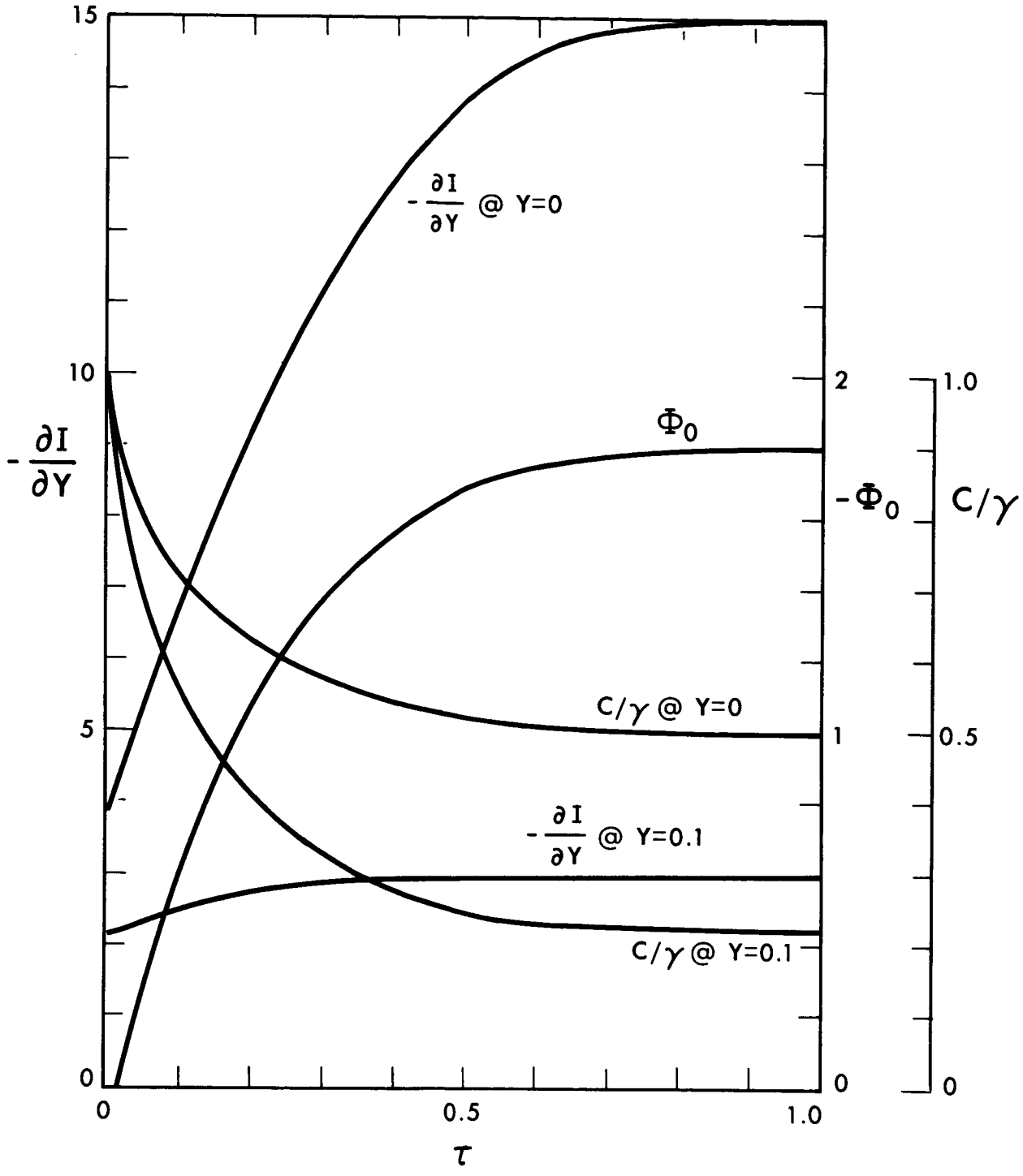

Figure 14. Transient Behavior of Cadmium Anode (5N KOH). $\xi = 50.$, $\Delta = 0.1$, $\beta = 10.$ (Tafel Overpotential)

qualitative effect of system parameters upon this behavior. An accurate overpotential expression would be needed before any quantitative analysis could be undertaken. Moreover, the discharge of a cadmium anode actually involves significant changes in the properties of the matrix, associated with conversion of the solid reactant, counter to the assumptions of this model. Other factors, such as the solubility of $Cd(OH)_2$ in the electrolyte further complicate the situation. The present treatment, however, demonstrates the importance deriving accurate characterization of kinetic and transport phenomena for the system if performance prediction is to be successful. It also indicates the importance of consideration of operation in the mass transport transient condition.

4.3 Analysis of Ferri-Ferrocyanide Cathode

A reaction useful for possible experimental investigation of current distribution in porous electrodes is the ferricyanide-ferrocyanide redox couple, conveniently in NaOH solution. This system has several desirable properties: it is stable when light and oxygen are excluded; the reactant and product are both dissolved species in the electrolyte, allowing reaction to proceed with no significant alteration of the electrode matrix; the reaction does not involve water; the reaction may be run cathodically to appreciable overpotentials without hydrogen evolution; the electrolyte and reaction are compatible with nickel electrodes; the ionic strength of the solution remains relatively constant; and, the system has been extensively studied and many of

its properties are well established. For any practicable current distribution measurement this couple has, however, the severe limitation of a highly nonuniform current distribution at steady state in porous media. This will be discussed later in this section. The ferri-ferrocyanide reaction in NaOH is also representative of systems with excess inert electrolyte; thus analysis of porous electrode using this reaction will present a contrast to the binary system treated in Section 4.2.

If the cathode is selected for analysis, the reaction occurring is

$$Fe(CN)_6^{-3} - Fe(CN)_6^{-4} \longrightarrow - e^- . \qquad (4.3\text{-}1)$$

In a 2N NaOH solution* the species present in the electrolyte are $Fe(CN)_6^{-3}$, $Fe(CN)_6^{-4}$, Na^+, and OH^-. These will be designated, in the order mentioned, by the indices 1 through 4, giving

$$z_1 = -3;\ z_2 = -4;\ z_3 = +1;\ z_4 = -1$$
$$\nu_1 = +1;\ \nu_2 = -1;\ \nu_3 = \nu_4 = 0 \qquad (4.3\text{-}2)$$
$$c_4^o = 2 \times 10^{-3} \text{gmol/cm}^3;\ c_3^o = 2 \times 10^{-3} + 3c_1^o + 4c_2^o \text{ gmol/cm}^3$$

In 2N NaOH, diffusion coefficients for the Na^+ and OH^- ions have not been established as known functions of concentration, as was also the case for KOH as mentioned in the previous section. Using molecular diffusion data from International Critical Tables[36], converted from 15°C to 25°C

---

* This concentration is selected on the basis of availability of data and suitability for suppression of hydrogen evolution.

by considering $D\mu/T$ constant, the value $D_{NaOH}=1.6 \times 10^{-5}$ cm^2/sec is found for 2N NaOH solutions. This, taken with the observation that at concentrations above 1 N, the anion transference number is approximately 0.8 (see Landolt-Bornstein[37]), gives $D_4=4.1 \times 10^{-5}$ cm^2/sec. The value will, however, be decreased in the presence of other components in the electrolyte, as noted by Vinograd and McBain[38] among others. Based upon quite subjective considerations the approximation

$$D_4F = 3.2 \text{ cm}^2 \text{ coul/gmol sec} \qquad (4.3\text{-}3)$$

has been selected for the diffusion coefficient-Faraday product for OH^-. No claim is made for the accuracy of this choice, although it certainly is a sufficiently good approximation for this example. The corresponding value for Na^+ is then

$$D_3F = 0.8 \text{ cm}^2 \text{ coul/gmol sec.} \qquad (4.3\text{-}4)$$

From the data of Eisenberg, Tobias, and Wilke, the diffusion coefficients of $Fe(CN)_6^{-3}$ and $Fe(CN)_6^{-4}$ in 2N NaOH at 25°C are 0.527×10^{-5} and 0.418×10^{-5} cm^2/sec, respectively.[39] The approximation

$$D_1F = D_2F = 0.5 \text{ cm}^2 \text{ coul/gmol sec} \qquad (4.3\text{-}5)$$

is appropriate, considering the uncertainty of the other transport parameter data.

The electrode kinetics of the ferri-ferrocyanide couple have been reported for many conditions of reaction. The data of Petrocelli and Paolucci, measured for 0.4M $Fe(CN)_6^{-3}$ and 0.4M $Fe(CN)_6^{-4}$ in 2N NaOH on bright platinum seem

appropriate for this analysis.[40] According to these authors, a redox type overpotential expression with

$$\alpha = 0.5$$
$$i_o = 0.025 \text{ amp/cm}^2 \qquad (4.3\text{-}6)$$

characterizes the reaction.

The electrode structure parameters for this system will depend upon the nature of experimental apparatus that might be chosen. If fissures or other artificially constructed idealized pores are considered, practical values might be*

$$a = 200 \text{ cm}^2/\text{cm}^3$$
$$\ell = 0.33 \text{ cm}. \qquad (4.3\text{-}7)$$

No porosity conversion need be considered, the fluxes and current densities referred to effective pore cross section being appropriate in the context of this example. For this analysis, equivalent transfer layer thickness will be taken as zero except for a few cases when δ=0.03 cm was investigated for comparison.

In analyzing behavior under a variety of operating conditions the following values of ferro and ferricyanide concentration and of total current density have been chosen. In all cases equal ferro and ferricyanide concentrations were used.

$$c_1^o,\ c_2^o = 0.02,\ 0.10,\ 0.20 \text{ M}$$
$$i^* = 0.001,\ 0.003,\ 0.01,\ 0.03,\ 0.10,\ 0.30 \text{ amp/cm}^2 \qquad (4.3\text{-}8)$$

---

* Because of the high exchange current density, a and ℓ should be as small as permits electrode construction and current distribution measurements.

These values represent quite well the range of operation of such a system that would be of experimental interest.

Corresponding to the values cited in the preceding paragraphs, the input parameters characteristic of this system are:

$$\begin{aligned} N &= 4 \\ z_1 &= -3;\ z_2 = -4;\ z_3 = +1;\ z_4 = -1 \\ \nu_1 &= +1;\ \nu_2 = -1;\ \nu_3 = 0;\ \nu_4 = 0 \\ \pi_1 &= 0.156;\ \pi_2 = 0.156;\ \pi_3 = 0.250 \\ \alpha &= 0.5 \\ \xi &= 80. \end{aligned} \qquad (4.3\text{-}9)$$

The operating conditions listed are represented by the parameters:

$$\begin{aligned} \Delta &= 0,\ 0.1 \\ \gamma_1 = \gamma_2 &= 0.01,\ 0.05,\ 0.10\ (\gamma_3 = 1.07,\ 1.35,\ 1.70) \\ \beta &= 0.05,\ 0.15,\ 0.50,\ 1.50,\ 5.0,\ 15.0. \end{aligned} \qquad (4.3\text{-}10)$$

As in the analysis of the cadmium anode, not all possible combinations of the operating parameters were subjected to analysis. The cases calculated are listed in Table IV, the selection being made to investigate the effects of variations of β, γ, and Δ, in each case with other operating parameters held constant.

The behavior of the ferri-ferrocyanide cathode as calculated for the steady state is detailed by the curves contained in Appendix VII for each case considered. The curves are as described for Appendix V in Section 4.2. In their interpretation the dimensionless variables involved may be converted

TABLE IV

Cases of Operation Considered for the Ferri-Ferrocyanide Cathode in 2N NaOH (Overpotential per Petrocelli and Paolucci[40])

Case Number	Δ	γ_1, γ_2	β
B1	0.0	0.05,0.05	0.05
B2	↓	↓	0.15
B3(T)	↓	↓	0.50
B4	↓	↓	1.5
B5(T)	↓	↓	5.0
B6	↓	↓	15.
B7	↓	0.01,0.01	0.05
B8(T)	↓	↓	0.50
B9	↓	↓	5.0
B10	↓	0.10,0.10	0.05
B11(T)	↓	↓	0.50
B12	↓	↓	5.0
B13	0.1	0.05,0.05	0.015
B14	↓	↓	0.05

to dimensional form as follows: pore current density (inlet) is 0.02β (amp/cm^2); transfer current density is $3 \times 10^{-4}\beta \frac{\partial I}{\partial Y}$ (amp/cm^2 pore wall); distances are 0.33Y (cm); overpotential is $0.0256\ \Phi$ (volts).

The performance of the electrode at steady state is summarized in Figures 15 through 17. The influence of current drain, β, on transfer current distribution for $\gamma_1=\gamma_2=0.05$ and $\Delta=0$ is illustrated in Figure 15. As was the case with the cadmium anode, a limiting distribution is reached at low values of β which is not affected by further reductions in β. In contrast with the cadmium anode case, however, the high degree of nonuniformity of current distribution, even at this limiting condition, should be noted. This phenomenon has required that only one-tenth of the electrode be represented on the distance axis of Figures 15 and 16, and that the $-\frac{\partial I}{\partial Y}$ axis be shifted up an order of magnitude from the scale used in Section 4.2.

This nonuniformity of current distribution is the result of the combined effect of the high exchange current density (or parameter ξ) for the system and the presence of the excess inert electrolyte, NaOH. The latter influence is demonstrated by observing the changes in current distribution occasioned by altering the bulk concentrations of $Fe(CN)_6^{-3}$ and $Fe(CN)_6^{-4}$ (simultaneously) as shown in Figure 16. This action is equivalent, with appropriate adjustment of β and ξ, to changing the concentration of NaOH. The distribution of transfer current becomes more uniform as γ_1 and γ_2 increase but remains highly nonuniform for any case where the system

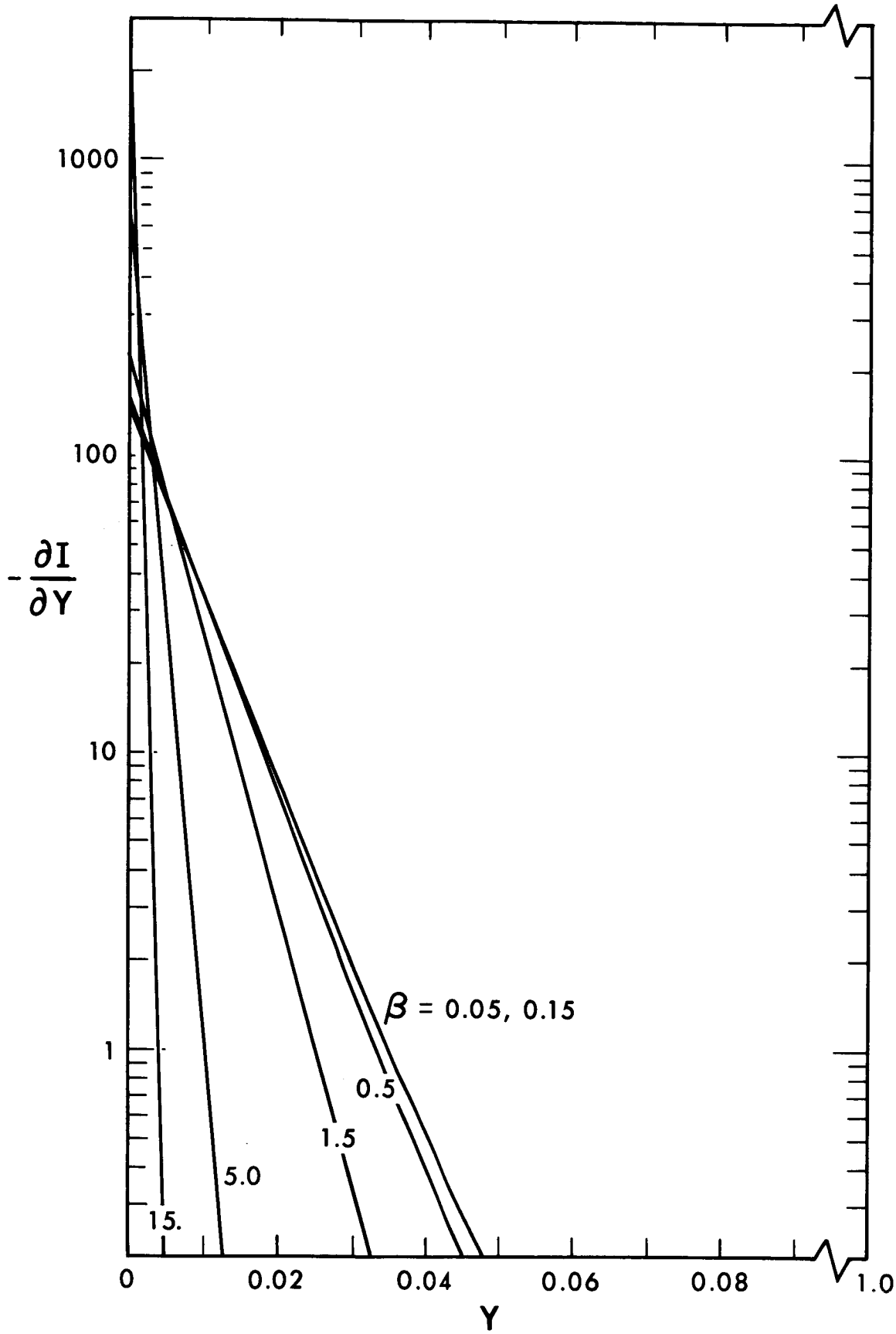

Figure 15. Current Distribution at Steady State for $Fe(CN)_6^{-3}$ - $Fe(CN)_6^{-4}$ Cathode (2N NaOH). ξ = 80., $\gamma_1 = \gamma_2$ = 0.05, Δ = 0.

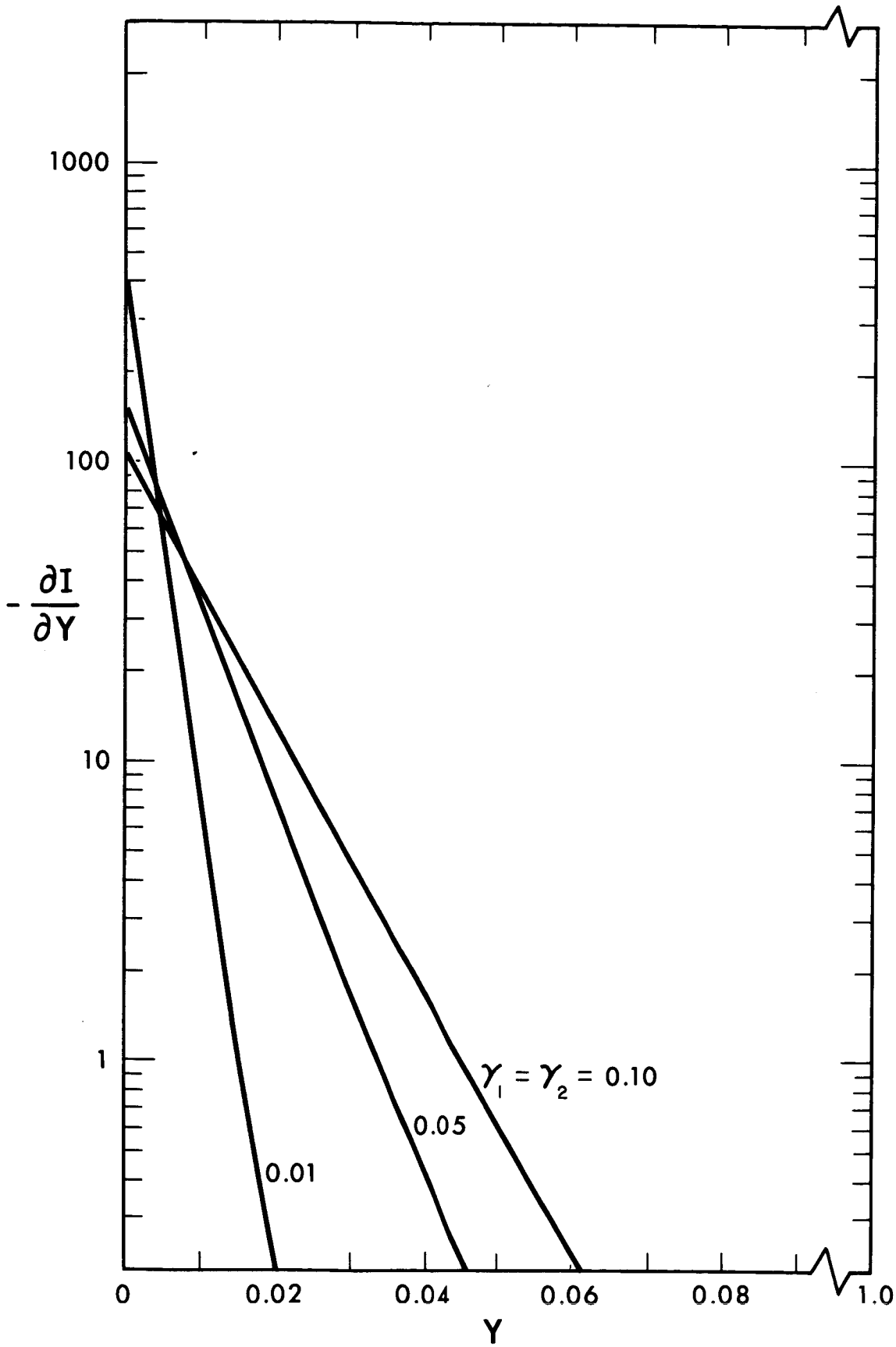

Figure 16. Current Distribution at Steady State for $Fe(CN)_6^{-3}$ - $Fe(CN)_6^{-4}$ Cathode (2N NaOH). $\xi = 80.$, $\Delta = 0$, $\beta = 0.5$.

can even remotely be considered to contain "supporting electrolyte".

Electrode overpotential is represented as a function of β in Figure 17. Again, as in the case of the cadmium anode, the relationship is linear up to reasonably large values of β (~2), the slope (position on the logarithmic plot used) being dependent on the values of γ_1 and γ_2. Since these curves represent the case for $\Delta=0$, no limiting current behavior occurs; rather, the overpotentials deviate negatively from the linear behavior as β becomes large and approaching ultimately a proportionality to $\ln\beta$. In no case of steady state operation for the ferri-ferrocyanide cathode is there any significant penetration of the reaction into the depth of the electrode.

The behavior of the system under transient conditions was analyzed for several of the cases previously enumerated, these being designated by a "(T)" in Table IV. The calculated results for these cases are contained in the graphs in Appendix VIII. Typical of the transient performance of the electrode is that for $\gamma_1 = \gamma_2 = 0.05$, $\Delta=0$, $\beta=0.5$, which is represented by the time plots in Figure 18. Here the initially rapid rise in overpotential, and in transfer current density at the front of the electrode, is apparent; the appropriate time conversion is $t = 3.4 \times 10^3 \tau$ sec. The change in current distribution with time is shown in another way by the curves of Figure 19, representing transfer current as a function of position at various elapsed times. The corresponding

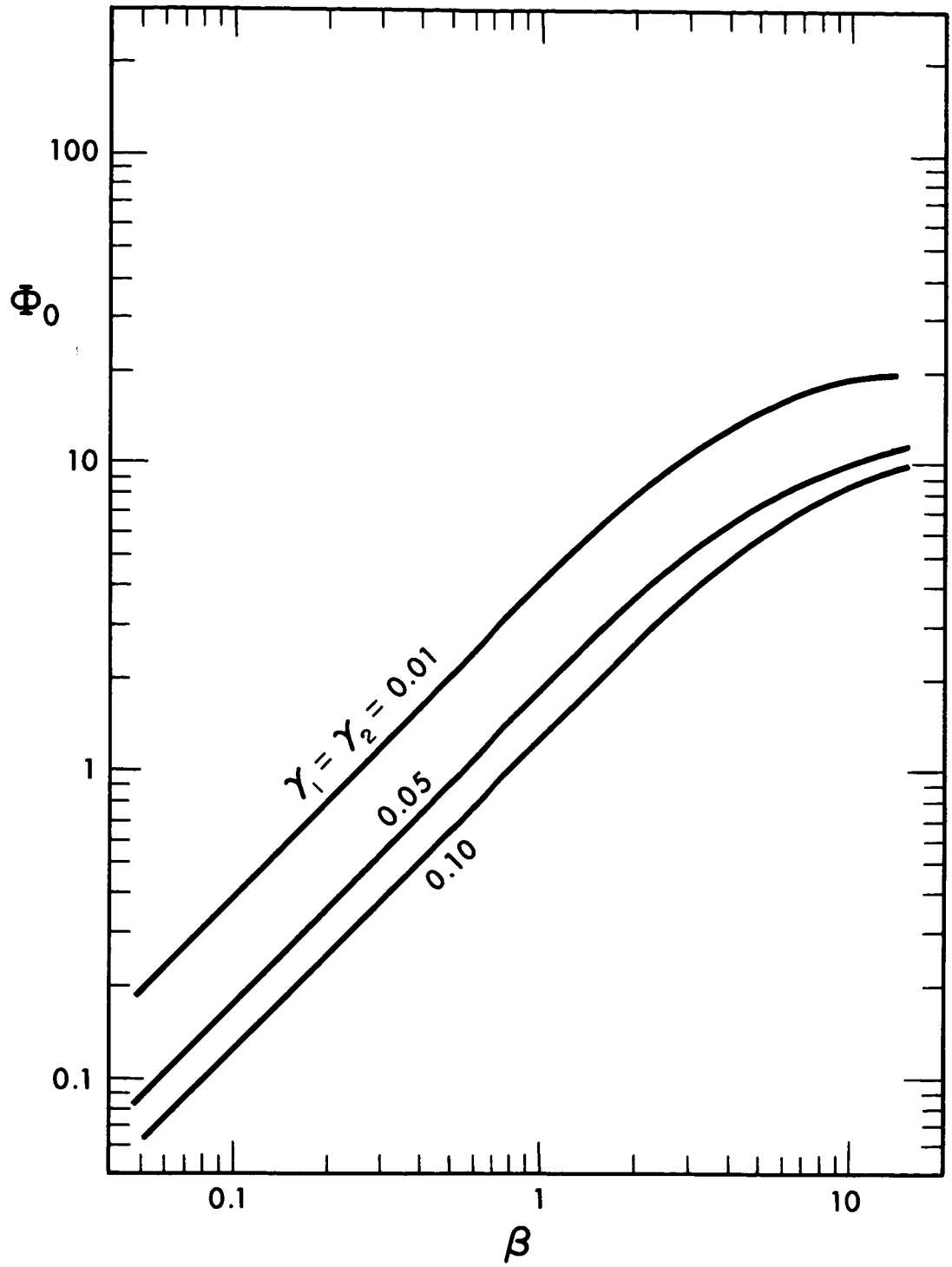

Figure 17. Electrode Overpotential at Steady State for $Fe(CN)_6^{-3}$ - $Fe(CN)_6^{-4}$ Cathode (2N NaOH). ξ = 80., Δ = 0.

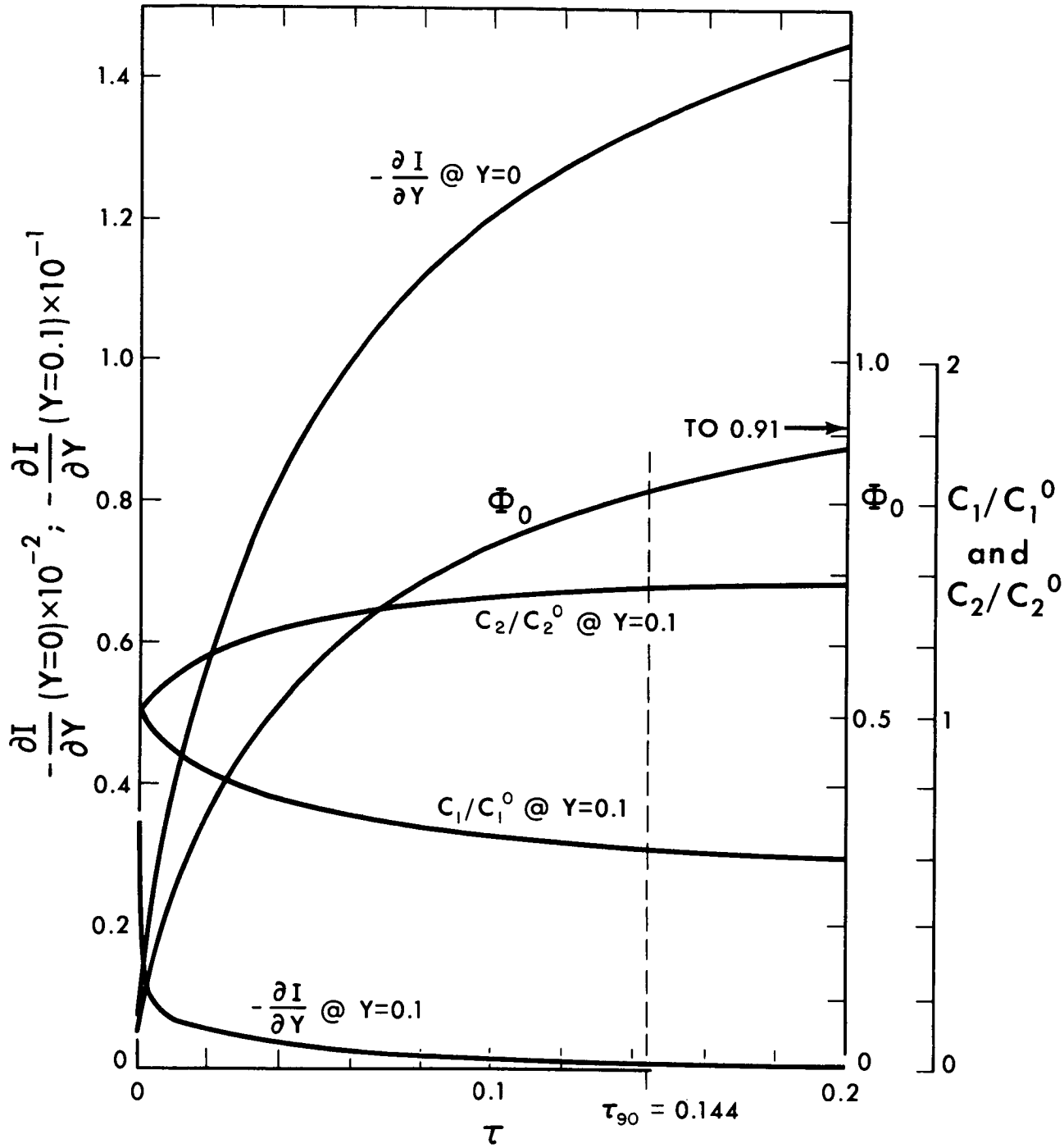

Figure 18. Transient Behavior of $Fe(CN)_6^{-3}$ - $Fe(CN)_6^{-4}$ Cathode (2N NaOH). ξ = 80., $\gamma_1 = \gamma_2$ = 0.05, Δ = 0, β = 0.5.

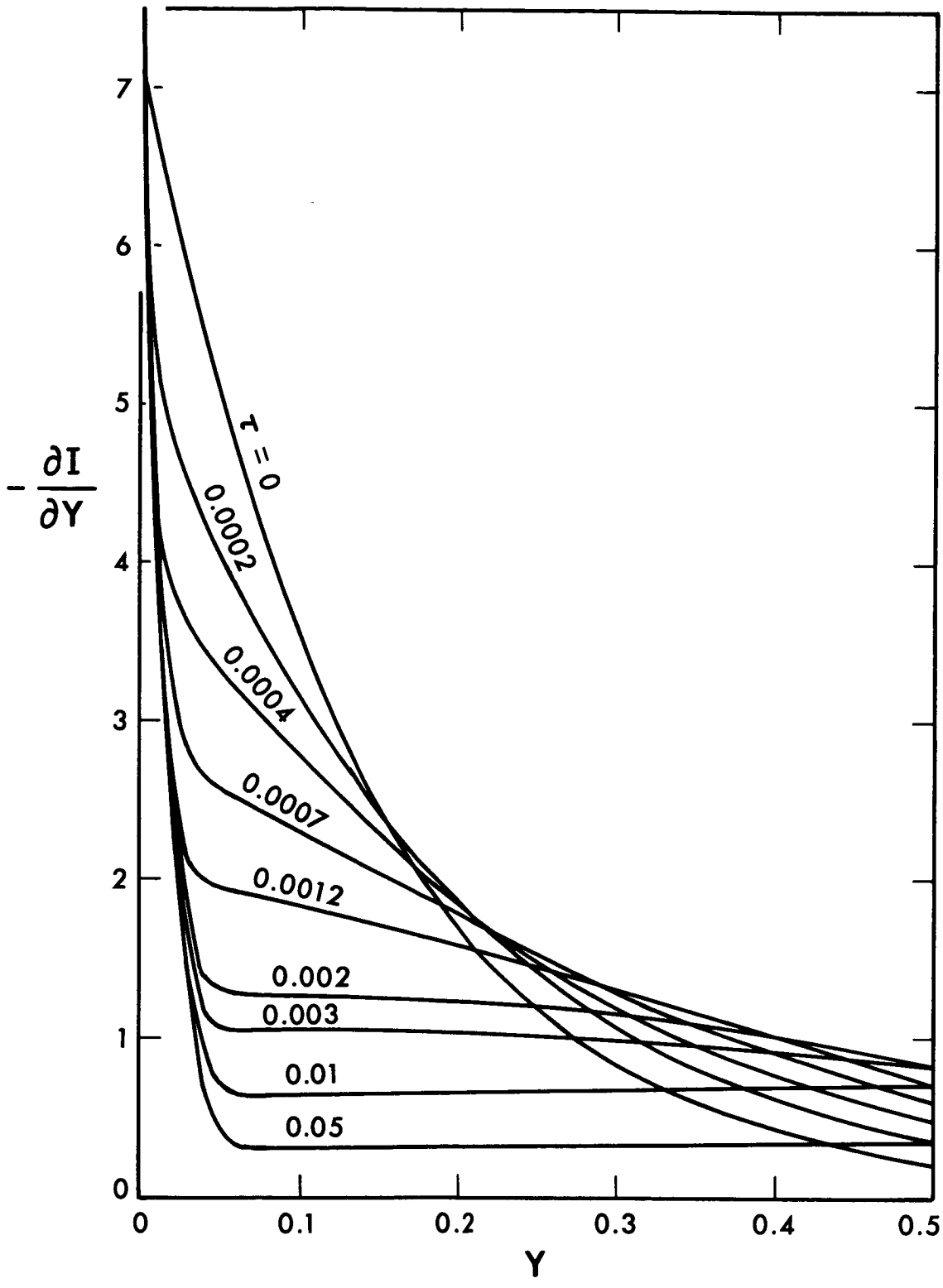

Figure 19. Current Distribution at Several Elapsed Times for $Fe(CN)_6^{-3}$ - $Fe(CN)_6^{-4}$ Cathode (2N NaOH). $\gamma = 80.$, $\gamma_1 = \gamma_2 = 0.05$, $\Delta = 0$, $\beta = 0.5$.

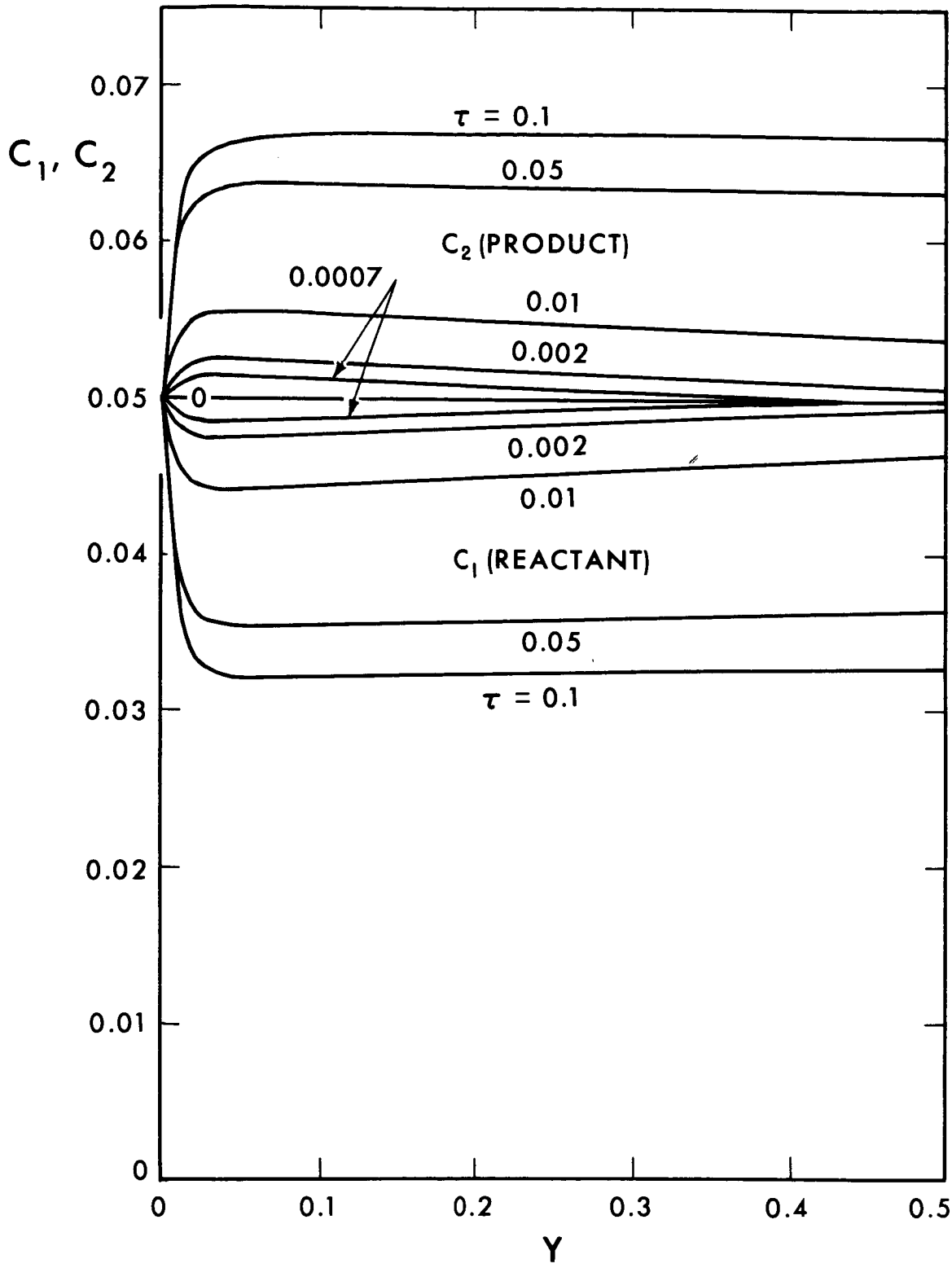

Figure 20. Concentration Distribution of Reactant and Product at Several Elapsed Times for $Fe(CN)_6^{-3}$ - $Fe(CN)_6^{-4}$ Cathode (2N NaOH). ξ = 80., $\gamma_1 = \gamma_2$ = 0.5, Δ = 0, β = 0.5.

distributions of reactant and product concentrations are given in Figure 20, where transient effects can be followed in the absence of the concentration changes at the face of the electrode imposed by an external transfer layer.

The initially moderately nonuniform current distribution is altered with passage of time by the rapid depression of reaction rate at areas sufficiently distant from the face of the electrode to create inhibitions of reactant supply (and product removal) and yet close enough to the face to have favorable potentials. Increasing reaction rates are noted for areas very close to the face, due to their favorable accessibility to bulk electrolyte, and by areas deep in the electrode, due to their store of as yet unused reactant. The effects of increasing overpotential and consumption of reactant (along with increasing product concentrations) tend to create a very uniform current distribution in all but the front part of the electrode during the transient. This uniform level decreases and its starting location moves deeper into the electrode as the concentrations approach their steady state values and diffusive transport becomes important at successively deeper points in the pores. The family of current distribution curves at increasing times generates an envelope, at least in the front portion of the electrode, which closely follows the steady state distribution which will ultimately be reached. Eventually the reaction occurs at significant rates over only the narrow portion of the electrode previously mentioned as active at steady state. The characteristic times

for this process, as defined in Section 4.2, vary over the range of τ_{90}=0.01 to 1, that is, 30 to 3000 sec.

This analysis of the behavior of the ferri-ferrocyanide cathode indicates its disadvantages for steady state investigations of current distribution in porous electrodes, together with its suitability for some transient measurements. The highly nonuniform current distributions at steady state would preclude any measurements of such distributions. However, the initial distributions are sufficiently uniform to permit design of meaningful transient experiments. The transient effects are marked and take place over periods of time well suited for experimental observation. For the case depicted in Figures 18 and 19 current distributions over a period of about 1 minute would fall in a range amenable to measurement. Other, perhaps more suitable, systems can be analyzed to obtain predictions of steady state behavior which may be experimentally verifiable. Lack of basic kinetic and transport data prevents this analysis in most cases, at the present time.

5. CONCLUSIONS

Certain general characteristics of the behavior of porous electrode systems, at least as far as they can be represented by the one dimensional model of this dissertation, will be summarized in the paragraphs that follow. These behavior patterns are significant. However, they do not constitute the principal results of this investigation, but, rather, only an illustration of the application of the end product of the study. What was sought was not data but a procedure that would be used to develop performance predictions for electrode systems of interest. Such a procedure has been developed and has been demonstrated on the calculation of behavior of realistic systems. The limitations of this work lie in the limitations on applicability of the procedure, as enumerated in Chapter 2. Its value lies in the ability of the procedure to analyze performance of a flooded porous electrode, given complete and accurate data for the transport and kinetic behavior of the system involved.

5.1 Behavior of Porous Electrode Systems at Steady State

The operation of a flooded non-flow, porous electrode at steady state is characterized by a moderately to highly non-uniform distribution of electrode reaction (transfer current) in depth in the electrode (see Figures 4, 5, 6 and 15). This nonuniformity profoundly affects the overpotential-current relationship for the electrode causing it to deviate widely

from the overpotential expression for the reacting system. At low currents the relationship is linear (but does not have the same slope as the local overpotential expression at vanishing transfer current). At higher currents it deviates toward lower overpotentials from this linear relation, except in the presence of external resistance to transport of the reactant to the electrode face (equivalent transfer layer), when, of course, it increases sharply as limiting current is approached. The general overpotential behavior of a porous electrode cannot be simply described nor easily determined from the overpotential expression for the reaction. Such approximations as that proposed by Ksenzhek* are applicable only under extremely restrictive conditions. Each case of interest must be separately analyzed. The nonuniform current distribution also reduces the portion of the electrode which significantly contributes to the electrode reaction (see Figure 10). In many electrodes only a very narrow portion adjacent to the face is effective.

The distribution of transfer current in an electrode becomes more nonuniform with increasing values of the parameters ξ and β, and decreasing values of γ for the reactant.

---

* Ksenzhek[16] proposed that the overpotential for a porous electrode, with a reaction represented by a Tafel type overpotential expression, was a linear function of the logarithm of current density with a slope equal one-half the Tafel slope for the reaction. To do this he assumed the potential was constant throughout the electrolyte in the pores.

Thus high values of exchange current density, specific electrode surface, or electrode depth, all of which lead to high ξ values, and high current drains, which give high β values, cause nonuniform distributions. These conditions, with the exception of large electrode depth, are commonly encountered (and desirable) in porous electrode applications. If β is decreased, that is, if lower current drains are considered, the current distribution becomes more uniform only up to a point, approaching a limit which still may be very nonuniform. This effect can be observed in Figures 4 and 15. Lower values of ξ again lead to more uniform electrode reactions only within the limit imposed by the nonuniformity of the distribution at $\xi=0$. This latter case corresponds to the distributions calculated with a Tafel type overpotential expression, such as those shown in Figure 13.

By and large, the nonuniformity of reaction at the steady state is not subject to control without incurring other undesirable effects, principally increased overpotential.

5.2 Transient Behavior in Porous Electrode Systems

The transient behavior of a porous electrode system, taken in this work to be the behavior over the period from completion of the circuit until steady state is achieved at constant current drain, involves the complex phenomena of reaction distributions which are not only nonuniform but changing with time. The course of such a transient process, leading from a moderately nonuniform initial state to a highly nonuniform steady state, has been described in some

detail in Section 4.3 and illustrated in Figures 18, 19, and 20 (along with others). It is significant to note that although the reactant content is but slowly depleted in those deep portions of the electrode where transfer current densities are small, reactant supply from the electrolyte in the depth of the electrode to the areas near the face where reaction rates are high is usually quite small compared to supply from the electrode face. Thus the presence of a reservoir of reactant in the pores often significantly affects the course of the process only in those parts of the electrode where very little current is transferred.

The transient processes are characterized by times (to say 90% of total overpotential change as cited earlier) on the order of 10 to 10^4 sec. Since many applications of porous electrodes involves operating periods which are not long compared to this time range, transient behavior should be carefully considered in analysis of cells involving porous electrodes. The magnitude of the characteristic time, in dimensionless form, is relatively constant over wide ranges of operating conditions for cases where migration is the most significant reactant transport mechanism, that is for binary electrolytes. In this case changes in concentration have no effect on the dimensionless representation, and increasing current increases reactant transport as well as consumption. For cases where migration is only a secondary reactant transport means, excess inert electrolyte being present, the duration of the transient phenomena are strongly

influenced by manner of operation. Here, characteristic times are decreased by increasing β or decreasing γ of the reacting species, corresponding to raising current drain and to lowering reactant concentrations, respectively. If the reactant (and product) are transported almost entirely by diffusion, τ_{90} is roughly proportional to γ and to $1/\beta$. However, for most systems transient periods would not be short for any practicable combination of these parameters. Kinetic parameters have a relatively small influence on the characteristic times. Decreasing the depth of the electrode reduces the duration of transients, but, because of the effects mentioned in the preceding paragraph, not so much as the dependence of the τ to t conversion upon ℓ^2 would lead one to expect. For systems where the reactant species are in large concentration, as in most batteries, the transients are quite long and relatively independent of current. Operation in the steady state may be the exception rather than the rule.

It was mentioned in Section 2.1 and developed in Appendix I that time constants for transient behavior in porous electrodes would be long compared to electrical time constants for discharge of double layer capacitance. This is now clearly seen to be the case, the electrical time constants having typically values in the range of 10^{-4} to 10^{-1} sec. This constitutes additional justification for ignoring capacitative terms in equation (2.1-9) and those developed from it, in spite of the importance assigned to their effect by some previous investigators (see Section 1.2).

5.3 Influence of Overpotential Expression

The calculational procedure developed in this investigation was based upon no particular form of the overpotential, or electrode reaction rate, expression. However, as discussed in Section 2.4, the Tafel and redox type overpotential relationships were selected for use in example calculations, the redox type being considered a realistic representation for most electrode reactions which might be encountered. However, other choices could be made for such expressions, based upon the kinetics of the electrode reaction involved. The nature of the rate (overpotential) expression used in the analysis of a porous electrode to a very large extent determines the behavior that will be predicted for the electrode.

The effect of the choice of overpotential expression upon the analysis is well illustrated by the case of the cadmium anode, described in Section 4.2. This electrode, for $\xi=50.$ and $\Delta=0.1$ has been analyzed using, in turn, the redox type expression, the Tafel representation corresponding to this redox expression at high overpotential, and the linear formulation corresponding to it at low overpotential (and in the absence of concentration overpotential-see Section 2.4). The current distributions resulting from these analyses at $\beta=1.0$ are presented in Figure 21 and the electrode overpotential curves in Figure 22.

For the case chosen, the Tafel expression yields current distributions which are much too uniform, compared to the

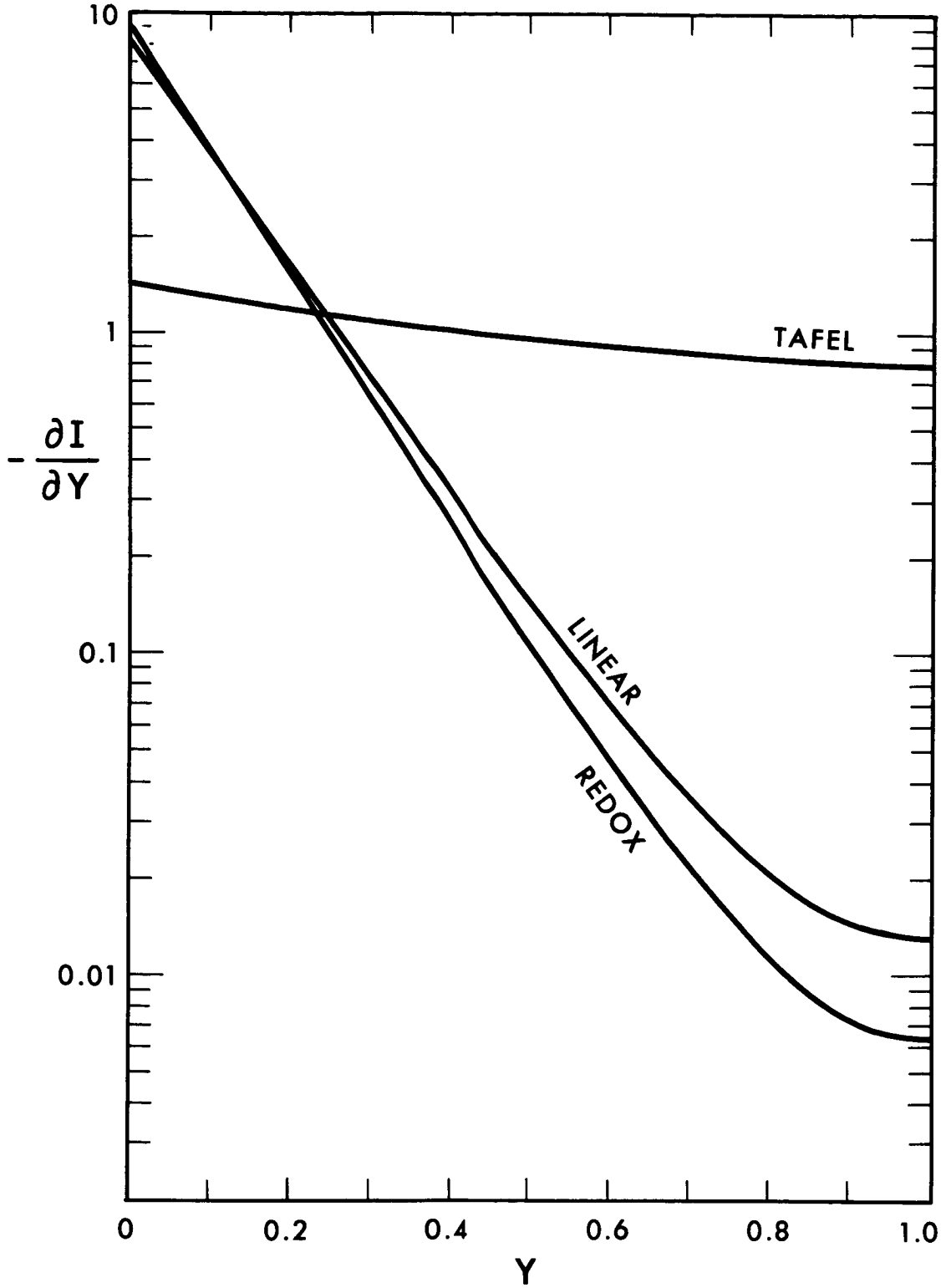

Figure 21. Current Distribution at Steady State for Cadmium Anode (5N KOH). $\xi = 50.$, $\Delta = 0.1$, $\beta = 1.0$.
(Calculated using overpotential expressions indicated.)

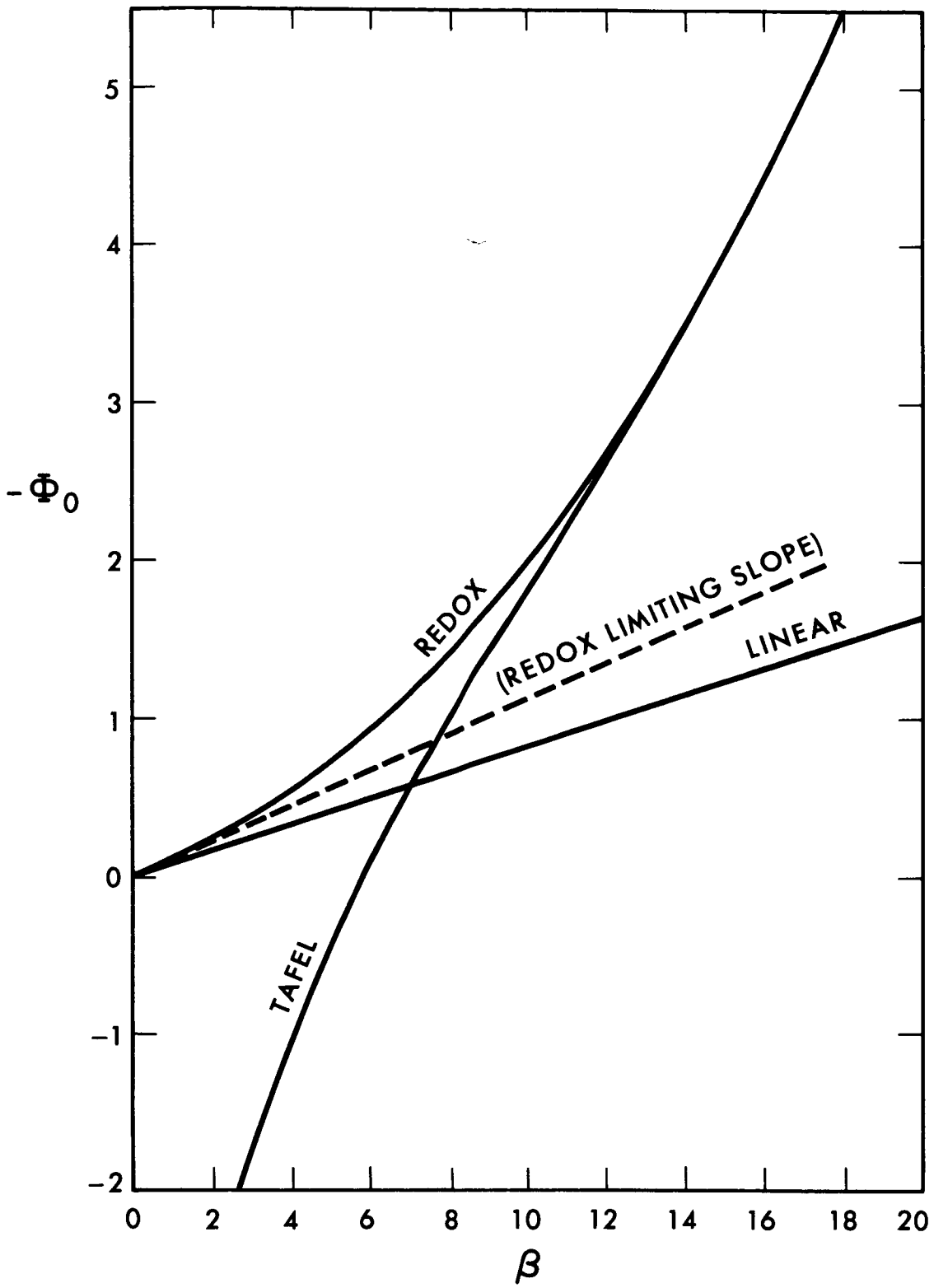

Figure 22. Electrode Overpotential at Steady State for Cadmium Anode (5N KOH). $\xi = 50.$, $\Delta = 0.1$, $\beta = 1.0$. (Calculated using overpotential expressions indicated)

distributions calculated with the redox formula. The linear expression here gives behavior that deviates only moderately from the redox case. At a higher value of β the Tafel based curve would more closely approximate that for the redox, while the distribution resulting from the linear approximation would deviate much more widely. At very high values of β the Tafel and redox expressions yield current distributions which are almost identical in that portion of the electrode where significant reaction takes place. However, this only occurs at values of β which are too large to correspond to any practical condition of electrode operation. At vanishing values of β the redox based curve and that derived for the linear approximation are identical.

The overpotential behavior of the electrode, as based on a redox type expression, is compared to the behavior for Tafel and linear type expressions in Figure 22. The overpotentials predicted by the Tafel form are asymptotic to those predicted with the redox expression as β becomes large (here β=20 corresponds to limiting current). The linear approximation gives overpotentials close to those calculated for the redox case at small β, but the limiting slope of the latter overpotential curve at low β does not correspond with the slope of the straight line overpotential relation resulting from use of this linearization. Most significantly, over the range of β=1 to 10, which corresponds to the conditions of operation expected for a cadmium anode, analyses based on the Tafel or on the linear expression are inadequate.

They predict electrode performance not even remotely approximating that from an analysis based on the redox overpotential equation.

It can be concluded that the type of overpotential expression utilized in the analysis of a porous electrode, and the values of the parameters used in that expression, is critical. The redox type formulation has been shown to be valid for a number of systems (see Vetter[22]) but cannot be assumed arbitrarily. The use of a Tafel type expression may be valid for some systems, but its employment as an approximation to a redox form is clearly counterindicated. Such an analysis could have value only under conditions where the reverse term in the redox expression is negligible in all portions of the electrode where significant reaction takes place; this condition usually requires prohibitively large overpotentials. The linearization of the redox expression, around vanishing overpotential or any other chosen overpotential value, can have validity only over a narrow range of overpotentials, and thus of transfer current densities. However, porous electrodes are characterized by a simultaneous existence of wide ranges of transfer current densities at different positions in the electrode. The only condition to which such an analysis might reasonably be applied is that of vanishing current drain. In using any overpotential expression in analyzing porous electrode behavior, the effect of variations in the form and in the parameters of the expression within the range of their uncertainty must

certainly be investigated. The use of several values of exchange current density in Section 4.2 is an example. It may be found that in many cases meaningful analysis of the behavior of the electrode system is not possible without more precisely known overpotential expressions.

5.4 Proposed Extensions of the Investigation

This investigation has established a model for a flooded porous electrode with no hydrodynamic flow of electrolyte in the pores, and, from this model, developed a procedure for analysis of the dynamic behavior of the electrode. In defining and analyzing this model certain limitations have been imposed by assumptions introduced concerning the system and its behavior. While certain of these assumptions (e.g., that of constant transport parameters) are necessary because of lack of data for alternate treatments, this work could be extended to eliminate the necessity of others. Such extensions would logically include the introduction of flow terms in the flux equations (and corresponding source terms in the conservation equations) to account for the generation (or elimination) of electrolyte volume in the course of the reaction and the consideration of electrode matrices which possess significant electrical resistance.

Also, a pressing need exists for extension of this sort of analysis to cases where the properties of the electrode matrix change in course of the charging or discharging of the electrode. All real battery systems fall in this category.

Unfortunately, little is known about the nature of these effects on a local basis at the present time; such a knowledge is prerequisite to incorporation of these considerations into porous electrode analysis. However, models should be developed which account for such phenomena in a general way and can be adapted to the characteristics of a particular matrix when these become known. Some first efforts, of a very approximate nature, have been made in this direction by Winsel[18].

Finally, experiments confirming the results of applications of this procedure are required. These should include measurements of overpotential as a function of current drain and distribution of transfer current in depth for well described porous electrodes of both random (sintered, etc.) configuration and idealized geometry (micro fissures and cylinders). The current distribution measurements require sectioning of the electrode in depth without destroying its uniformity, a difficult undertaking where resolution to fractional millimeters might be required. Such experiments could only be based upon a redox system for which complete and accurate overpotential and transport properties were available due to the sensitivity of the analysis to these factors, particularly the former. The ferri-ferrocyanide couple discussed in Section 4.3 meets these requirements as well as any other available, but even here, uncertainty in diffusion coefficients and exchange current densities would limit verification to qualitative comparisons only.

Ultimately, the significance of this work consists primarily in three aspects: First, it relates the dynamic behavior of flooded porous electrodes to the basic transport and kinetic phenomena determining such behavior. Second, it demonstrates the general characteristics of the transient and steady state performance of such electrodes and the influence of conditions of operation upon the performance. And, third, it provides a method of predicting performance of systems for which adequate basic information is available. At the same time, this analysis again indicates the great need for accurate fundamental data for electrochemical systems.

APPENDICES

APPENDIX I

Capacitance Effects in Porous Electrode Dyamics

If the considerable capacitance of the electric double layer over the extended interface in a porous electrode is considered, it is apparent that the expression given in Section 2.1 for conservation of current should also include a capacitive term. Thus equation (2.1-9) would become

$$\nabla \cdot \underline{i} = S_i - a\,\sigma \frac{\partial \phi}{\partial t} = -a\left(i^s + \sigma \frac{\partial \phi}{\partial t}\right) \qquad \text{(I-1)}$$

where σ = interface capacitance per unit area (F/cm^2). However, $\frac{\partial \phi}{\partial t}$ is significant only during the initial charging of the capacitance (at switch-on time). This proceeds, as shown by Ksenzhek[16], with a time constant

$$\theta_{el} = \rho\, a\, \sigma\, \ell^2 \qquad \text{(I-2)}$$

where ρ = effective resistivity of electrolyte in pores(ohm cm)

ℓ = characteristic dimension of system (cm).

The time constant for the mass transport process is of the order of the diffusion time constant

$$\theta_{dif} = \frac{\ell^2}{D} \qquad \text{(I-3)}$$

Using a typical value for electrolyte resistivity of the order ρ = 1 ohm cm, for surface area of $a = 10^5\ cm^2/cm^3$, and for surface capacity of 20 $\mu F/cm^2$

$$\theta_{el} \simeq 2\ell^2 \text{ sec}$$

which is in agreement with the results of Euler[14] if $\ell = 10^{-2}$-10^{-3} cm. Similarly using a value of $D = 10^{-5}\text{cm}^2/\text{sec}$ it is seen that the order of magnitude of the diffusion time constant is

$$\theta_{dif} \simeq 10^5 \ \ell^2 \text{ sec}$$

Comparing these results

$$\frac{\theta_{el}}{\theta_{dif}} \simeq 2 \times 10^{-5}$$

and therefore the capacitative effects occur only in the very first part of a transient process. For the purpose of this study they can be considered as completed instantaneously and thus ignored.

APPENDIX II

Formulation of Overpotential Expressions for Numerical Analysis

The overpotential expressions chosen for discussion in Section 2.4, the Tafel and redox types, may be put in the form of equation (3.2-1) as follows:

$$\text{Tafel:}\quad p(\Phi,C_i) = C_r\left\{\frac{\chi}{\gamma_r}\exp\left[\alpha n\Phi\right]\right\} \tag{II-1}$$

$$\therefore\quad A_j = \begin{cases} 0 & j\neq r \\ \dfrac{\chi}{\gamma_r}\exp\left[\alpha n\Phi\right] & j=r \end{cases} \tag{II-2}$$

$$B_j = \begin{cases} C_r\dfrac{\chi}{\gamma_r}\exp\left[\alpha n\Phi\right] & j\neq r \\ 0 & j=r \end{cases} \tag{II-3}$$

$$\text{Redox:}\quad p(\Phi,C_i) = C_r\left\{\frac{\chi}{\gamma_r}\exp[\alpha n\Phi]\right\} + C_p\left\{\frac{-\chi}{\gamma_p}\exp[(\alpha-1)n\Phi]\right\} \tag{II-4}$$

$$\therefore\quad A_j = \begin{cases} 0 & j\neq r, j\neq p \\ \dfrac{\chi}{\gamma_r}\exp\left[\alpha n\Phi\right] & j=r \\ \dfrac{-\chi}{\gamma_p}\exp\left[(\alpha-1)n\Phi\right] & j=p \end{cases} \tag{II-5}$$

$$B_j = \begin{cases} \chi\left\{\dfrac{C_r}{\gamma_r}\exp[\alpha n\Phi] - \dfrac{C_p}{\gamma_p}\exp[(\alpha-1)n\Phi]\right\} & j\neq r, j\neq p \\ -\dfrac{C_p}{\gamma_p}\chi\exp[(\alpha-1)n\Phi] & j=r \\ \dfrac{C_r}{\gamma_r}\chi\exp[\alpha n\Phi] & j=p \end{cases} \tag{II-6}$$

In finite difference form A_j, B_j are evaluated in terms of Φ and C_i for a given Y and τ index, that is in terms of $\Phi(J,K)$, $C_i(J,K)$, and may thus be expressed as $A_j(J,K)$, $B_j(J,K)$

APPENDIX III

Accommodation of Source Term Discontinuities in Finite Difference Representation of Conservation Equations

The species source term in equations (3.3-10) exists only in the electrode proper ($Y > 0$) and is zero in the equivalent transfer layer ($-\Delta < Y < 0$). A difficulty arises in assigning values to this term at the point of the finite difference approximation corresponding to $Y = 0$ (at the face of the electrode). In order to find the correct source term for this point consider (3.3-10) applied in the transfer layer (primed variables)

$$\frac{1}{\pi_j}\frac{\partial C_j'}{\partial \tau} = \frac{\partial^2 C_j'}{\partial Y^2} + z_j\left(C_j'\frac{\partial^2 \Phi}{\partial Y^2} + \frac{\partial C_j'}{\partial Y}\frac{\partial \Phi'}{\partial Y}\right), \quad -\Delta \le Y \le 0 \qquad \text{(III-1)}$$

and in the electrode proper

$$\frac{1}{\pi_j}\frac{\partial C_j}{\partial \tau} = \frac{\partial^2 C_j}{\partial Y^2} + z_j\left(C_j\frac{\partial^2 \Phi}{\partial Y^2} + \frac{\partial C_j}{\partial Y}\frac{\partial \Phi}{\partial Y}\right) + S_j, \quad 0 \le Y \le 1 \qquad \text{(III-2)}$$

with appropriate boundary conditions at $Y = -\Delta$ and $Y = 1$, and with the linking conditions at $Y = 0$

$$C_j' = C_j \quad ; \quad \Phi' = \Phi \qquad \text{(III-3)}$$

$$-\pi_j\left[\frac{\partial C_j'}{\partial Y} + z_j C_j'\frac{\partial \Phi'}{\partial Y}\right] = -\pi_j\left[\frac{\partial C_j}{\partial Y} + z_j C_j\frac{\partial \Phi}{\partial Y}\right], \qquad \text{(III-4)}$$

equation (III-4) being equivalent to

$$\frac{\partial C_j'}{\partial Y} = \frac{\partial C_j}{\partial Y} \quad ; \quad \frac{\partial \Phi'}{\partial Y} = \frac{\partial \Phi}{\partial Y}. \qquad \text{(III-5)}$$

In finite difference form, using the notation of Section 3.3, (III-1) and (III-2) become

$$\left[1-z_j\,\frac{P'(J,K)}{4}\right]C'_j(J-1,K)+\left[z_jQ'_j(J,K)-\frac{2}{\lambda_j(K)}-2\right]C'_j(J,K)$$

$$+\left[1+z_j\,\frac{P'(J,K)}{4}\right]C'_j(J+1,K)=F'_j(J,K)\qquad J=1,LF\qquad\text{(III-6)}$$

and for J=LF,L

$$\left[1-z_j\,\frac{P(J,K)}{4}\right]C_j(J-1,K)+\left[z_jQ_j(J,K)-T_jA_j(J,K)-\frac{2}{\lambda_j(K)}-2\right]C_j(J,K)$$

$$+\left[1+z_j\,\frac{P(J,K)}{4}\right]C_j(J+1,K)=F_j(J,K)+T_jB_j(J,K)$$

$$=F'_j(J,K)+\left(T_j-z_j\,\frac{h^2}{\kappa}\,\gamma_j\right)B'_k(J,0)+T_jB_j(J,K)\qquad\text{(III-7)}$$

with the linking conditions

$$C'_j(LF,K)=C_j(LF,K);\ P'(LF,K)=P(LF,K);\ Q'(LF,K)=Q(LF,K)\qquad\text{(III-8)}$$

$$\frac{C'_j(LF+1,K)-C'_j(LF-1,K)}{2h}=\frac{C_j(LF+1,K)-C_j(LF-1,K)}{2h}.\qquad\text{(III-9)}$$

Substituting (III-9) and (III-8) into (III-6) taken at J=LF

$$2C'_j(LF-1,K)+\left[z_jQ_j(LF,K)-\frac{2}{\lambda_j(K)}-2\right]C_j(LF,K)$$

$$+\left[1+z_j\,\frac{P(LF,K)}{4}\right]\left[C_j(LF+1,K)-C_j(LF-1,K)\right]=F'_j(LF,K).\qquad\text{(III-10)}$$

Then solving (III-10) for $C_j(LF-1,K)$ and substituting this result into (III-7) taken at J=LF

$$2\,\frac{\left[1-z_j\frac{P(LF,K)}{4}\right]}{\left[1+z_j\frac{P(LF,K)}{4}\right]}\,C'_j(LF-1,K)+\left[\left\{\frac{\left[1-z_j\frac{P(LF,K)}{4}\right]}{\left[1+z_j\frac{P(LF,K)}{4}\right]}+1\right\}\times\right.$$

$$\left.\left\{z_jQ_j(LF,K)-\frac{2}{\lambda_j(K)}-2\right\}-T_jA_j(LF,K)\right]C_j(LF,K)+2C_j(LF+1,K)$$

$$=\left\{\frac{\left[1-z_j\frac{P(LF,K)}{4}\right]}{\left[1+z_j\frac{P(LF,K)}{4}\right]}+1\right\}F'_j(LF,K)+\left(T_j-z_j\frac{h^2}{\kappa}\,\gamma_j\right)B_k(LF,0)+T_jB_j(LF,K)$$

$$\text{(III-11)}$$

results. If this is multiplied by $\left[1+z_j\frac{P(LF,K)}{4}\right]/2$ and it is noted that C_j' and C_j no longer overlap so that the prime can be dropped, the expression simplifies to

$$\left[1-z_j\frac{P(LF,K)}{4}\right]C_j(LF-1,K)+\left[z_jQ_j(LF,K)-\frac{\left[1+z_j\frac{P(LF,K)}{4}\right]}{2}T_jA_j(LF,K)\right.$$
$$\left.-\frac{2}{\lambda_j(K)}-2\right]C_j(LF,K)+\left[1+z_j\frac{P(LF,K)}{4}\right]C_j(LF+1,K)$$
$$=F_j'(LF,K)+\frac{\left[1+z_j\frac{P(LF,K)}{4}\right]}{2}\left\{\left(T_j-z_j\frac{h^2}{\kappa}\gamma_j\right)B_k(LF,0)+T_jB_j(LF,K)\right\} \qquad \text{(III-12)}$$

Therefore, at J=LF, the finite difference approximation is the same as within the electrode (J>LF) but with the source terms $A_j(LF,K)$, $B_j(LF,K)$, and $B_k(LF,0)$ weighted by the factor

$$\frac{\left[1+z_j\frac{P(LF,K)}{4}\right]}{2}=\frac{1}{2}+z_j\frac{P(LF,K)}{8} \qquad \text{(III-13)}$$

APPENDIX IV

FORTRAN II Program for Implementation of Calculations

The analysis is implemented for an IBM 7090 digital computing system by a FORTRAN II program. This consists in a main routine (CODE-1), which merely prepares input parameters for calculation, a principal subroutine (ODE), in which most computations are performed, and several accessory subroutines (INTEG, TDIAG, PDIAG, STEP), which carry out certain detailed aspects of the calculations. A subroutine (TFC) is used to introduce whatever overpotential expression may be desired, and another (PHIFE) to provide initial estimates of Φ.

The program input (to CODE-1) consists of five punched cards per case, as follows:

1. (I4, 9F4.0, 4F8.3): N, z_1,---,z_5,ν_1,---,ν_4,π_1,---,π_4
2. (F8.3, 2E12.3): α, ξ, η
3. (4F8.4, E12.3, F8.4): γ_1,---,γ_4, β, Δ
4. (5E8.1): h, g_o, ϵ_1, ϵ_2, C_{ins}
5. (8I4, F8.2, 28X, I4, F8.2): M1, M2, M3, M4, NR, MP, MK, MNI, TML, M7, FDAMP

The last card listed above is for control of program options where the indicators have the following significance:

M1 (1 = STEADY STATE; 2 = TRANSIENT)

M2 (1 = NO ITERATION OUTPUT; 2 = ITERATION OUTPUT)

M3 (1 = NO AUX OUTPUT [TIME, ITER. COUNT]; 2 = AUX OUTPUT)

M4 (1 = EXIT ON ELAPSED TIME; 2 = EXIT ON ITERATION COUNT; 3 = EXIT ONLY ON CONVERGENCE)

NR (0 = NO BINARY TAPE OUTPUT; > 0 = BINARY TAPE WITH CASE NO. = NR)

MP (NO. OF CALCULATION PTS PER OUTPUT PT)

MK (NO. OF TIME STEPS CALCULATED PER OUTPUT)

MNI (ITERATION LIMIT FOR EXIT)

TML (TIME LIMIT FOR EXIT)

M7 (0 = ALT. Φ CALCULATION & FIXED CURRENT; 1 = ALT Φ CALCULATION & FIXED POTENTIAL; 2 = FIXED CURRENT; 3 = FIXED POTENTIAL)

FDAMP (0 = MAX DAMPING FACTOR = 1; > 0 = MAX DAMPING FACTOR = FDAMP).

Within the programs, the following equivalences exist between FORTRAN variables and external variables.

NC	N	
V(I)	ν_i	NOTE: I = 1,5
Z(I)	z_i	
P(I)	π_i	
G(I)	γ_i	
DELTA	Δ	
BETA	β	
ALFA	α	
PC	$\chi = \xi/\beta$	
PE	η	
PN	n	
H	h	

DTI	g_o	
DT	$g(K)$	
EPS	ϵ_1	
DEV	ϵ_2	
CINSIG	C_{ins}	
C(J,I)	$C_i(J,K)$	J = 1,250
PHI(J)	$\Phi(J,K)$	
PHIS(J)	$\Phi^*(J,K)$	
TC(J)	$[-\partial I/\partial Y]_{(J,K)}$	
Y	Y	
TAU	τ	
L	L	
LF	LF	
PHI1	$\Phi(1)$	
FK(J,I)	$F_i(J,K)$	
FKP(J)	$F_p(J,K)$	
A(J)	A(J)	
B(J)	B(J)	
DP(J)	P(J,K)	
DP2(J)	Q(J,K)	
DC(J)	R(J,K)	
DC2(J)	S(J,K)	
CAPPA	κ	
FL(I)	$1/\lambda_i(K)$	
FLK(I)	$1/\lambda_i(K-1)$	

Other FORTRAN variables are as defined in the routine concerned.

The program output is in the form of printed tables of $-\frac{\partial I}{\partial Y}$ (called J), Φ, and C_i at regular intervals of Y, a table being printed for each MKth time step. Values of $-\frac{\partial I}{\partial Y}$ at Y = 0, 1. by 0.1 can be printed at each iteration as desired (M2 = 2). Error terminations and failures to converge give diagnostic outputs.

The main program, CODE-1, and principal subroutine, ODE, are listed below. They are followed by the necessary accessary subroutines. Examples of the subroutines TFC and PHIFE are also listed; however, these programs should be written (with connection to ODE as in the example) to correspond to the overpotential expression in effect and the associated estimated behavior.

```
MAIN PROGRAM - DATA READ IN AND SET UP
CCODE-1  ANALYSIS OF ONE DIMENSIONAL POROUS ELECTRODE SYSTEM
C                          17 MAY 63 - E A GRENS
   01 FORMAT(I4,9F4.0,4F8.3)
   02 FORMAT(F8.3,2E12.3)
   03 FORMAT(4F8.4,E12.3,F8.4)
   04 FORMAT(5E8.1)
   05 FORMAT(8I4,F8.2,28X,I4,F8.2)
   11 FORMAT(8H1FOR THE,I2,51H COMPONENT SYSTEM CHARACTERIZED BY THE PAR
     1AMETERS -)
   12 FORMAT(5X,1HZ,I1,1H=,F3.0,9X,1HV,I1,1H=,F3.0,9X,1HP,I1,1H=,F6.3,
     1     9X,1HG,I1,1H=,F7.4)
   13 FORMAT(5X,5HALFA=,F5.2,5X,3HXI=,1PE9.2,3X,6HDELTA=,0PF7.4,5X,
     1     5HBETA=,1PE9.2,23X,A6,14H POLARIZATION))
   14 FORMAT(19HOCALCULATED WITH H=,1PE8.1,5H, DT=,1PE8.1,10H, EPSILON=,
     1     1PE8.1,6H, DEV=,1PE8.1,9H, CINSIG=,1PE8.1)
   15 FORMAT(100X,7H(RUN NR,I4,1H))
      DIMENSION Z(5),V(5),P(5),G(5),DUM1(3750),DUM2(2)
      COMMON DUM1,ALFA,H,DUM2,NC,DUM3,PC,PE,Z,V,P,G,BETA,DELTA,DT,
     1     EPS,DEV,CINSIG,DTI
      NRS=0
READ CARDS CONTAINING SYSTEM AND OPERATION PARAMETERS
   20 READ INPUT TAPE 2,1,NC,(Z(I),I=1,5),(V(I),I=1,4),(P(I),I=1,4)
   30 IF(NC)31,31,21
   31 IF(NRS)33,33,32
   32 CALL REWUNL(8)
   33 CALL EXIT
   21 READ INPUT TAPE 2,2,ALFA,XI,PE
      READ INPUT TAPE 2,3,(G(I),I=1,4),BETA,DELTA
      READ INPUT TAPE 2,4,H,DTI,EPS,DEV,CINSIG
      READ INPUT TAPE 2,5,M1,M2,M3,M4,NR,MP,MK,MNI,TML,M7,FDAMP
SET UP BINARY TAPE FOR RECORDING OUTPUT IF NR NOT 0
   40 IF(NR)22,22,41
   41 IF(NRS)42,42,22
   42 CALL REWIND(8)
      NRM=NR-1
      NRS=NRS+NR
      CALL POSITT(8,NRM,0)
      CALL ETTEST(8,INDIC)
      IF(INDIC)43,22,43
   43 NR=0
ESTABLISH PARAMETERS FOR I=NC
   22 V(NC)=0.
      P(NC)=1.
      G(NC)=1.
CALCULATE XI
      PC=XI/BETA
PRINT OUT PARAMETERS DESCRIBING CASE
   70 IF(ABSF(PE-1.)-0.001)71,72,72
   71 TYPE=6H(TAFEL
      GO TO 23
   72 TYPE=6H(REDOX
   23 CALL STEP(TDTM,1)
   25 WRITE OUTPUT TAPE 3,11,NC
   50 IF(NR)26,26,51
   51 WRITE OUTPUT TAPE 3,15,NR
      WRITE TAPE 8,NR
      WRITE TAPE 8,NC,(Z(I),I=1,NC),(V(I),I=1,NC),(P(I),I=1,NC),
     1     (G(I),I=1,NC),ALFA,XI,PE,DELTA,BETA
   26 DO 27 I=1,NC
```

```
   27 WRITE OUTPUT TAPE 3,12,I,Z(I),I,V(I),I,P(I),I,G(I)
      WRITE OUTPUT TAPE 3,13,ALFA,XI,DELTA,BETA,TYPE
      WRITE OUTPUT TAPE 3,14,H,DT,EPS,DEV,CINSIG
GO TO SUBROUTINE ODE FOR COMPUTATION OF CASE
   28 CALL ODE(M1,M2,M3,M4,NR,MP,MK,MN1,TML,M7,FDAMP)
WRITE END OF FILE ON BINARY TAPE IF USED
   60 IF(NR)20,20,61
   61 CALL EOF(8)
      GO TO 20
      END
```

```
  100 SUBROUTINE ODE(M1,M2,M3,M4,MN,MP,MK,MNI,TML,M7,FDAMP)
C     SUBROUTINE FOR ANALYSIS OF ONE DIMENSIONAL POROUS ELECTRODE SYSTEM
C                          12 JUL 63 - E A GRENS
NOTE - ALL SECTIONS WITH STATEMENT NRS IN M// SERIES CONCERN FIXED PHI(1)
CALCULATION OPTION
  101 FORMAT(9H0FOR TAU=,1PE10.3,6H AT N=,I4,6H, TEL=,0PF6.2,6H, ERR=,
     11PE10.3,7H, DAMP=,0PF6.2,52H, AND THE VALUES OF J FOR Y FROM 0 TO
     21 (BY 0.1) ARE)
  102 FORMAT(10X,1P11E10.3)
  103 FORMAT(6H0AFTER,I5,15H ITERATIONS AND,F6.2,44H MINUTES INITIAL POT
     1ENTIAL HAD NOT CONVERGED)
  104 FORMAT(46H0THE STEADY STATE CONDITION OF THE SYSTEM IS -)
  105 FORMAT(9X,26H(THE CALCULATION REQUIRED ,F5.2,12H MINUTES AND,I4,
     112H ITERATIONS))
  106 FORMAT(8H0AT TAU=,1PE10.3,33H THE CONDITION OF THE SYSTEM IS -)
  107 FORMAT(8H0AT TAU=,1PE10.3,4H, N=,I4,67H, CALCULATIONS WERE TERMINA
     1TED AT VALUES BELOW. TOTAL ELAPSED TIME=,0PF6.2,8H, ERROR=,
     21PE10.3)
  108 FORMAT(22H0FOR TAU GREATER THAN ,1PE10.3,43H, THE SYSTEM IS ESSENT
     1IALLY AT STEADY STATE)
  109 FORMAT(1H0,3X,1HY,12X,1HJ,14X,3HPHI,13X,A2,14X,A2,14X,A2,14X,
     1A2,14X,A2)
  110 FORMAT(1X,F6.3,1P7E16.4)
  111 FORMAT(54H0LIMITING CURRENT IS REACHED WITH RESPECT TO COMPONENT,
     1I2)
      DIMENSION Z(5),V(5),P(5),G(5),T(5),FL(5),C(250,5),CSS(250,5),
     1    PHIS(250),PHI(250),PHISS(250),TCS(250),TC(250),TCP(250),
     2    TCSS(250),FK(250,4),FKP(250),DP(250),DP2(250),DC(250),
     3    DC2(250),QM(250),Q(250),QP(250),R(250),A(250),B(250),U(250),
     4    FLK(5),PHISO(250),TCO(250),OC(5),TD(5),CH(5),PHIIN(250),
     5    AO(250,4),BO(250,4),PHUS(250),CNCO(250),PHILT(250)
      COMMON A,B,TCS,TCP,QM,Q,QP,R,PHIS,PHI,C,ALFA,H,LF,L,NC,PN,PC,PE,
     1    Z,V,P,G,BETA,DELTA,DT,EPS,DEV,CINSIG,DTI,INC,LFM,LFP,LI,WF,
     2    IR,IP,N,M7,CIGNOR,KTYPE,KEY,KFLD,KINIT,PHIFAC
SET UP OVERPOTENTIAL EXPRESSION OPTION
  117 IF(ABSF(PE-1.)-0.001)118,119,119
  118 KTYPE=1
      GO TO 120
  119 KTYPE=2
  120 CALL CLOCKT(TIS)
ESTABLISH PRINTOUT COLUMN HEADINGS
      CH(1)=2HC1
      CH(2)=2HC2
      CH(3)=2HC3
      CH(4)=2HC4
      CH(5)=2HC5
INITIALIZE INTERNAL PARAMETERS
      PN=0.
      NCM=NC-1
  124 DO 125 I=1,NCM
  125 PN=PN+V(I)*Z(I)
      S=0.
  126 DO 127 I=1,NC
  127 S=S+Z(I)*Z(I)*P(I)*G(I)
      CAPPA=S/(PN*BETA)
      T4=H*H/CAPPA
      T10=PN*BETA*H
  128 DO 129 I=1,NC
      TD(I)=2.*H*H/P(I)
```

```
  130 GO TO (133,131),KTYPE
  131 IXP=XFIXF(LOGF(CINSIG)/4.6)
  132 CIGNOR=10.**IXP
      GO TO 135
  133 CIGNOR=CINSIG
  135 IF(FDAMP-0.01)136,137,137
  136 DAMAX=1.
      GO TO 138
  137 DAMAX=FDAMP
  138 DAMCK=DAMAX+0.01
  140 L=XFIXF((1.+DELTA)/H)+1
      LF=XFIXF(DELTA/H)+1
      LM=L-1
      LFM=LF-1
      LFP=LF+1
      LI=LF-(LFM/MP)*MP
      INC=XFIXF(0.1/H)
      IR=0
      IP=0
      K=0
      DO 143 I=1,2
      IF(V(I))141,143,142
  141 IP=I*(KTYPE-1)
      GO TO 143
  142 IR=I
  143 CONTINUE
      IF(IP*IP-IR*IP)399,144,144
  144 PHIFAC=1.
      IF(NC-2)148,148,145
CHARACTERIZE SYSTEM AS TO PRESENCE OF EXCESS INERT ELECTROLYTE
  145 DO 147 I=1,NC
      IF(V(I))147,147,146
  146 IF(G(I)-0.25)147,148,148
  147 CONTINUE
      KFLD=1
      GO TO 150
  148 KFLD=2
SET UP CALCULATION PROCEDURE OPTIONS
  150 GO TO (151,153),KFLD
  151 IF(M7-2)152,153,153
  152 KMP=2
      GO TO 156
  153 KMP=1
ESTABLISH INITIAL DAMPING
      GO TO (154,156),KFLD
  154 GO TO (155,156),KTYPE
  155 DAMS=1.
      GO TO 600
  156 DAMS=0.9**6
BINARY TAPE OUTPUT (OPTIONAL
  600 IF(MN)157,157,601
  601 INT=XFIXF(0.01/H)
      LIT=LF-(LFM/INT)*INT
      YI=FLOATF(LIT-1)*H-DELTA
      WRITE TAPE 8,YI
BYPASS STEADY STATE CALCULATION IF M1=3
  157 GO TO (160,160,158),M1
  158 KINIT=1
      CALL PHIFE
      DO 159 J=1,L
```

```
  159 PHISS(J)=1.2*PHI(J)
      GO TO 200
SET UP STEADY STATE CALCULATION
  160 DAMP=DAMS
  161 N=1
      MC=0
      KP=1
      ERR=0.
      CALL CLOCKT(TI)
      KEY=2
      KINIT=1
      TAU=9.999E+33
      CALL PHIFE
      DO 163 J=1,L
      DO 162 I=1,NCM
      C(J,I)=G(I)
  162 FK(J,I)=0.
      FKP(J)=0.
      PHIS(J)=PHI(J)-PHI(1)
  163 PHISO(J)=PHIS(J)
      DO 164 I=1,NC
  164 FL(I)=0.
      DO 165 J=LF,L
  165 TC(J)=1.
CONDUCT PROCEDURE FOR A TIME STEP WITH STEADY STATE SET UP
      GO TO 400
PRINT STEADY STATE RESULTS FOR STEADY STATE CALC ONLY
  170 GO TO (171,180),M1
  171 WRITE OUTPUT TAPE 3,104
      GO TO (610,172),M3
  172 WRITE OUTPUT TAPE 3,105,TEL,N
BINARY TAPE OUTPUT (OPTIONAL)
  610 IF(MN)173,173,611
  611 WRITE TAPE 8,TAU
      DO 612 J=LIT,L,INT
  612 WRITE TAPE 8,TC(J),PHI(J),(C(J,I),I=1,NC)
  173 WRITE OUTPUT TAPE 3,109,(CH(I),I=1,NC)
      DO 179 J=LI,L,MP
      GO TO (174,178),M3
  174 DO 176 I=1,NC
      IF(C(J,I)/G(I)-CIGNOR)175,175,176
  175 C(J,I)=0.
  176 CONTINUE
      IF(TC(J)-10.*CIGNOR)177,177,178
  177 TC(J)=0.
  178 Y=FLOATF(J-1)*H-DELTA
  179 WRITE OUTPUT TAPE 3,110,Y,TC(J),PHI(J),(C(J,I),I=1,NC)
      RETURN
SAVE STEADY STATE RESULTS IN TRANSIENT CALCULATIONS
  180 DO 182 J=1,L
      DO 181 I=1,NC
  181 CSS(J,I)=C(J,I)
      TCSS(J)=TC(J)
  182 PHISS(J)=PHI(J)
      NS=N
      TELS=TEL
BINARY TAPE OUTPUT (OPTIONAL)
  615 IF(MN)200,200,616
  616 WRITE TAPE 8,TAU
      DO 617 J=LIT,L,INT
```

```
  617 WRITE TAPE 8,TC(J),PHI(J),(C(J,I),I=1,NC)
SET UP CALCULATION AT TAU =0
  200 N=1
      MC=0
      KP=1
      KEY=1
      KINIT=2
      ERP=0.
      DAMP=DAMS
      PHIFAC=1.
      CALL CLOCKT(TI)
  201 CALL PHIFE
      DO 202 J=1,L
      PHIS(J)=PHI(J)-PHI(1)
      DO 202 I=1,NC
  202 C(J,I)=G(I)
      WF=0.5
CONDUCT CALCULATION AT TAU=0
  210 CALL TFC(PHI1,NC,1)
      DO 211 J=2,L
      QM(J)=1.
      QP(J)=1.
      Q(J)=-2.-T4*PC*PN*FLOATF(KTYPE-1)
  211 R(J)=T4*(B(J)-PC*PN*PHIS(J)*FLOATF(KTYPE-1))
      CALL TDIAG(1,L,0.,PHUS)
      IF(N-1)212,212,214
  212 DO 213 J=1,L
  213 PHIS(J)=PHUS(J)
      GO TO 700
  214 DO 215 J=1,L
  215 PHIS(J)=PHISO(J)*(1.-DAMP)+PHUS(J)*DAMP
  700 GO TO (217,701),KP
  701 CALL TFC(PHI1,NC,4)
      IF(M-2)230,230,702
  702 IF(ABSF(TCP(LF)-TC(LF))-CIGNOR)222,222,703
  703 IF((TCP(LF)-TC(LF))*(TC(LF)-TCO(LF)))224,222,222
  217 CALL TFC(PHI1,NC,2)
      IF(NC)483,483,218
  218 IF(N-2)230,230,219
  219 IF(ABSF(PHI1-PHI(1))-EPS/10.)222,222,220
  220 IF((PHI1-PHI(1))*(PHI(1)-PHI10))224,221,221
  221 IF((PHI1-PHI(1))*(PHI10-PHI102))224,222,222
  222 DAMP=DAMP/0.9
      IF(DAMP-1.01)226,223,223
  223 DAMP=1.
      GO TO 226
  224 IF(DAMP-0.11)226,225,225
  225 DAMP=0.9*DAMP
  226 DO 227 J=1,L
  227 PHIS(J)=PHISO(J)*(1.-DAMP)+PHUS(J)*DAMP
  704 GO TO (228,230),KP
  228 CALL TFC(PHI1,NC,2)
      IF(NC)483,483,230
  230 PHI102=PHI10
      PHI10=PHI(1)
      SUM=0.
  705 GO TO (232,706),KP
  706 CALL TFC(PHI1,NC,4)
      TCO(LF)=TC(LF)
  707 TC(LF)=TCP(LF)
```

```
  232 DO 233 J=1,L
      SUM=SUM+ABSF((PHI(J)-PHIS(J))/PHI1-1.)
      PHI(J)=PHIS(J)+PHI1
  233 PHISO(J)=PHIS(J)
  234 ERP=H*SUM/DAMP
  235 CALL CLOCKT(TN)
      TEL=TN-TI
  710 GO TO (236,711),KP
  711 IF(0.10*EPS-ERP)712,713,713
  712 M=M+1
      GO TO 240
  713 CALL TFC(PHI1,NC,3)
      DO 714 J=LF,L
  714 TCS(J)=TCP(J)
      GO TO 742
  236 IF(TEL-0.70)237,237,238
  237 IF(0.5*EPS-ERP)240,250,250
  238 IF(5.*EPS-ERP)240,250,250
  240 GO TO (241,242,243),M4
  241 IF(TEL-1.00)243,243,245
  242 IF(N -MNI-2*(KP-1)*MNI)243,245,245
  243 N=N+1
  715 IF(N -MNI)210,716,210
  716 IF(M7-1)210,783,210
  245 WRITE OUTPUT TAPE 3,103,N,TEL
      RETURN
  250 CALL TFC(PHI1,NC,3)
  252 DO 253 J=1,L
      PHIIN(J)=PHI(J)
  253 TC(J)=TCP(J)
SET UP PRINT FOR TAU=0
  260 K=0
      TAU=0.
      TAUO=0.
      TCK=TC(LF)
      FORFAC=0.1
DETERMINE AND RECORD OVERPOTENTIAL TREND
      IF(PHIIN(LF)-PHISS(LF))261,262,262
  261 TND=+1.
      GO TO 300
  262 TND=-1.
PRINT TIME STEP RESULTS
  300 WRITE OUTPUT TAPE 3,106,TAU
BINARY TAPE OUTPUT (OPTIONAL)
  620 IF(MN)301,301,621
  621 WRITE TAPE 8,TAU
      DO 622 J=LIT,L,INT
  622 WRITE TAPE 8,TC(J),PHI(J),(C(J,I),I=1,NC)
  301 GO TO (303,302),M3
  302 WRITE OUTPUT TAPE 3,105,TEL,N
  303 WRITE OUTPUT TAPE 3,109,(CH(I),I=1,NC)
      DO 311 J=LI,L,MP
      DO 304 I=1,NC
  304 OC(I)=C(J,I)
      GO TO (305,309),M3
  305 DO 307 I=1,NC
      IF(C(J,I)/G(I)-CIGNOR)306,306,307
  306 OC(I)=0.
  307 CONTINUE
      IF(TC(J)-10.*CIGNOR)308,308,309
```

```
  308 TCOPJ=0.
      GO TO 310
  309 TCOPJ=TC(J)
  310 Y=FLOATF(J-1)*H-DELTA
  311 WRITE OUTPUT TAPE 3,110,Y,TCOPJ,PHI(J),(OC(I),I=1,NC)
INITIALIZE TIME STEP CALCULATIONS
  320 KEY=1
      KINIT=1
      K=K+1
      N=1
      MC=0
      KP=1
      ERR=0.
      DAMP=DAMS
      CALL CLOCKT(TI)
  321 IF(K-1)322,322,330
CALCULATE TIME STEP TERMS FOR INITIAL TIME STEP
  322 S=H*H/DT
      DO 323 I=1,NC
      FL(I)=S/P(I)
  323 FLK(I)=FL(I)
      WF=0.5
      CALL TFC(PHI1,NC,1)
      DO 327 J=2,L
      DO 325 I=1,NCM
  325 FK(J,I)=(T(I)-Z(I)*T4*G(I))*B(J)-2.*FL(I)*G(I)
      GO TO (326,327),KMP
  326 FKP(J)=-T4*B(J)-2.*FL(NC)/Z(NC)
  327 CONTINUE
      GO TO 350
CALCULATE TIME STEP TERMS FOR SUSEQUENT TIME STEPS
  330 CALL STEP(TDTM,2)
  331 DO 334 J=2,L
      DO 334 I=1,NCM
      IF(C(J,I)/G(I)-CINSIG)334,334,332
  332 S=-C(J,I)/FK(J,I)
      TDT=TD(I)*(S+2.*FL(I)*S*S)
      IF(TDTM-TDT)334,334,333
  333 TDTM=TDT
  334 CONTINUE
      IF(ABSF(TC(LF)/TCK-1.)-0.2)335,335,336
  335 CALL STEP(TDTM,3)
      GO TO 338
  336 CALL STEP(TDTM,4)
  336 S=H*H/DT
      DO 339 I=1,NC
      FLK(I)=FL(I)
  339 FL(I)=S/P(I)
  340 DO 349 J=2,L
      DO 345 I=1,NCM
      IF(C(J,I)/G(I)-CINSIG)341,341,344
  341 IF(C(J,I)-1.0E-35)342,342,343
  342 FK(J,I)=-2.*C(J,I)*FL(I)
      GO TO 345
  343 FK(J,I)=-2.*FL(I)*C(J,I)*EXPF(FK(J,I)/(C(J,I)*FL(I))+
     1    2.*FLK(I)/FL(I))
      GO TO 345
  344 FK(J,I)=-FK(J,I)-2.*(FL(I)+FLK(I))*C(J,I)
  345 CONTINUE
      GO TO (346,349),KMP
```

```
  346 FKP(J)=-FKP(J)-2.*(FL(NC)+FLK(NC))*C(J,NC)/Z(NC)
  349 CONTINUE
ESTABLISH STARTING ESTIMATES OF PHI FOR TIME STEP
  350 TAU=TAU+DT
      TCK=TC(LF)
      DO 351 J=1,L
  351 PHILT(J)=PHI(J)
  355 FORS=FORFAC*FLOATF(KFLD-1)
      DO 359 J=1,L
      IF(J-LF)356,356,357
  356 FORM=FORS
      GO TO 358
  357 FORM=FORS*(TC(J)/TC(LF)+FLOATF(K-1))/FLOATF(K)
  358 PHI(J)=PHILT(J)*(1.-FORM)+PHISS(J)*FORM
      PHIS(J)=PHI(J)-PHI(1)
  359 PHISO(J)=PHIS(J)
CONDUCT SOLUTION OF EQUATION SYSTEM FOR TIME STEP
START ITERATION WITH PHI VALUES FROM LAST ITERATION
  400 DO 401 J=2,LM
      DP(J)=PHIS(J+1)-PHIS(J-1)
  401 DP2(J)=PHIS(J+1)+PHIS(J-1)-2.*PHIS(J)
      DP2(L)=2.*(PHIS(LM)-PHIS(L))
FIND NEW VALUES FOR C(J,I) FOR I NOT NC
      DO 429 I=1,NCM
      IF(ABSF(T(I))-1.E-20)410,410,402
  402 WF=(1.+Z(I)*DP(LF)/4.)/2.
      CALL TFC(PHI1,I,1)
      GO TO (403,405),KFLD
  403 GO TO (404,410),KMP
  404 IF(N-1)410,408,406
  405 IF(N-MNI/2)410,408,406
  406 DO 407 J=2,L
      A(J)=(A(J)+AO(J,I))/2.
      B(J)=(B(J)+BO(J,I))/2.
      AO(J,I)=A(J)
  407 BO(J,I)=B(J)
      GO TO 410
  408 DO 409 J=2,L
      AO(J,I)=A(J)
  409 BO(J,I)=B(J)
  410 DO 411 J=2,LM
      S= Z(I)*DP(J)/4.
      QM(J)=1.-S
  411 QP(J)=1.+S
      S=2.*FL(I)+2.
      IF(IR*IP)421,421,412
  412 IF(I-IR)413,414,413
  413 IF(I-IP)421,414,421
  414 DO 415 J=2,L
      Q(J)=Z(I)*DP2(J)-T(I)*A(J)-S
      R(J)=FK(J,I)
  415 B(J)=-T(I)*B(J)
      IF(I-IR)417,416,417
  416 CALL PDIAG(1,L,G(IR),U,1)
      GO TO 429
  417 CALL PDIAG(1,L,G(IP),U,2)
      DO 420 J=1,L
      IF(U(J))418,418,419
  418 C(J,IR)=0.
      GO TO 420
```

```
  419 C(J,IR)=U(J)
  420 CONTINUE
      CALL PDIAG(1,L,G(IP),U,3)
      GO TO 423
  421 DO 422 J=2,L
      Q(J)=Z(I)*DP2(J)-T(I)*A(J)-S
  422 R(J)=FK(J,I)+T(I)*B(J)
      CALL TDIAG(1,L,G(I),U)
  423 DO 428 J=1,L
      IF(U(J))424,424,425
  424 C(J,I)=0.
      GO TO 428
  425 C(J,I)=U(J)
  428 CONTINUE
  429 CONTINUE
FIND C(J,NC) VALUES BY ELECTRONEUTRALITY
  430 DO 433 J=1,L
      SUM=0.
      DO 431 I=1,NCM
  431 SUM=SUM+C(J,I)*Z(I)
      CNCO(J)=C(J,NC)
      C(J,NC)=-SUM/Z(NC)
      IF(C(J,NC))432,432,433
  432 C(J,NC)=0.
  433 CONTINUE
  440 GO TO (460,441),KMP
FIND NEW VALUES OF PHI(J) BY ALTERNATE PROCEDURE
  441 DO 443 J=2,L
      DC2(J)=0.
      DC(J)=0.
      DO 442 I=1,NC
      DC2(J)=DC2(J)+Z(I)*Z(I)*P(I)*C(J,I)
  442 DC(J)=DC(J)+Z(I)*P(I)*(C(J,I)-C(J-1,I))
  443 CONTINUE
      GO TO (444,447),KP
  444 CALL TFC(PHI1,NC,2)
      IF(NC)483,483,445
  445 DO 446 J=1,L
  446 PHI(J)=PHI1+PHIS(J)
  447 CALL TFC(PHI1,NC,3)
      DO 448 J=LF,L
      TCS(J)=TCP(J)
  448 CONTINUE
      PHUS(1)=0.
      CALL INTEG(H,LF,L,CUR)
      IF(LF-2)452,450,450
  450 DO 451 J=2,LF
  451 PHUS(J)=PHUS(J-1)-(T10*CUR+DC(J))/DC2(J)
  452 DO 455 J=LFP,L
      IF((L-J)-((L-J)/2)*2)453,453,454
  453 CALL INTEG(H,J,L,CUR)
      GO TO 455
  454 CALL INTEG(H,J,LM,CUR)
      CUR=CUR+H*TCS(L)
  455 PHUS(J)=PHUS(J-1)-(T10*CUR+DC(J))/DC2(J)
      GO TO 500
FIND NEW VALUES OF PHI(J) BY BASIC PROCEDURE
  460 DO 464 J=2,LM
      IF(C(J,NC))462,461,462
  461 DC(J)=0.
```

```
      DC2(J)=0.
      GO TO 463
  462 DC(J)=(C(J+1,NC)-C(J-1,NC))/C(J,NC)
      DC2(J)=(C(J+1,NC)+C(J-1,NC))/C(J,NC)-2.
  463 S=DC(J)/4.
      QM(J)=1.-S
  464 QP(J)=1.+S
      IF(C(L,NC))466,465,466
  465 DC2(L)=0.
      GO TO 467
  466 DC2(L)=2.*(C(LM,NC)/C(L,NC)-1.)
  467 S=2.*FL(NC)/Z(NC)
      DO 469 J=2,L
      Q(J)=-2.
      R(J)=-DC2(J)/Z(NC)
      IF(C(J,NC))468,469,468
  468 R(J)=R(J)+FKP(J)/C(J,NC)+S
  469 CONTINUE
      CALL TDIAG(1,L,0.,PHUS)
RESTART ITERATION PROCEDURE WITH NEW ESTIMATES IF PHI(J) VALUES DIVERGE
  500 GO TO (501,520),KEY
  501 DO 502 J=1,L
      IF(ABSF(PHUS(J))-70.)502,502,525
  502 PHIS(J)=PHUS(J)
      CALL TFC(PHI1,NC,2)
      IF(NC)483,483,503
  503 LIMIT=0
      DO 512 J=1,L
      PHI(J)=PHI1+PHIS(J)
      PDS=PHI(J)-PHISS(J)
      IF(TND*PDS)505,505,504
  504 LIMIT=+1
      XSS=ABSF(PDS/PHISS(J))
      FSS=1./(2.+10.*XSS)
      PHI(J)=PHISS(J)+FSS*PDS
      GO TO 512
  505 IF(LIMIT)507,507,506
  506 PHI(J)=PHISS(J)+0.5*PDS
  507 PDI=PHIIN(J)-PHI(J)
      IF(TND*PDI)509,509,508
  508 LIMIT=-1
      XIN=ABSF(PDI/PHIIN(J))
      FIN=1./(2.+10.*XIN)
      PHI(J)=PHIIN(J)-FIN*PDI
      GO TO 512
  509 IF(LIMIT)510,512,512
  510 PHI(J)=PHIIN(J)-0.5*PDI
  512 PHUS(J)=PHI(J)-PHI(1)
INCREASE OR DECREASE DAMPING ACCORDING TO BEHAVIOR OF TC(J)
  520 IF(N-1)521,521,523
  521 DO 522 J=1,L
  522 PHIS(J)=PHUS(J)
      GO TO 720
  523 DO 524 J=1,L
  524 PHIS(J)=PHISO(J)*(1.-DAMP)+PHUS(J)*DAMP
  720 GO TO (530,721),KP
  721 CALL TFC(PHI1,NC,4)
  722 IF(M-2)550,550,532
  525 GO TO (526,497),KEY
  526 GO TO (502,527),KFLD
```

```
  527 N=1
      ERR=0.
      DAMP=(DAMP+DAMS)/2.
      FORFAC=FORFAC*(1.-FORFAC)-0.01
      IF(FORFAC)399,355,355
  530 CALL TFC(PHI1,NC,2)
      IF(NC)483,483,531
  531 IF(N-2)550,550,532
  532 CALL TFC(PHI1,NC,4)
      DO 537 J=LF,L,INC
  725 GO TO (533,726),KP
  726 IF((L-LF)/3+LF-J)537,537,533
  533 IF(DAMP-0.53)535,534,534
  534 IF(ABSF(TCP(J)-TC(J))-2.*CIGNOR)537,537,536
  535 IF(ABSF(TCP(J)-TC(J))-20.*CIGNOR)537,537,536
  536 IF((TCP(J)-TC(J))*(TC(J)-TCO(J)))542,537,537
  537 CONTINUE
  540 DAMP=DAMP/0.9
      IF(DAMP-DAMCK)545,541,541
  541 DAMP=0.9*DAMP
      GO TO 550
  542 IF(DAMP-0.01)545,543,543
  543 DAMP=0.9*DAMP
  545 DO 546 J=1,L
  546 PHIS(J)=PHISO(J)*(1.-DAMP)+PHUS(J)*DAMP
  727 GO TO (547,550),KP
  547 CALL TFC(PHI1,NC,2)
      IF(NC)483,483,550
  550 DO 551 J=1,L
      PHI(J)=PHIS(J)+PHI1
  551 PHISO(J)=PHIS(J)
      CALL TFC(PHI1,NC,3)
      DO 552 J=LF,L,INC
  552 TCO(J)=TC(J)
      CALL CLOCKT(TN)
      TEL=TN-TIS
CHECK FOR CONVERGENCE OF ITERATIONS FOR THE TIME STEP
  560 IF(N-1)470,470,730
  730 GO TO (561,731),KP
  731 SUM=0.
      ERMAX=0.
      DO 735 J=LF,L
      GO TO (733,732),KFLD
  732 TCP(J)=(TCP(J)+TC(J))/2.
  733 ERR=ABSF(TCP(J)-TC(J))
      SUM=SUM+ERR
      IF(ERR-ERMAX)735,735,734
  734 ERMAX=ERR
  735 TC(J)=TCP(J)
      GO TO (737,736),KFLD
  736 ERR=ERR/10.
      ERMAX=ERMAX/10.
  737 ERR=H*SUM
      IF(EPS-ERR/DAMP)738,739,739
  738 M=M+1
      GO TO 472
  739 IF(10.*EPS-ERMAX/DAMP)738,740,740
  740 DO 741 J=LF,L
  741 TCS(J)=TC(J)
  742 CALL INTEG(H,LF,L,CUR)
```

```
      GO TO (744,743),KINIT
  743 IF(ABSF(CUR-1.)-0.1*EPS)770,745,745
  744 IF(ABSF(CUR-1.)-EPS)770,745,745
  745 IF(CUR-1.)746,770,747
  746 INDP=-1
      GO TO 748
  747 INDP=+1
  748 IF(IND+INDP)750,760,750
  750 IND=INDP
      PHI1L=PHI1
      IF(IND)751,751,752
  751 PHI1=PHI1+DELPHI
      GO TO 753
  752 PHI1=PHI1-DELPHI
  753 CURL=CUR
      M=1
      DAMP=1.
      MC=MC+1
  754 GO TO (400,210),KINIT
  760 PHI1=PHI1L+(1.-CURL)*(PHI1-PHI1L)/(CUR-CURL)
      DELPHI=0.1*DELPHI
      IND=0
      MC=MC+1
      M=1
      DAMP=1.
  761 GO TO (400,210),KINIT
  770 M=0
      KP=1
      DAMP=1.
  771 GO TO (585,252),KINIT
  561 ERMAX=0.
      SUM=0.
      DO 578 J=LF,L
      GO TO (564,562),KFLD
  562 IF(N-MNI/2)564,563,563
  563 TCP(J)=(TCP(J)+TC(J))/2.
  564 ERR=ABSF(TCP(J)-TC(J))
      SUM=SUM+ERR
      DIV=MAX1F(ABSF(TCP(J)),ABSF(TC(J)))
  570 GO TO (571,573),KTYPE
  571 IF(ABSF(TCP(J))-10.*CIGNOR)572,572,574
  572 IF(ABSF(TC(J))-10.*CIGNOR)578,578,574
  573 DIV=MAX1F(1.,DIV)
  574 ERR=ERR/DIV
      IF(TCP(J)+CIGNOR)575,576,576
  575 ERMAX=1.
      GO TO 578
  576 IF(ERR-ERMAX)578,578,577
  577 ERMAX=ERR
  578 TC(J)=TCP(J)
      ERR=H*SUM
      EPP=EPS
      GO TO (582,580),KTYPE
  580 IF(N-MNI)582,582,581
  581 ERMAX=ERMAX/10.
      REV=1.+9.*MINOF(2*(N-MNI),MNI)/FLOATF(MNI)
      EPP=REV*EPS
  582 IF(EPP-ERR/DAMP)472,583,583
  583 IF(EPP-ERMAX/DAMP)472,585,585
  585 IF(LFM-1)596,586,586
```

```
  586 DO 587 J=1,LFM
  587 TC(J)=0.
      DO 590 I=1,NCM
      IF(V(I))590,590,588
  588 DO 589 J=LF,LFP
      IF(C(J,I)/G(I)-CINSIG)591,591,589
  589 CONTINUE
  590 CONTINUE
      GO TO 596
  591 GO TO (592,593,592),M1
  592 WRITE OUTPUT TAPE 3,111,I
      RETURN
  593 GO TO (594,595),KEY
  594 WRITE OUTPUT TAPE 3,106,TAU
  595 WRITE OUTPUT TAPE 3,111,I
      GO TO (399,180),KEY
CONVERGENCE OF ITERATION PROCEDURE - GO TO CHECK FOR STEADY STATE
  596 GO TO (360,170),KEY
  470 DO 471 J=LF,L
  471 TC(J)=TCP(J)
  472 GO TO (480,473),M2
PRINT ITERATION SUMMARY (OPTIONAL)
  473 WRITE OUTPUT TAPE 3,101,TAU,N,TEL,ERR,DAMP
      WRITE OUTPUT TAPE 3,102,(TC(J),J=LF,L,INC)
CHECK FOR EXCEEDING PROGRAM TIME LIMIT
  480 GO TO (481,482,485),M4
  481 IF(TEL-TML)485,485,483
  482 IF(N-MNI-2*(KP-1)*MNI)485,483,483
  483 WRITE OUTPUT TAPE 3,107,TAU,N,TEL,ERMAX
      WRITE OUTPUT TAPE 3,109,(CH(I),I=1,NC)
      DO 484 J=LI,L,MP
      Y=FLOATF(J-1)*H-DELTA
TERMINATE CALCULATIONS FOR EXCESSIVE ELAPSED TIME (OR ITERATIONS)
  484 WRITE OUTPUT TAPE 3,110,Y,TC(J),PHI(J),(C(J,I),I=1,NC)
      GO TO (370,399),KEY
COMMENCE ANOTHER ITERATION
  485 N=N+1
  775 GO TO (776,400),KP
  776 GO TO (780,490),KEY
CHECK FOR VERY HIGH PHI ESTIMATES - RESTART WITH LOWER ESTIMATE IF HIGH
  490 IF(N-MNI/3)491,493,491
  491 IF(N-MNI)492,499,492
  492 IF(N-(3*MNI)/2)400,498,400
  493 LFH=LF+(L-LF)/2
      DO 495 J=LF,LFH,INC
      IF(TC(J)+1.0)496,494,494
  494 IF(TC(J)+0.1)497,495,495
  495 CONTINUE
      GO TO 780
  496 PHIFAC=0.3*PHIFAC
      GO TO 161
  497 PHIFAC=0.9*PHIFAC
      GO TO 161
  498 IF(TC(LF)-TCR)497,780,780
  499 TCR=TC(LF)
  780 IF(N-MNI)400,781,400
  781 IF(MC-1)782,400,400
  782 IF(M7-1)783,784,783
  783 IF(M7-3)400,784,400
  784 IND=0
```

```
      MC=1
      M=1
      KP=2
      PHI1=PHI(1)
      IF(ABSF(PHI1)-1.)785,785,786
  785 IF(ABSF(PHI1)-0.1)788,788,787
  786 DELPHI=1.
      GO TO 789
  787 DELPHI=0.1
      GO TO 789
  788 DELPHI=0.01
  789 DELPHI=DELPHI*PN/ABSF(PN)
      GO TO (790,210),KINIT
  790 GO TO (791,400),KEY
  791 DELPHI=0.1*DELPHI
      GO TO 400
CHECK FOR APPROACH TO STEADY STATE
  360 CALL CLOCKT(TN)
      TEL=TN-TI
      DO 366 J=LF,L,INC
      IF(ABSF(TCSS(J))-10.*CIGNOR)361,361,362
  361 IF(ABSF(TC(J))-10.*CIGNOR)366,366,380
  362 FACTOR=LOGF(TCSS(J))
      IF(FACTOR)363,363,364
  363 ADEV=(1.-FACTOR+FACTOR*FACTOR/50.)*DEV
      GO TO 365
  364 ADEV=DEV/FACTOR
  365 IF(ABSF(TC(J)/TCSS(J)-1.)-ADEV)366,366,380
  366 CONTINUE
STEADY STATE REACHED - PRINT STEADY STATE RESULTS
      WRITE OUTPUT TAPE 3,108,TAU
  370 WRITE OUTPUT TAPE 3,104
  630 IF(MN)371,371,631
  631 TAU=-1.
      WRITE TAPE 8,TAU
  371 GO TO (373,372),M3
  372 WRITE OUTPUT TAPE 3,105,TELS,NS
  373 WRITE OUTPUT TAPE 3,109,(CH(I),I=1,NC)
      DO 379 J=LI,L,MP
      GO TO (374,378),M3
  374 DO 376 I=1,NC
      IF(CSS(J,I)/G(I)-CIGNOR)375,375,376
  375 CSS(J,I)=0.
  376 CONTINUE
      IF(TCSS(J)-10.*CIGNOR)377,377,378
  377 TCSS(J)=0.
  378 Y=FLOATF(J-1)*H-DELTA
  379 WRITE OUTPUT TAPE 3,110,Y,TCSS(J),PHISS(J),(CSS(J,I),I=1,NC)
      RETURN
CHECK FOR FAILURE TO REACH STEADY STATE AT REASONABLE TAU
  380 IF(500.*DTI-TAU)381,390,390
  381 GO TO 483
  390 GO TO (392,391),M3
START NEW TIME STEP
  391 IF(K-(K/MK)*MK)300,300,310
  392 IF(TAU-TAUO-DTI*FLOATF(MK))310,393,393
  393 TAUO=TAU
      GO TO 300
RETURN TO MAIN PROGRAM FOR NEW CASE
  399 RETURN
```

```
   01 SUBROUTINE INTEG(H,JI,JF,QU)
C     SUBROUTINE FOR INTEGRATION BY SIMPSONS RULE - 16 OCT 62 -E A GRENS
      DIMENSION U(250),DUM(500)
      COMMON DUM,U
   02 SUM1=0.
      SUM2=0.
      JIP=JI+1
      JIP2=JI+2
      JFM=JF-1
      JFM2=JF-2
   04 DO 05 J=JIP,JFM,2
   05 SUM1=SUM1+U(J)
   06 DO 07 J=JIP2,JFM2,2
   07 SUM2=SUM2+U(J)
   08 QU=(U(JI)+U(JF)+4.*SUM1+2.*SUM2)*H/3.
      RETURN
      END
```

```
   01 SUBROUTINE TDIAG(JI,JF,UI,U)
C     SUBROUTINE FOR SOLUTION OF SPECIAL TRIDIAGONAL MATRICES
C                          26 NOV 62 - E A GRENS
      DIMENSION QM(250),Q(250),QP(250),R(250),W(250),RS(250),U(250),
     1    DUM(1000)
      COMMON DUM,QM,Q,QP,R
   02 JIP=JI+1
      JFM=JF-1
      JFQ=JF-JI
   03 W(JI)=0.
      RS(JI)=UI
   04 DO 05 J=JIP,JFM
      S=Q(J)-QM(J)*W(J-1)
      W(J)=QP(J)/S
   05 RS(J)=(R(J)-QM(J)*RS(J-1))/S
   06 U(JF)=(R(JF)-2.*RS(JFM))/(Q(JF)-2.*W(JFM))
   08 DO 09 JP=1,JFQ
      JQ=JF-JP
   09 U(JQ)=RS(JQ)-W(JQ)*U(JQ+1)
      RETURN
      END
```

```
   01 SUBROUTINE PDIAG(JI,JF,VI,U,MODE)
C      SUBROUTINE FOR SIMULTANEOUS SOLUTION OF TWO LINEARLY LINKED
C      TRIDIAGONAL MATRICES (2)     18 JUN 63 - E A GRENS
      DIMENSION QM(250),QMR(250),Q(250),QR(250),QP(250),QPR(250),B(250),
     1    BR(250),R(250),RR(250),U(250),V(250),A(250),DUM(500)
      COMMON A,B,DUM,QM,Q,QP,R
   02 JIP=JI+1
      JFM=JF-1
      JFQ=JF-JI
   03 GO TO (10,20,30),MODE
   10 U(JI)=VI
      UI=VI
   11 DO 12 J=JIP,JF
      QMR(J)=QM(J)
      QR(J)=Q(J)
      QPR(J)=QP(J)
      BR(J)=B(J)
   12 RR(J)=R(J)
      RETURN
   20 V(JI)=VI
      QPR(JI)=0.
      QP(JI)=0.
      BR(JI)=0.
      B(JI)=0.
      RR(JI)=UI
      R(JI)=VI
      QMR(JF)=2.
      QM(JF)=2.
   21 DO 22 J=JIP,JF
      DA=1.-BR(J-1)*B(J-1)
      AR=QMR(J)/DA
      ZR=-AR*BR(J-1)
      A=QM(J)/DA
      Z=-A*B(J-1)
      DENR=QR(J)-AR*QPR(J-1)
      DEN=Q(J)-A*QP(J-1)
      QPR(J)=QPR(J)/DENR
      QP(J)=QP(J)/DEN
      BR(J)=(BR(J)-ZR*QP(J-1))/DENR
      B(J)=(B(J)-Z*QPR(J-1))/DEN
      RR(J)=(RR(J)-AR*RR(J-1)-ZR*R(J-1))/DENR
   22 R(J)=(R(J)-A*R(J-1)-Z*RR(J-1))/DEN
      QPR(JF)=0.
      QP(JF)=0.
   24 DO 25 K=1,JFQ
      J=JF-K+1
      RHR=RR(J)-QPR(J)*U(J+1)
      RH=R(J)-QP(J)*V(J+1)
      DU=1.-B(J)*BR(J)
      U(J)=(RHR-RH*BR(J))/DU
   25 V(J)=(RH-RHR*B(J))/DU
      RETURN
   30 DO 31 J=JI,JF
   31 U(J)=V(J)
      RETURN
```

```
   01 SUBROUTINE STEP(TDTM,MODE)
C      SUBROUTINE FOR CALCULATION OF INITIAL TIME STEP AND FOR TIME STEP
C      MODIFICATION (FORM 3) -  3 JUL 63 - E A GRENS
       DIMENSION Z(5),V(5),G(5),P(5),DUM(3750),DUM2(8),DUM3(5)
       COMMON DUM,DUM2,Z,V,P,G,BETA,DELTA,DT,EPS,DEV,CINSIG,DTI,DUM3,
      1    IR,IP,N,M7,CIGNOR
   02 GO TO (10,20,30,40),MODE
   10 IF(IR)16,16,14
   14 DT=G(IR)/(5.0*V(IR)*BETA)
   15 IF(DTI-DT)16,50,50
   16 DT=DTI
      GO TO 50
   20 TDTM=10.*DTI
      GO TO 50
   30 IF(TDTM-DT)32,32,31
   31 DT=DT+0.5*(TDTM-DT)
      GO TO 50
   32 DT=TDTM
      GO TO 50
   40 IF(TDTM-DT)41,41,42
   41 DT=TDTM
      GO TO 50
   42 IF(DT-DTI)43,43,44
   43 DT=DT
      GO TO 50
   44 DT=DT-0.5*(DT-DTI)
   50 RETURN
      END
```

```
   01 SUBROUTINE TFC(PHI1,I,MODE)
C     SUBROUTINE FOR CALCULATION OF OVERPOTENTIAL-TRANSFER CURRENT
C     RELATIONSHIPS FOR REDOX POLARIZATION  (FORM 4)
C                              18 JUN 63 - E A GRENS
   02 FORMAT(44HOOVERPOTENTIAL CALCNLATION DOES NOT CONVERGE)
      DIMENSION Z(5),V(5),P(5),G(5),C(250,5),PHIS(250),PHI(250),
     1     TCS(250),TCP(250),A(250),B(250),CR(250),CP(250),DUM(1000)
      COMMON A,B,TCS,TCP,DUM,PHIS,PHI,C,ALFA,H,LF,L,NC,PN,PC,PE,Z,V,P,G,
     1     BETA,DELTA,DT,EPS,DEV,CINSIG,DTI,INC,LFM,LFP,LI,WF,IR,IP,N,M7,
     2     CIGNOR,KTYPE,KEY,KFLD,KINIT,PHIFAC
   03 GO TO (06,04),KEY
   06 GO TO (70,04),KINIT
   04 IF(N-1)05,05,70
   05 T2=ALFA*PN
      T3=(ALFA-1.)*PN
      GO TO (07,09),KTYPE
   07 DO 08 J=LF,L
   08 CP(J)=0.
      TP=0.
      GO TO 85
   09 IF(IP)80,80,82
   80 DO 81 J=LF,L
   81 CP(J)=PC
      GO TO 85
   82 TP=PC/G(IP)
   85 IF(IR)86,86,88
   86 DO 87 J=LF,L
   87 CR(J)=PC
      GO TO 70
   88 TR=PC/G(IR)
   70 GO TO (77,79,79,79),MODE
   77 IF(IR*IP)71,71,78
   78 IF(I-IP)10,10,99
   79 IF(I-1)71,90,71
   71 GO TO (74,99),KTYPE
   99 IF(IP)74,74,72
   72 DO 73 J=LF,L
   73 CP(J)=TP*C(J,IP)
   74 IF(IR)90,90,75
   75 DO 76 J=LF,L
   76 CR(J)=TR*C(J,IR)
   90 GO TO (10,20,30,40),MODE
   10 DO 11 J=1,LFM
      A(J)=0.
   11 B(J)=0.
      IF(I-IR)15,12,15
   12 DO 14 J=LF,L
      A(J)=TR*EXPF(T2*PHI(J))
      IF(IP)13,13,91
   91 B(J)=-TP*EXPF(T3*PHI(J))
      GO TO 14
   13 B(J)=-CP(J)*EXPF(T3*PHI(J))
   14 CONTINUE
      A(LF)=WF*A(LF)
      B(LF)=WF*B(LF)
      RETURN
   15 IF(I-IP)18,16,18
   16 DO 17 J=LF,L
      A(J)=-TP*EXPF(T3*PHI(J))
```

```
92 B(J)=TR*EXPF(T2*PHI(J))
   GO TO 17
93 B(J)=CR(J)*EXPF(T2*PHI(J))
17 CONTINUE
   A(LF)=WF*A(LF)
   B(LF)=WF*B(LF)
   RETURN
18 DO 19 J=LF,L
   A(J)=0.
   B(J)=CR(J)*EXPF(T2*PHI(J))-CP(J)*EXPF(T3*PHI(J))
19 CONTINUE
   B(LF)=WF*B(LF)
   RETURN
20 GO TO (21,25),KTYPE
21 DO 22 J=LF,L
22 TCS(J)=CR(J)*EXPF(T2*PHIS(J))
23 CALL INTEG(H,LF,L,QT)
24 PHI1=-LOGF(QT)/T2
   RETURN
25 DO 26 J=LF,L
26 TCS(J)=CR(J)*EXPF(T2*PHIS(J))
   CALL INTEG(H,LF,L,QF)
27 DO 29 J=LF,L
29 TCS(J)=CP(J)*EXPF(T3*PHIS(J))
   CALL INTEG(H,LF,L,QR)
60 IF(ABSF(ALFA-0.5)-0.1)61,61,63
61 PHI1=2.*LOGF((1.+SQRTF(1.+4.*QF*QR))/(2.*QF))/PN
62 IF(ABSF(ALFA-0.5)-1.E-06)50,50,64
63 PHI1=LOGF(QR/QF)/PN
64 NP=0
65 NP=NP+1
66 S2=QF*EXPF(T2*PHI1)
   S3=QR*EXPF(T3*PHI1)
   PHI1P=PHI1-(S2-S3-1.)/(T2*S2-T3*S3)
   ERP=ABSF(PHI1P/PHI1-1.)
   PHI1=PHI1P
67 IF(ERP-EPS)50,50,68
68 IF(NP-30)65,69,69
69 NC=0
   WRITE OUTPUT TAPE 3,02
   RETURN
30 IF(LFM-1)34,32,32
32 DO 33 J=1,LFM
33 TCP(J)=0.
34 DO 35 J=LF,L
35 TCP(J)=CR(J)*EXPF(T2*PHI(J))-CP(J)*EXPF(T3*PHI(J))
   RETURN
40 DO 41 J=LF,L,INC
41 TCP(J)=CR(J)*EXPF(T2*(PHIS(J)+PHI1))-CP(J)*EXPF(T3*(PHIS(J)+PHI1))
50 RETURN
   END
```

```
   01 SUBROUTINE PHIFE
C       SUBROUTINE FOR INITIAL ESTIMATE OF PHI - UNIFORM CONCENTRATION
C       DISTRIBUTION (CASE 5) - 18 JUN 63 - E A GRENS
        DIMENSION Z(5),V(5),P(5),G(5),PHI(250),DUM1(2250),DUM2(1250),
      1     DUM3(10)
        COMMON DUM1,PHI,DUM2,ALFA,H,LF,L,NC,PN,PC,PE,Z,V,P,G,BETA,DELTA,
      1     DUM3,IR,IP,N,M7,CIGNOR,KTYPE,KEY,KFLD,KINIT,PHIFAC
   02 T2=ALFA*PN
        GO TO (05,20),KINIT
   05 IF(IR)06,06,07
   06 EC=1.
        GIR=G(NC)
        GO TO 08
   07 EC=1.-BETA*DELTA*(V(IR)/G(IR)-ABSF(PN)/(ABSF(Z(NC))+ABSF(Z(IR))
      1     *G(IR)))/P(IR)
        GIR=G(IR)
   08 CEF=(1.+0.002*BETA+0.05*EC*GIR/BETA)/(EC*GIR+0.002*BETA
      1     +0.05*EC*GIR/BETA)
        ETC=(0.4*BETA+BETA*LOGF(BETA)/10.+0.1*EXPF(-BETA))*CEF+1.
        GO TO (11,12),KTYPE
   11 SS=PC*EC/ETC
        PHIJ=-LOGF(SS)/T2
        GO TO 15
   12 BS=SQRTF(20.*BETA/PC)
        PHIJ=2.2*BS/(PN*(1.+0.27*LOGF(10.*EC*GIR)+0.025*BS*BS))
   15 DO 16 J=1,L
   16 PHI(J)=PHIJ*PHIFAC
        RETURN
   20 GO TO (21,22),KTYPE
   21 PHIJ=-LOGF(PC)/T2
        GO TO 15
   22 PHIJ=LOGF((1.+SQRTF(1.+4.*PC*PC))/(2.*PC))/T2
        GO TO 15
        END
```

APPENDIX V.

Steady State Behavior of Cadmium Anode (5N KOH)

The steady state behavior of the cadmium anode example, as calculated according to the one dimensional model, is contained in this appendix. For each case treated a graph is included presenting curves of transfer current distribution, overpotential, and concentration as functions of depth in the porous electrode. The non-dimensional variables are used and overpotential is presented as a ratio to its value, Φ_o, at the electrode face (electrode overpotential).

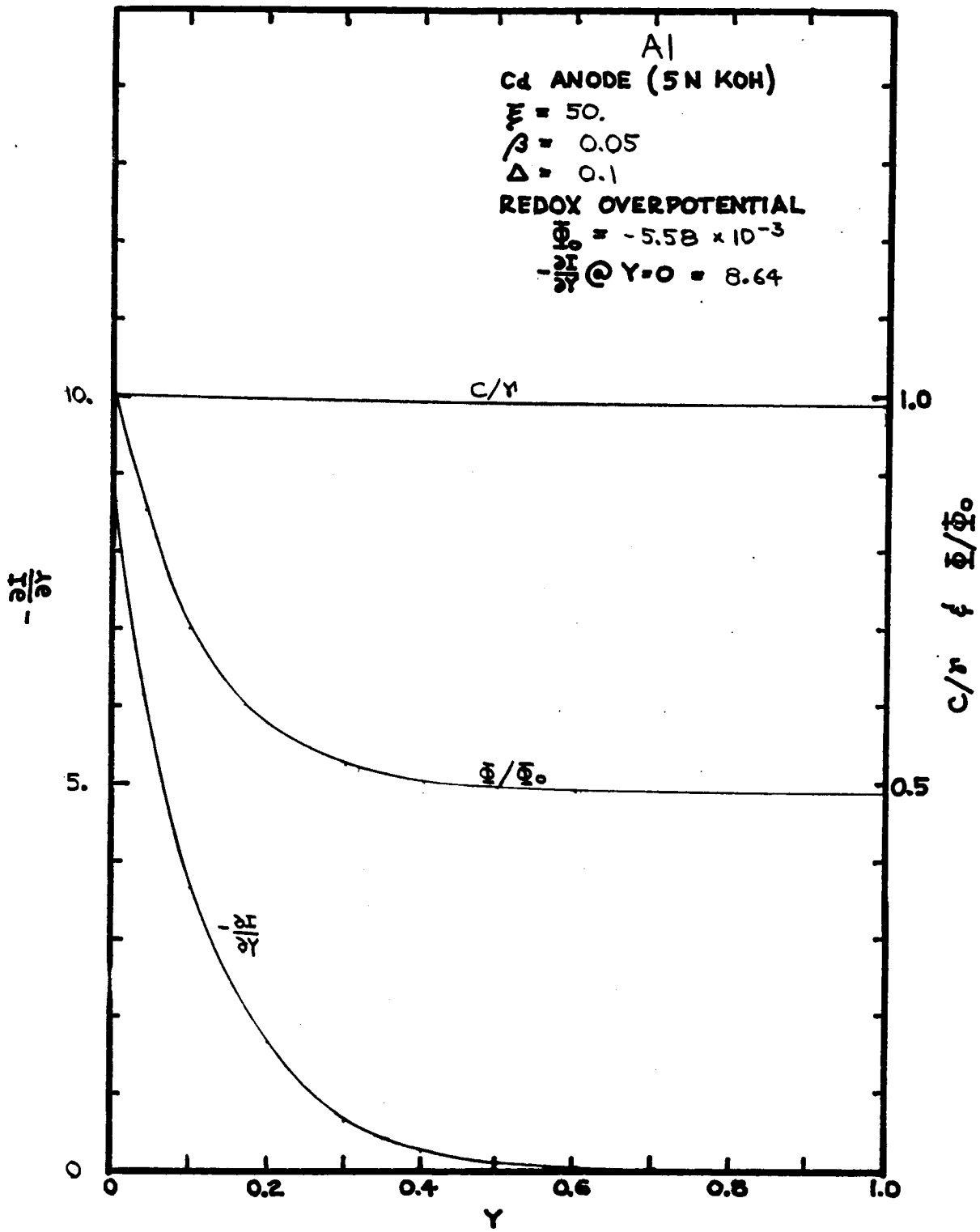
A1
Cd ANODE (5 N KOH)
ξ = 50.
β = 0.05
Δ = 0.1
REDOX OVERPOTENTIAL
Φ₀ = -5.58 x 10⁻³
-∂I/∂Y @ Y=0 = 8.64
C/I
Φ/Φ₀
-∂I/∂Y
10.
5.
0
1.0
0.5
0
0.2
0.4
0.6
0.8
1.0
Y
-∂I/∂Y
C/I & Φ/Φ₀

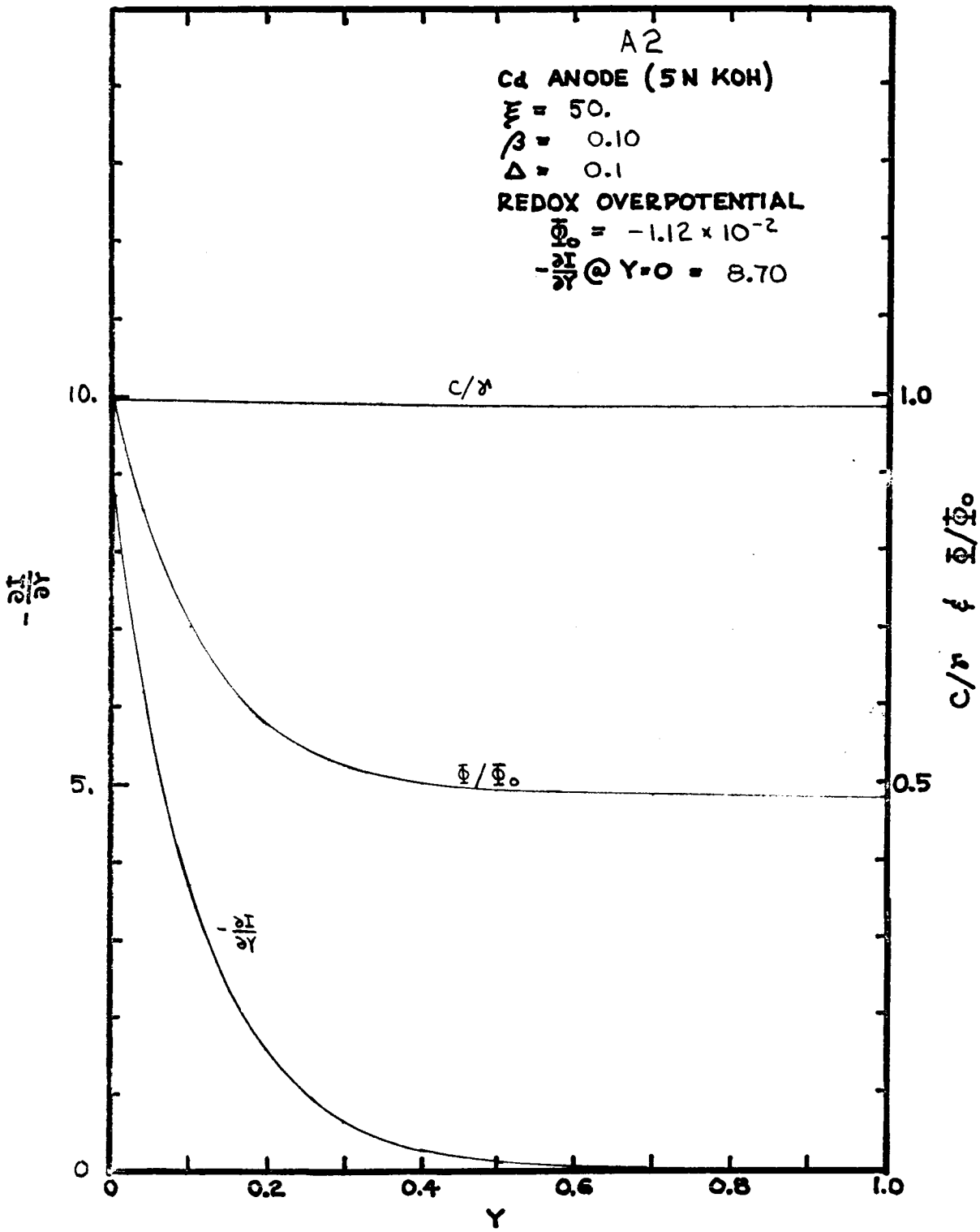
A2
Cd ANODE (5N KOH)
ξ = 50.
β = 0.10
Δ = 0.1
REDOX OVERPOTENTIAL
Φ₀ = −1.12 × 10⁻²
−∂I/∂Y @ Y=0 = 8.70
C/γ
Φ/Φ₀
−∂Ie/∂Y
10.
5.
0
1.0
0.5
0
0.2
0.4
0.6
0.8
1.0
Y
−∂Ie/∂Y
C/γ & Φ/Φ₀

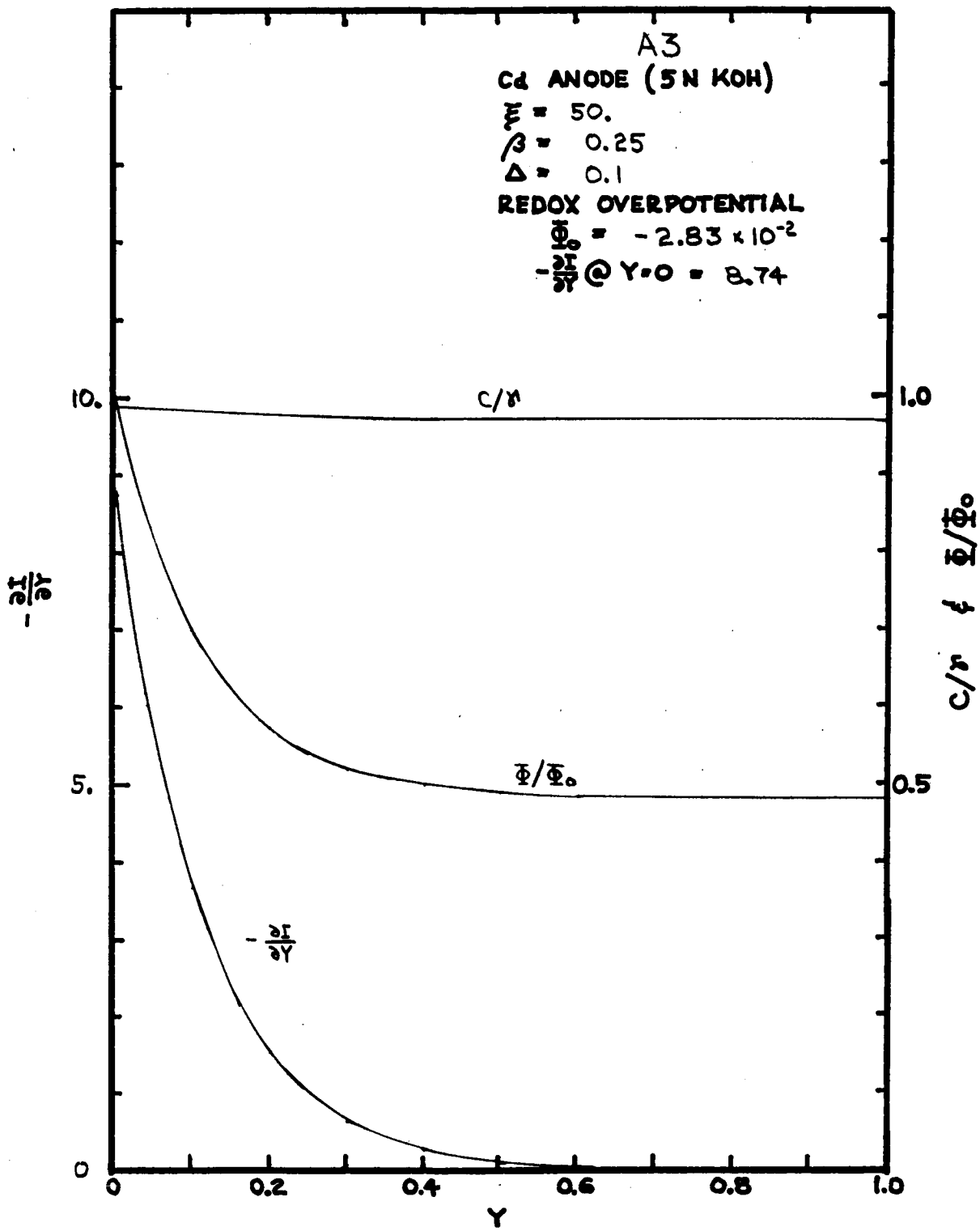
A3
Cd ANODE (5 N KOH)
ξ = 50.
β = 0.25
Δ = 0.1
REDOX OVERPOTENTIAL
Φ₀ = -2.83 × 10⁻²
-∂I/∂Y @ Y=0 = 8.74
C/γ
Φ/Φ₀
-∂I/∂Y
10.
5.
0
1.0
0.5
0
0.2
0.4
0.6
0.8
1.0
Y
-∂I/∂Y
C/γ & Φ/Φ₀

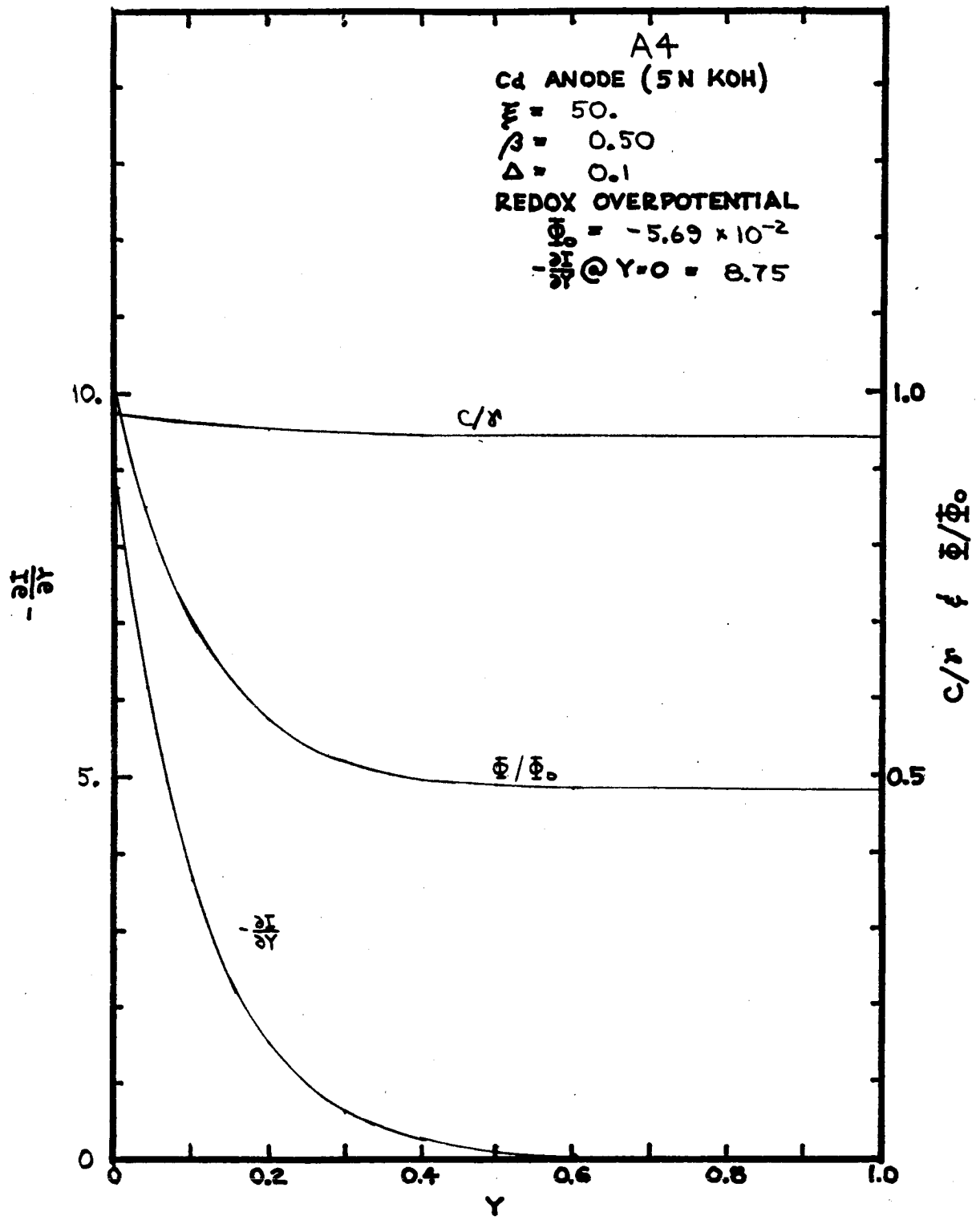
A4
Cd ANODE (5N KOH)
ξ = 50.
β = 0.50
Δ = 0.1
REDOX OVERPOTENTIAL
Φ₀ = -5.69 × 10⁻²
-∂I/∂Y @ Y=0 = 8.75
C/γ
Φ/Φ₀
-∂I/∂Y
10.
5.
0
1.0
0.5
0
0.2
0.4
0.6
0.8
1.0
Y
-∂I/∂Y
C/γ & Φ/Φ₀

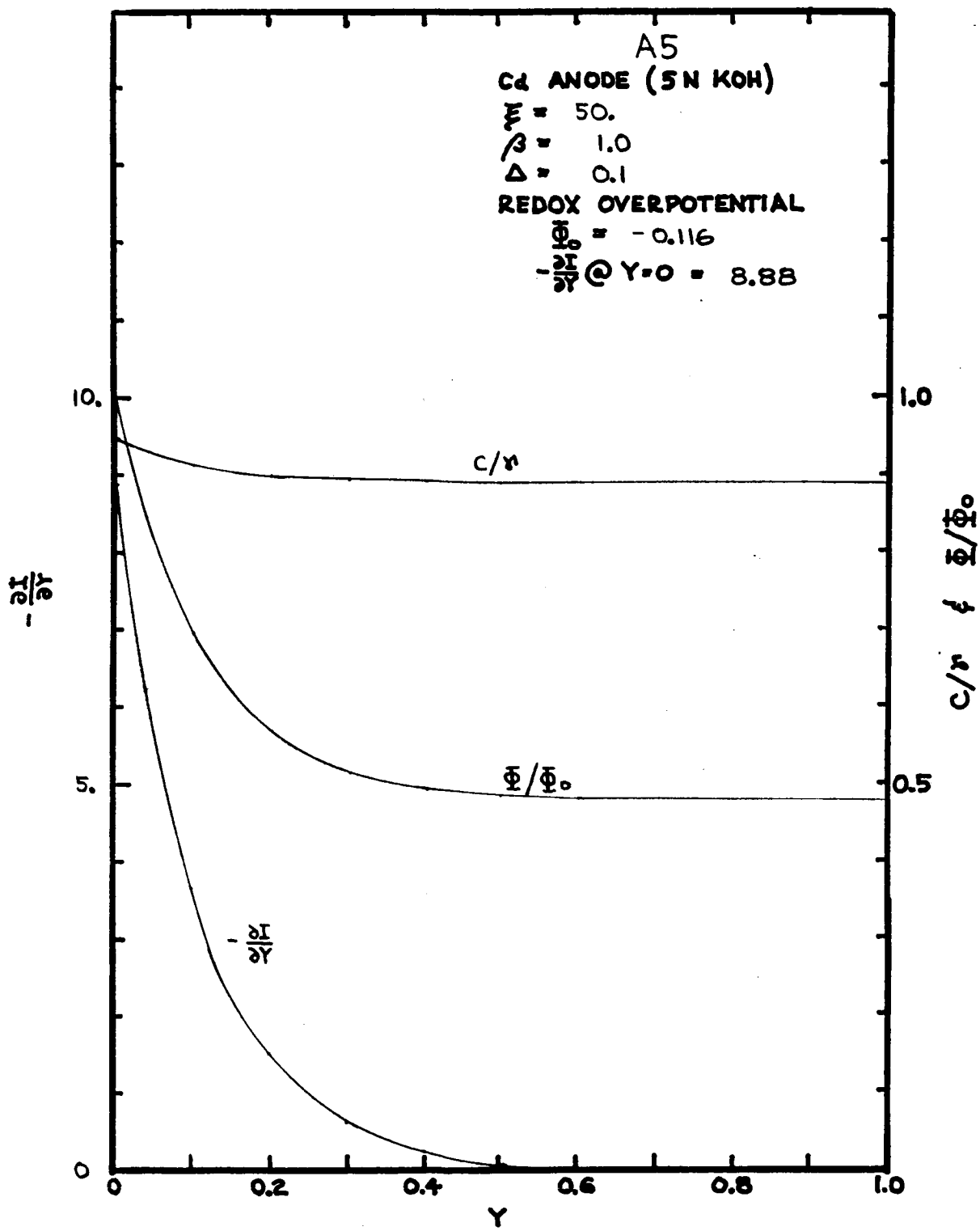
A5
Cd ANODE (5 N KOH)
ξ = 50.
β = 1.0
Δ = 0.1
REDOX OVERPOTENTIAL
Φ₀ = -0.116
-∂I/∂r @ Y=0 = 8.88
10.
5.
0
1.0
0.5
0
0.2
0.4
0.6
0.8
1.0
Y
C/r
Φ/Φ₀
-∂I/∂Y
-∂I/∂r
C/r & Φ/Φ₀

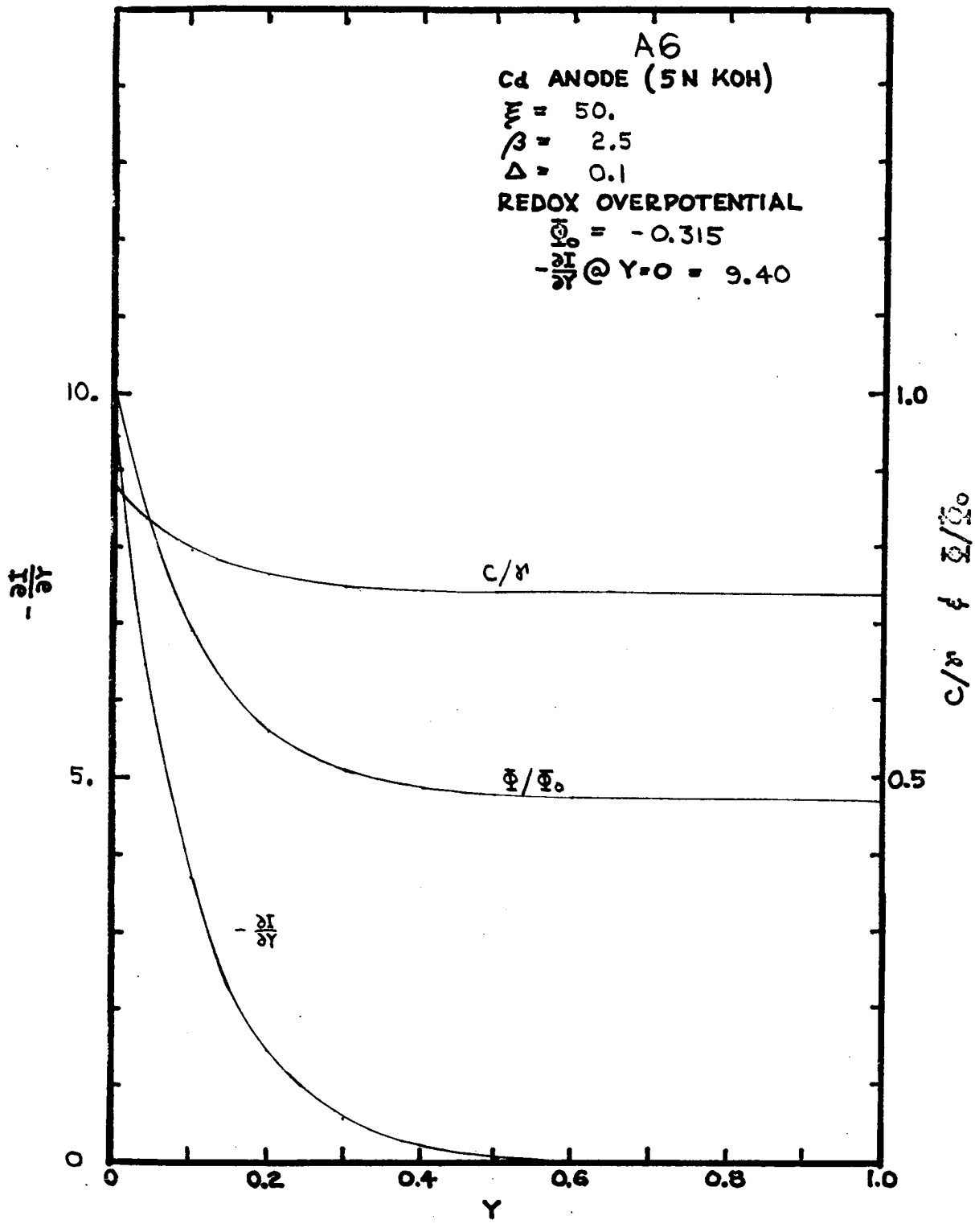
A6
Cd ANODE (5N KOH)
ξ = 50.
β = 2.5
Δ = 0.1
REDOX OVERPOTENTIAL
Φ₀ = -0.315
-∂I/∂Y @ Y=0 = 9.40
10.
5.
0
1.0
0.5
0
0.2
0.4
0.6
0.8
1.0
Y
C/γ
Φ/Φ₀
-∂I/∂Y
-∂I/∂e
C/γ & Ω/Ω₀

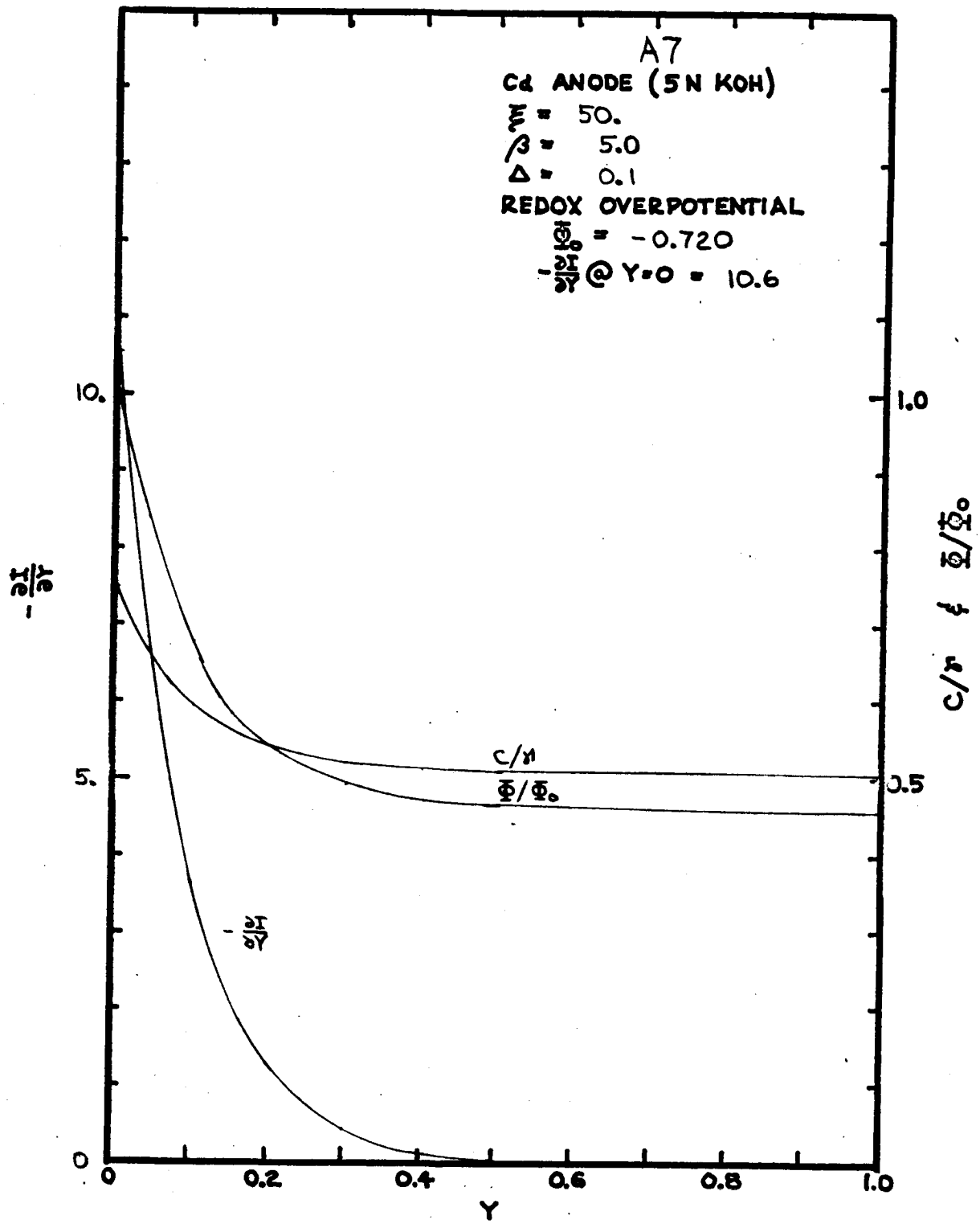
A7
Cd ANODE (5 N KOH)
ξ = 50.
β = 5.0
Δ = 0.1
REDOX OVERPOTENTIAL
Φ/Φ₀ = -0.720
-∂Φ/∂ξ @ Y=0 = 10.6
10.
5.
0
1.0
0.5
0
0.2
0.4
0.6
0.8
1.0
Y
-∂Φ/∂ξ
C/κ & Φ/Φ₀
C/κ
Φ/Φ₀
-∂Φ/∂Y

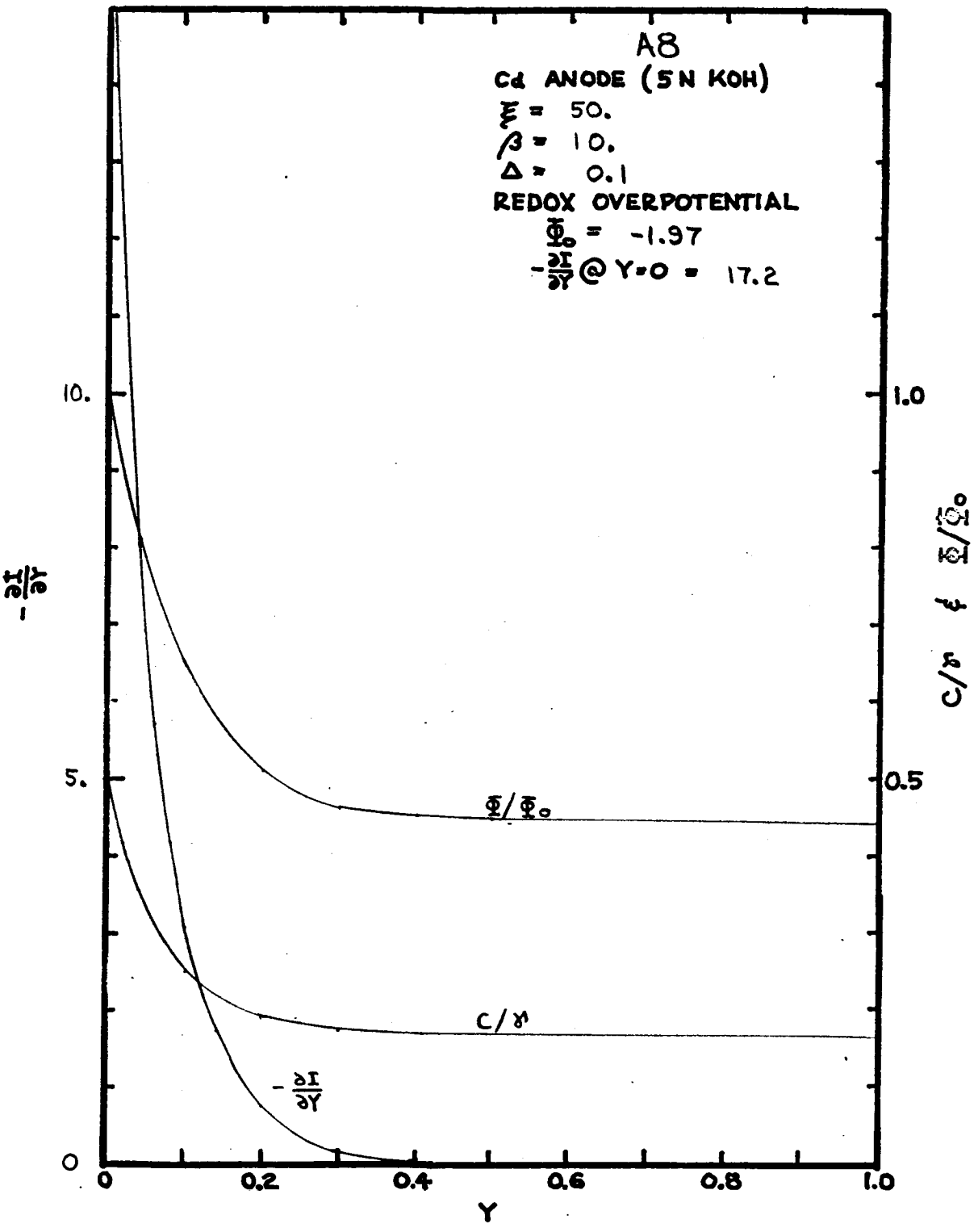
A8
Cd ANODE (5 N KOH)
ξ = 50.
β = 10.
Δ = 0.1
REDOX OVERPOTENTIAL
Φ₀ = -1.97
-∂I/∂Y @ Y=0 = 17.2
10.
5.
0
1.0
0.5
0
0.2
0.4
0.6
0.8
1.0
Y
-∂I/∂Y
Φ/Φ₀
C/γ
C/γ ξ Ξ/Ξ₀

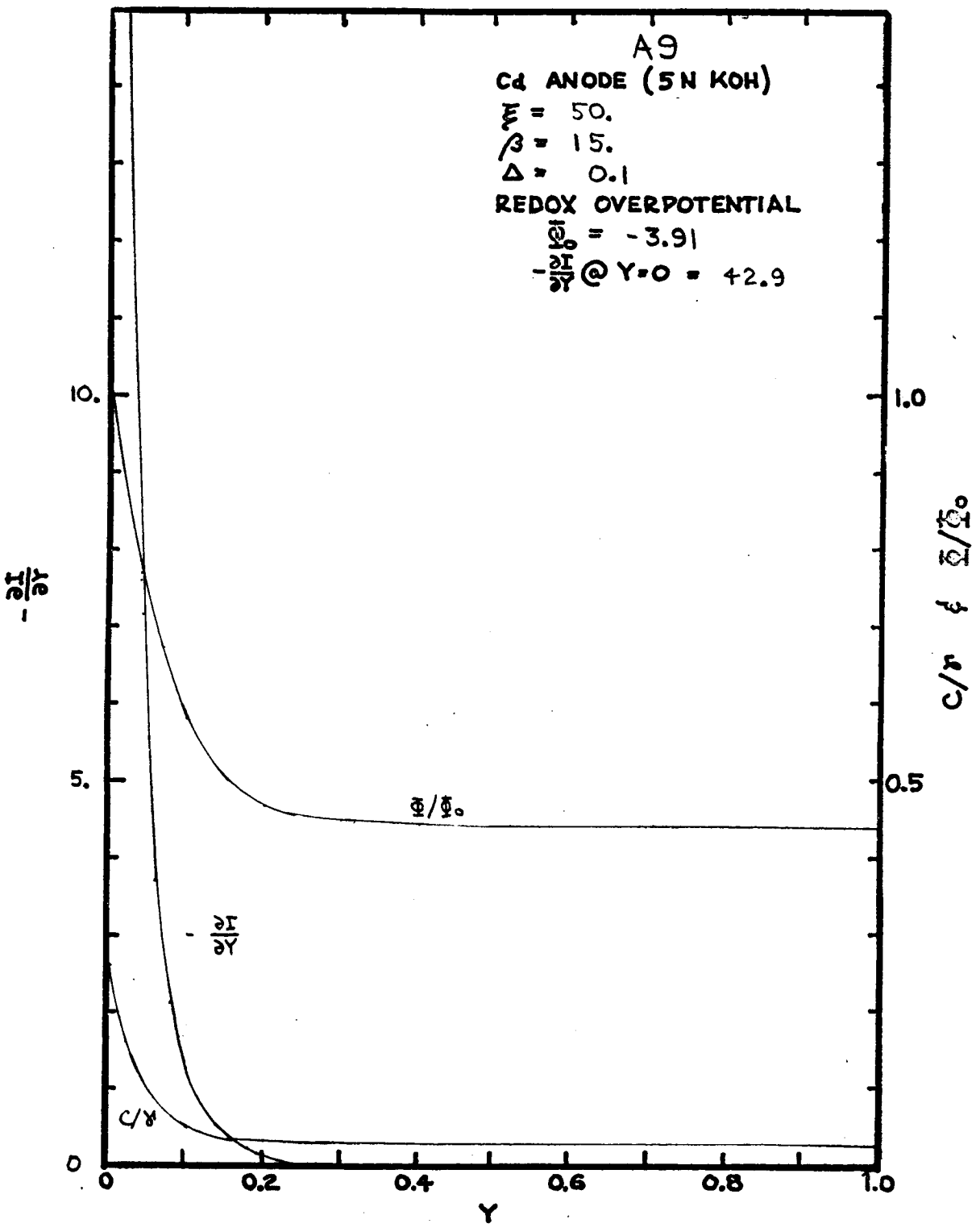
A9
Cd ANODE (5N KOH)
ξ = 50.
β = 15.
Δ = 0.1
REDOX OVERPOTENTIAL
$\frac{F\phi_0}{RT}$ = -3.91
$-\frac{\partial}{\partial Y}\frac{F\phi}{RT}$ @ Y=0 = 42.9
$-\frac{\partial}{\partial Y}\frac{F\phi}{RT}$
Φ/Φ_0
C/γ
C/γ & Φ/Φ_0
Y
0
0.2
0.4
0.6
0.8
1.0
5.
10.
0.5
1.0

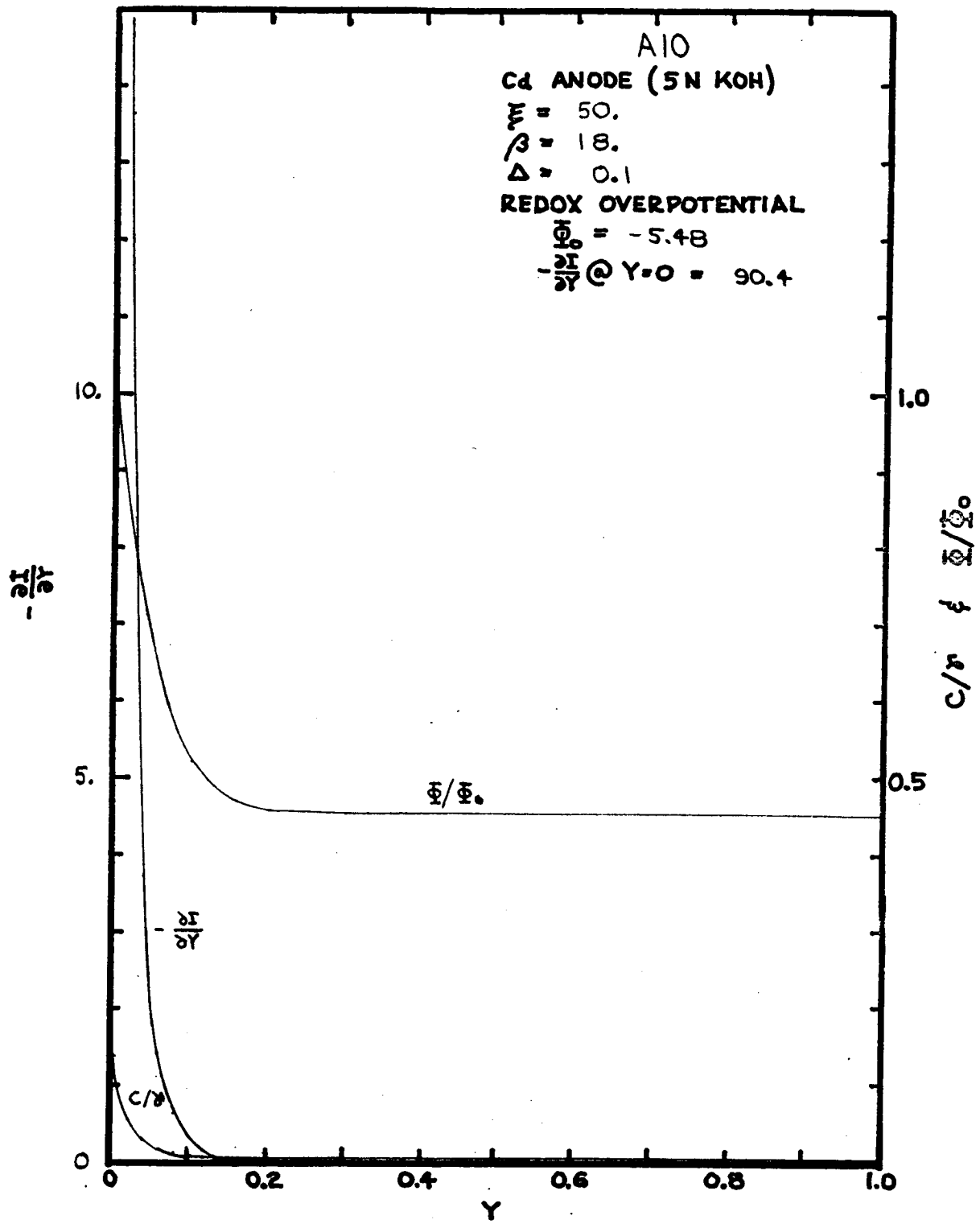
A10
Cd ANODE (5N KOH)
Ξ = 50.
β = 18.
Δ = 0.1
REDOX OVERPOTENTIAL
Φ₀ = -5.48
-∂Φ/∂ξ @ Y=0 = 90.4
10.
5.
0
1.0
0.5
0
0.2
0.4
0.6
0.8
1.0
Y
Φ/Φ₀
-∂Φ/∂ξ
C/β
C/β & Φ/Φ₀

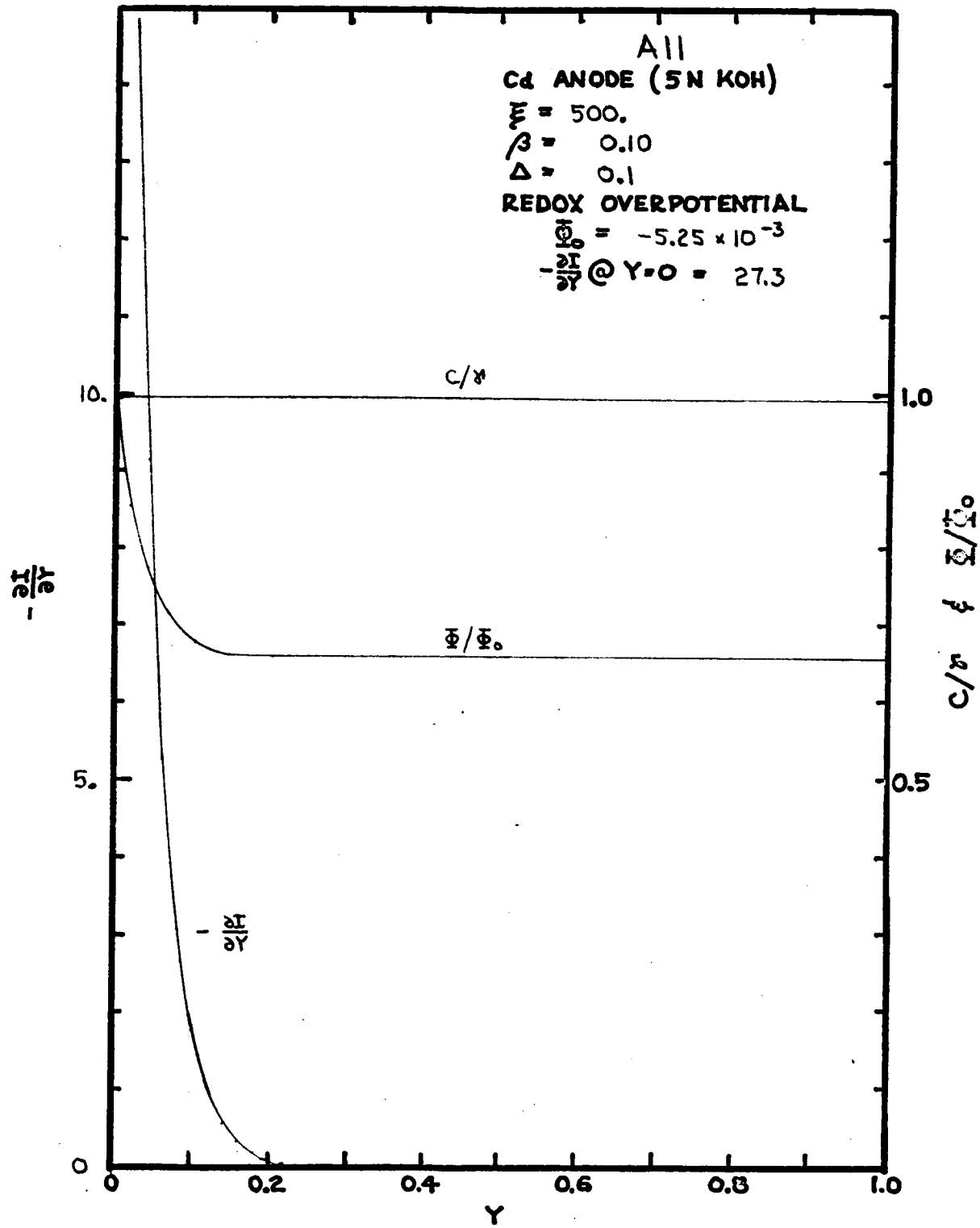
A11
Cd ANODE (5 N KOH)
ξ = 500.
β = 0.10
Δ = 0.1
REDOX OVERPOTENTIAL
Φ₀ = −5.25 × 10⁻³
−∂Σ/∂Y @ Y=0 = 27.3
C/κ
Φ/Φ₀
−∂Σ/∂Y
10.
5.
0
1.0
0.5
0
0.2
0.4
0.6
0.8
1.0
Y
−∂Σ/∂Y
C/κ & Φ/Φ₀

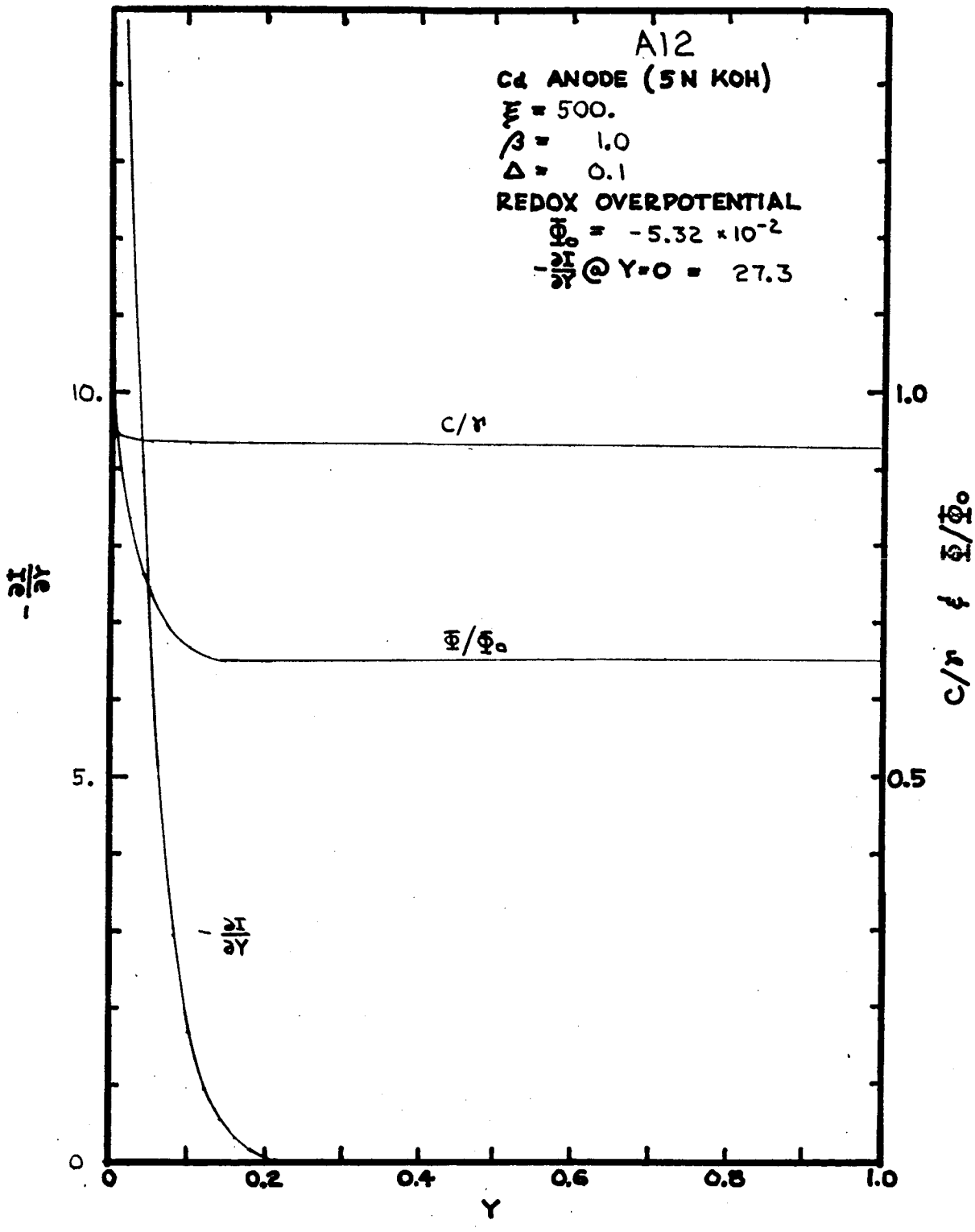
A12
Cd ANODE (5N KOH)
ξ = 500.
β = 1.0
Δ = 0.1
REDOX OVERPOTENTIAL
Φ₀ = -5.32 × 10⁻²
-∂I/∂Y @ Y=0 = 27.3
C/r
Φ/Φ₀
-∂I/∂Y
-∂I/∂Y
C/r & Φ/Φ₀
Y
10.
5.
0
1.0
0.5
0
0.2
0.4
0.6
0.8
1.0

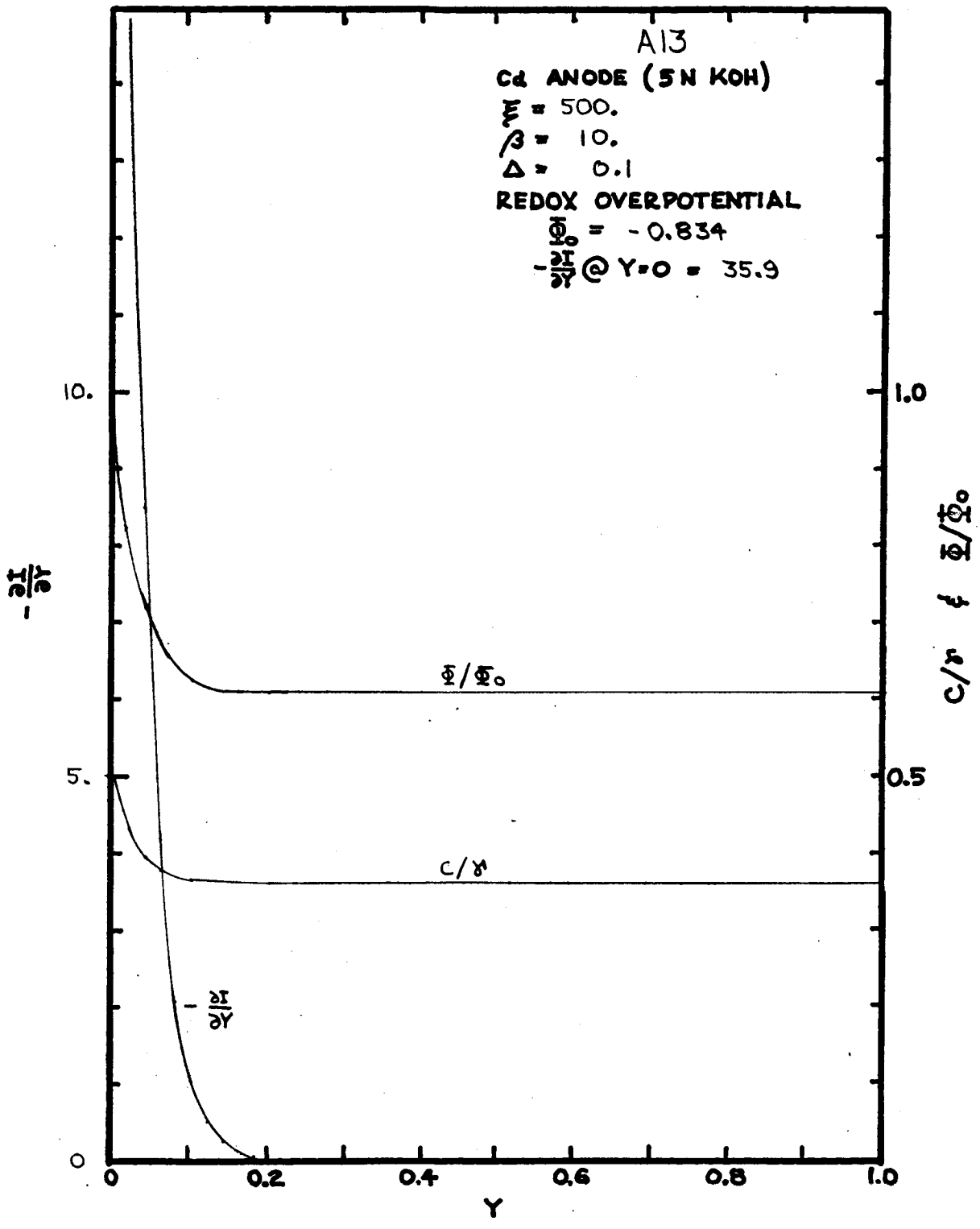
A13
Cd ANODE (5N KOH)
ξ = 500.
β = 10.
Δ = 0.1
REDOX OVERPOTENTIAL
Φ₀ = -0.834
-∂I/∂Y @ Y=0 = 35.9
10.
5.
0
1.0
0.5
0
0.2
0.4
0.6
0.8
1.0
Y
-∂I/∂Y
Φ/Φ₀
C/γ
C/γ & Φ/Φ₀
-∂I/∂Y

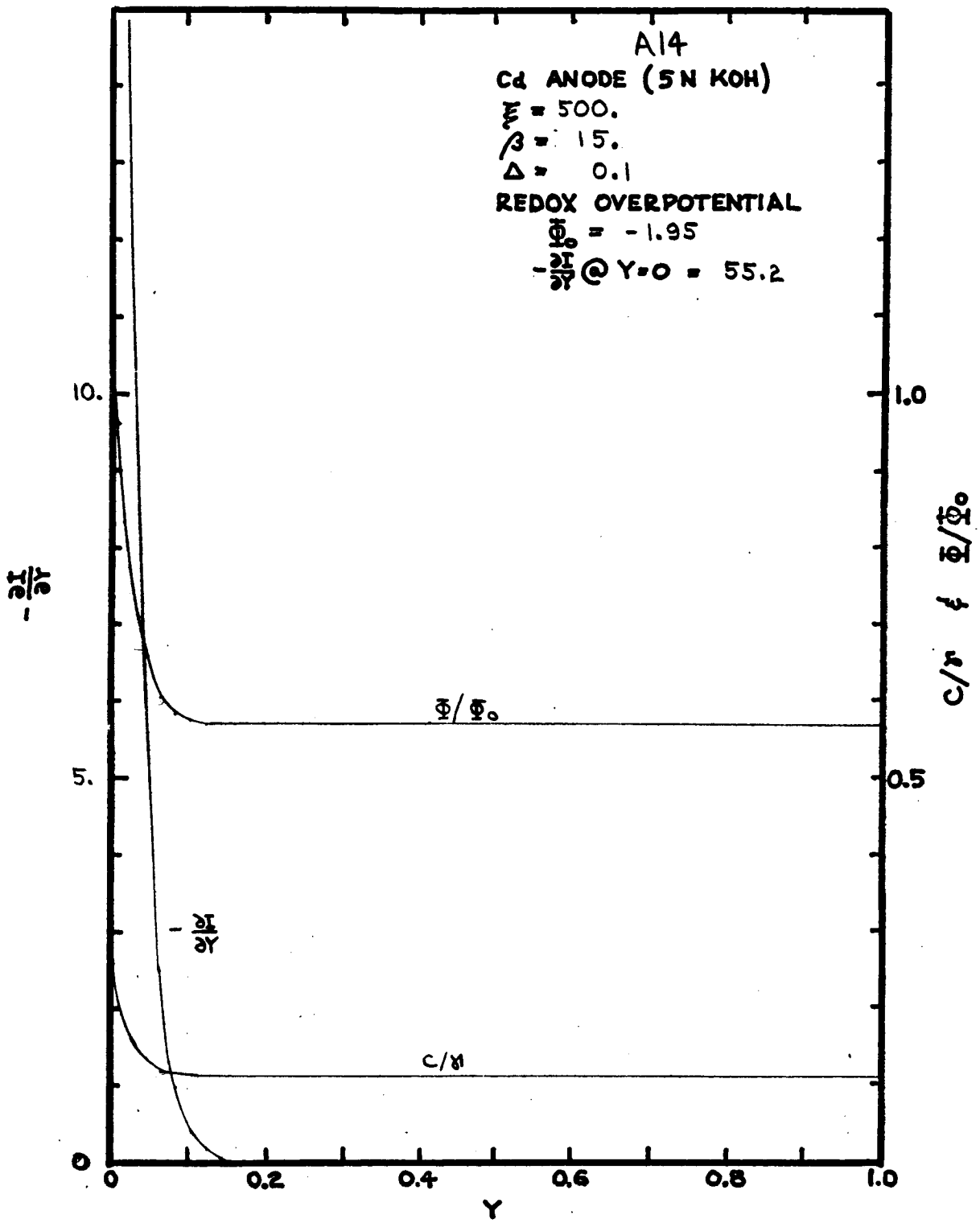
A14
Cd ANODE (5 N KOH)
ξ = 500.
β = 15.
Δ = 0.1
REDOX OVERPOTENTIAL
Φ₀ = -1.95
-∂I/∂Y @ Y=0 = 55.2
10.
5.
0
1.0
0.5
0
0.2
0.4
0.6
0.8
1.0
Y
Φ/Φ₀
-∂I/∂Y
C/R
C/R & Φ/Φ₀

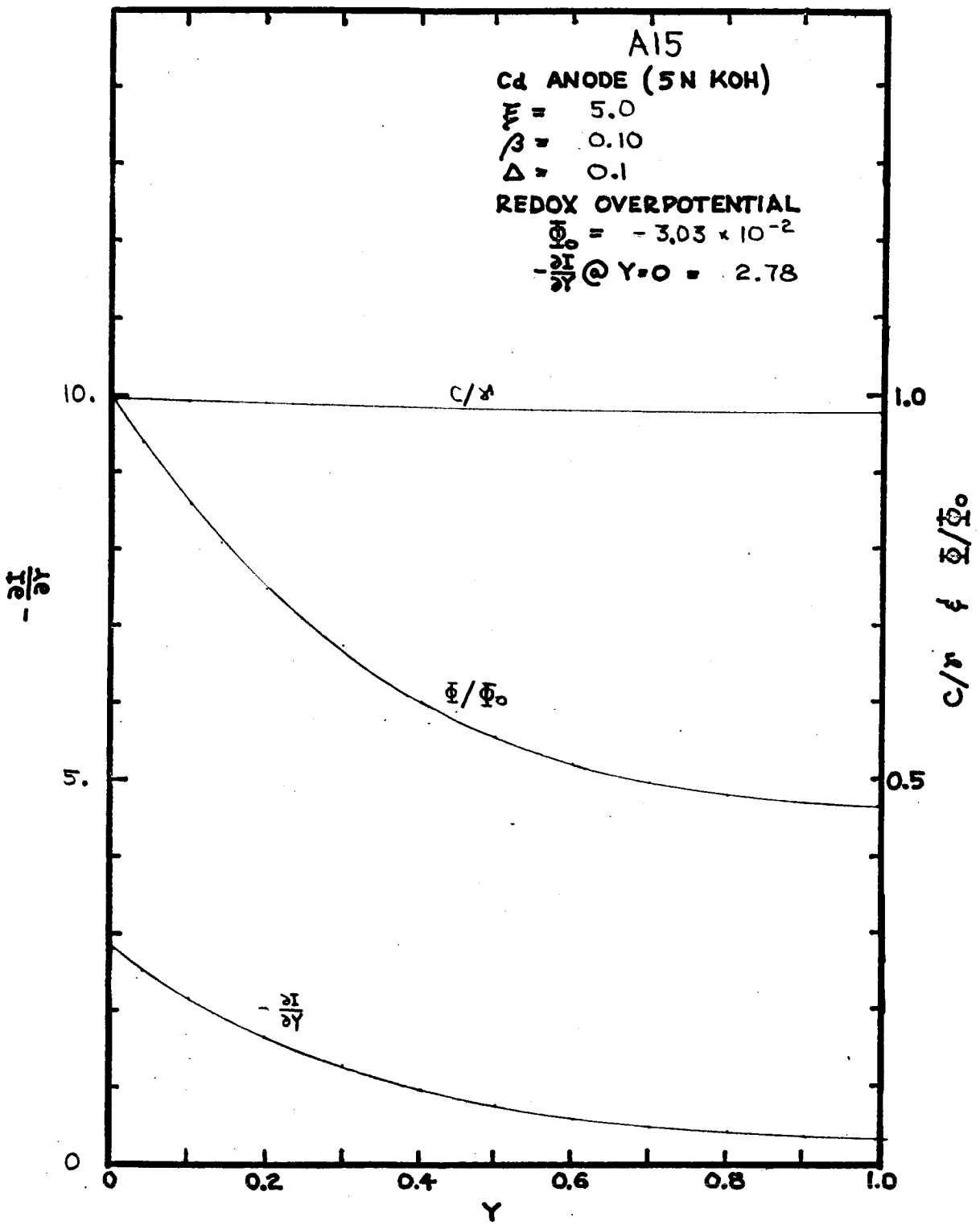
A15
Cd ANODE (5N KOH)
ξ = 5.0
β = 0.10
Δ = 0.1
REDOX OVERPOTENTIAL
Φ₀ = -3.03 × 10⁻²
-∂I/∂Y @ Y=0 = 2.78
C/κ
Φ/Φ₀
-∂I/∂Y
10.
5.
0
1.0
0.5
0
0.2
0.4
0.6
0.8
1.0
Y
-∂I/∂Y
C/κ & Φ/Φ₀

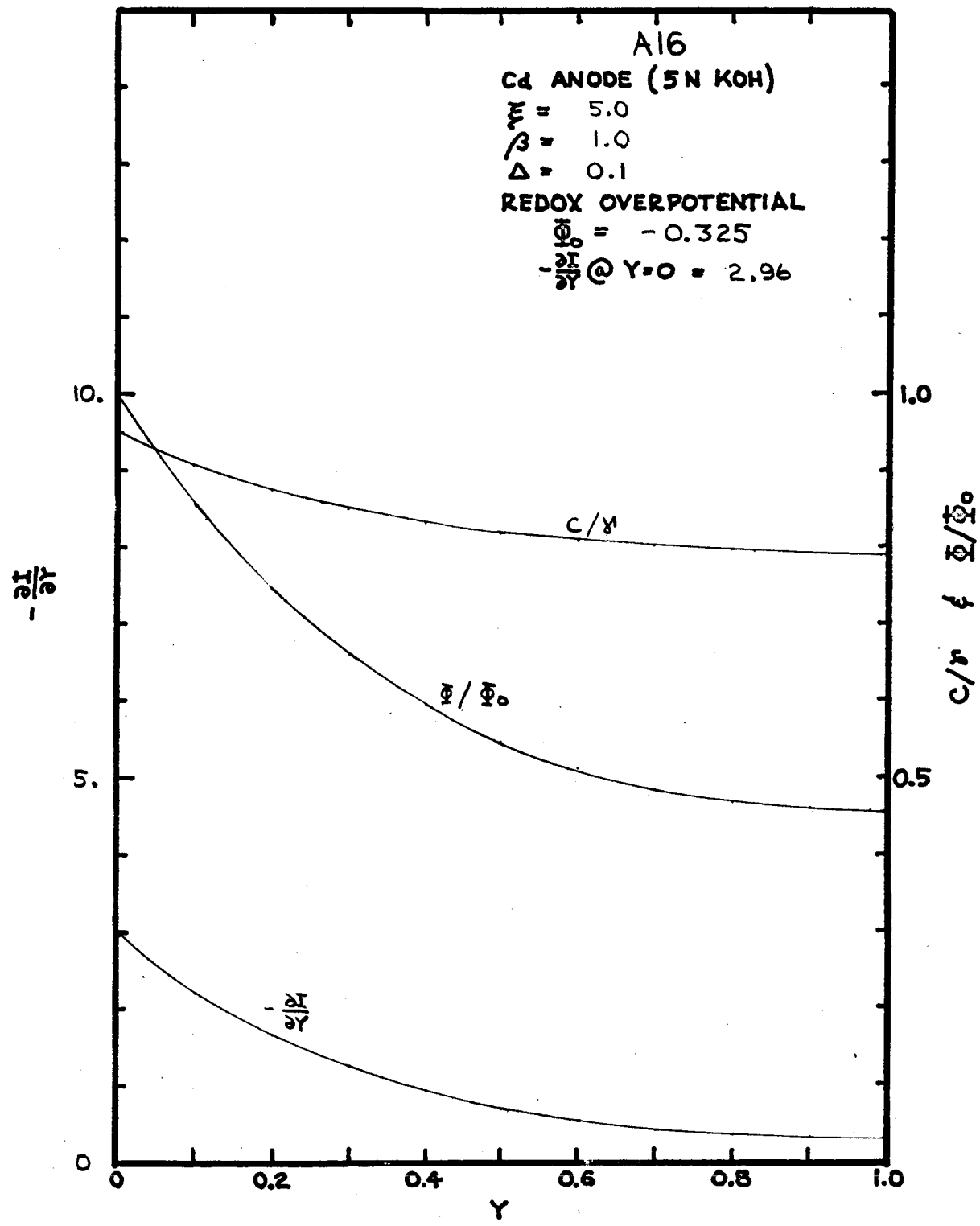
A16
Cd ANODE (5N KOH)
ξ = 5.0
β = 1.0
Δ = 0.1
REDOX OVERPOTENTIAL
Φ0 = -0.325
-∂η/∂Y @ Y=0 = 2.96
10.
5.
0
1.0
0.5
0
0.2
0.4
0.6
0.8
1.0
Y
C/γ
Φ/Φ0
-∂η/∂Y
C/γ & Φ/Φ0

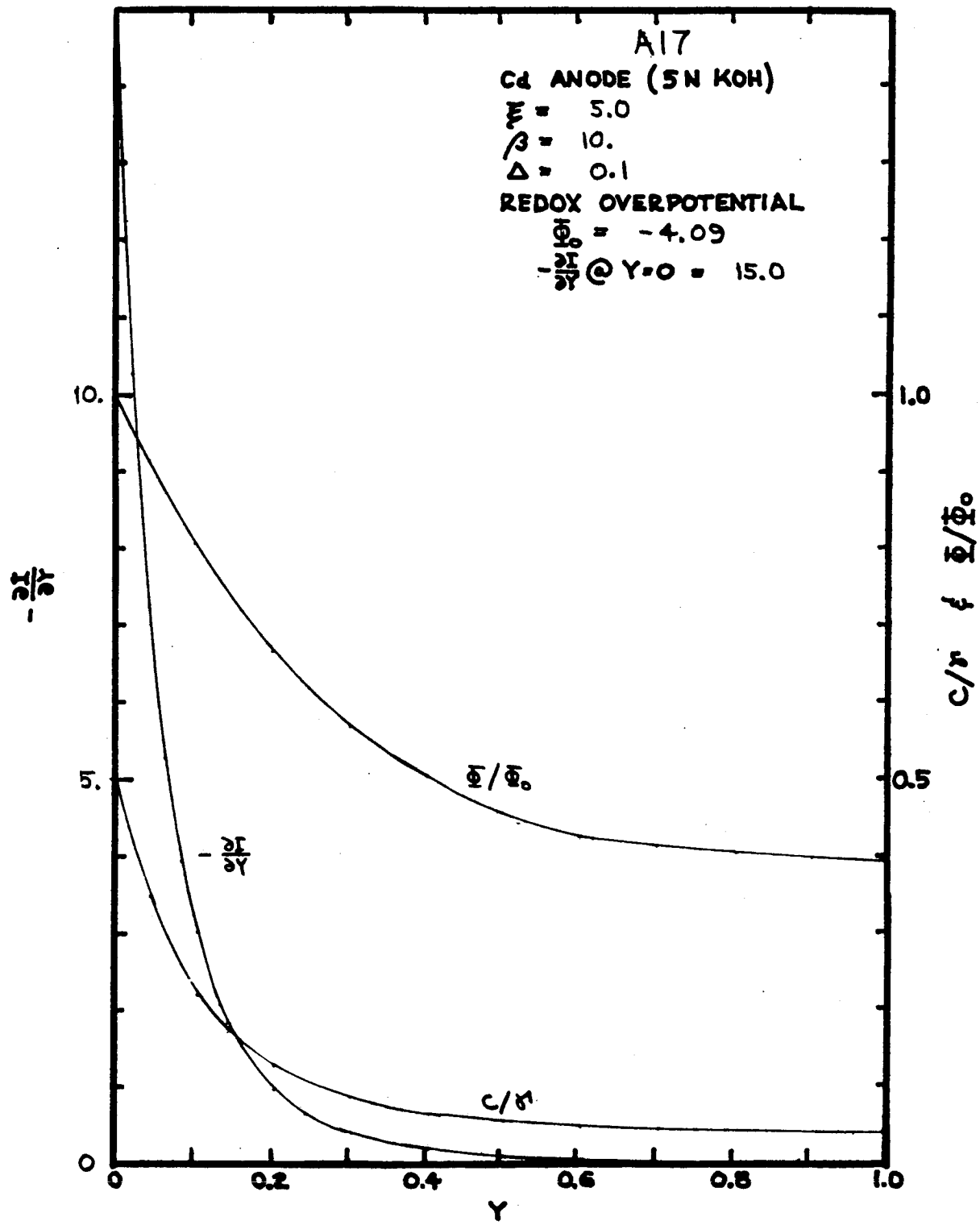
A17
Cd ANODE (5N KOH)
ξ = 5.0
β = 10.
Δ = 0.1
REDOX OVERPOTENTIAL
Φ₀ = -4.09
-∂Ψ/∂ξ @ Y=0 = 15.0
10.
5.
0
1.0
0.5
0
0.2
0.4
0.6
0.8
1.0
Y
-∂Ψ/∂ξ
C/κ & Φ/Φ₀
Φ/Φ₀
-∂Ψ/∂Y
C/κ

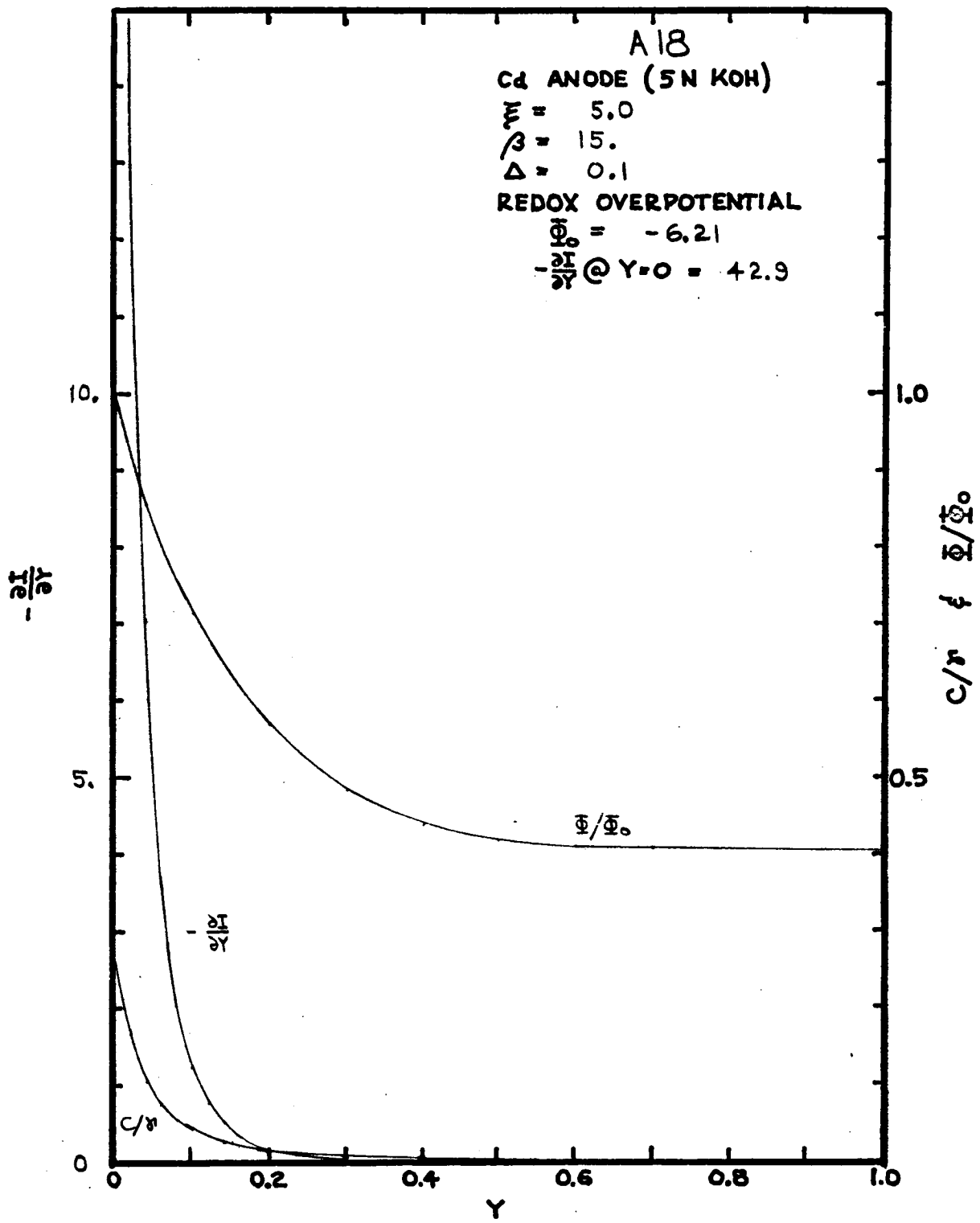
A18
Cd ANODE (5N KOH)
ξ = 5.0
β = 15.
Δ = 0.1
REDOX OVERPOTENTIAL
Φ₀ = -6.21
-∂i/∂Y @ Y=0 = 42.9
10.
5.
0
1.0
0.5
0
0.2
0.4
0.6
0.8
1.0
Y
-∂i/∂Y
Φ/Φ₀
-∂i/∂Y
C/R
C/R & Φ/Φ₀

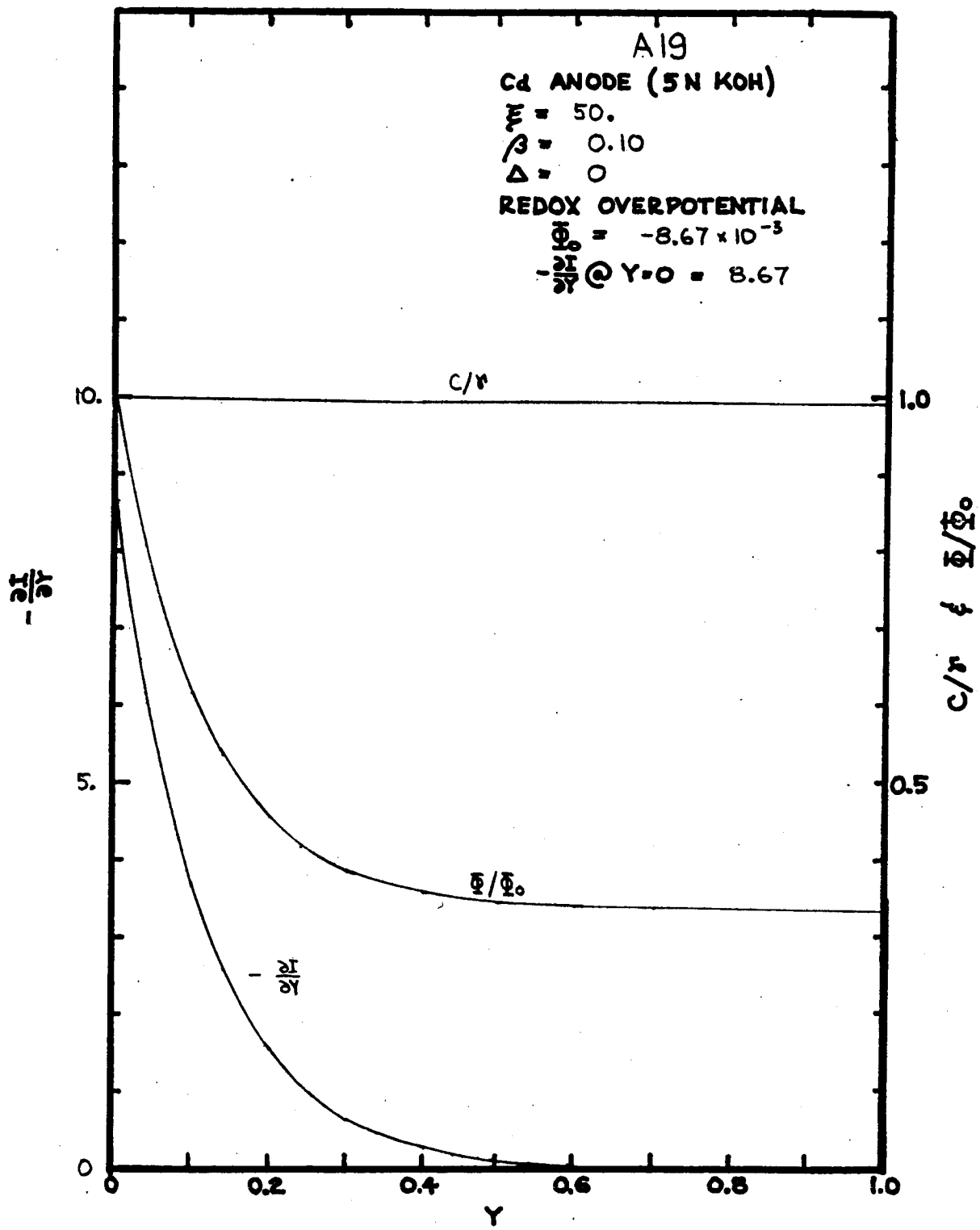
A19
Cd ANODE (5N KOH)
ξ = 50.
β = 0.10
Δ = 0
REDOX OVERPOTENTIAL
Φ₀ = -8.67 × 10⁻³
-∂Φ/∂Y @ Y=0 = 8.67
C/r
Φ/Φ₀
-∂Φ/∂Y
10.
5.
0
1.0
0.5
0
0.2
0.4
0.6
0.8
1.0
Y
-∂Φ/∂Y
C/r & Φ/Φ₀

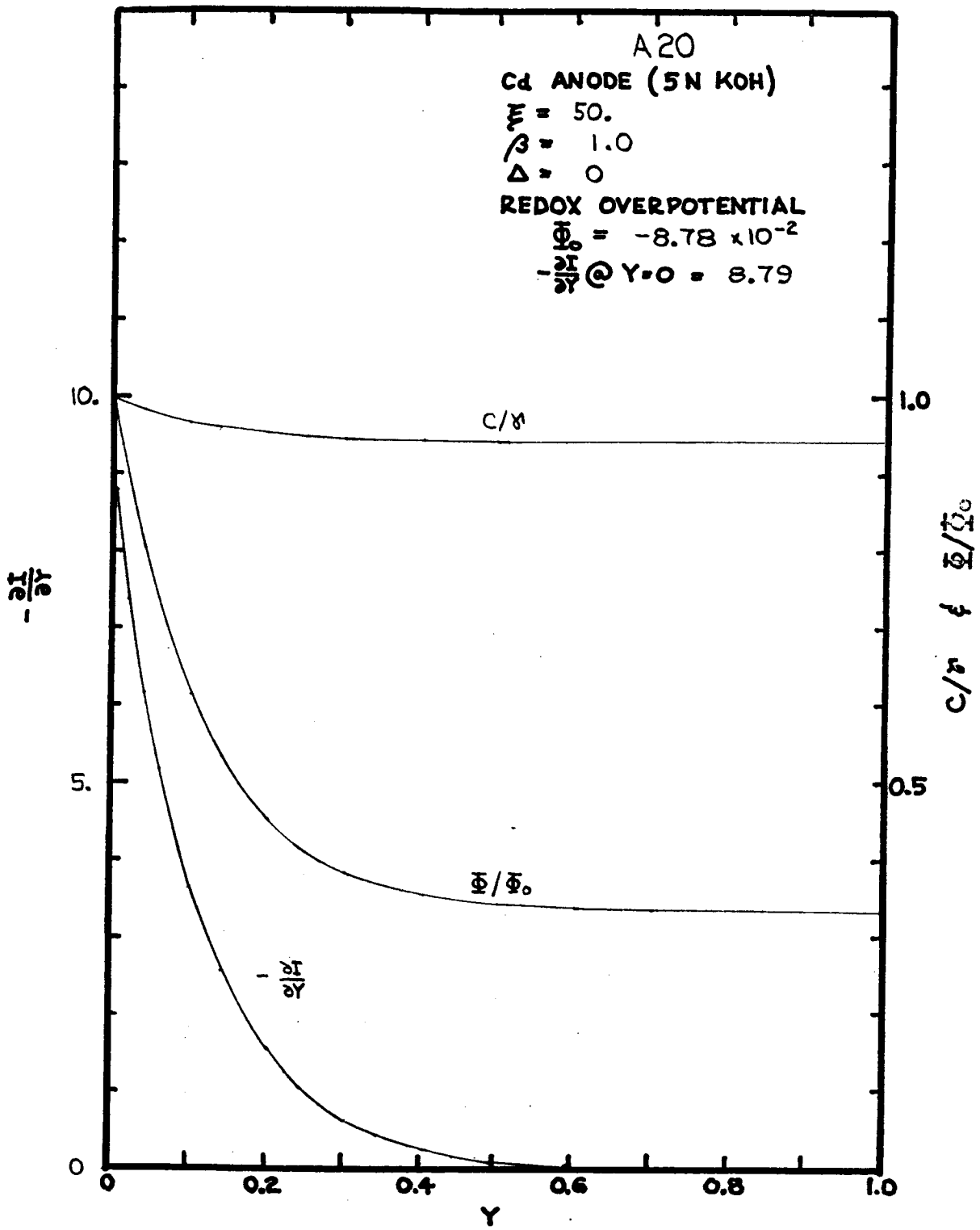
A20
Cd ANODE (5N KOH)
ξ = 50.
β = 1.0
Δ = 0
REDOX OVERPOTENTIAL
Φ₀ = -8.78 x10⁻²
-∂I/∂Y @ Y=0 = 8.79
C/γ
Φ/Φ₀
-∂I/∂Y
-∂I/∂Y
C/γ & Φ/Φ₀
Y
10.
5.
0
1.0
0.5
0
0.2
0.4
0.6
0.8
1.0

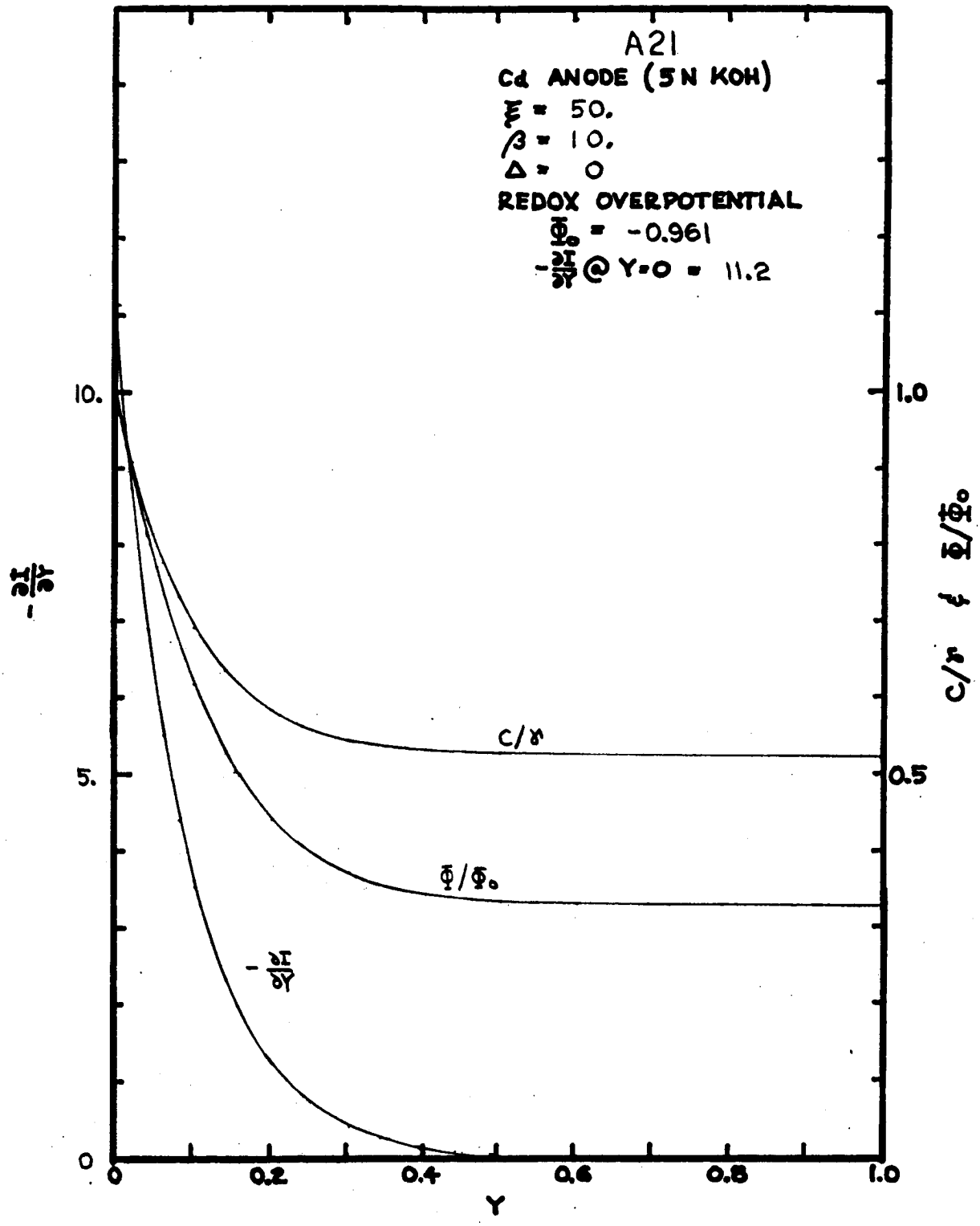
A21
Cd ANODE (5N KOH)
ξ = 50.
β = 10.
Δ = 0
REDOX OVERPOTENTIAL
Φ₀ = -0.961
-∂Φ/∂Y @ Y=0 = 11.2
10.
5.
0
1.0
0.5
0
0.2
0.4
0.6
0.8
1.0
Y
C/γ
Φ/Φ₀
-∂Φ/∂Y
C/γ & Φ/Φ₀

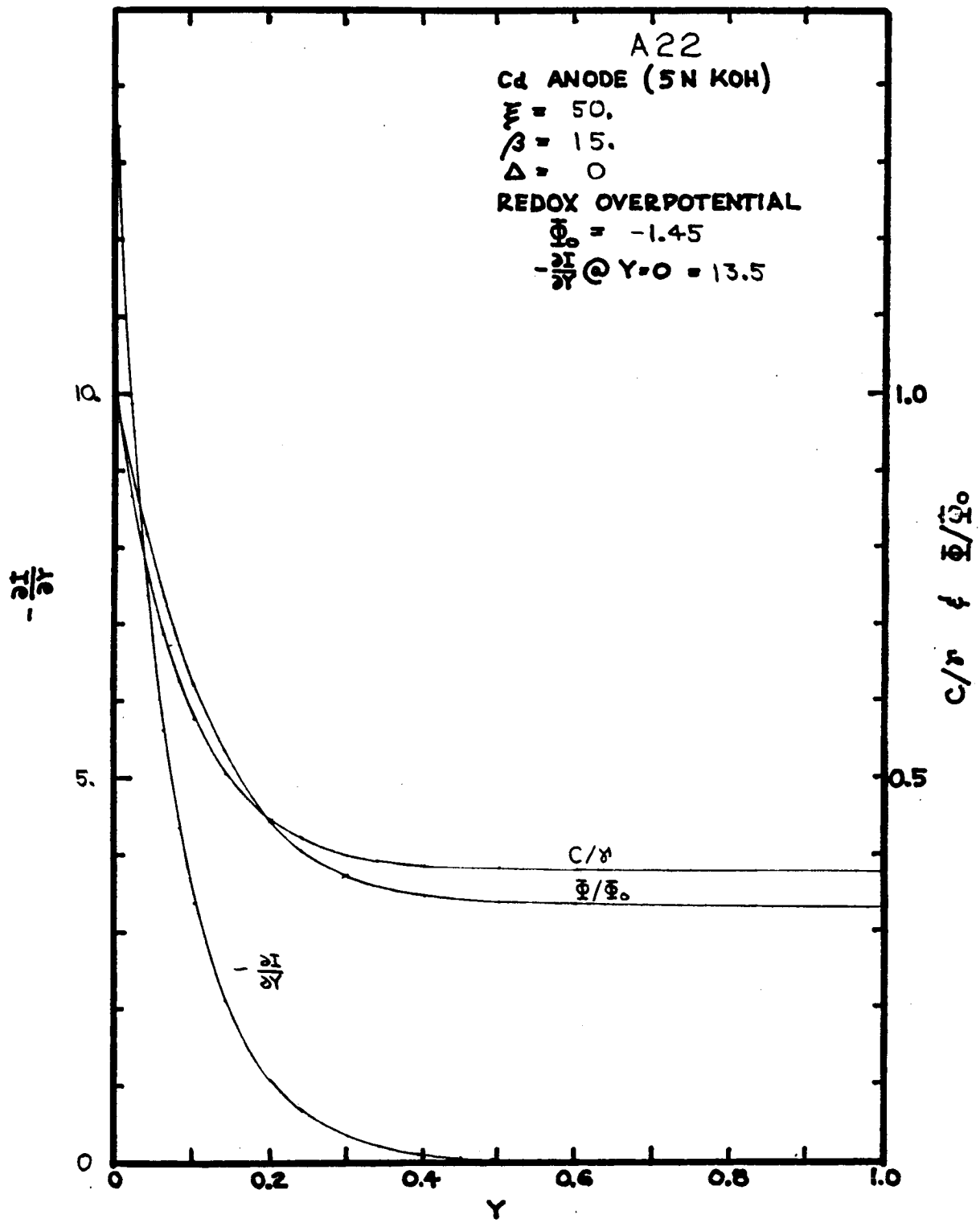
A22
Cd ANODE (5N KOH)
ξ = 50.
β = 15.
Δ = 0
REDOX OVERPOTENTIAL
Φ₀ = -1.45
-∂Γ/∂Y @ Y=0 = 13.5
10.
5.
0
1.0
0.5
0
0.2
0.4
0.6
0.8
1.0
Y
C/γ
Φ/Φ₀
-∂Γ/∂Y
C/γ & Φ/Φ₀

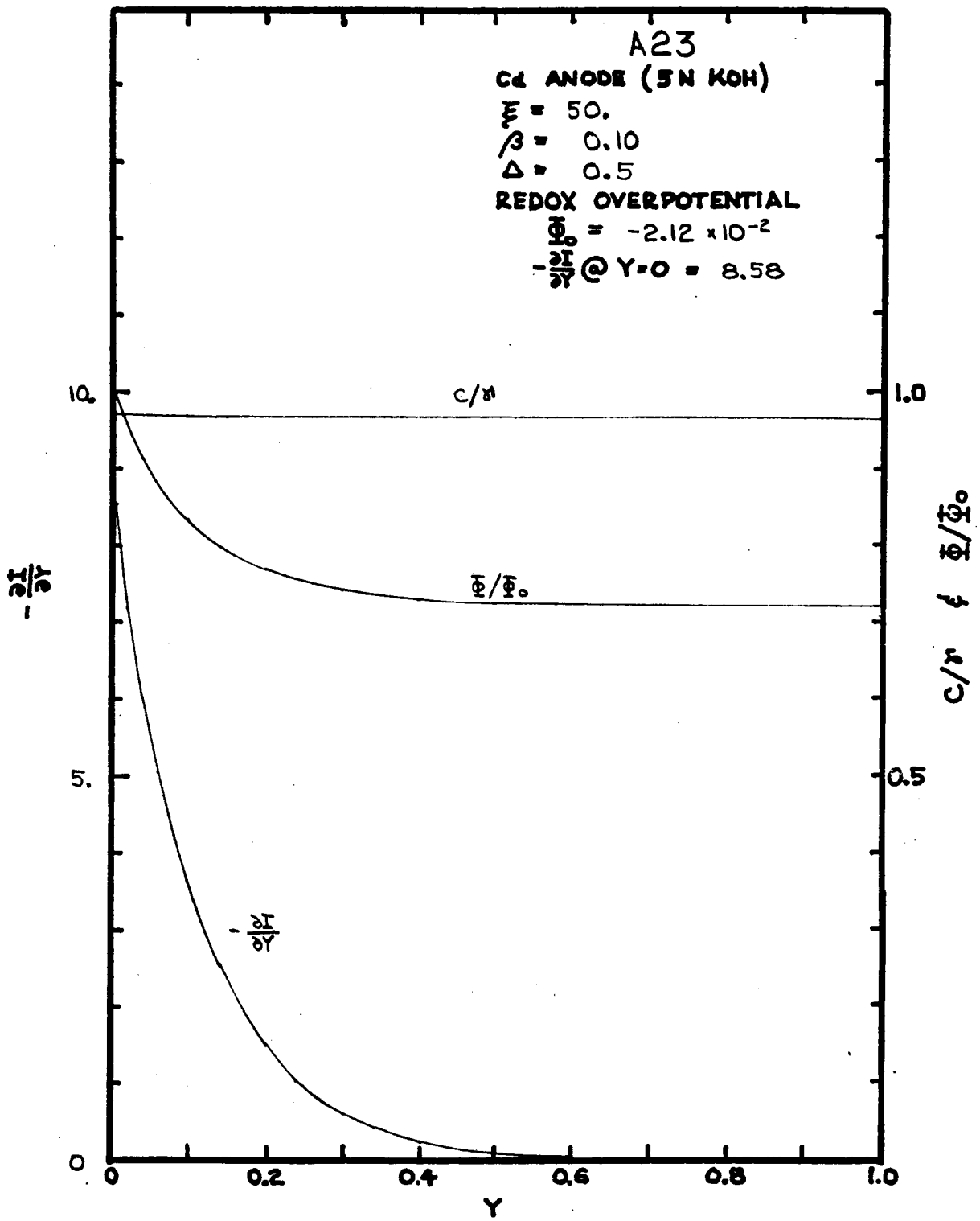
A23
Cd ANODE (5N KOH)
ξ = 50.
β = 0.10
Δ = 0.5
REDOX OVERPOTENTIAL
Φ₀ = -2.12 x10⁻²
-∂I/∂Y @ Y=0 = 8.58
C/κ
Φ/Φ₀
-∂I/∂Y
10.
5.
0
1.0
0.5
0
0.2
0.4
0.6
0.8
1.0
Y
-∂I/∂Y
C/κ & Φ/Φ₀

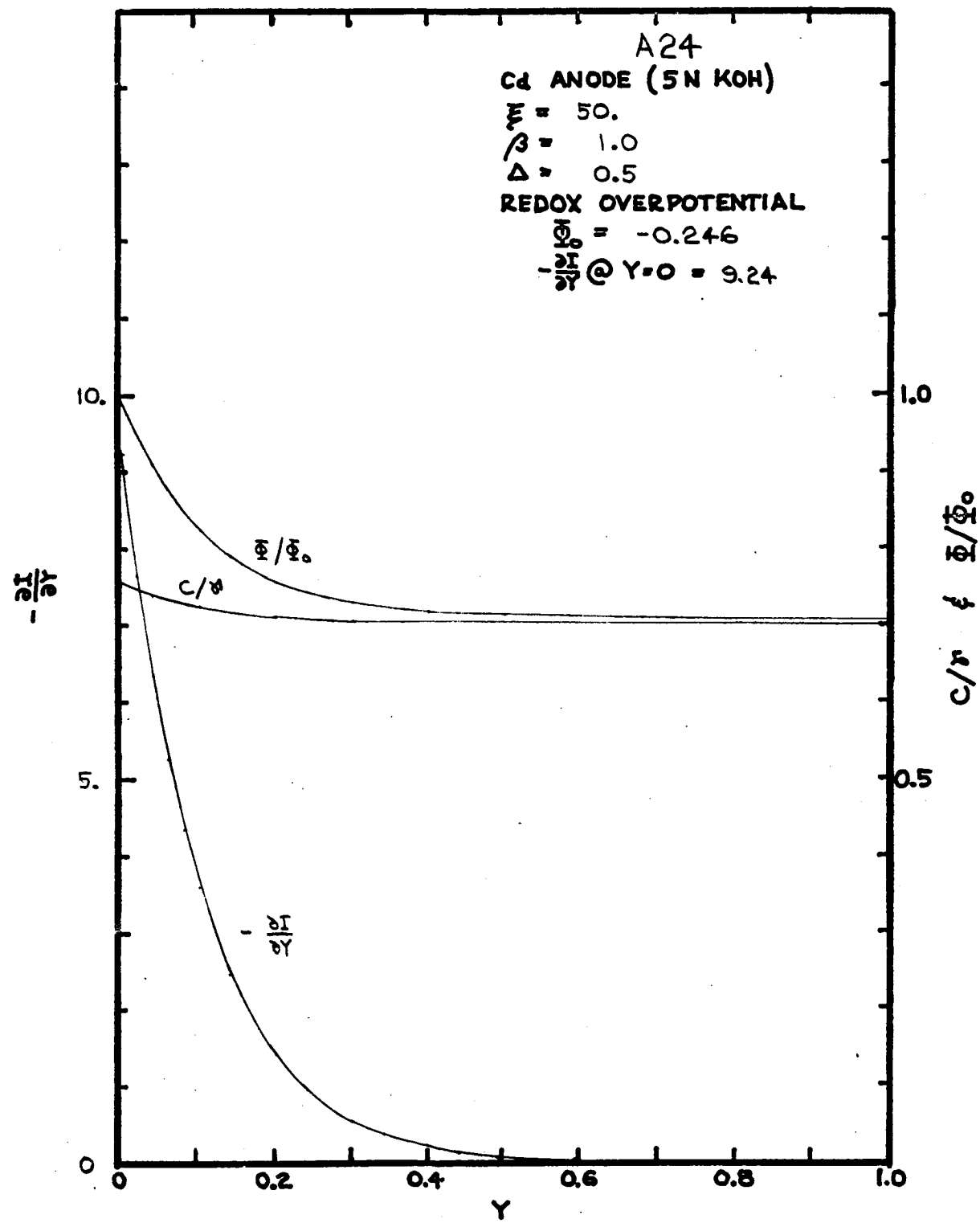
A24
Cd ANODE (5N KOH)
ξ = 50.
β = 1.0
Δ = 0.5
REDOX OVERPOTENTIAL
Φ0 = -0.246
-∂I/∂Y @ Y=0 = 9.24
10.
5.
0
1.0
0.5
0
0.2
0.4
0.6
0.8
1.0
Y
Φ/Φ0
C/β
-∂I/∂Y
C/β & Φ/Φ0

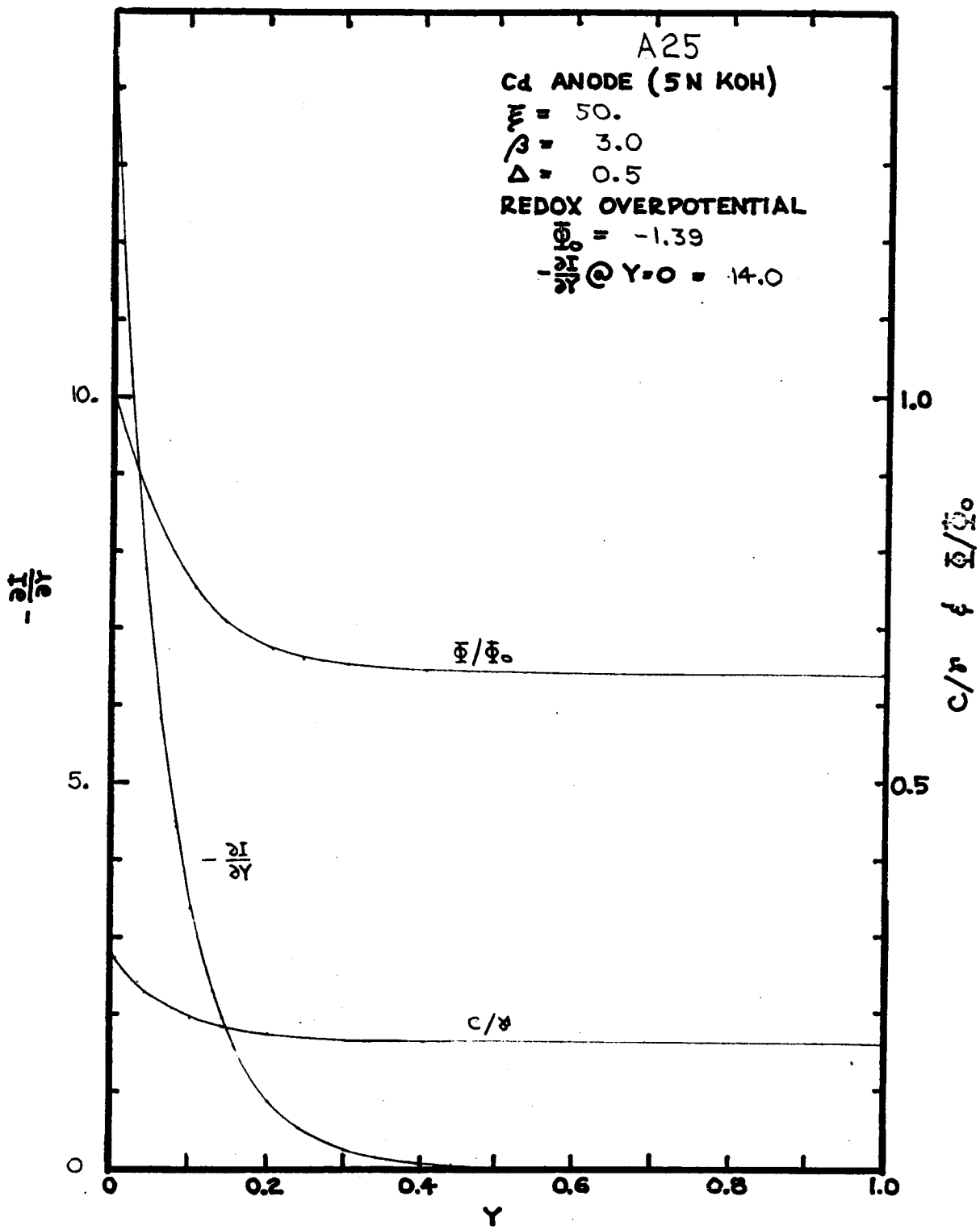
A25
Cd ANODE (5N KOH)
ξ = 50.
β = 3.0
Δ = 0.5
REDOX OVERPOTENTIAL
Φ₀ = -1.39
-∂I_R/∂Y @ Y=0 = 14.0
10.
5.
0
1.0
0.5
0
0.2
0.4
0.6
0.8
1.0
Y
Φ/Φ₀
-∂I_R/∂Y
C/ϑ
-∂I_R/∂Y
C/ϑ ϑ Φ/Φ₀

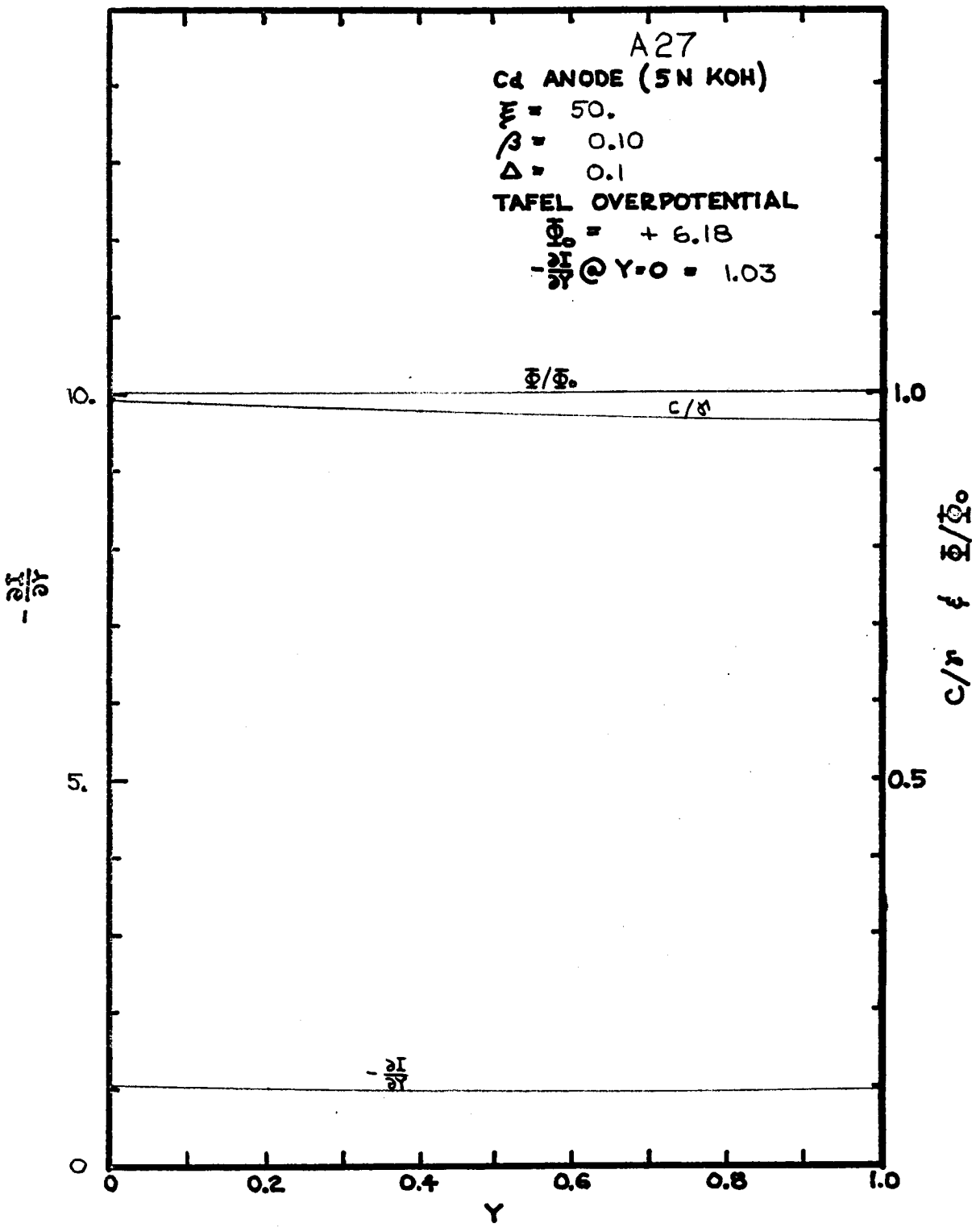
A27
Cd ANODE (5N KOH)
ξ = 50.
β = 0.10
Δ = 0.1
TAFEL OVERPOTENTIAL
Φ₀ = + 6.18
-∂Ic/∂Y @ Y=0 = 1.03
Φ/Φ₀
C/β
-∂Ic/∂Y
-Ic
10.
5.
0
1.0
0.5
0
0.2
0.4
0.6
0.8
1.0
Y
-∂Ic/∂Y
C/β & Φ/Φ₀

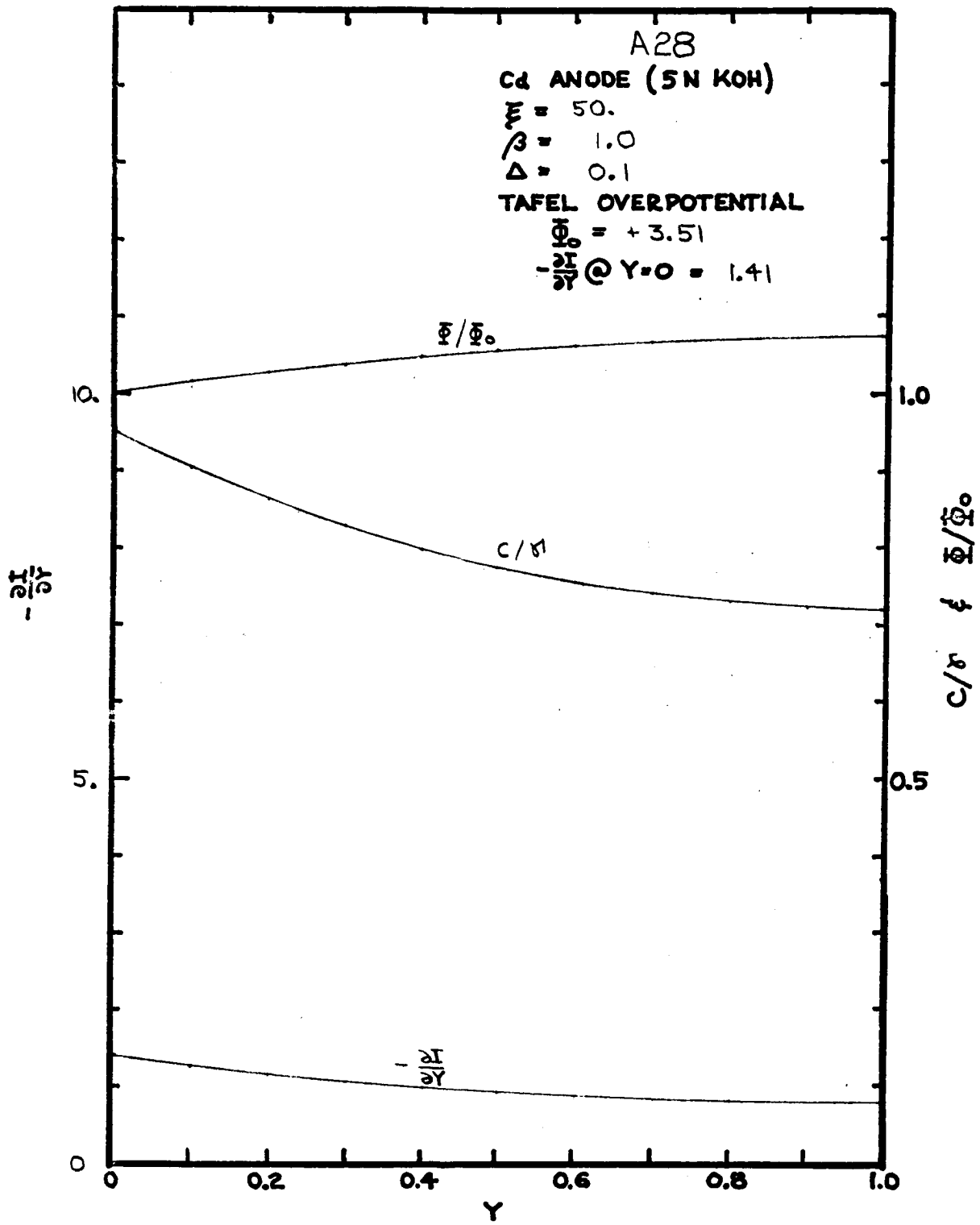
A28
Cd ANODE (5N KOH)
ξ = 50.
β = 1.0
Δ = 0.1
TAFEL OVERPOTENTIAL
Φ₀ = +3.51
-∂Σr/∂Y @ Y=0 = 1.41
Φ/Φ₀
C/β
-∂Σr/∂Y
10.
5.
0
1.0
0.5
0
0.2
0.4
0.6
0.8
1.0
Y
C/β & Φ/Φ₀

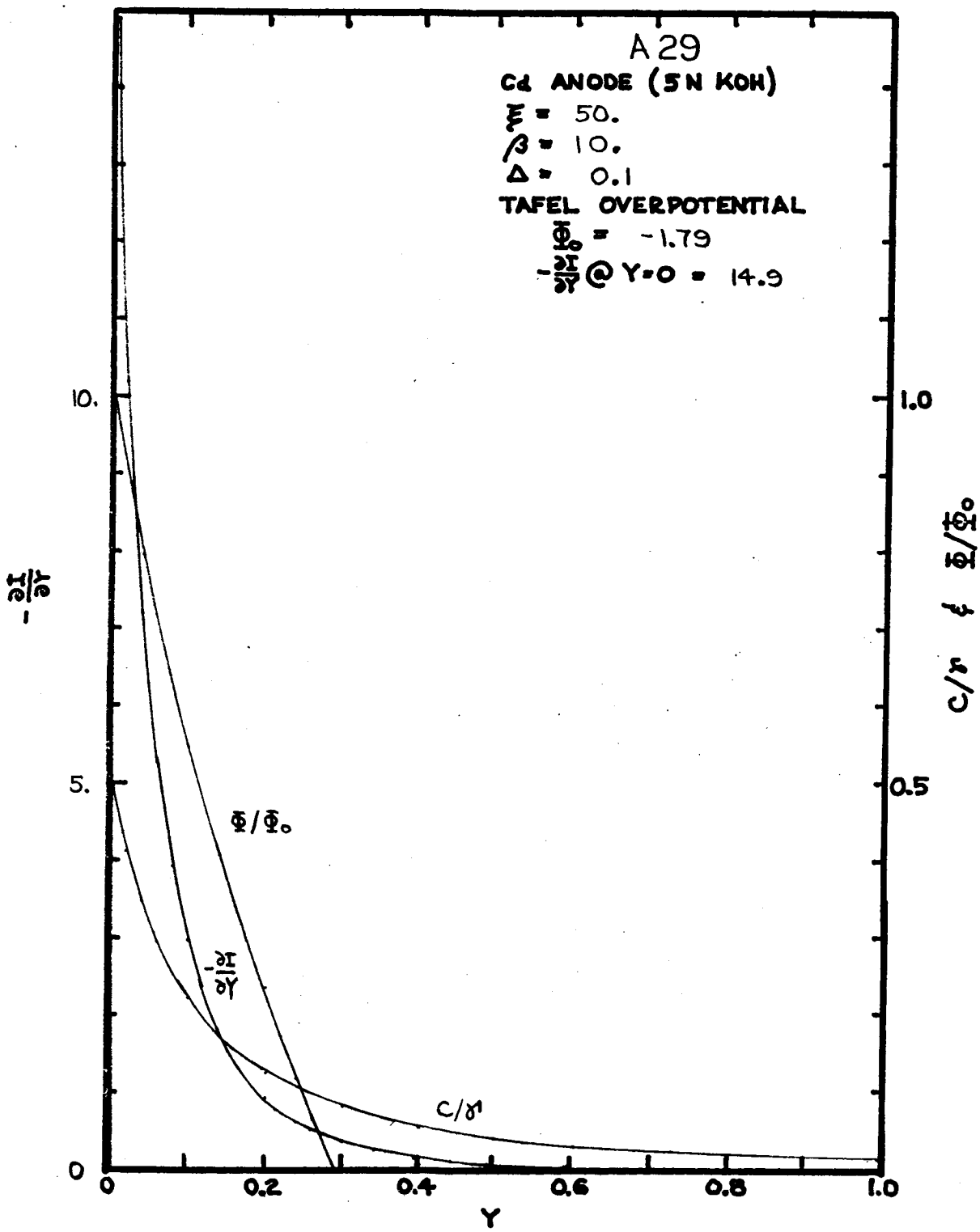
A 29
Cd ANODE (5N KOH)
ξ = 50.
β = 10.
Δ = 0.1
TAFEL OVERPOTENTIAL
Φ₀ = -1.79
-∂I/∂Y @ Y=0 = 14.9
10.
5.
0
1.0
0.5
0
0.2
0.4
0.6
0.8
1.0
Y
-∂I/∂Y
C/γ & Φ/Φ₀
Φ/Φ₀
-∂I/∂Y
C/γ

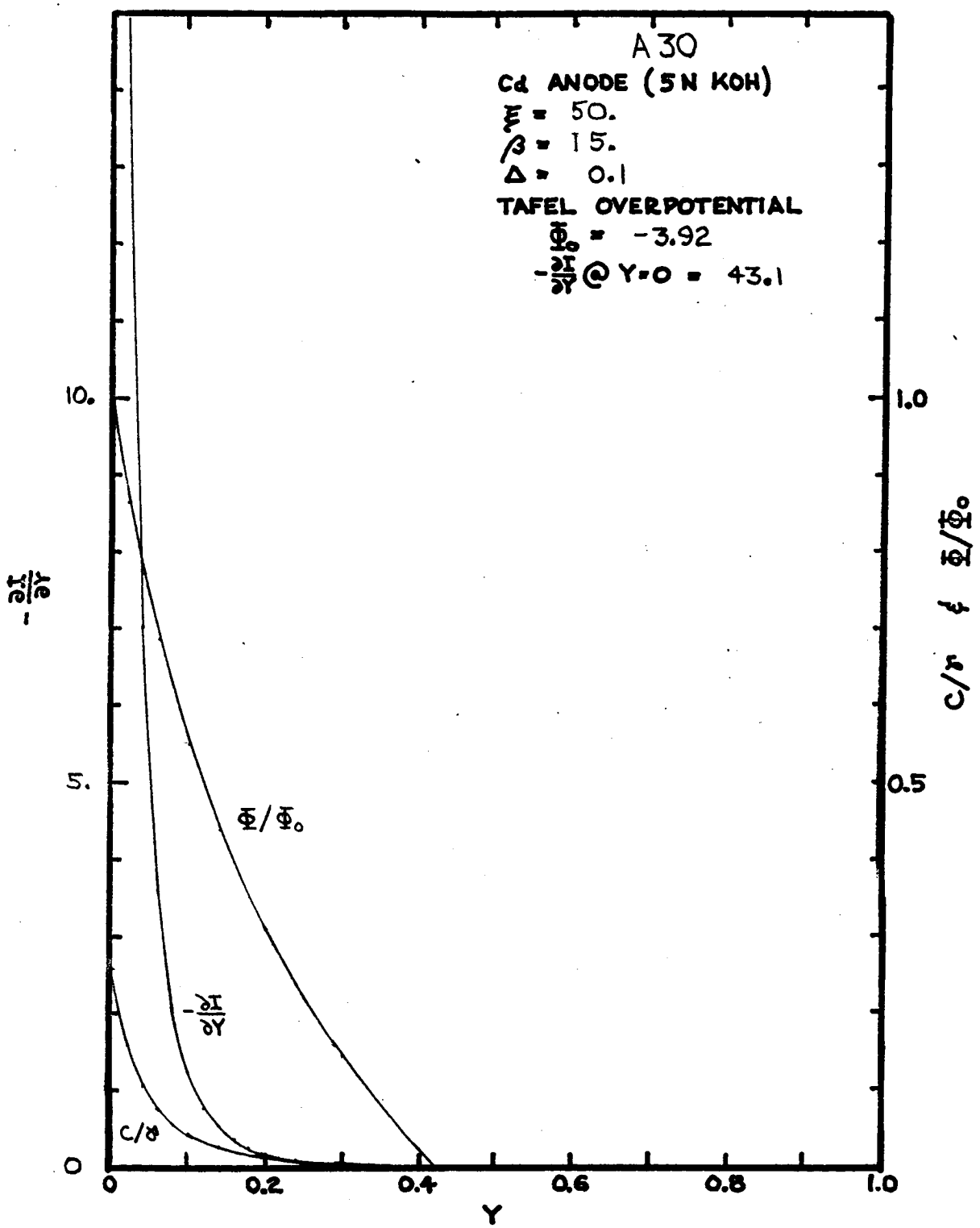
A 30
Cd ANODE (5N KOH)
ξ = 50.
β = 15.
Δ = 0.1
TAFEL OVERPOTENTIAL
Φ₀ = -3.92
-∂Φ/∂Y @ Y=0 = 43.1
10.
5.
0
1.0
0.5
0
0.2
0.4
0.6
0.8
1.0
Y
-∂C/∂Y
C/n & Φ/Φ₀
Φ/Φ₀
-∂Φ/∂Y
C/n

APPENDIX VI.

Transient Behavior of Cadmium Anode (5N KOH)

The transient behavior of the cadmium anode example, as calculated according to the one dimensional model, is contained in this appendix. For each case treated a graph is included presenting plots, vs. elapsed time since circuit completion, of transfer current density at Y = 0, electrolyte concentration at Y = 0.1, and electrode overpotential. The non-dimensional variables are used and overpotential is presented as a ratio to its steady state value.

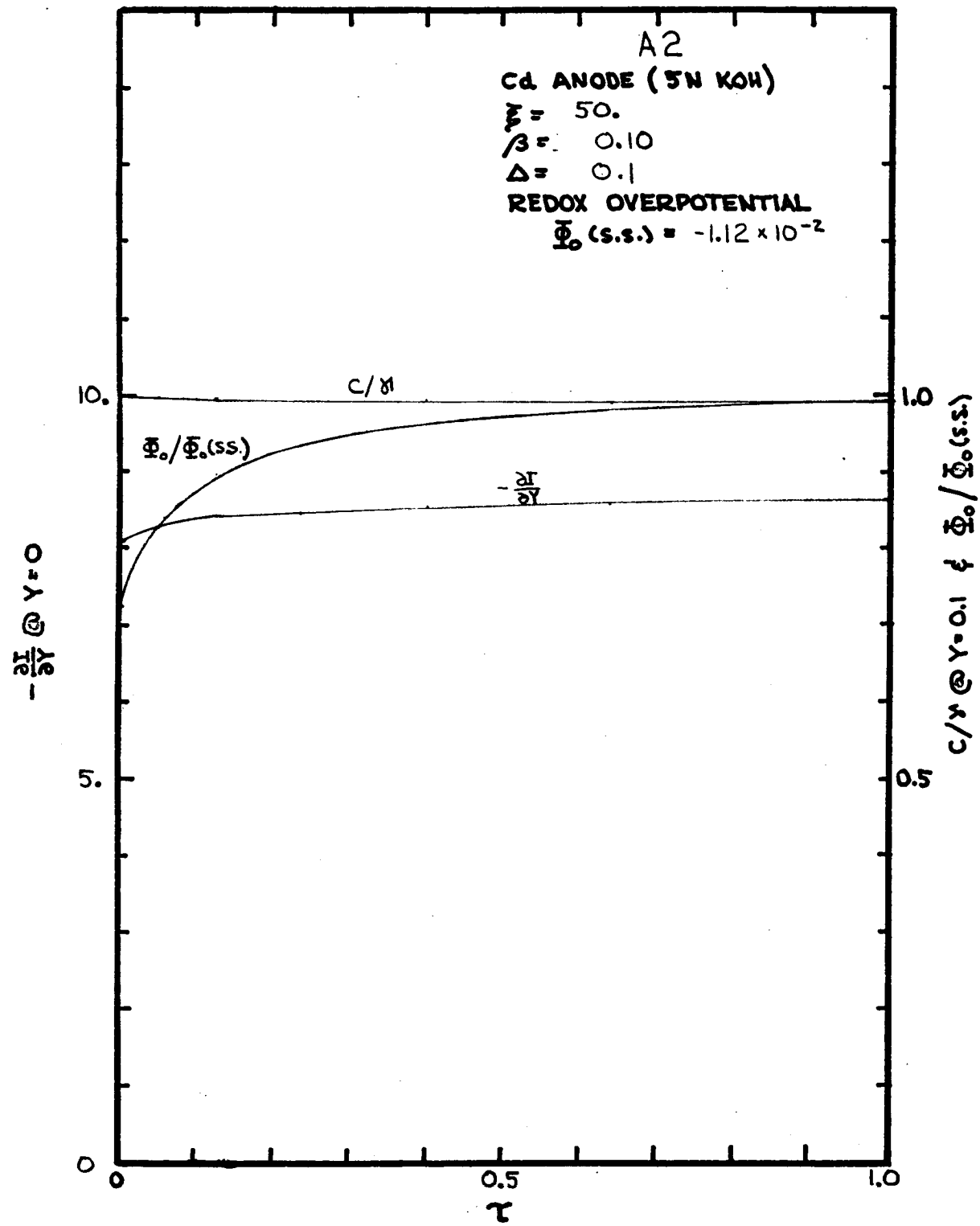
A2
Cd ANODE (5N KOH)
ξ = 50.
β = 0.10
Δ = 0.1
REDOX OVERPOTENTIAL
Φ₀ (s.s.) = -1.12 × 10⁻²
C/γ
Φ₀/Φ₀(ss.)
-∂R/∂Y
10.
5.
0
1.0
0.5
0
0.5
1.0
τ
-∂Γ/∂Y @ Y=0
C/γ @ Y=0.1 & Φ₀/Φ₀(s.s.)

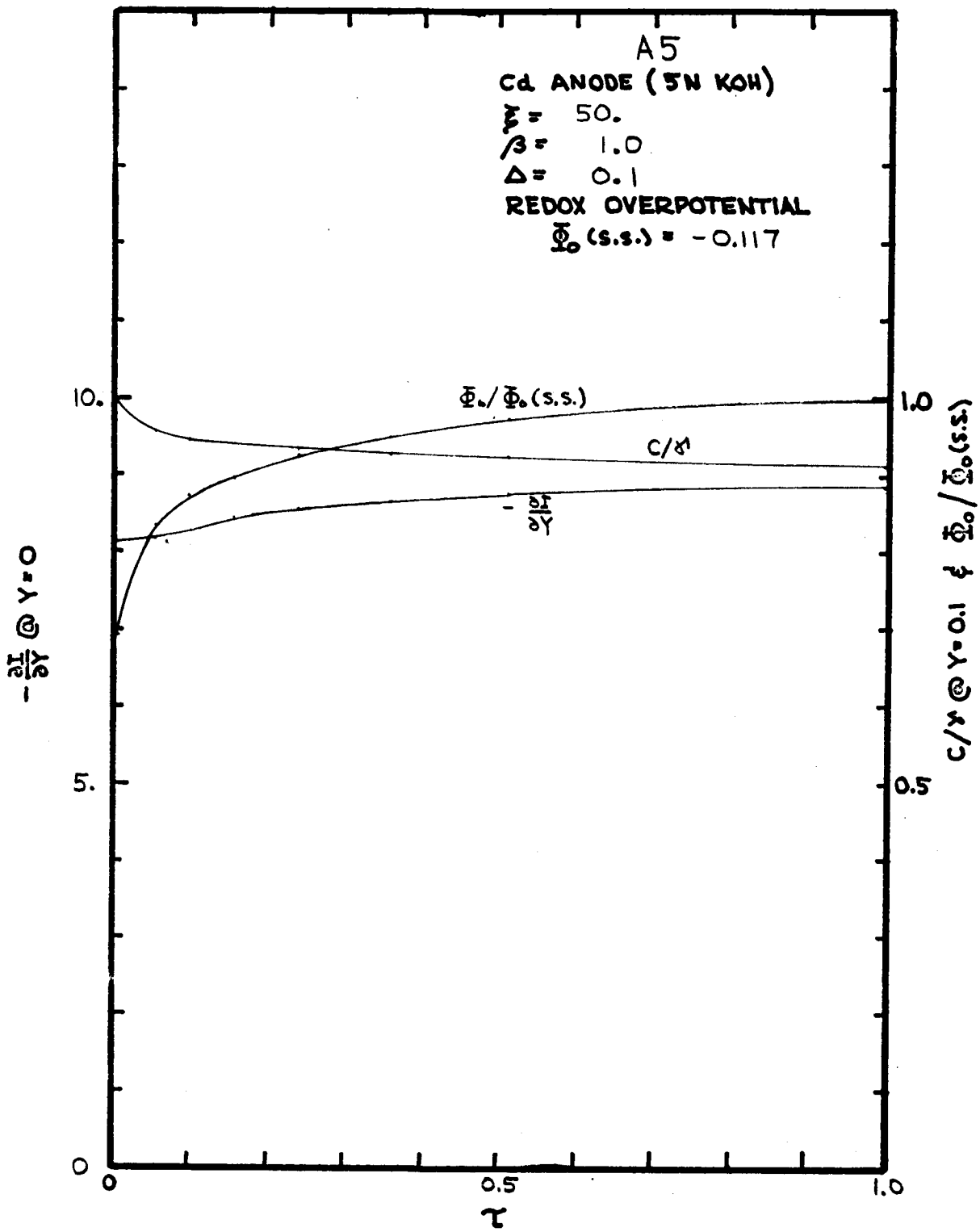
A5
Cd ANODE (5N KOH)
ξ = 50.
β = 1.0
Δ = 0.1
REDOX OVERPOTENTIAL
Φ₀ (s.s.) = -0.117
Φ/Φ₀(s.s.)
C/σ
-∂I/∂Y
10.
5.
0
0
0.5
1.0
τ
1.0
0.5
-∂I/∂Y @ Y=0
C/σ @ Y=0.1 & Φ/Φ₀(s.s.)

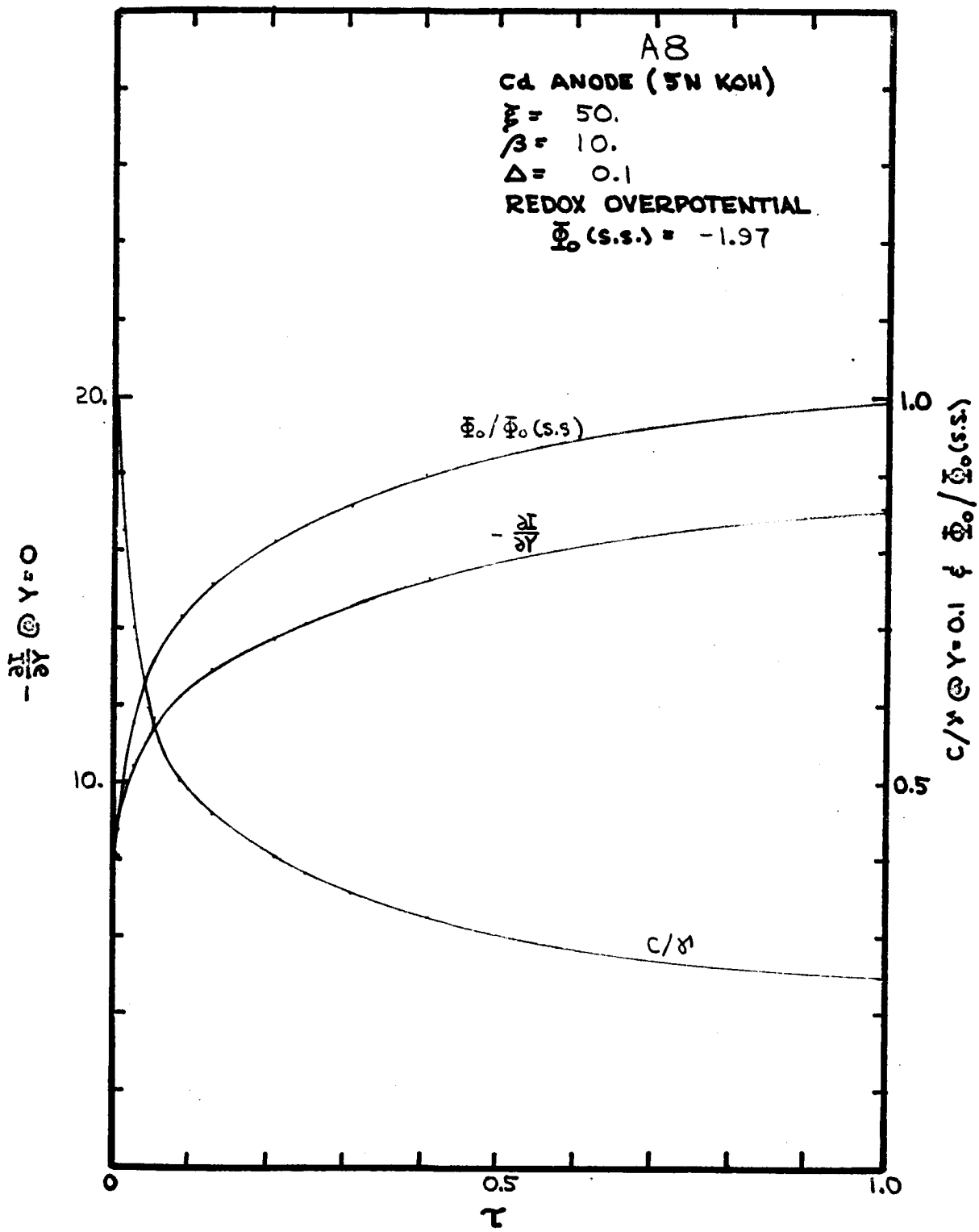
A8
Cd ANODE (5N KOH)
ξ = 50.
β = 10.
Δ = 0.1
REDOX OVERPOTENTIAL
Φ₀ (s.s.) = -1.97
20.
10.
1.0
0.5
0
0.5
1.0
τ
Φ₀/Φ₀(s.s)
-∂R/∂Y
C/γ
-∂I/∂Y @ Y=0
C/γ @ Y=0.1 & Φ₀/Φ₀(s.s)

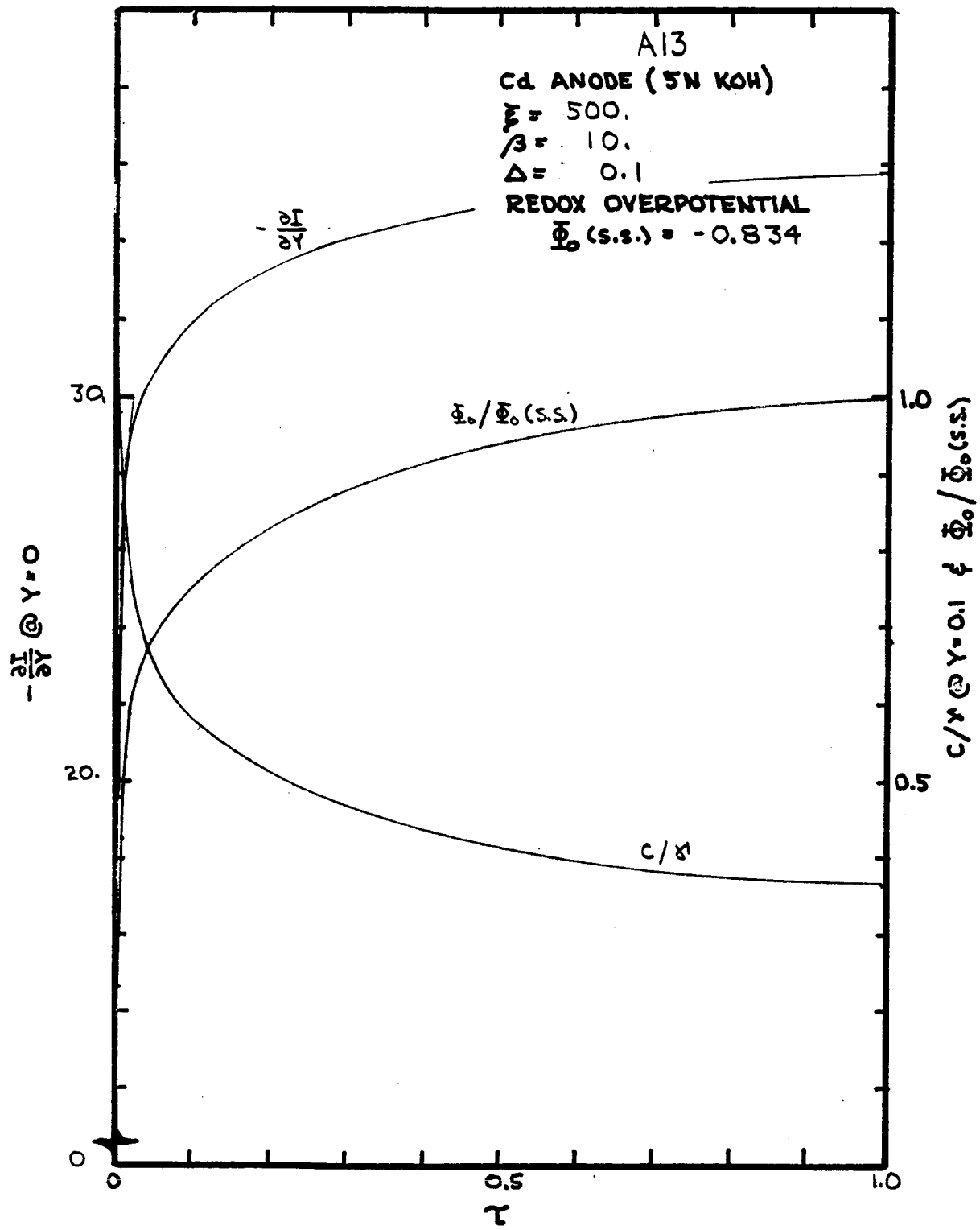
A13
Cd ANODE (5N KOH)
ξ = 500.
β = 10.
Δ = 0.1
REDOX OVERPOTENTIAL
Φ₀ (s.s.) = -0.834
$-\frac{\partial \Phi}{\partial Y}$
Φ_0/Φ_0(s.s.)
C/γ
$-\frac{\partial \Phi}{\partial Y}$ @ Y = 0
C/γ @ Y = 0.1 & Φ_0/Φ_0(s.s.)
30.
20.
0
1.0
0.5
0
0.5
1.0
τ

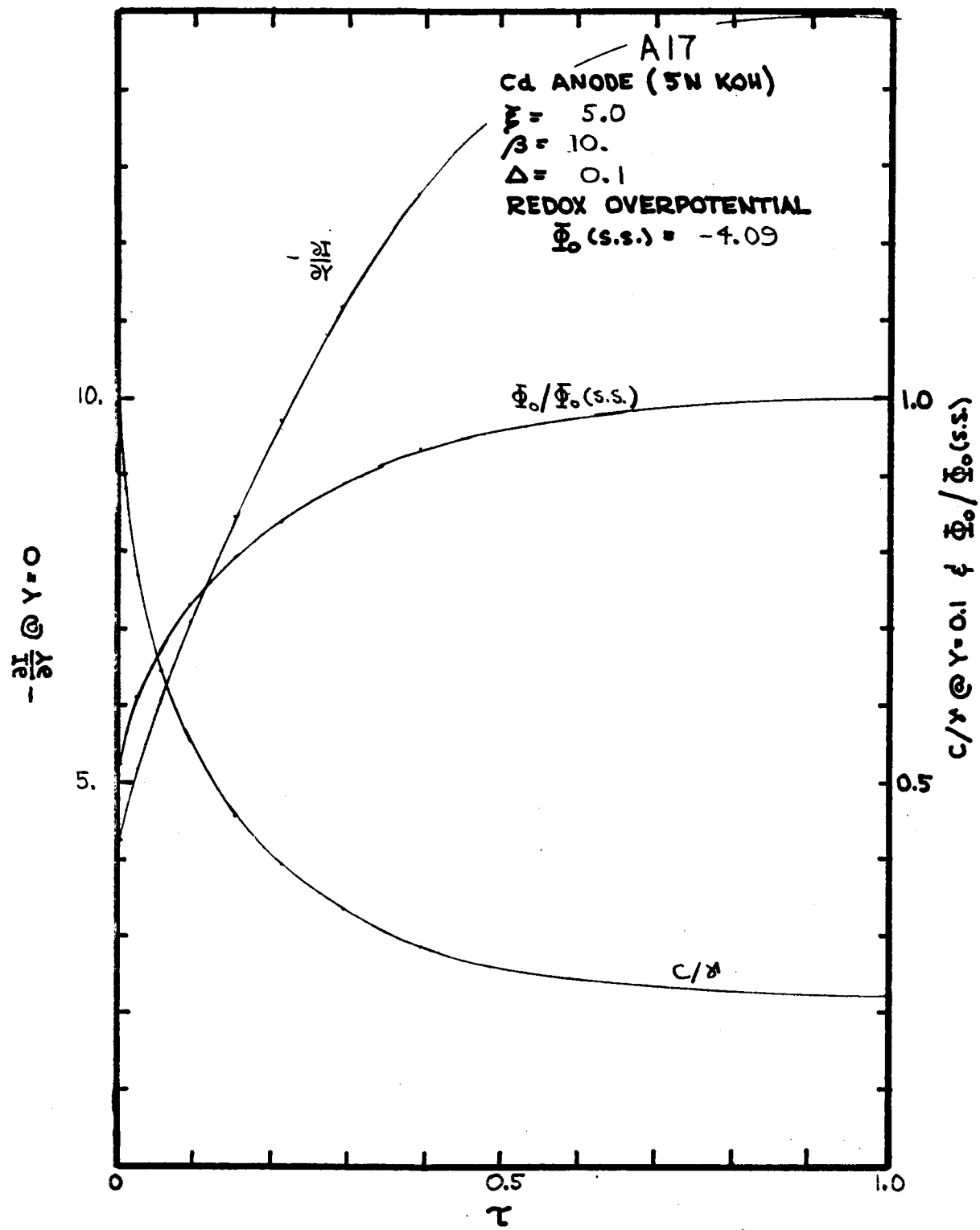
A17
Cd ANODE (5N KOH)
ξ = 5.0
β = 10.
Δ = 0.1
REDOX OVERPOTENTIAL
Φ₀ (s.s.) = -4.09
$-\frac{\partial \Phi}{\partial Y}$
$\Phi_0/\Phi_0(s.s.)$
C/γ
$-\frac{\partial I}{\partial Y}$ @ Y = 0
C/γ @ Y = 0.1 & $\Phi_0/\Phi_0(s.s.)$
10.
5.
1.0
0.5
0
0.5
1.0
τ

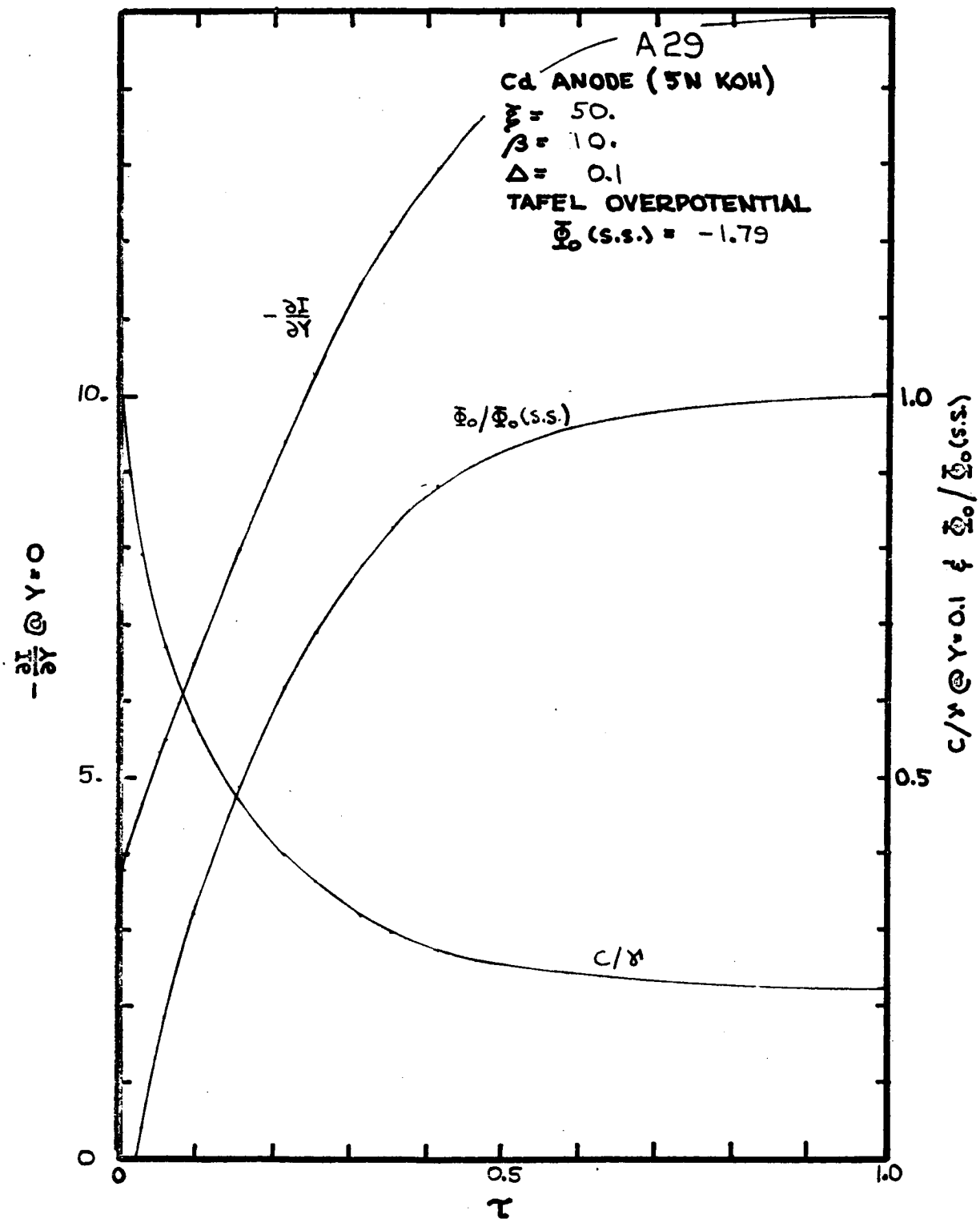
A29
Cd ANODE (5N KOH)
ξ = 50.
β = 10.
Δ = 0.1
TAFEL OVERPOTENTIAL
Φ₀ (s.s.) = −1.79
$-\frac{\partial I}{\partial Y}$
$\Phi_0/\Phi_0(s.s.)$
C/γ
$-\frac{\partial I}{\partial Y}$ @ Y = 0
C/γ @ Y = 0.1 & $\Phi_0/\Phi_0(s.s.)$
τ
0
5.
10.
0.5
1.0
0.5
1.0

APPENDIX VII.

Steady State Behavior of Ferri-ferrocyanide Cathode (2N NaOH)

The steady state behavior of the ferri-ferrocyanide cathode example, as calculated according to the one dimensional model, is contained in this appendix. For each case treated a graph is included presenting curves of transfer current distribution, overpotential, and reactant and product concentrations as functions of depth in the porous electrode. The non-dimensional variables are used and overpotential is presented as a ratio to its value, Φ_o, at the electrode face (electrode overpotential).

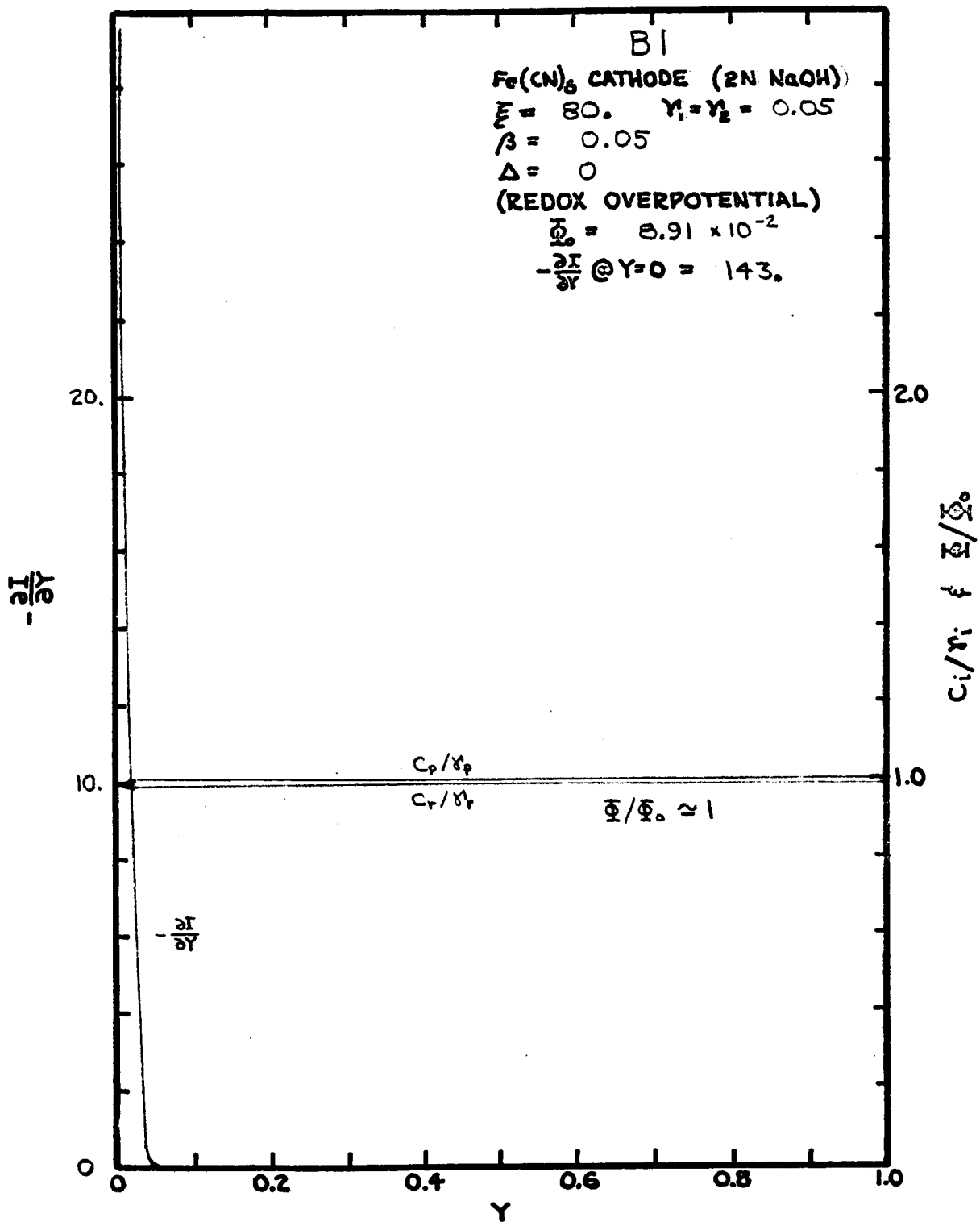
B1
Fe(CN)6 CATHODE (2N NaOH)
ξ = 80. γ1 = γ2 = 0.05
β = 0.05
Δ = 0
(REDOX OVERPOTENTIAL)
Φ0 = 8.91 x 10^-2
-∂I/∂Y @ Y=0 = 143.
20.
10.
0
2.0
1.0
0
0.2
0.4
0.6
0.8
1.0
Y
-∂I/∂Y
-∂Φ/∂Y
Cp/γp
Cr/γr
Φ/Φ0 ≃ 1
Ci/γi ; Φ/Φ0

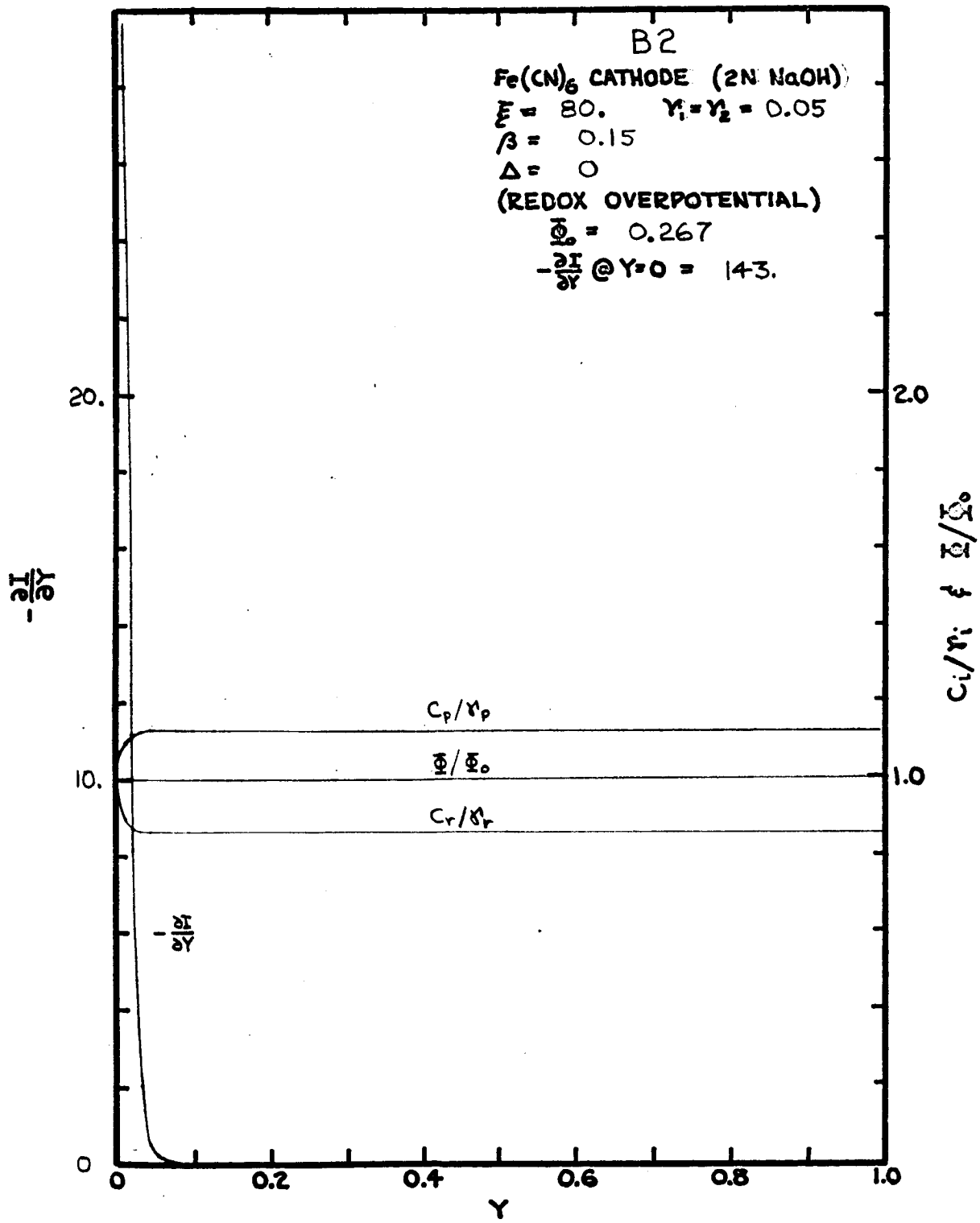
B2
Fe(CN)6 CATHODE (2N NaOH)
ξ = 80. γ1 = γ2 = 0.05
β = 0.15
Δ = 0
(REDOX OVERPOTENTIAL)
Φ0 = 0.267
-∂I/∂Y @ Y=0 = 143.
20.
10.
0
2.0
1.0
0
0.2
0.4
0.6
0.8
1.0
Y
-∂I/∂Y
Cp/γp
Φ/Φ0
Cr/γr
-∂lnΦ/∂Y
Ci/γi & Φ/Φ0

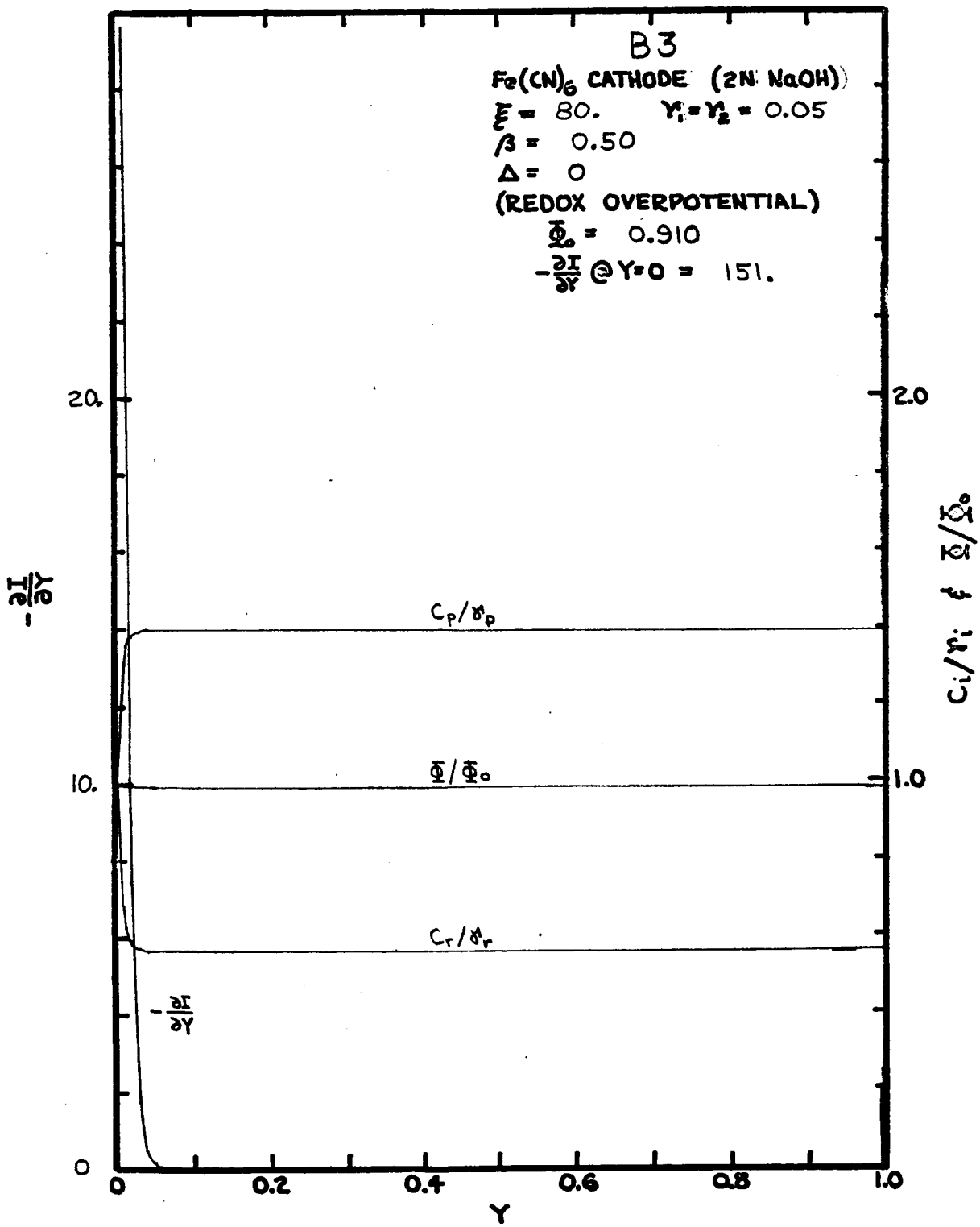
B3
Fe(CN)6 CATHODE (2N NaOH)
ξ = 80. γ1 = γ2 = 0.05
β = 0.50
Δ = 0
(REDOX OVERPOTENTIAL)
Φo = 0.910
-∂I/∂Y @ Y=0 = 151.
20.
10.
0
2.0
1.0
0
0.2
0.4
0.6
0.8
1.0
Y
-∂I/∂Y
Cp/γp
Φ/Φo
Cr/γr
-∂R/∂Y
Ci/γi & Φ/Φo

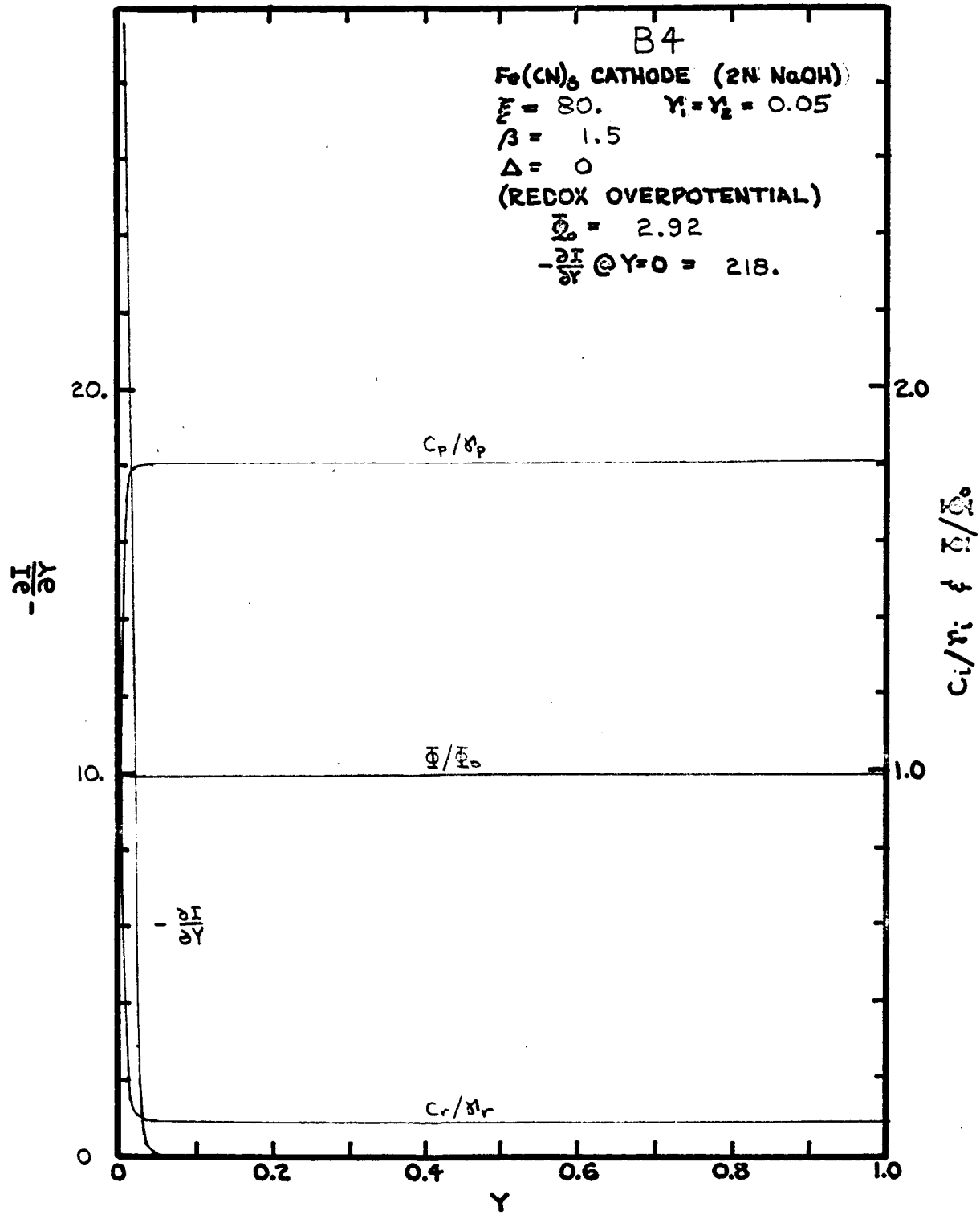
B4
Fe(CN)6 CATHODE (2N NaOH)
ξ = 80. γ1 = γ2 = 0.05
β = 1.5
Δ = 0
(REDOX OVERPOTENTIAL)
Φ0 = 2.92
-∂I/∂Y @ Y=0 = 218.
20.
10.
0
2.0
1.0
Cp/γp
Φ/Φ0
-∂Ie/∂Y
Cr/γr
0
0.2
0.4
0.6
0.8
1.0
Y
-∂Ie/∂Y
Ci/γi & Φ/Φ0

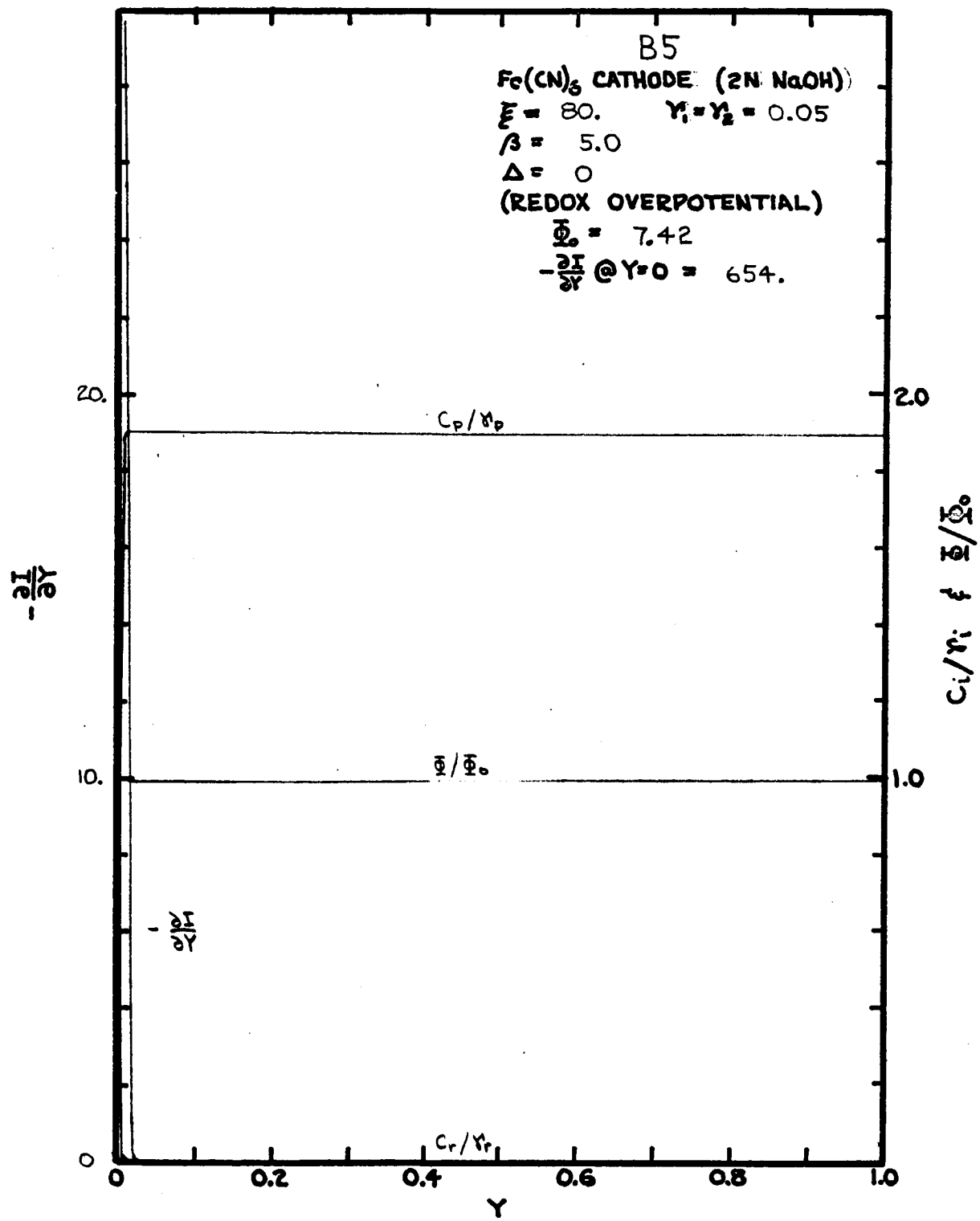
B5
Fe(CN)6 CATHODE (2N NaOH)
ξ = 80. γ1 = γ2 = 0.05
β = 5.0
Δ = 0
(REDOX OVERPOTENTIAL)
Φ0 = 7.42
-∂I/∂Y @ Y=0 = 654.
Cp/γp
Φ/Φ0
Cr/γr
-∂I/∂Y
-∂I/∂Y
Ci/γi & Φ/Φ0
20.
10.
0
2.0
1.0
0
0.2
0.4
0.6
0.8
1.0
Y

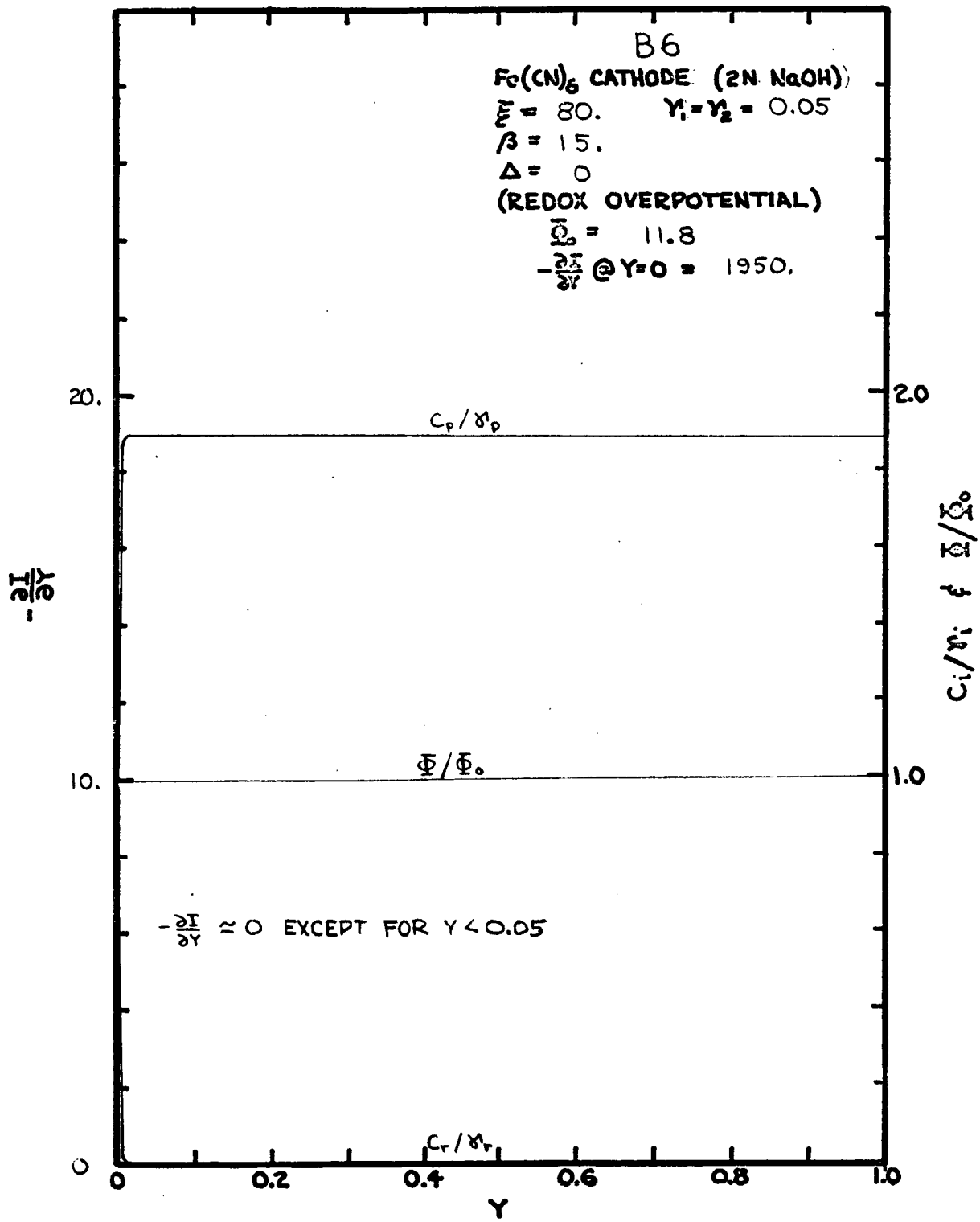
B6
$Fe(CN)_6$ CATHODE (2N NaOH)
ξ = 80. $\gamma_1 = \gamma_2$ = 0.05
β = 15.
Δ = 0
(REDOX OVERPOTENTIAL)
$\bar{\Omega}_o$ = 11.8
$-\frac{\partial I}{\partial Y}$ @ Y=0 = 1950.
C_p/γ_p
Φ/Φ_o
C_r/γ_r
$-\frac{\partial I}{\partial Y} \simeq 0$ EXCEPT FOR $Y < 0.05$
$-\frac{\partial I}{\partial Y}$
C_i/γ_i & $\Phi/\bar{\Omega}_o$
Y
20.
10.
0
2.0
1.0
0
0.2
0.4
0.6
0.8
1.0

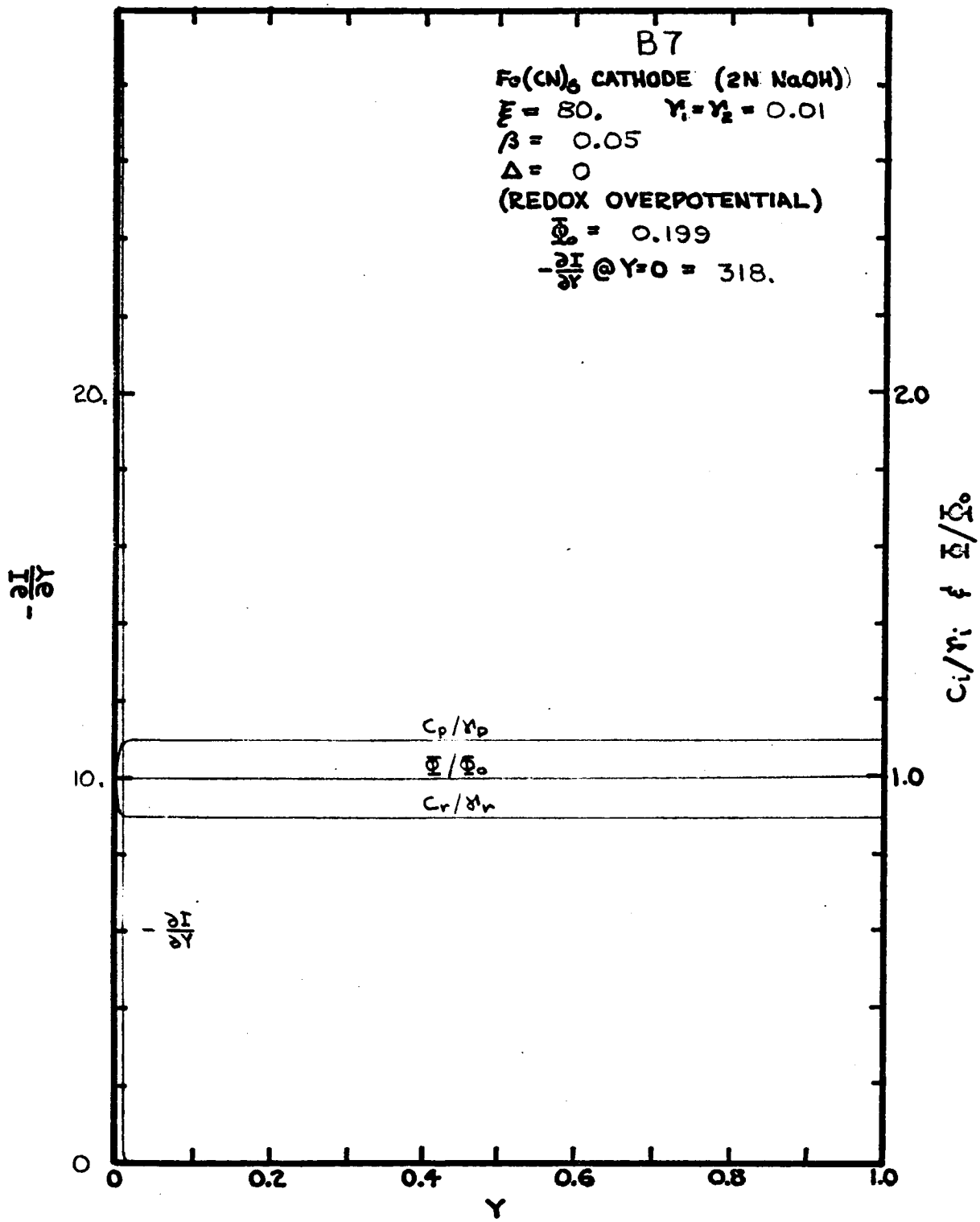
B7
Fe(CN)6 CATHODE (2N NaOH)
ξ = 80. γ1 = γ2 = 0.01
β = 0.05
Δ = 0
(REDOX OVERPOTENTIAL)
Φ0 = 0.199
-∂I/∂Y @ Y=0 = 318.
20.
10.
0
2.0
1.0
0
0.2
0.4
0.6
0.8
1.0
Y
-∂I/∂Y
-∂I/∂ξ
Cp/γp
Φ/Φ0
Cr/γr
Ci/γi & I/I0

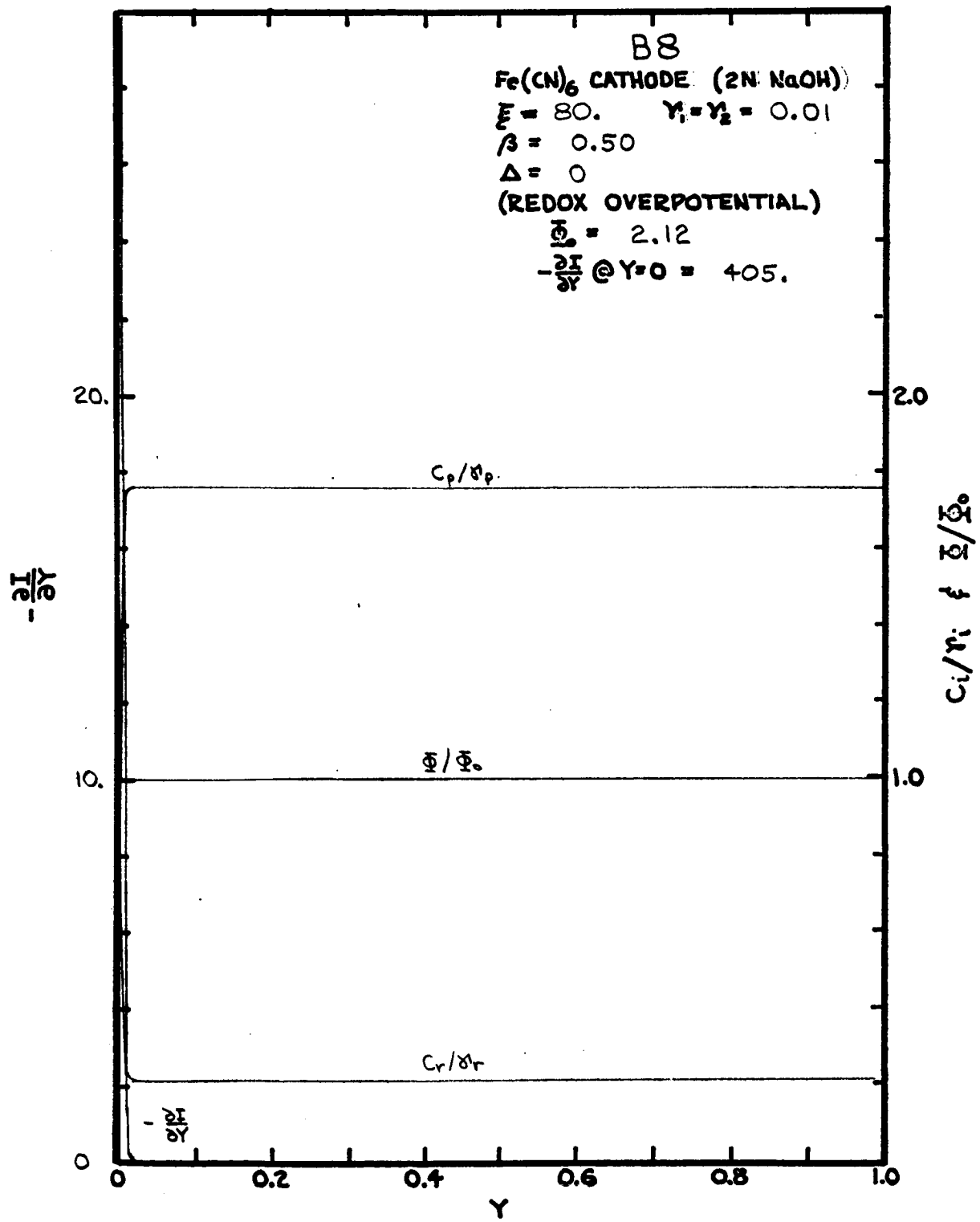
B8
Fe(CN)6 CATHODE (2N NaOH)
ξ = 80. Y1 = Y2 = 0.01
β = 0.50
Δ = 0
(REDOX OVERPOTENTIAL)
Φ0 = 2.12
-∂I/∂Y @ Y=0 = 405.
20.
10.
0
2.0
1.0
Cp/γp
Φ/Φ0
Cr/γr
-∂I/∂Y
0
0.2
0.4
0.6
0.8
1.0
Y
-I ∂I/∂Y
Ci/γi & Φ/Φ0

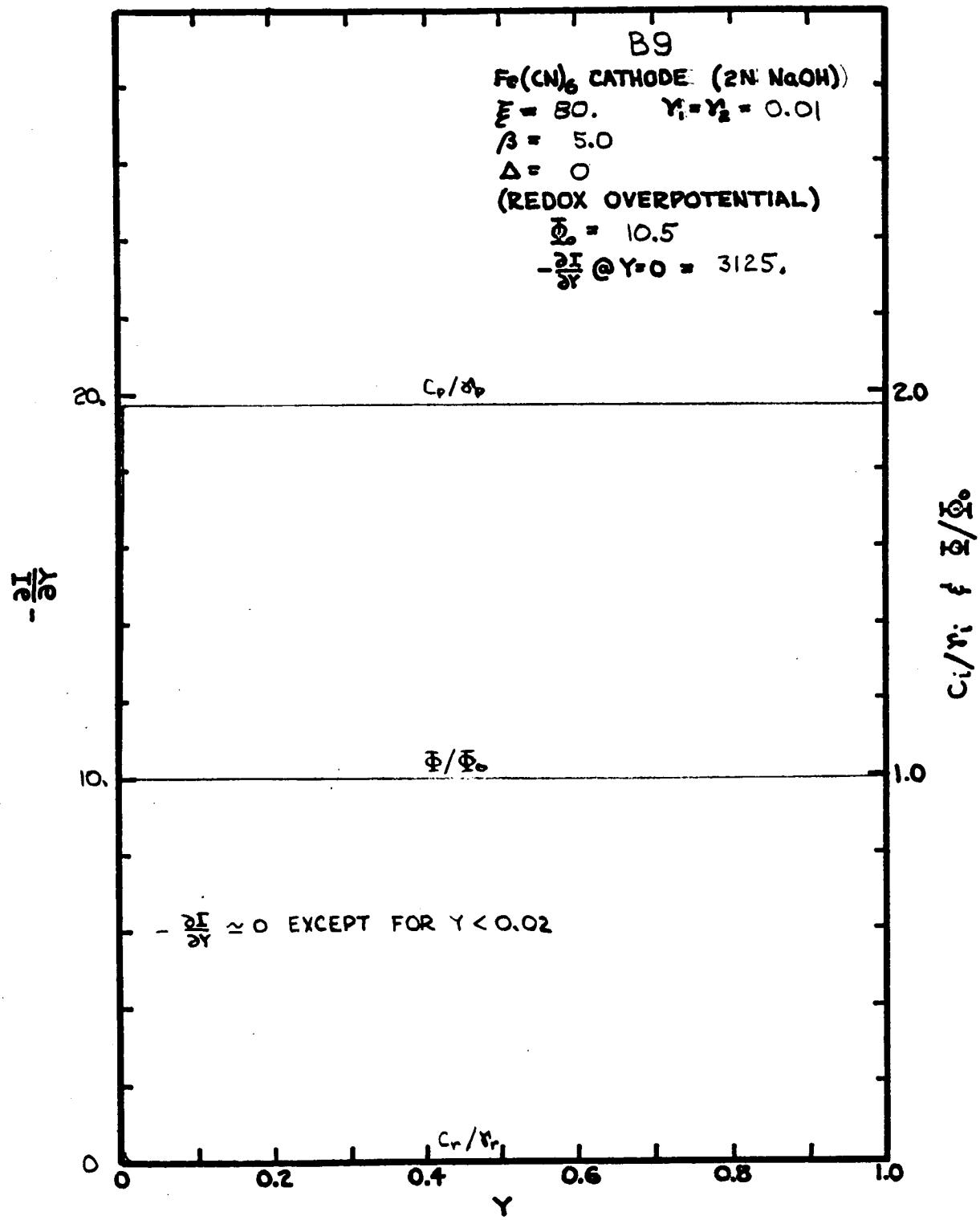
B9
Fe(CN)6 CATHODE (2N NaOH)
ξ = 80. γ1 = γ2 = 0.01
β = 5.0
Δ = 0
(REDOX OVERPOTENTIAL)
Φo = 10.5
-∂I/∂Y @ Y=0 = 3125.
Cp/γp
Φ/Φo
-∂I/∂Y ≃ 0 EXCEPT FOR Y < 0.02
Cr/γr
-∂I/∂Y
Ci/γi ; I/Φo
20.
10.
0
2.0
1.0
0
0.2
0.4
0.6
0.8
1.0
Y

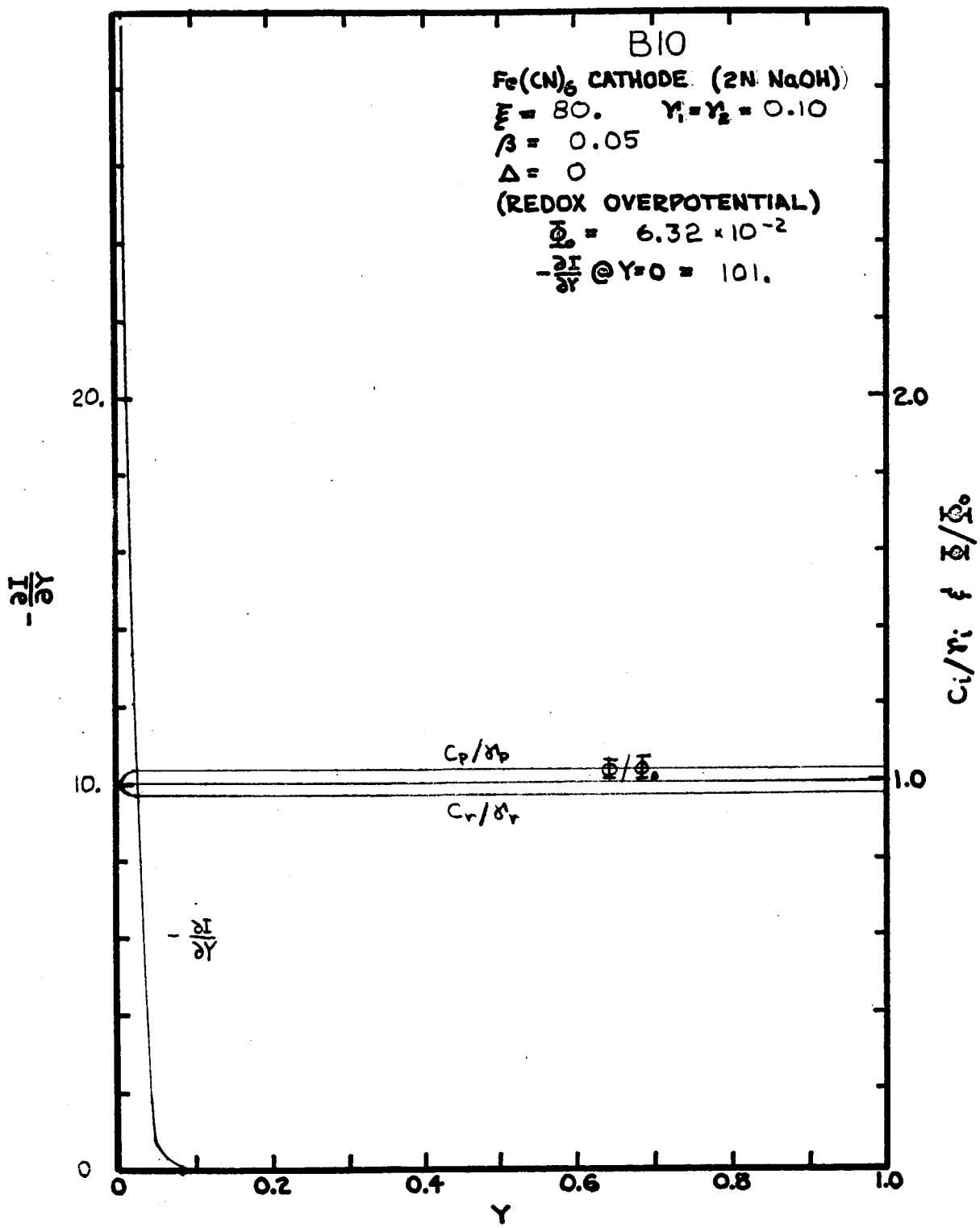
B10
Fe(CN)6 CATHODE (2N NaOH)
ξ = 80. γ1 = γ2 = 0.10
β = 0.05
Δ = 0
(REDOX OVERPOTENTIAL)
Φ0 = 6.32 × 10-2
-∂I/∂Y @ Y=0 = 101.
20.
10.
0
2.0
1.0
0
0.2
0.4
0.6
0.8
1.0
Y
-∂I/∂Y
Cp/γp
Φ/Φ0
Cr/γr
-∂I/∂Y
Ci/γi & ∂I/∂Φ0

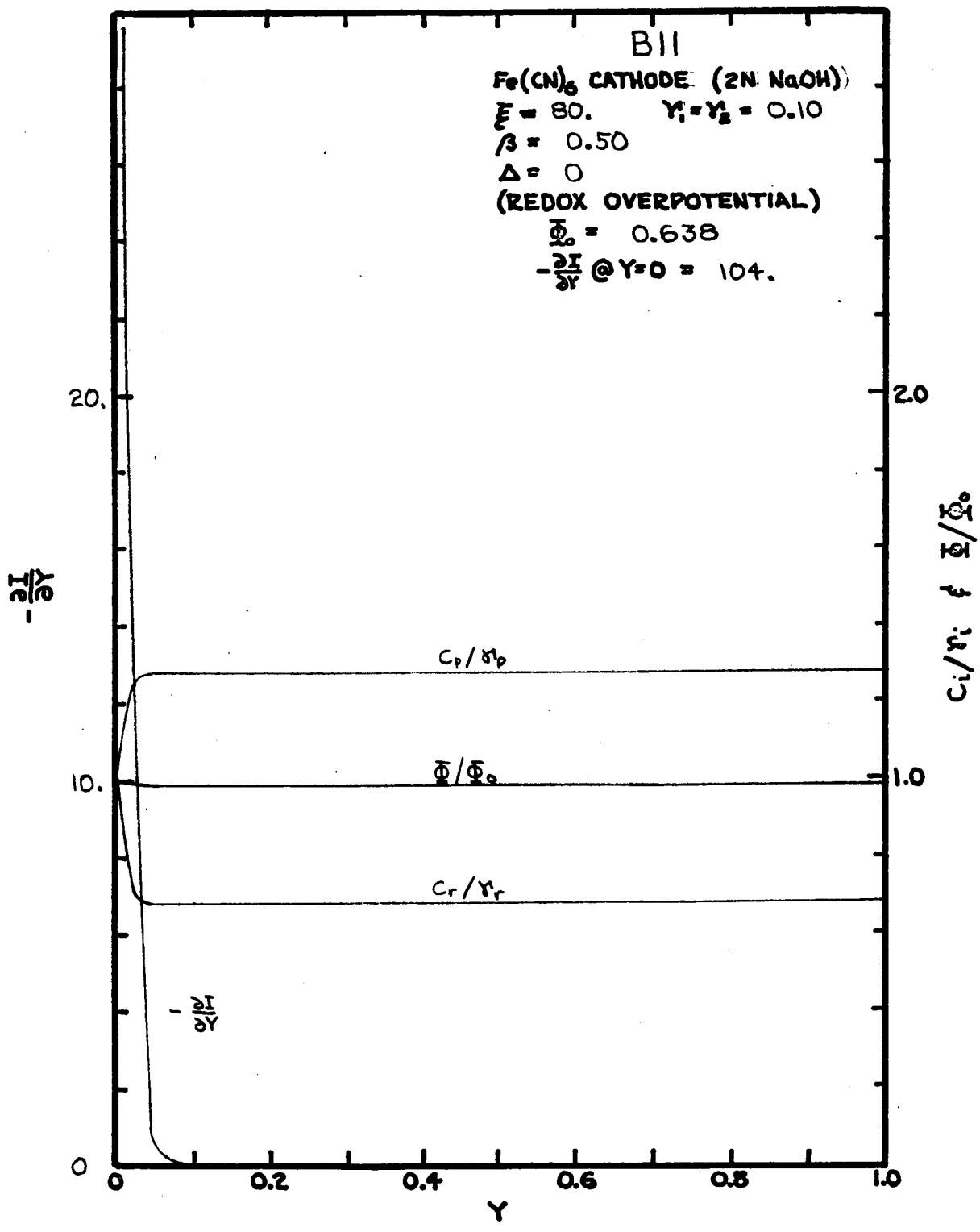
B11
$Fe(CN)_6$ CATHODE (2N NaOH)
ξ = 80. $\gamma_1 = \gamma_2$ = 0.10
β = 0.50
Δ = 0
(REDOX OVERPOTENTIAL)
Φ_0 = 0.638
$-\frac{\partial I}{\partial Y}$ @ Y=0 = 104.
$-\frac{\partial I}{\partial Y}$
C_i/γ_i & Φ/Φ_0
C_p/γ_p
Φ/Φ_0
C_r/γ_r
$-\frac{\partial I}{\partial Y}$
20.
10.
0
2.0
1.0
0
0.2
0.4
0.6
0.8
1.0
Y

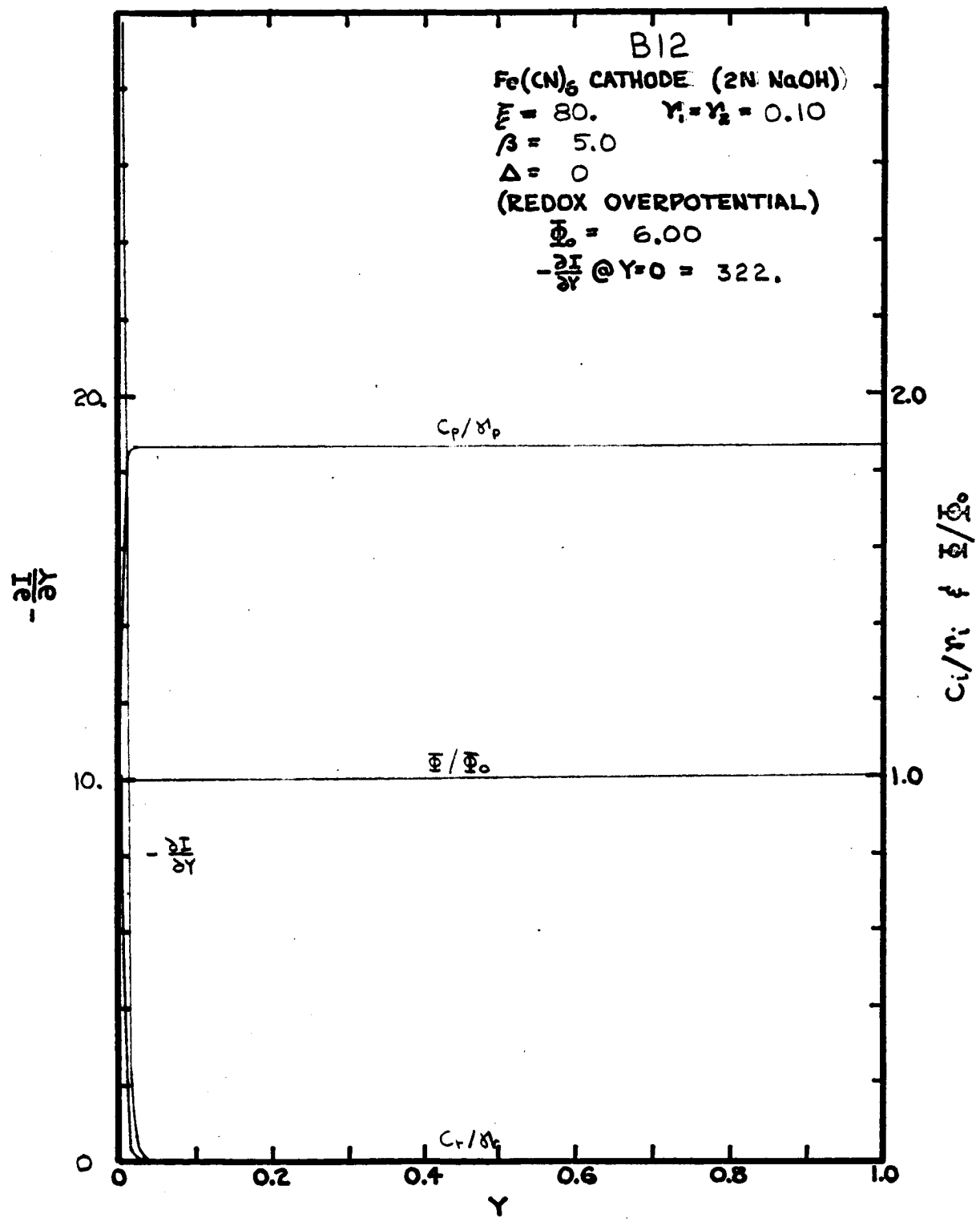
B12
Fe(CN)6 CATHODE (2N NaOH)
ξ = 80. γ1 = γ2 = 0.10
β = 5.0
Δ = 0
(REDOX OVERPOTENTIAL)
Φ0 = 6.00
-∂I/∂Y @ Y=0 = 322.
Cp/γp
Φ/Φ0
-∂I/∂Y
Cr/γr
-∂I/∂Y
Ci/γi & Φ/Φ0
Y
0
0.2
0.4
0.6
0.8
1.0
10.
20.
2.0
1.0

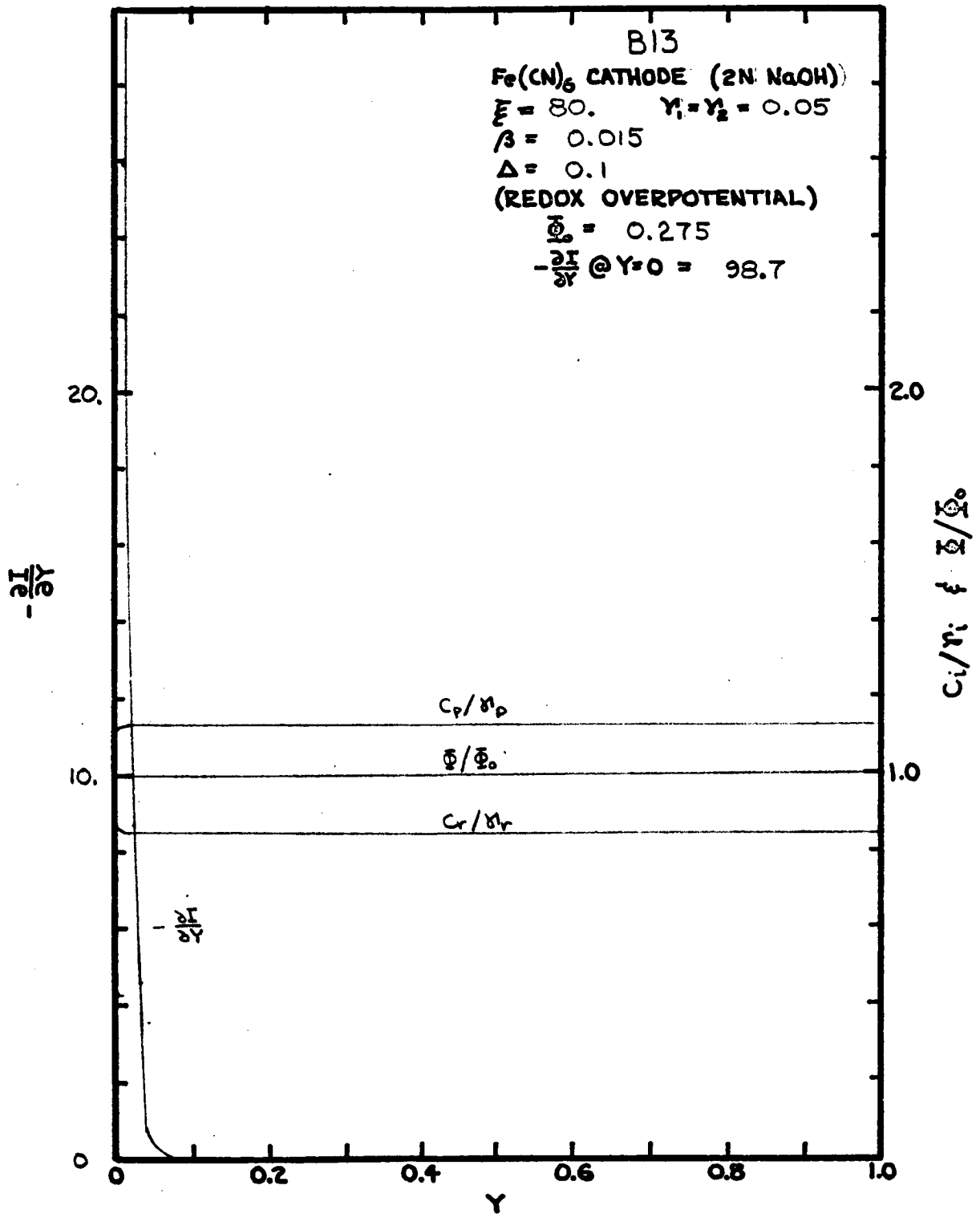
B13
Fe(CN)6 CATHODE (2N NaOH)
ξ = 80. γ1 = γ2 = 0.05
β = 0.015
Δ = 0.1
(REDOX OVERPOTENTIAL)
Φ0 = 0.275
-∂I/∂Y @ Y=0 = 98.7
20.
10.
0
2.0
1.0
0
0.2
0.4
0.6
0.8
1.0
Y
-∂²I/∂Y²
-∂I/∂Y
Cp/γp
Φ/Φ0
Cr/γr
Ci/γi & Φ/Φ0

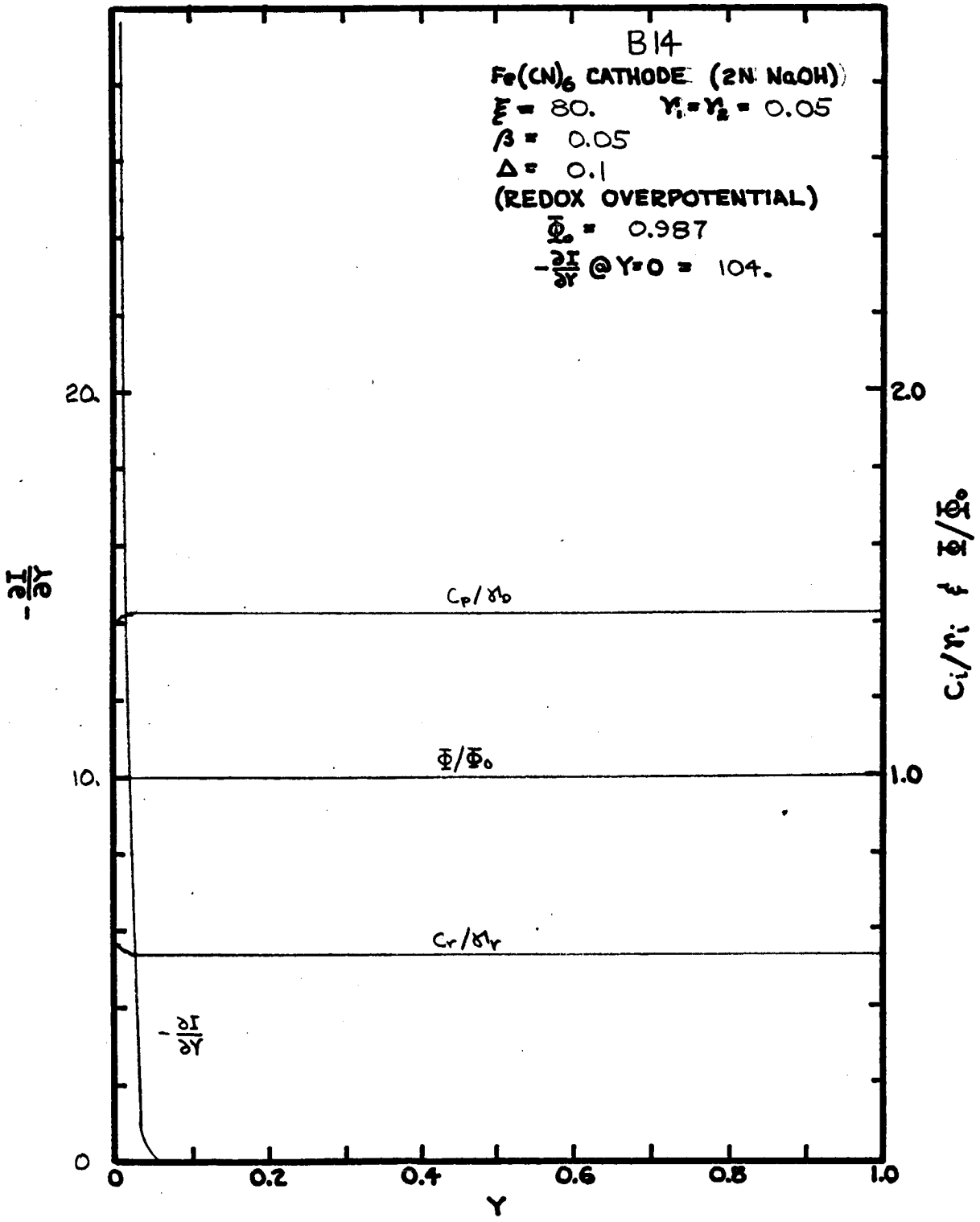
B14
Fe(CN)6 CATHODE (2N NaOH)
ξ = 80. γ1 = γ2 = 0.05
β = 0.05
Δ = 0.1
(REDOX OVERPOTENTIAL)
Φ0 = 0.987
-∂I/∂Y @ Y=0 = 104.
20.
10.
0
2.0
1.0
0
0.2
0.4
0.6
0.8
1.0
Y
-∂I/∂Y
Cp/γ0
Φ/Φ0
Cr/γr
-∂R/∂Y
Ci/γi & E/E0

APPENDIX VIII.

Transient Behavior of Ferri-ferrocyanide Cathode (2N NaOH)

The transient behavior of the ferri-ferrocyanide cathode example, as calculated according to the one dimensional model, is contained in this appendix. For each case treated a graph is included presenting plots, vs. elapsed time since circuit completion, of transfer current density at Y = 0, reactant and product concentrations at Y = 0.1, and electrode overpotential. The non-dimensional variables are used and overpotential is presented as a ratio to its steady state value.

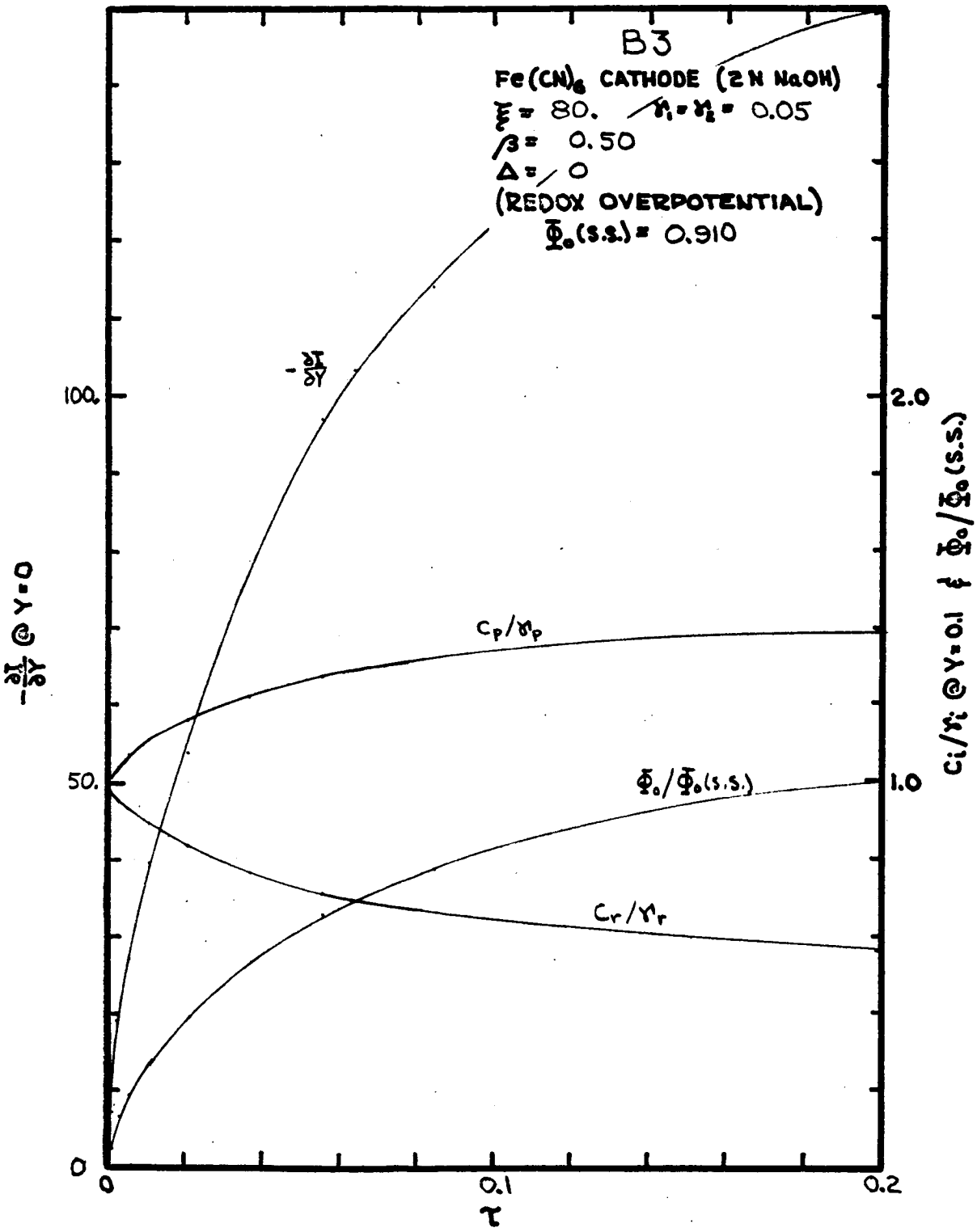
B3
Fe(CN)$_6$ CATHODE (2 N NaOH)
ξ = 80. $\gamma_1 = \gamma_2$ = 0.05
β = 0.50
Δ = 0
(REDOX OVERPOTENTIAL)
$\bar{\Phi}_0$(S.S.) = 0.910
$-\frac{\partial I}{\partial Y}$
C_p/γ_p
$\Phi_0/\bar{\Phi}_0$(S.S.)
C_r/γ_r
$-\frac{\partial I}{\partial Y}$ @ Y = 0
C_i/γ_i @ Y = 0.1 & $\Phi_0/\bar{\Phi}_0$(S.S.)
100.
50.
0
2.0
1.0
0
0.1
0.2
τ

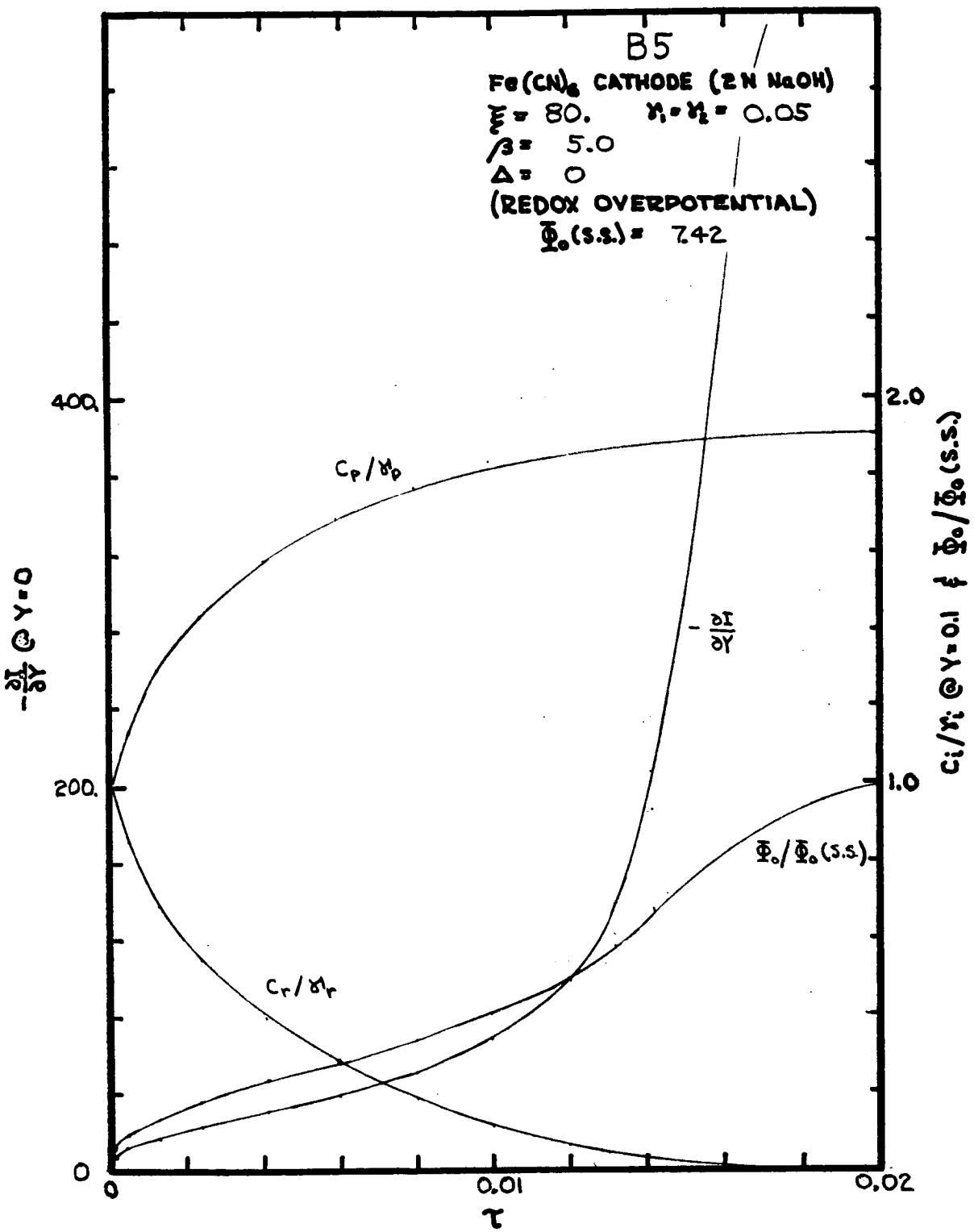
B5
Fe(CN)$_6$ CATHODE (2 N NaOH)
ξ = 80. $\gamma_1 = \gamma_2$ = 0.05
β = 5.0
Δ = 0
(REDOX OVERPOTENTIAL)
$\bar{\Phi}_0$(S.S.) = 7.42
400.
200.
0
2.0
1.0
$-\frac{\partial C_i}{\partial Y}$ @ Y = 0
C_i/γ_i @ Y = 0.1 & $\bar{\Phi}_0/\bar{\Phi}_0$(S.S.)
C_p/γ_p
$-\frac{\partial \Gamma}{\partial Y}$
$\bar{\Phi}_0/\bar{\Phi}_0$(S.S.)
C_r/γ_r
0
0.01
0.02
τ

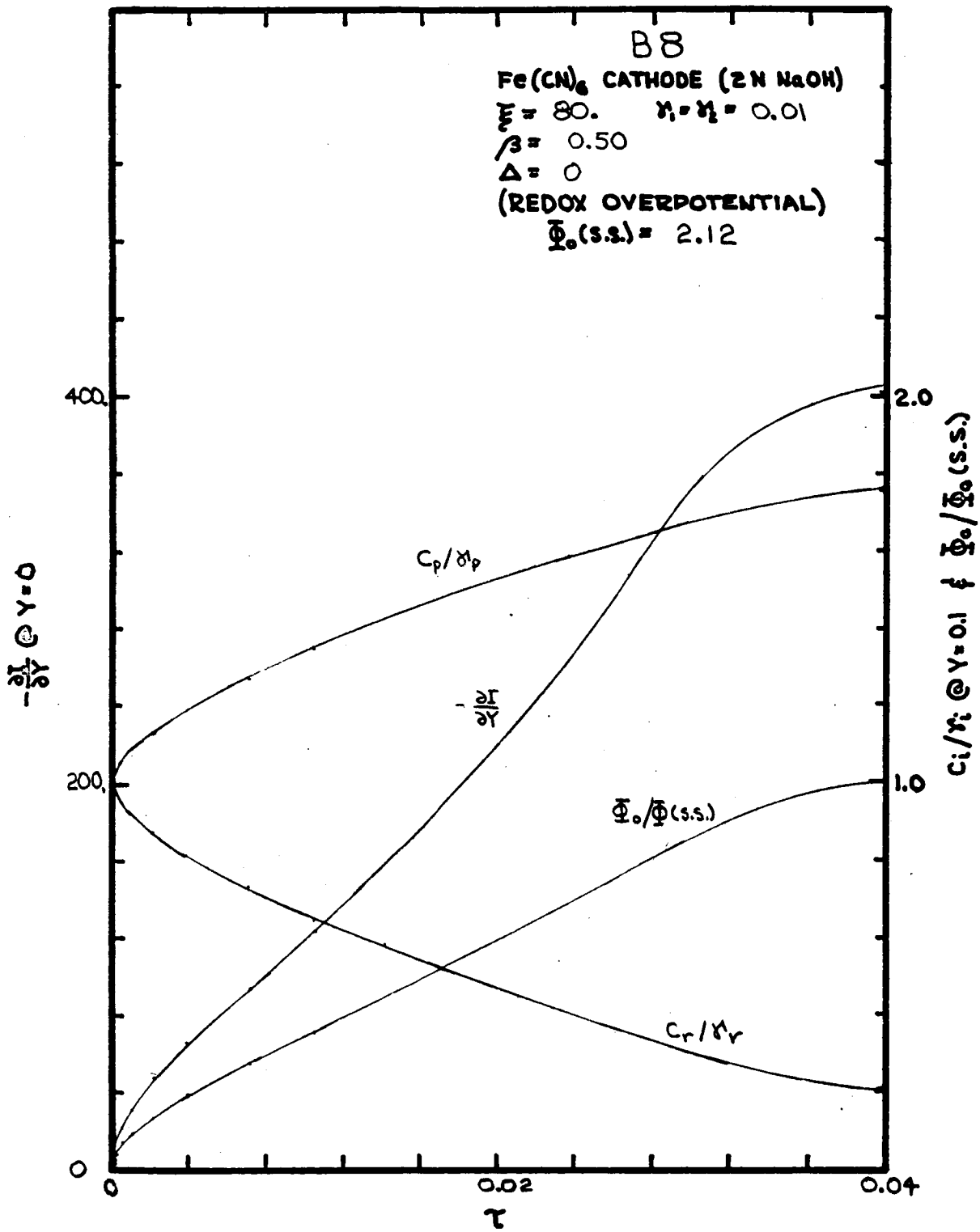
B8
Fe(CN)6 CATHODE (2 N NaOH)
ξ = 80. γ1 = γ2 = 0.01
β = 0.50
Δ = 0
(REDOX OVERPOTENTIAL)
Φ0(S.S.) = 2.12
400.
200.
0
2.0
1.0
0
0.02
0.04
τ
Cp/γp
-∂Φ/∂Y
Φ0/Φ(S.S.)
Cr/γr
-∂Y/∂Y @ Y=0
Ci/γi @ Y=0.1 & Φ0/Φ0(S.S.)

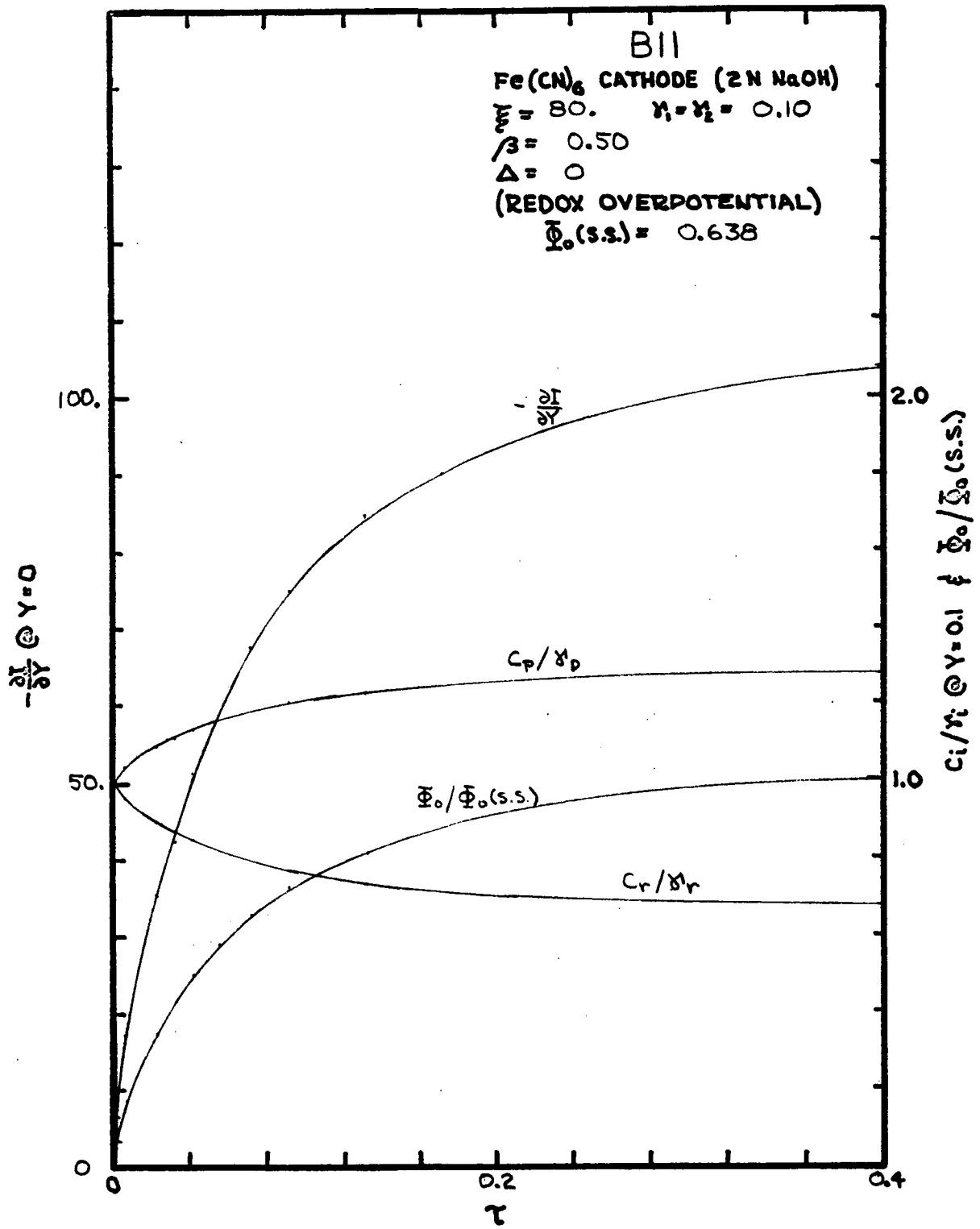
B11
Fe(CN)6 CATHODE (2 N NaOH)
ξ = 80. γ1 = γ2 = 0.10
β = 0.50
Δ = 0
(REDOX OVERPOTENTIAL)
Φ0(s.s.) = 0.638
100.
50.
0
2.0
1.0
0
0.2
0.4
τ
$-\frac{\partial I_R}{\partial Y}$
$-\frac{\partial I}{\partial Y}$ @ Y=0
C_P/γ_P
$\Phi_0/\Phi_0(s.s.)$
C_r/γ_r
C_i/γ_i @ Y=0.1 & $\Phi_0/\Phi_0(s.s.)$

NOTATION

English Letters

A_j	Coefficient of C_j in overpotential expression
a	Specific surface of matrix (cm^{-1})
B_j	Term of overpotential expression not involving C_j linearly
C_j	Concentration of species j (dimensionless) = c_j/c_k^o
c_j	Concentration of species j ($gmol/cm^3$)
c_j^o	Concentration of species j in bulk electrolyte ($gmol/cm^3$)
D_j	Diffusion coefficient of species j (cm^2/sec)
e^-	Symbol for electron
F	Faraday's constant (96,500 coul/equiv)
g_i	Time increment (dimensionless) at step i
h	Distance increment (dimensionless)
I	Current density in electrolyte (dimensionless) = i/i*
i	Current density in electrolyte (amp/cm^2)
i_o	Exchange current density in electrode reaction (amp/cm^2)
i^s	Transfer current density (amp/cm^2)
i*	Current density in electrolyte at pore entrance (amp/cm^2)
J	Index for space variable Y
K	Index for time variable τ
k	Boltzmann constant (1.38×10^{-16} erg/°K)
L	Value of J at Y=1 (= $(1+\Delta)/h+1$)
LF	Value of J at Y=0 (= $\Delta/h+1$)
ℓ	Thickness (or half thickness) of porous electrode model(cm)
M_j	Symbol for species j
N_j	Flux of species j ($gmol/cm^2$-sec)

n Number of Faradays of charge transfered per gmol of reaction (positive for cathodic)

P Porosity

R Gas constant

r General position vector

S_j Source term for species j ($gmol/cm^3$-sec)

T Temperature (°K)

t Time (sec)

u_j Mobility of species j (cm/sec-dyne)

v Electrolyte velocity (cm/sec)

Y Distance into porous electrode (dimensionless) = y/ℓ

y Distance into porous electrode (cm)

z_j Charge number of species j

Greek Letters

α Transfer coefficient in overpotential expression

β $i^*\ell/nFD_k c_k^o$

γ_j c_j^o/c_k^o

Δ Equivalent transfer layer thickness (dimensionless) = δ/ℓ

δ Equivalent transfer layer thickness (cm)

ϵ Electronic charge (1.60×10^{-19} coul)

η Overpotential parameter

θ Dispersion angle of pore structure

κ Electrolyte conductivity (dimensionless)

λ_j $\pi_j\, g/h^2$

μ Viscosity (poise)

ν_j Stoichiometric coefficient of species j

ξ $a\ell^2 i_o/nFD_k c_k^o$

π_j D_j/D_k

τ Time (dimensionless) = $D_k t/\ell^2$

Φ Potential in electrolyte (dimensionless) = $F(\phi-\phi_e)/RT$

Φ_o Φ evaluated at Y=0

Φ^* $\Phi - \Phi|_{Y=-\Delta}$

ϕ Potential in electrolyte (volts)

ϕ_e Equilibrium electrode potential at c_j^o (volts)

χ ξ/β

ω Tortuosity factor of pore structure

Subscripts

j Species in electrolyte identification

p Product species

r Reactant species

Superscripts

' Pertaining to superficial or exterior measured quantities

BIBLIOGRAPHY

1. K. Fischbeck, Z. Anorg. Chem. 148, 97 (1925).
2. K. Fischbeck and E. Einecke, Z. Anorg. Chem. 167, 21 (1927).
3. K. Fischbeck and E. Einecke, Z. Anorg. Chem. 175, 335 (1928).
4. V. S. Daniel-Bekh, Zh. Fiz. Khim. SSSR 22, 697 (1948).
5. J. J. Coleman, Trans. Electrochem. Soc. 90, 545 (1946).
6. J. J. Coleman, J. Electrochem. Soc. 98, 26 (1951).
7. O. S. Ksenzhek and V. V. Stender, Doklady Akad. Nauk SSSR 106, 487 (1956).
8. O. S. Ksenzhek and V. V. Stender, Doklady Akad. Nauk SSSR 107, 280 (1956).
9. O. S. Ksenzhek and V. V. Stender, Zh. Fiz. Khim. 31, 117 (1957).
10. O. S. Ksenzhek, Ukrain. Khim. Zh. 23, 443 (1957).
11. R. M. Perskaya and I. A. Zaideman, Zh. Fiz. Khim. 33, 50 (1959).
12. J. Euler and W. Nonnenmacher, Electrochimica Acta 2, 268 (1960).
13. R. Buvet, M. Guillou, and B. Warszawski, Electrochimica Acta 6, 113 (1962).
14. J. Euler, Electrochimica Acta 4, 27 (1961).
15. J. Euler, Electrochimica Acta 7, 205 (1962).
16. O. S. Ksenzhek, Russ. J. Phys. Chem. 36, 121 (1962).
17. O. S. Ksenzhek, Russ. J. Phys. Chem. 36, 331 (1962).
18. A. Winsel, Z. Elektrochemie 66, 287 (1962).
19. J. S. Newman and C. W. Tobias, J. Electrochem. Soc. 109, 1183 (1962).
20. B. Levich, Physicochemical Hydrodynamics (Prentice-Hall, Englewood Cliffs, N. J., 1962), Ch. VI.

21. H. S. Harned, Chem. Rev. 40, 461 (1947).

22. K. J. Vetter, Elektrochemische Kinetik (Springer, Berlin, 1961).

23. G. E. Forsythe and W. R. Wasow, Finite Difference Methods for Partial Differential Equations (Wiley, New York, 1960), Ch. 2.

24. L. Lapidus, Digital Computation for Chemical Engineers (McGraw-Hill, New York, 1962), Ch. 6.

25. J. Crank and P. Nicholson, Proc. Cambridge Phil. Soc. 43, 50 (1947).

26. G. E. Forsythe and W. R. Wasow, loc. cit., Sec. 17.2.

27. G. H. Bruce, D. W. Peaceman, H. H. Rachford, and J. D. Rice, Trans. A.I.M.E. 198, 79 (1953).

28. J. Douglas, Jr. and T. M. Gallie, Jr., Proc. Amer. Math. Soc. 6, 787 (1955).

29. G. E. Forsythe and W. R. Wasow, loc. cit., Sec. 15.1.

30. F. Kornfeil, Proc. Ann. Battery Res. and Dev. Conf. (12th) Ft. Monmouth, N. J. (1958), 25-7.

31. H. S. Harned and B. B. Owen, The Physical Chemistry of Electrolytic Solutions (A.C.S. Monograph, Reinhold, New York, 1958), Table 6-8-2.

32. A. R. Gordon, J. Chem. Phys. 5, 522 (1937).

33. R. C. Reid and T. K. Sherwood, The Properties of Gases and Liquids (McGraw-Hill, New York, 1958), 296 ff.

34. H. S. Harned and B. B. Owen, loc. cit., 12-2-7A.

35. K. J. Vetter, loc. cit., Sec. 162.

36. National Research Council, International Critical Tables (McGraw-Hill, New York, 1926), 5:66.

37. Landolt-Bornstein, Physikalisch-Chemische Tabellen (Springer, Berlin, 1931), 1103.

38. J. R. Vinograd and J. W. McBain, J. Am. Chem. Soc. 63, 2008 (1941).

39. M. Eisenberg, C. W. Tobias, and C. R. Wilke, J. Electrochem. Soc. 103, 413 (1956).

40. J. V. Petrocelli and A. A. Paolucci, J. Electrochem. Soc. 98, 291 (1951).

ACKNOWLEDGEMENT

I wish to express my appreciation to Professor C. W. Tobias for his advice and direction in the conduct of this study; and to Professors E. F. Orlemann and I. Fatt for their review of this thesis.

This work was performed under Research Grant NsG 150-61 from the National Aeronautics and Space Administration.